

**SBORNÍK VYBRANÝCH
IMPAKTOVANÝCH PRACÍ
ZA ROK 2013**



Obsah

ÚVODNÍ SLOVO	5
Přehled publikovaných prací	6
A CONTROLLED TRIAL OF REVASCLARIZATION IN ACUTE STROKE	7
MYELOMA STEM CELL CONCEPTS, HETEROGENEITY AND PLASTICITY OF MULTIPLE MYELOMA	15
SAFETY AND EFFICACY OF ENDOVASCULAR SONOLYSIS USING THE EKOSONIC™ ENDOVASCULAR SYSTEM IN ACUTE STROKE PATIENTS	29
SHOULD MEAN ARTERIAL PRESSURE BE INCLUDED IN THE DEFINITION OF AMBULATORY HYPERTENSION IN CHILDREN?	36
ECTOPIC LIVER - DIFFERENT MANIFESTATIONS, ONE SOLUTION	43
CLINICALLY IMPORTANT INTERACTION BETWEEN METOPROLOL AND PROPRAFENONE	48
OBJECTIVE EVALUATION OF THE EFFECT OF AUTOLOGOUS PLATELET CONCENTRATE ON POST-OPERATIVE SCARRING IN DEEP BURNS	51
EXTRAESOPHAGEAL REFLUX: WHAT IS THE BEST PARAMETER FOR PH-MONITORING DATA ANALYSIS FROM THE PERSPECTIVE OF PATIENT RESPONSE TO PROTON PUMP INHIBITORS?	65
CHROMOENDOSCOPY TO DETECT EARLY SYNCHRONOUS SECOND PRIMARY ESOPHAGEAL CARCINOMA IN PATIENTS WITH SQUAMOUS CELL CARCINOMAS OF THE HEAD AND NECK?	70
INVESTIGATION OF AN AUTOLOGOUS BLOOD TREATMENT STRATEGY FOR TEMPOROMANDIBULAR JOINT HYPERMOBILITY IN A PIG MODEL	75
POSSIBLE ROLE OF NANO-SIZED PARTICLES IN CHRONIC TONSILLITIS AND TONSILLAR CARCINOMA: A PILOT STUDY	81
TAKAYASU ARTERITIS IN A 10-MONTH-OLD BOY	86
THE ROLE OF ADRENOMEDULLIN AND GALANIN IN RECURRENT VASOVAGAL SYNCOPE: A CASE CONTROL STUDY	90
ENDOSCOPIC VS OPEN SAPHENOUS VEIN HARVEST FOR CORONARY ARTERY BYPASS GRAFTING: A LEG-RELATED MORBIDITY AND HISTOLOGICAL COMPARISON	96
PRIMARY NEUROENDOCRINE CARCINOMA OF THE KIDNEY	101

ÚVODNÍ SLOVO

Vážení kolegové,

dostáváte do rukou první číslo sborníku nejlepších vědeckých prací publikovaných v impaktovaných časopisech v roce 2013. Sborník je souhrnem 15 prací, které v roce 2013 získali nejvyšší impakt faktor a představují přehled nejkvalitnějších autorských prací ve Fakultní nemocnici Ostrava.

Publikační činnost je nedílnou součástí vědecké práce zaměstnanců fakultní nemocnice a odráží špičkovou kvalitu poskytované zdravotní péče. Naše nemocnice se snaží poskytnout svým pacientům tu nejkvalitnější péči a ta se odráží i ve vědecké a publikační činnosti.

Kvalitní autorský text, který je otištěn v prestižním impaktovaném časopise, je trvalou stopou naší vědecké práce. Nárůst kvalitních publikovaných výsledků vědecké práce představuje dnes nedílnou součást vědecko-výzkumné činnosti, bez které se fakultní nemocnice neobejde.

Naším dlouhodobým cílem je zvyšovat úroveň Fakultní nemocnice Ostrava jako registrované výzkumné organizace a to nejen prostřednictvím vědeckých sdělení na odborných seminářích a kongresech, ale rovněž publikovanými výsledky vědecko-výzkumné činnosti, které jsou registrovány a hodnoceny v rámci RIV a tím nastavují i začlenění nemocnice mezi kvalitní výzkumné organizace.

Přeji Vám hodně úspěchů ve Vaší publikační činnosti, kterou nemocnice bude svým zázemím trvale podporovat.

MUDr. Václav Procházka, Ph.D., MSc
Náměstek ředitele FNO pro vědu a výzkum

Dear colleagues,

You are holding in your hands the first issue of the Collection of the best original scientific works published in high-impact journals in 2013. The Collection presents a summary of fifteen scientific articles, which were given the highest impact factor in 2013, and which represent an overview of the best original works from the University Hospital Ostrava for that year.

Publication activity is an integral part of scientific work of the employees of the university hospital and reflects the topmost quality of the provided medical care. Our hospital strives to provide the highest-quality care to our patients, which is also reflected in our scientific and publication activities.

A high-quality original text published in a prestigious high-impact journal is a permanent mark of our scientific work. The increasing number of published first-class results of the scientific work is an integral part of the activities realized in the area of research and development, without which the operation of the university hospital would not be possible.

Our long-term goal is to improve the level of the University Hospital Ostrava as a registered research organization, not only through scientific presentations at expert conferences and congresses, but also by the means of published results of research and development activities, which are registered and evaluated within the national Register of R&D results, and thus predetermine also the ranking of the hospital among top-class research organizations.

I wish you much success in your publication activities, which will be thoroughly supported by the hospital and its facilities.

Václav Procházka, MD, Ph.D., MSc
Vice-President for Research and Development

Přehled publikovaných prací

číslo	autor	název	časopis	licence ze dne
1.	Roubec Martin	A controlled trial of revascularization in acute stroke	Radiology	2. dubna 2014
2.	Hájek Roman	Myeloma stem cell concepts, heterogeneity and plasticity of multiple myeloma	British journal of haematology	7. dubna 2014
3.	Kuliha Martin	Safety and efficacy of endovascular sonolysis using the EkoSonic endovascular system in patients with acute stroke	American journal of neuroradiology	22. dubna 2014
4.	Šuláková Terezie	Should mean arterial pressure be included in the definition of ambulatory hypertension in children?	Pediatric nephrology	27. března 2014 (č. 3357090030260)
5.	Zonča Pavel	Ectopic liver: Different manifestations, one solution	World journal of gastroenterology	12. dubna 2014
6.	Đuricová Jana	Clinically important interaction between metoprolol and propafenone	Canadian family physician	2. dubna 2014
7.	Klosová Hana	Objective evaluation of the effect of autologous platelet concentrate on post-operative scarring in deep burns	Burns	23. dubna 2014 (č. 3374580799917)
8.	Zeleník Karol	Extraesophageal reflux: what is the best parameter for pH-monitoring data analysis from the perspective of patient response to proton pump inhibitors?	Gastroenterology Research and Practice	1. dubna 2014
9.	Komínek Pavel	Chromoendoscopy to detect early synchronous second primary esophageal carcinoma in patients with squamous cell carcinomas of the head and neck?	Gastroenterology Research and Practice	1. dubna 2014
10.	Štembírek Jan	Investigation of an autologous blood treatment strategy for temporomandibular joint hypermobility in a pig model	International journal of oral and maxillofacial surgery	28. dubna 2014 (č. 3377611027768)
11.	Zeleník Karol	Possible role of nano-sized particles in chronic tonsillitis and tonsillar carcinoma: a pilot study	European archives of oto-rhino-laryngology and Head & Neck	8. dubna 2014 (č. 3364151139022)
12.	Pískovský Tomáš	Takayasu arteritis in a 10-month-old boy	VASA	3. dubna 2014
13.	Plášek Jiří	The role of adrenomedullin and galanin in recurrent vasovagal syncope: a case control study	Biomedical papers	3. dubna 2014
14.	Brát Radim	Endoscopic vs open saphenous vein harvest for coronary artery bypass grafting: A leg-related morbidity and histological comparison	Biomedical papers	3. dubna 2014
15.	Dvořáčková Jana	Primary neuroendocrine carcinoma of the kidney	Biomedical papers	3. dubna 2014

A CONTROLLED TRIAL OF REVASCULARIZATION IN ACUTE STROKE

Martin Roubec, MD, PhD, Martin Kuliha, MD, Václav Procházka, MD, PhD, Jan Krajča, MD, Daniel Czerný, MD, Tomáš Jonszta, MD, Antonín Krajina, MD, PhD, Daniel Šaňák, MD, PhD, FESO, Kateřina Langová, MS, PhD, Roman Herzig, MD, PhD, FESO, and David Školoudík, MD, PhD, FESO

From the Comprehensive Stroke Center, Department of Neurology, Faculty of Medicine, Ostrava University and University Hospital Ostrava, 17 Listopadu 1790, CZ-708 52 Ostrava-Poruba, Czech Republic (M.R., M.K., D. Školoudík); Comprehensive Stroke Center, Department of Neurology, Faculty of Medicine and Dentistry, Palacký University and University Hospital, Olomouc, Czech Republic (M.K., D. Šaňák, R.H., D. Školoudík); Comprehensive Stroke Center, Department of Radiology, University Hospital Ostrava, Ostrava, Czech Republic (V.P., J.K., D.C., T.J.); Comprehensive Stroke Center, Department of Radiology, Faculty of Medicine Charles University and University Hospital Hradec Králové, Hradec Králové, Czech Republic (A.K.); and Department of Biophysics, Faculty of Medicine and Dentistry, Institute of Molecular and Translational Medicine, Palacký University, Olomouc, Czech Republic (K.L.).

Originally published in: *Radiology*, 2013; 266: 871-878

Consent to the publication of 2nd April 2014

ABSTRACT

Purpose

To compare safety and utility of intraarterial revascularization with use of stents to no revascularization in patients who either failed to respond to intravenous thrombolysis (IVT) or have contraindications to IVT.

Materials and Methods

The case-control study was approved by local ethics committees; all patients signed informed consent. One hundred thirty-one patients (74 men; mean age, 65.9 years \pm 12.3; range, 25-86 years) with acute ischemic stroke (AIS) due to middle cerebral artery (MCA) occlusion were enrolled; 75 underwent IVT. No further recanalization therapy was performed in 26 (35%) IVT-treated patients with MCA recanalization (group 1). Patients with IVT failure after 60 minutes were allocated to endovascular treatment (group 2A) or no further therapy (group 2B). Patients with contraindication to IVT were allocated to endovascular treatment within 8 hours since AIS onset (group 3A) or to no recanalization therapy (group 3B). Neurologic deficit at admission, MCA recanalization, symptomatic intracerebral hemorrhage (SICH), and 3-month clinical outcome were evaluated. Favorable clinical outcome was defined as modified Rankin scale score 0-2 at 3 months after stroke onset. Two-sided Mann-Whitney U test, independent samples t test, Fisher exact test, multivariate logistic regression analysis of baseline variables, and complete MCA recanalization for the prediction of favorable clinical outcome were used for statistical evaluation.

Results

Median National Institutes of Health Stroke Scale score at admission was 13.5, 16.0, 15.5, 15.0, and 16.0 in groups 1, 2A, 2B, 3A, and 3B, respectively (P

> .05); SICH occurred in one of 26 (3.8%), one of 23 (4.3%), one of 26 (3.8%), one of 31 (3.2%), and one of 25 (4.0%) patients, respectively (P > .05). MCA recanalization after endovascular treatment was achieved in 50 of 54 (92.6%) patients. Favorable outcome was significantly different between groups 2A and 2B (10 of 23 [43.5%] and four of 26 [15.4%], respectively; P = .03) and groups 3A and 3B (14 of 31 [45.2%] and two of 25 [8.0%], respectively; P = .004) and was dependent on MCA recanalization (odds ratio, 5.55; P = .006).

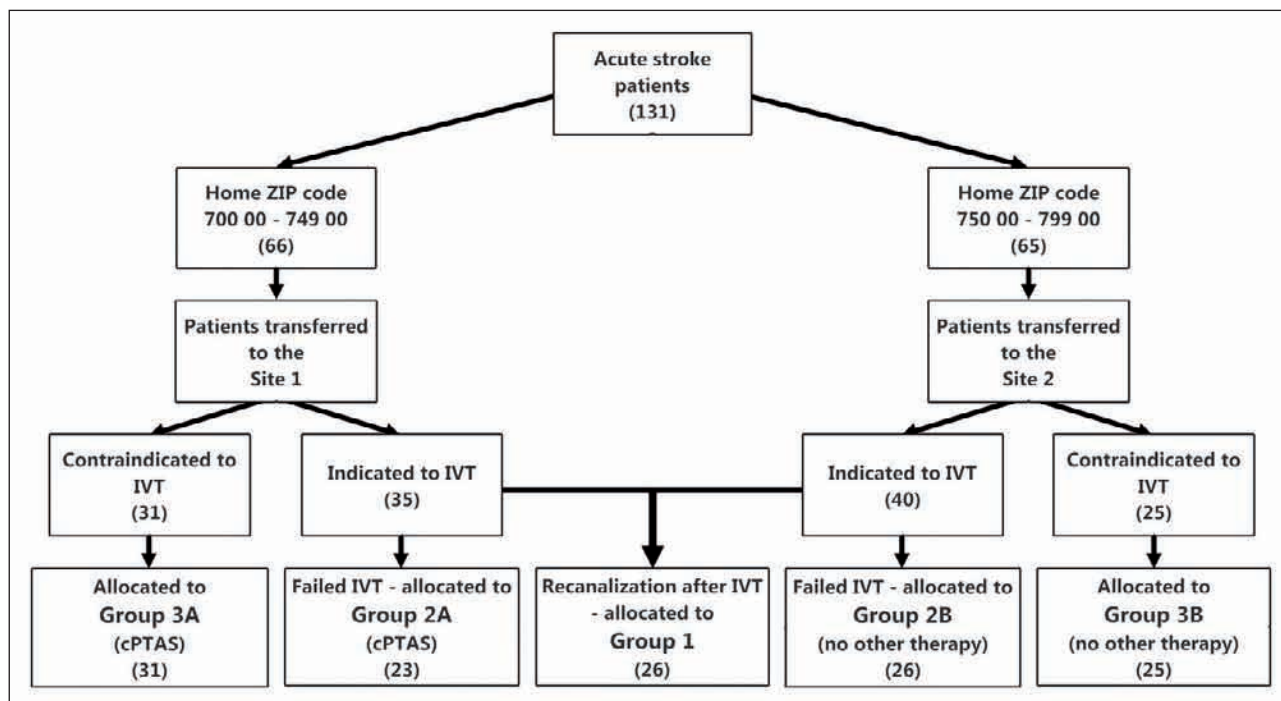
Conclusion

In this controlled trial, intraarterial revascularization with stents was an effective and safe-effective treatment option in patients with acute MCA occlusion with contraindication to IVT or after IVT failure.

INTRODUCTION

One of the most important prognostic factors in patients with acute ischemic stroke with intracranial artery occlusion is the time to recanalization (1-4). Spontaneous recanalization is possible, but it is difficult to accurately specify its rate. According to previous studies, the rate of spontaneous recanalization of the middle cerebral artery (MCA) occlusion 6-8 hours from stroke onset is somewhere between 14% and 28%, most likely closer to 17% (5). Moreover, delayed spontaneous recanalization cannot usually prevent irreversible damage of the brain tissue with permanent neurologic deficit. That is why the effort to accelerate recanalization of the occluded artery becomes crucial.

Currently, the following options for acceleration of recanalization of the intracranial artery occlusion are available: intravenous thrombolysis (IVT), intraarterial or combined thrombolysis, mechanical recanalization techniques using several mechanical devi-



ces for thrombectomy and/or stent placement, and remote or local sonolysis (1-4,6-17). Cerebral percutaneous transluminal angioplasty (PTA) with stent placement is one of the methods available that can be used to accelerate and achieve recanalization of MCA occlusion (18-26).

The purpose of this study was to compare the safety and utility of intraarterial revascularization with use of stents to no revascularization in patients who either fail to respond to IVT or have contraindication to IVT.

MATERIALS AND METHODS

The entire study was conducted in accordance with the Helsinki Declaration of 1975 (as revised in 2004 and 2008). The study was approved by the local ethics committees of the two participating hospitals (University Hospital Ostrava, University Hospital Olomouc). All patients signed informed consent forms for the eligible and available treatment. Independent witnesses verified the signatures in cases where there were any technical problems.

Patients

A prospective bicenter case-control study was conducted. One hundred thirty-one consecutive patients with acute ischemic stroke were enrolled during more than 24 months (66 in Ostrava, site 1 and 65 in Olomouc, site 2; case-to-control subject ratio, 1:1). Patient inclusion criteria were acute ischemic stroke with MCA occlusion at computed tomographic (CT) angiography, National Institutes of Health Stroke Scale (NIHSS) score of 4-25 at admission, age of 18-90 years, and start of therapy within 8 hours of symptom onset. Patients with modified Rankin score greater than 1 before stroke onset (four patients), acute ischemic lesion in region other than ICA (three

patients), intracranial hemorrhage (one patient), or brain tumor at CT (one patient) were excluded due to potentially worse prognosis caused by the concomitant diseases.

Diagnostics

At admission, a physical examination, blood samples, electrocardiogram, chest x-ray, and standard neurologic evaluation by a certified neurologist using the NIHSS were performed, followed by brain CT or magnetic resonance (MR) imaging and by CT angiography or MR angiography of the cervical and brain arteries. Duplex ultrasonography (US) of the cervical portion of the carotid and vertebral arteries and transcranial color-coded duplex US were performed at the end of IVT or 1 hour after stroke unit admission and 24 hours after stroke onset in all patients. Artery recanalization was evaluated by using Thrombolysis in Brain Ischemia criteria (27).

Treatment

Patients were treated at two comprehensive stroke centers, with 24-hour, 7-days-a-week accessibility to IVT and cerebral PTA with stent placement. They underwent the standard treatment (28,29). All patients who fulfilled the Safe Implementation of Thrombolysis in Stroke-Monitoring Study, or SITS-MOST, criteria for IVT were treated by using recombinant tissue plasminogen activator, or rt-PA, at a dose of 0.9 mg per kilogram of body weight within 4.5 hours after stroke onset (28-30).

Zip code allocation was performed to allocate patients to different therapeutic groups (Figure). Because of the specific allocation of stroke care in the Czech Republic, where patients with acute stroke are transferred only to the stroke center or comprehensive stroke center according to the place of residence, we decided to use a zip code allocation.

We used two neighboring regions (catchment area of two comprehensive stroke centers) with similar population (each about 1 000 000 inhabitants) and identical demographic and socioeconomic structures (31,32). Patients were treated at the two centers with similar acuity and quality of care. The cerebral PTA with stent placement was performed at one hospital by one team of interventional radiologists for the preservation of standard procedure.

No further recanalization therapy was performed in all IVT-treated patients (26 patients, 35%) with successful MCA recanalization (Thrombolysis in Brain Ischemia score, 3 or 4; group 1). All patients with IVT failure after 60 minutes with a home zip code CZ-700 00 to CZ-749 00 were treated with cerebral PTA and stents (23 patients, group 2A); no further recanalization therapy was used in all 26 patients after IVT failure with a home zip code CZ-750 00 to CZ-799 00 (group 2B). All patients with proved MCA occlusion with contraindication to IVT within 8.0 hours after ischemic stroke onset and home zip code CZ-700 00 to CZ-749 00 were treated with cerebral PTA and stents (31 subjects, group 3A), whereas all 25 patients with contraindication to IVT and home zip code CZ-750 00 to CZ-799 00 were not treated with any recanalization technique (group 3B).

All patients who underwent cerebral PTA with stent placement received intravenously 500 mg of acetylsalicylic acid at the end of the endovascular procedure. Subsequently, within the next 2 hours, 150 mg of oral clopidogrel, followed by a 6-week dual oral antiplatelet therapy (100-mg acetylsalicylic acid daily plus 75-mg clopidogrel daily) were used as instituted therapy regimen. In patient who did not undergo cerebral PTA with stent placement, anticoagulation therapy (oral, subcutaneous, or intravenous) and oral administration of acetylsalicylic acid or other antiplatelet agents was used as standard treatment 24 hours after stroke onset according to guidelines set by the European Stroke Organization (28,29).

PTA and Stent Placement

Digital subtraction angiography (Innova 4100; GE Healthcare, Waukesha, Wis) was performed by using a Seldinger technique via the femoral or brachial artery under sedation or with general anesthesia. At the start of the procedure, heparin at 50 IU per kilogram of patient's body weight was administered intraarterially. Verification of vessel occlusion was performed in all patients by using four-vessel contrast material-enhanced (Omnipaque; GE Healthcare AS, Oslo, Norway) diagnostic angiography with 4- or 5-F pre-shaped catheters inserted over 0.03-inch hydrophilic wires. The 6-F guiding catheter was introduced subsequently into the target brain-supplying vessel with the same hydrophilic wire and microcatheter and with the support of a 0.014-inch microwire and was advanced past the occluded intracranial vessel segment. The intraluminal position of the microcath-

eter was checked and a search of any periprocedural complications was made. All the catheters were continuously flushed with heparinized saline. The microcatheter was then replaced with a collapsed balloon catheter on a guidewire into the location of occlusion. The balloon was then inflated to a fixed size by using water pressures at 6-20 MPa. After widening of the blood vessel for improved flow, the balloon was deflated and withdrawn. Depending on the location and local anatomic conditions, different stents were inserted at the time of balloon placement to ensure the vessel remained open. The following stents and balloons of various calibers have been used off-label in this study: 25 Enterprise (Cordis Neurovascular, Miami Lakes, Fla), seven Wingspan, 11 Gateway, one Neuroform, five Wallstent (Boston Scientific, San Leandro, Calif), one Multilink, two Acculink (Abbott Vascular, Santa Clara, Calif), and two Zilver (Cook, Bloomington, Ind) devices. Repeated diagnostic angiography of the treated region was performed to assess recanalization grade according to Thrombolysis in Cerebral Ischemia (TICI) criteria (Table 1) (33).

Evaluation of Recanalization

All IVT-treated patients underwent transcranial color-coded duplex US examination at the beginning and at the end of the IVT treatment to detect recanalization or occlusion. TIBI (thrombolysis in brain ischemia) criteria in the IVT-treated patients were used for evaluation of MCA recanalization at the end of IVT (34). Transcranial color-coded duplex US (GE Vivid 7 Pro, GE Medical Systems, Horten Norway, 3S 1.5-3.6-MHz probe at site 1; Philips HD 11, Bothel, Wash, P4-1 probe at site 2) was performed by an experienced sonographer using a 1.5-4-MHz transcranial probe from both temporal bone windows. For patients who underwent cerebral PTA with stent placement, the efficacy of recanalization was evaluated at the end of the procedure by using TICI criteria. Recanalization with TICI grade IIa or IIb was diagnosed as partial and that with TICI grade IIc or III was diagnosed as complete (33). Two experienced, independent, blinded radiologists (T.J., A.K.) evaluated all findings before definitive assessment of the diagnosis was made. Interrater variability of angiographic findings was evaluated. The final diagnosis of recanalization based on TICI criteria was made after agreement of both radiologists. In the case of initial disagreement, both radiologists performed re-evaluation of their findings and, in the case of existing disagreement, assessment of the more experienced radiologist (A.K.) was considered as the final result.

Clinical Evaluation

Neurologic and physical examinations were performed before therapy commencement (IVT, cerebral PTA with stent placement, or acetylsalicylic acid administration) and 24 hours and 90 days after the

Table 1: TICl Criteria

TICl Flow Grade	Characteristic
Grade 0	No perfusion
Grade I	Perfusion past the initial occlusion, but no distal branch filling
Grade IIa	Partial perfusion with incomplete distal filling of < 50% of the expected territory
Grade IIb	Partial perfusion with incomplete distal filling of 50%–99% of the expected territory
Grade IIc	Near complete perfusion but with delay in contrast runoff
Grade III	Full perfusion with normal filling of distal branches in a normal hemodynamic fashion

Table 2: Patient Demographic Data

Variable	Group 1	Group 2A	Group 2B	PValue	Group 3A	Group 3B	PValue
No. of subjects	26	23	26		31	25	
Age (y)*	65.4 ± 12.2	63.2 ± 12.6	67.9 ± 11.6	.187 [†]	62.8 ± 11.2	66.8 ± 13.7	.192 [†]
No. of men	14 (53.8)	13 (56.5)	12 (46.2)	.571 [†]	20 (64.5)	15 (60.0)	.786 [†]
Arterial hypertension	19 (73.1)	17 (73.9)	20 (76.9)	>.99 [†]	25 (80.6)	18 (72.0)	.532 [†]
Diabetes mellitus	5 (19.2)	4 (17.4)	5 (19.2)	>.99 [†]	7 (22.6)	4 (16.0)	.737 [†]
Hyperlipidemia	6 (23.8)	4 (17.4)	6 (23.1)	.731	6 (19.4)	4 (16.0)	>.99 [†]
Atrial fibrillation	9 (34.6)	8 (34.8)	10 (38.5)	>.99 [†]	9 (29.0)	8 (32.0)	>.99 [†]
Smoking	6 (23.8)	6 (26.1)	7 (26.9)	>.99 [†]	3 (9.7)	4 (16.0)	.688 [†]
Heavy alcohol consumption	2 (7.7)	1 (4.3)	1 (3.8)	>.99 [†]	2 (6.5)	1 (4.0)	>.99 [†]
ICA occlusion/stenosis > 50%	5 (19.2)	4 (17.4)	5 (19.2)	>.99 [†]	6 (19.4)	5 (20.0)	>.99 [†]
Left hemisphere	12 (46.2)	14 (60.9)	15 (57.7)	>.99 [†]	15 (48.4)	14 (56.0)	.602 [†]
Medical history of acetylsalicylic acid	9 (34.6)	8 (34.8)	9 (34.6)	>.99 [†]	13 (41.9)	10 (40.0)	>.99 [†]

start of therapy. A certified neurologist performed the evaluation of neurologic symptoms using NIHSS in all visits. A modified Rankin Scale (mRS) was used for evaluation of disability at 90 days. Favorable clinical outcome was defined as mRS score 0-2 3 months after stroke onset.

All adverse events were recorded. All changes in physical examination, worsening of neurologic symptoms (≥ 4 points with NIHSS), and all disorders prolonging or requiring hospitalization were recorded as adverse events.

Intracranial bleeding detected in the brain of control subjects at CT or MR examination 24 hours after therapy onset was recorded. Intracranial bleeding with worsening of neurologic symptoms (≥ 4 points according to NIHSS) was evaluated as a symptomatic intracranial hemorrhage (8); other intracranial bleedings were evaluated as asymptomatic intracranial hemorrhage.

Statistical Analysis

Kolmogorov-Smirnov and Shapiro-Wilk tests of normality were used for testing the fit of the parameters calculated to a normal distribution. Data with a normal distribution are reported as means \pm standard deviation. All parameters not fitting to a normal distribution are presented as median and interquartile range. Two-sided Mann-Whitney U test, independent samples t test, Fisher exact test, and multivariate logistic regression analysis were used for statistical evaluation. The univariate analysis was used for testing recanalization in patients treated with cerebral PTA and stents (groups 2A and 3A) for the prediction

of good clinical outcome and also the following variables: age, sex, presence of diabetes mellitus, arterial hypertension, hyperlipidemia, atrial fibrillation, smoking, serum level of glucose and blood pressure at admission, prior use of statins and antiplatelets, onset-to-treatment interval and baseline NIHSS score, and MCA recanalization. Multivariable logistic regression analysis with backward selection procedure was performed on the basis of variables with univariate P values of less than .05. The Cohen κ statistic was applied to assess correlation between the two radiologists with regard to artery recanalization evaluation using TICl criteria. Statistical analyses were performed with SPSS 14.0 software (SPSS, Chicago, Ill). Statistical significance was defined as a P value of less than .05.

RESULTS

A total of 131 patients (74 men and 57 women; mean age, 65.8 years \pm 12.2; range, 25-86 years) with acute ischemic stroke due to MCA main stem occlusion were enrolled. Seventy-five patients fulfilling the criteria underwent IVT within 4.5 hours after ischemic stroke onset. Table 2 lists patient demographic data. NIHSS scores at admission did not differ significantly among groups. Median NIHSS score was 13.5 in IVT-treated patients with successful MCA recanalization, 16.0 in patients with IVT failure and treatment with cerebral PTA and stents, 15.5 in patients with IVT failure and no further recanalization.

Table 3: Clinical Results in Particular Subgroups

Variable	Group 1	Group 2A	Group 2B	PValue	Group 3A	Group 3B	PValue
Baseline NIHSS score*	13.5 (6–22)	16 (11–19)	15.5 (12–18)	.651 [†]	15 (10–22.5)	16 (15–19)	.192 [†]
NIHSS score at day 7*	4 (1–14)	9 (4–27)	14.5 (7–21)	.191 [†]	6 (2–18)	16 (14–19)	.019 [†]
90-day mRS score*	2 (1–4)	3 (2–5)	5 (3–5.5)	.053 [†]	3 (1–5)	5 (4–6)	.039 [†]
mRS score of 0–3 at day 90	17 (65.3)	12 (52.2)	7 (26.9)	.073 [†]	16 (51.6)	3 (12.0)	.002 [†]
mRS score of 0–2 at day 90	15 (57.7)	10 (43.5)	4 (15.4)	.034 [†]	14 (45.2)	2 (8.0)	.004 [†]
SICH	1 (3.8)	1 (4.3)	1 (3.8)	>.99 [†]	1 (3.2)	1 (4.0)	>.99 [†]
Malignant infarction	3 (11.5)	3 (13.0)	3 (11.5)	>.99 [†]	5 (16.1)	2 (8.0)	.443 [†]
7-day Mortality	3 (11.5)	3 (13.0)	3 (11.5)	>.99 [†]	5 (16.1)	3 (12.0)	.720 [†]
3-month Mortality	5 (21.7)	6 (26.1)	6 (23.1)	>.99 [†]	9 (29.0)	7 (28.0)	>.99 [†]

Table 4: Procedural Data and Recanalization Rate in the Particular Groups

Variable	Group 1	Group 2A	Group 2B	Group 3A	PValue
Time to IVT (min)*	142.4 ± 28.4	140.8 ± 33.5	146.9 ± 30.5	Not applicable	.516 [†]
Time to cerebral PTA with stents (min)*	Not applicable	249.5 ± 57.5	Not applicable	274.8 ± 111.5	.291 [†]
Length of procedure (min)*	Not applicable	47.0 ± 13.1	Not applicable	65.0 ± 25.0	.001 [†]
Complete MCA recanalization (TICI IIc–III)	Not applicable	9 (39.1)	Not applicable	12 (38.7)	>.99 [†]
Partial MCA recanalization (TICI IIa–IIb)	Not applicable	12 (52.2)	Not applicable	17 (54.8)	>.99 [†]
No recanalization (TICI 0–I)	Not applicable	2 (8.7)	Not applicable	2 (6.5)	>.99 [†]

Table 5: Results of Univariate Analysis of Baseline Variables for the Prediction of Good Functional Outcome (mRS score 0-2)

Variable	mRS Score 0–2)	mRS Score 3–6	PValue
No. of subjects	28	26	
Mean age (y)*	60.2 ± 17.3	65.6 ± 11.2	.178 [†]
No. of men	17 (60.7)	16 (61.5)	>.99 [†]
Diabetes mellitus	6 (21.4)	5 (19.2)	>.99 [†]
Arterial hypertension	21 (75.0)	21 (80.8)	.747 [†]
Hyperlipidemia	5 (17.9)	5 (19.2)	>.99 [†]
Atrial fibrillation	9 (32.1)	8 (30.8)	>.99 [†]
Active smoking	5 (17.9)	4 (15.4)	>.99 [†]
Admission systolic blood pressure (mmHg)*	153 ± 25	158 ± 27	.481 [†]
Admission diastolic blood pressure (mmHg)*	88 ± 12	93 ± 12	.158 [†]
Prior use of antiplatelet therapy	12 (42.9)	10 (38.5)	.787 [†]
Prior use of statins	7 (25.0)	2 (7.7)	.144 [†]
Stroke onset-to-treatment interval (min)*	88 ± 12	93 ± 12	.158 [†]
Admission serum level of glucose (mmol/l) [§]	5.8 (5.0–7.7)	7.4 (5.6–10.2)	.034 [#]
Baseline NIHSS score [§]	12 (8–17)	18 (14–21)	.004 [#]
MCA recanalization	16 (57.1)	5 (19.2)	.006 [†]

on therapy, 15.0 in patients with contraindication to IVT and treatment with cerebral PTA and stents, and 16.0 in patients with contraindication to IVT and no recanalization technique ($P > .05$). General anesthesia was used in 14 (25.9%) patients who underwent cerebral PTA with stent placement. Symptomatic intracerebral hemorrhage (SICH) occurred in one of 26 (3.8%) IVT-treated patients with successful MCA recanalization, one of 23 (4.3%) patients with IVT failure and treatment with cerebral PTA and stents,

one of 26 (3.8%) patients with IVT failure and no further recanalization therapy, one of 31 (3.2%) patients with contraindication to IVT and treatment with cerebral PTA and stents, and one of 25 (4.0%) patients with contraindication to IVT and no recanalization technique ($P > .05$, Table 3). Periprocedural complications occurred in one patient (4.3%) treated with cerebral PTA and stents after IVT failure and in one patient (3.2%) with contraindication to IVT and treatment with cerebral PTA and stents.

After cerebral PTA with stent placement, partial MCA recanalization was achieved in 29 (53.7%) patients and complete recanalization was achieved in 21 (38.9%) patients. Findings of recanalization at the end of cerebral PTA with stent placement in patients with IVT failure (group 2A) and in patients with contraindication to IVT (group 3A), as well as the time to onset of therapy (IVT, cerebral PTA with stent placement) and the length of cerebral PTA with stent placement procedure are presented in Table 4. When the Enterprise, Gateway, and the rest of endovascular devices were compared, MCA recanalization was achieved in 24 of 25 (96.0%), 11 of 11 (100%), and 15 of 18 (83.3%) devices, respectively, and, the median 90-day mRS score was 3, 3, and 4, respectively.

The interobserver agreement for the diagnosis of artery occlusion location was good ($\kappa = 0.635$, $P < .001$), with a full agreement in 73%, but interobserver agreement for arterial recanalization was poor ($\kappa = 0.277$, $P < .001$), with full agreement in only 44% of patients. However, a difference of more than three subpoints occurred in zero patients, and a two-subpoint difference occurred in only two patients.

Favorable 3-month clinical outcomes were achieved in 15 of 26 (57.7%) IVT-treated patients with recanalization within 60 minutes after IVT failure. Clinical outcomes were significantly better in patients treated with cerebral PTA and stents after IVT failure (group 2A) than in control subjects (group 2B), with favorable clinical outcome in 10 of 23 (43.5%) patients in group 2A and only four of 26 (15.4%) patients in group 2B ($P = .03$, Table 3). Also, clinical outcomes were significantly better in patients with contraindication to IVT who were treated with cerebral PTA and stents (group 3A) than in control subjects (group 3B), with favorable clinical outcome in 14 of 31 (45.2%) patients in group 3A and two of 25 (8.0%) patients in group 3B ($P = .004$). The favorable 3-month clinical outcome difference was not statistically significant between patients treated with IVT only (groups 1 and 2B) and those treated with cerebral PTA and stents only (group 3A) (36.5% vs 45.2%, $P > .05$). Seven-day mortality and 3-month mortality were not significantly different in the particular groups (Table 3). Results of univariate analysis of baseline variables for the prediction of good functional outcome are presented in Table 5. Baseline NIHSS score (odds ratio, 0.854; 95% confidence interval: 0.751, 0.971; $P = .004$) was identified as independent negative predictor and complete MCA recanalization (odds ratio, 5.550; 95% confidence interval: 1.477, 20.851; $P = .006$) was identified as independent positive predictor of good functional outcome at multivariate logistic regression analysis.

DISCUSSION

In this prospective, controlled trial we demonstrated that, compared with no further therapy, patients with MCA occlusion who either failed or with contraindication to IVT who undergo revascularization by using intracranial stents achieve superior outcomes. These promising clinical outcomes were seen in the setting of remarkably high rates of recanalization with use of such stents. Notably, we further demonstrated the safety of cerebral PTA with stent placement, with low incidence of SICH, periprocedural complications, and malignant infarction. These findings indicate that patients who do not respond to or have a contraindication to IVT should be offered local revascularization therapy.

The angiographic results of this study are superior to those of prior studies in which the Merci Retriever (Concentric Medical, Mountain View, Calif) was used. In the Multi MERCI study, partial or complete recanalization was achieved in only 55% of patients, with 9.8% of SICH and 5.5% of periprocedural complications. Independency (mRS score 0-2) was achieved in 36.0% of patients (9). The study with Penumbra system reported a higher recanalization rate than studies with Merci Retriever, and the recanalization rate with Penumbra system was comparable with results of the presented study. Partial recanalization was achieved in 54% of patients and complete recanalization was achieved in 33% of patients, with 5.7% of periprocedural complications and 11.2% of SICH. Nevertheless, a 90-day mRS score of 0-2 was reported in only 25% of patients (10).

Fitzsimmons et al (19) reported one of the first cases of cerebral revascularization with the deployment of a self-expansible stent in 2006. Most of the studies published to date have been retrospective single-center reports, with sample sizes ranging between nine and 20 patients (20-24). In these studies, the recanalization rate ranged between 60% and 100% (17,18,20,21,23,25), and good clinical outcome (mRS score 0-2 or NIHSS score ≤ 4) was reported between 36% and 74% (17,25). The recently reported preliminary data of a prospective stent-assisted recanalization in acute ischemic stroke, or SARIS, study of the first 20 acute stroke patients showed successful recanalization (Thrombolysis in Myocardial Infarction grade 2 or 3) in 100% of cases, with a 5% rate of SICH (26). The highest recanalization rates were achieved with the use of self-expanding retrievable Solitaire stents (eV3, Paris, France). In recent studies, partial or complete recanalization of brain artery was achieved in 84%-91% of patients, with 2%-10% of SICH and less than 9% of periprocedural complications (11-14). These results are similar to those achieved in 92.6% of patients with partial or complete recanalization of brain artery.

Several limitations of the study should be mentioned. This was a bicenter case-control study with the main goal to assess the safety and recanalization

rate of cerebral PTA with stent placement. Although the criteria for SICH evaluation are well defined, the evaluation of brain artery recanalization is still very subjective; however, in this study, blinded radiologists evaluated the vascular status. The open-label design of the study with only blinded evaluation of recanalization by using the TIC1 scale cannot prevent bias in clinical evaluation of dependency (mRS) after 3 months. The use of zip code to allocate patients to different therapeutic groups could also cause bias. Finally, the different time window between patients treated with IVT and cerebral PTA with stent placement prevents direct comparison of the two treatments.

Cerebral PTA with stent placement seems to be a safe endovascular therapeutic method for patients with acute ischemic stroke and might be effective both in patients with MCA occlusion after IVT failure and in patients with contraindication to IVT. Nevertheless, the safety and efficacy of cerebral PTA with stent placement, as endovascular method, needs to be compared directly with IVT and/or other conservative treatment within the same time window by a prospective randomized trial. Furthermore, studies comparing the safety and efficacy of self-expandable stents with self-expanding retrievable stents not requiring the use of dual antiplatelet therapy should be also performed in the future.

REFERENCES

- van der Worp HB, van Gijn J. Clinical practice: acute ischemic stroke. *N Engl J Med* 2007;357(6):572-579.
- Tissue plasminogen activator for acute ischemic stroke. The National Institute of Neurological Disorders and Stroke rt-PA Stroke Study Group. *N Engl J Med* 1995;333(24):1581-1587.
- Smith WS, Sung G, Starkman S, et al. Safety and efficacy of mechanical embolectomy in acute ischemic stroke: results of the MERCI trial. *Stroke* 2005;36(7):1432-1438.
- Kerber CW, Barr JD, Berger RM, Chopko BW. Snare retrieval of intracranial thrombus in patients with acute stroke. *J Vasc Interv Radiol* 2002;13(12):1269-1274.
- Kassem-Moussa H, Graffagnino C. Nonocclusion and spontaneous recanalization rates in acute ischemic stroke: a review of cerebral angiography studies. *Arch Neurol* 2002;59(12):1870-1873.
- Molina CA, Saver JL. Extending reperfusion therapy for acute ischemic stroke: emerging pharmacological, mechanical, and imaging strategies. *Stroke* 2005;36(10):2311-2320.
- Zangerle A, Kiechl S, Spiegel M, et al. Recanalization after thrombolysis in stroke patients: predictors and prognostic implications. *Neurology* 2007;68(1):39-44.
- Hacke W, Kaste M, Bluhmki E, et al. Thrombolysis with alteplase 3 to 4.5 hours after acute ischemic stroke. *N Engl J Med* 2008;359(13):1317-1329.
- Smith WS, Sung G, Saver J, et al. Mechanical thrombectomy for acute ischemic stroke: final results of the Multi MERCI trial. *Stroke* 2008;39(4):1205-1212.
- Tarr R, Hsu D, Kulcsar Z, et al. The POST trial: initial post-market experience of the Penumbra system—revascularization of large vessel occlusion in acute ischemic stroke in the United States and Europe. *J Neurointerv Surg* 2010;2(4):341-344.
- Machi P, Costalat V, Lobotesis K, et al. Solitaire FR thrombectomy system: immediate results in 56 consecutive acute ischemic stroke patients. *J Neurointerv Surg* 2012;4(1):62-66.
- Stampfl S, Hartmann M, Ringleb PA, Haehnel S, Bendszus M, Rohde S. Stent placement for flow restoration in acute ischemic stroke: a single-center experience with the Solitaire stent system. *AJNR Am J Neuroradiol* 2011;32(7):1245-1248.
- Castañó C, Dorado L, Guerrero C, et al. Mechanical thrombectomy with the Solitaire AB device in large artery occlusions of the anterior circulation: a pilot study. *Stroke* 2010;41(8):1836-1840.
- Roth C, Papanagiotou P, Behnke S, et al. Stent-assisted mechanical recanalization for treatment of acute intracerebral artery occlusions. *Stroke* 2010;41(11):2559-2567.
- Alexandrov AV, Demchuk AM, Burgin WS, Robinson DJ, Grotta JC; CLOTBUST Investigators. Ultrasound-enhanced thrombolysis for acute ischemic stroke: phase I—findings of the CLOTBUST trial. *J Neuroimaging* 2004;14(2):113-117.
- Skoloudik D, Bar M, Skoda O, et al. Safety and efficacy of the sonographic acceleration of the middle cerebral artery recanalization: results of the pilot thrombotripsy study. *Ultrasound Med Biol* 2008;34(11):1775-1782.
- Qureshi AI, Siddiqui AM, Suri MF, et al. Aggressive mechanical clot disruption and low-dose intra-arterial third-generation thrombolytic agent for ischemic stroke: a prospective study. *Neurosurgery* 2002;51(5):1319-1327; discussion 1327-1329.
- Levy EI, Mehta R, Gupta R, et al. Self-expanding stents for recanalization of acute cerebrovascular occlusions. *AJNR Am J Neuroradiol* 2007;28(5):816-822.
- Fitzsimmons BF, Becske T, Nelson PK. Rapid stent-supported revascularization in acute ischemic stroke. *AJNR Am J Neuroradiol* 2006;27(5):1132-1134.
- Breckenfeld C, Schroth G, Mattle HP, et al. Stent placement in acute cerebral artery occlusion: use of a self-expandable intracranial stent for acute stroke treatment. *Stroke* 2009;40(3):847-852.
- Mocco J, Hanel RA, Sharma J, et al. Use of a vascular reconstruction device to salvage acute ischemic occlusions refractory to traditional endovascular recanalization methods. *J Neurosurg* 2010;112(3):557-562.
- Suh SH, Kim BM, Roh HG, et al. Self-expanding stent for recanalization of acute embolic or dissecting intracranial artery occlusion. *AJNR Am J Neuroradiol* 2010;31(3):459-463.
- Linfante I, Samaniego EA, Geisbüscher P, Dabus G. Self-expandable stents in the treatment of acute ischemic stroke refractory to current thrombectomy devices. *Stroke* 2011;42(9):2636-2638.
- Zaidat OO, Wolfe T, Hussain SI, et al. Interventional acute ischemic stroke therapy with intracranial self-expanding stent. *Stroke* 2008;39(8):2392-2395.
- Nakano S, Iseda T, Yoneyama T, Kawano H, Wakisaka S. Direct percutaneous transluminal angioplasty for acute middle cerebral artery trunk occlusion: an alternative option to intra-arterial thrombolysis. *Stroke* 2002;33(12):2872-2876.
- Levy EI, Siddiqui AH, Cruemlich A, et al. First Food and Drug Administration-approved prospective trial of primary intracranial stenting for acute stroke: SARIS (stent-assisted recanalization in acute ischemic stroke). *Stroke* 2009;40(11):3552-3556.
- Demchuk AM, Burgin WS, Christou I, et al. Thrombolysis in brain ischemia (TIBI) transcranial Doppler flow grades predict clinical severity, early recovery, and mortality in patients treated with intravenous tissue plasminogen activator. *Stroke* 2001;32(1):89-93.
- European Stroke Organisation (ESO) Executive Committee; ESO Writing Committee. Guidelines for management of ischemic stroke and transient ischaemic attack 2008. *Cerebrovasc Dis* 2008;25(5):457-507.
- The European Stroke Organisation (ESO) Executive Committee and the ESO Writing Committee 2008, Update Guidelines January 2009 New Elements. ESO guideline update. http://www.eso-stroke.org/pdf/ESO_Extended_Thrombolysis_KSU.pdf. Published January 29, 2009. Accessed February 3, 2012.
- Toni D, Lorenzano S, Puca E, Principe M. The SITS-MOST registry. *Neurol Sci* 2006;27(Suppl 3):S260-S262.

31. Krajska sprava CSU v Ostrave. Statisticka rocenka Moravsko-slezskeho kraje 2011. Cesky statisticky urad. <http://www.czso.cz/csu/2011edicniplan.nsf/krajp/711302-11-xm>. Published December 30, 2011. Accessed August 1, 2012.
32. Krajska sprava CSU v Olomouci. Statisticky bulletin - Olomoucky kraj 1. az 4. ctvrtleti 2011. Cesky statisticky urad. <http://www.czso.cz/csu/2011edicniplan.nsf/krajp/711302-11-xm>. Published April 4, 2012. Accessed August 1, 2012.
33. Noser EA, Shaltoni HM, Hall CE, et al. Aggressive mechanical clot disruption: a safe adjunct to thrombolytic therapy in acute stroke? *Stroke* 2005;36(2):292-296.
34. Tomsick T. TIMI, TIBI, TICl: I came, I saw, I got confused. *AJNR Am J Neuroradiol* 2007;28(2):382-384.

MYELOMA STEM CELL CONCEPTS, HETEROGENEITY AND PLASTICITY OF MULTIPLE MYELOMA

Roman Hajek^{1,2,3,4}, Samuel A. Okubote¹ and Hana Svachova¹

¹ Babak Myeloma Group, Department of Pathological Physiology, Faculty of Medicine, Masaryk University, Brno, Czech Republic

² Department of Haemato-oncology, University Hospital Ostrava, Ostrava, Czech Republic

³ Department of Clinical Haematology, University Hospital Brno, Brno, Czech Republic

⁴ Faculty of Medicine, University of Ostrava, Ostrava, Czech Republic

Originally published in British journal of haematology 2013; 163(5): 551-564

Consent to the publication of 7th April 2014

SUMMARY

Multiple myeloma (MM) is a hematological malignancy characterized by accumulation of clonal plasma cells (PCs) in the bone marrow (BM). Although novel therapeutic strategies have prolonged survival of patients, the disease remains difficult to treat with a high risk of relapse. A failure of therapy is supposed to be associated with a persistent population of the so-called MM stem cells or myeloma initiating cells (MIC) that exhibit tumor-initiating potential, self-renewal and resistance to chemotherapy. However, the population responsible for the origin and sustainability of tumor mass has not been clearly characterized so far. This review summarizes current myeloma stem cell concepts and suggests that high phenotypic and intra-clonal heterogeneity together with plasticity potential of MM might be other contributing factors explaining discrepancies among particular concepts and contributing to the treatment failure.

Keywords

myeloma stem cells, malignant plasma cells, multiple myeloma, plasticity, precursor B cells.

INTRODUCTION

Modern molecular and cytogenetic approaches have progressed further to help in our understanding of multiple myeloma (MM) biology and have led to the development of targeted therapy that has improved management of this incurable disease. Despite therapeutic advances, MM is still accompanied by the threat of repeated relapses with a fatal ending. These observations indicate inefficient drug targeting of some MM cells. The existence of such persistent population, called myeloma stem cells or myeloma-initiating cells (MIC), has been suspected for more than two decades. However, the cells of origin remain elusive (Hamburger and Salmon, 1977; Bergsagel and Valeriotte, 1968; Park et al, 1971; Matsui et al, 2004; Yaccoby and Epstein, 1999). The timeline of increasing knowledge about putative

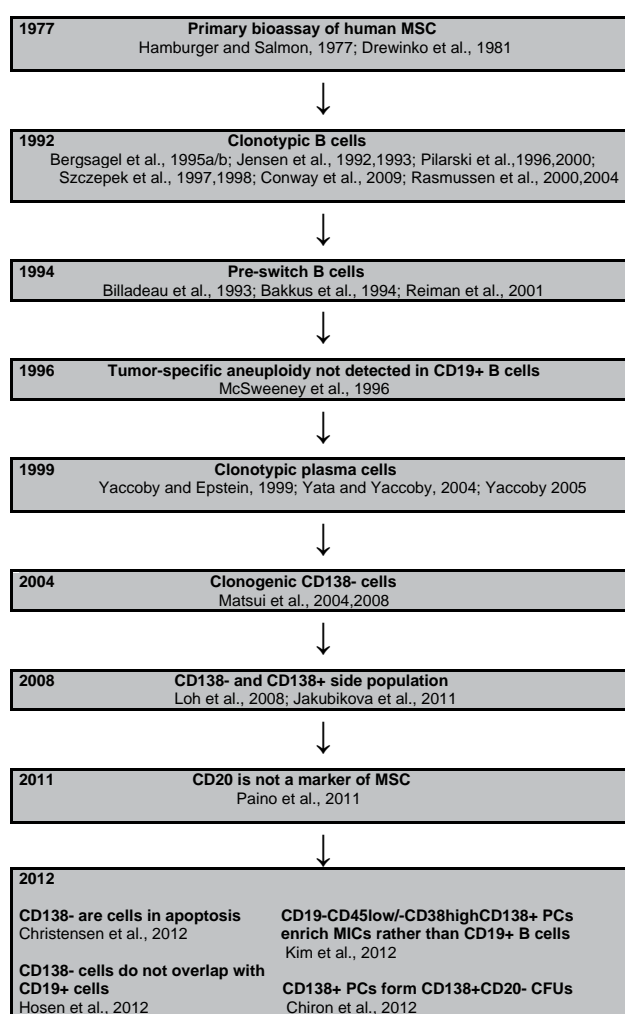


Figure 1: Timeline of myeloma stem cell concepts

An illustrative figure of several studies depicting different suspected cell population responsible for the maintenance and sustainability of MM.

MM stem cells is illustrated in Fig. 1. Discrepancies among MM stem cell concepts have arisen in parallel with high phenotypic and intra-clonal heterogeneity of clonal PCs, which might be another factor contributing to the failure of therapies and identification

of the population responsible for relapse. Myeloma PCs strongly depend on the supportive role of the bone marrow (BM) microenvironment (MEV), which is a source of essential growth factors and supports survival and dissemination of pathological PCs (Rajkumar et al, 2000; Rajkumar et al, 2002). Furthermore, hypoxic conditions of the tumor microenvironment enhance tumor progression by inducing angiogenesis, maintaining malignant phenotype and stimulating osteoclastogenesis (Colla et al, 2010). There is growing evidence suggesting that signals from pathological microenvironments can (reversibly) alter the phenotype of PCs. Such plasticity of PCs might result in obvious heterogeneity of MM and generate inconsistencies among MM stem cell concepts.

MYELOMA STEM CELL CONCEPTS

A number of laboratories have tried to identify a biologically distinct population of the so-called MM stem cells, responsible for the incurability of MM (Table I). The population responsible for the origin and sustainability of tumor mass has been suspected in the minor population of clonotypic or clonogenic CD138- cells retaining key stem cell properties, tumor-initiating potential, self-renewal and resistance to chemotherapy (Matsui et al, 2004; Bergsagel et al, 1995a; Bergsagel et al, 1995b; Szczepek et al, 1997; Jensen et al, 1993; Pilarsky et al, 2000; Rasmussen et al, 2000). However, even the dominant population of human CD138+ PCs was demonstrated to contain clonogenic cells; these cells show plasticity potential that might be responsible for the differentiation and acquirement of stem cell properties (Yaccoby, 2005; Yata and Yaccoby, 2004; Chiron et al, 2012; Kim et al, 2012).

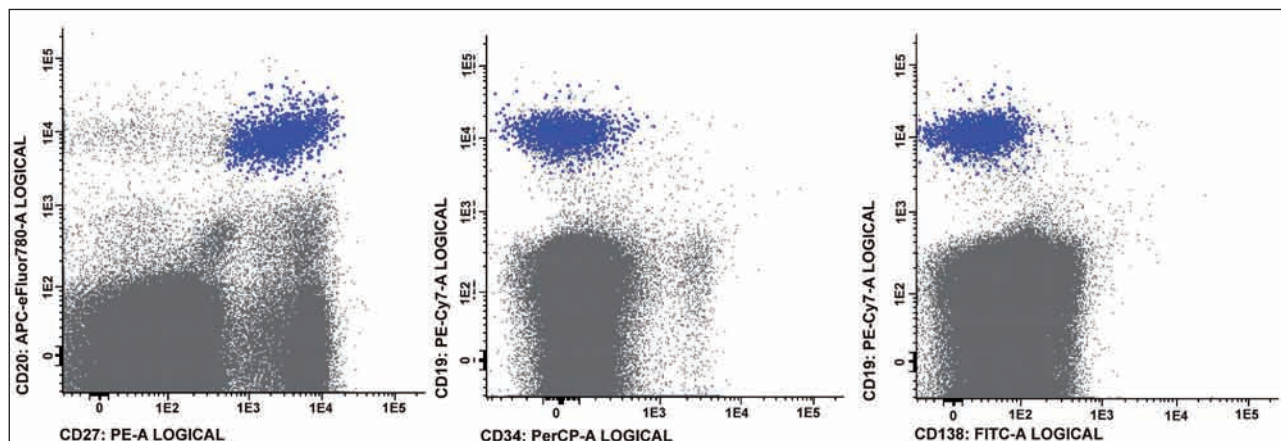
Table I: Candidates for putative neoplastic plasma cell precursors or myeloma stem cell

	Characteristics of the cells	Citation
Clonotypic B cells	PB CD19, CD38, CD10, CD11b, CD34 (HPCA-1), variable CD20, PCA-1, CD45RO, variable CD45, and CD56	Bergsagel et al (1995a); Bergsagel et al (1995b); Szczepek et al (1997); Jensen et al (1993); Pilarsky et al (2000); Pilarski et al (1996); Szczepek et al (1998); Pilarski and Jensen (1992); Jensen et al (1992)
	PB CD34±, CD38+, CD184+, CD31±, CD50±, CD138-, CD19-, CD20-	(Conway, et al 2009)
	PB CD19+CD27+CD38- memory B-like cells	Rasmussen et al (2000)
Clonotypic pre-switch B cells	pre-switch somatic hypermutated clonotypic cells (VDJ sequence still joined to Cμ gene)	Billadeau et al (1993); Bakkus et al (1994); Reiman et al (2001)
	PB and BM CD19, HLA class II or surface IgM	
Clonogenic CD138- cells	BM CD20+CD27+CD34-CD138- clonogenic myeloma stem cells	Matsui et al (2004); Matsui et al (2008); Peacock et al (2007); Huff and Matsui (2008)
Side population	Ability to exclude dyes sideways from the diagonal in FACS analysis plots	(Jakubikova, et al 2011, Loh, et al 2008)
	CD138- and CD138+	
Clonogenic plasma cells	BM CD38+CD45- PC (SCID-hu model)	(Yaccoby and Epstein 1999, Yaccoby, et al 2008, Yata and Yaccoby 2004)
	BM clonogenic CD38+CD138-CD45- PC (SCID-rab model)	
	BM CD38+CD138-CD45-CD19-CD34- PC (osteoclast co-culture)	(Yaccoby 2005)
	CD19-CD45low/-CD38high/CD138+ PCs	(Kim, et al 2012)
Intermediate PC precursors	CD138+CD44+ give rise to short-lived PC	(Munshi, et al 2011, O'Connor, et al 2002)
	CD138+CD44-/CD138-CD44+ give rise to long-lived PC in murine model	
	candidates for normal counterpart of transformed MM cells	

BM, bone marrow; FACS, fluorescent activated cell sorting; PB, peripheral blood; PC, plasma cell; HLA, human leucocyte antigen; HPCA, human progenitor cell antigen; SCID, severe combined immunodeficiency; VDJ, variable diverse joining.

Figure 2: Isotype switched and isotype unswitched memory B cells

An illustrative figure of putative multiple myeloma precursors; violet population - bone marrow isotype switched memory B cells, pink population - bone marrow isotype unswitched memory B cells.

**Clonotypic B cells**

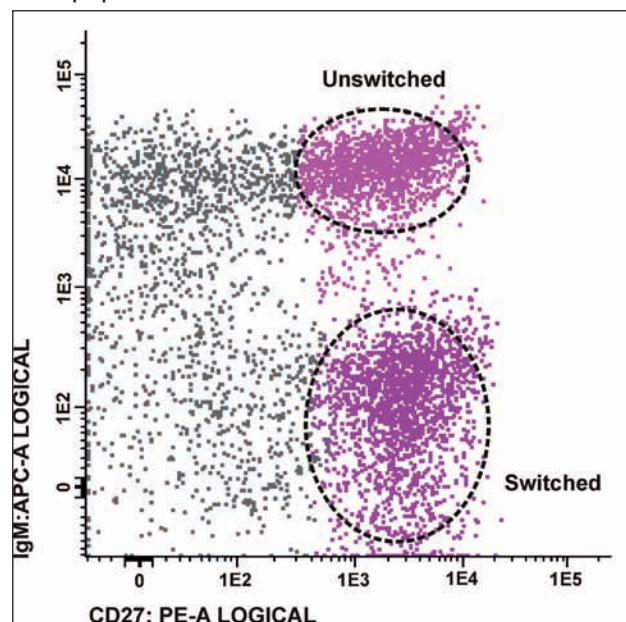
Myeloma precursors that share identical variable diversity joining (VDJ) regions, rearrangements of immunoglobulin heavy chain gene (IGH) with patient's tumor PCs and show a pre-plasma cell phenotype are referred to as clonotypic B cells (CBL) (Pilarski et al, 1996). They have been identified in peripheral blood (PB), lymph nodes and BM (Szczepek et al, 1998; Billadeau et al, 1993; Rasmussen et al, 2004). An extensive accumulation of somatic mutations in IGH gene and an absence of intraclonal variation suggest that CBLs originate from post-germinal center B cells (Bakkus et al, 1994). Additionally, phenotypic profile and amount of CBLs vary among studies - e.g., it is not clear if these cells resemble CD19+CD27+CD38- memory B-cells (Rasmussen et al., 2000; 2004) or carry a marker of hematopoietic stem cells, CD34 with or without the expression of CD19 surface marker (Szczepek et al, 1997; Pilarski et al, 2000; Conway et al, 2009). Furthermore, McSweeney et al. (1996) did not find BM CD19+ cells to be clonally restricted to kappa/lambda or revealed any deviations of expression patterns of B-cell maturation markers from normal B-cell components (McSweeney et al, 1996). These results do not support a hypothesis of disturbed B-cell maturation and the development of the disease from early stages of B-cell ontogeny. Moreover, DNA analysis proved that CD38++CD19- cells were mostly aneuploid, with a typical cell cycle profile indicating the presence of a proliferating population, while cells expressing CD19 were diploid. This suggests the existence of self-replicating PC compartments that have the capacity to replenish the tumor without the involvement of early B lymphocyte progenitors.

A number of studies that confirmed the presence of clonotypic B cells have been based mainly on the detection of the same IGH rearrangements by PCR-based methods. The percentage of MM patients with IGH-positive clonotypic B-cells ranged from 40% and 87% (Billadeau et al, 1993; Taylor et al, 2008). Limited dilution PCR assays detected the abundance of

CBLs in 0.24% - 25% of peripheral blood mononuclear cells (PBMC) and 66% of all peripheral B cells (Szczepek et al, 1998; Billadeau et al, 1993; Taylor et al, 2008; Trepel et al, 2012). This wide range of occurrence may result from methodological errors of the PCR technique or expression of atypical, non-clinical Ig transcripts (Trepel et al, 2012). Additionally, the presence of the same IGH rearrangements is a reliable marker of clonality but it does not confirm the malignancy of cells per se. Therefore, the detection of IGH rearrangements in CD19+ cells could indicate that a small clone of premalignant or premyelomatous B cells persists despite the transformation of other cells into malignant clones; however, this population does not actively contribute to myeloma clones (McSweeney et al, 1996). Rasmussen et al.

Figure 3: Clonogenic CD138- cells

An illustrative figure of putative multiple myeloma stem cells, bone marrow CD20+CD27+CD34-CD138-; blue population.



(2010) suggested that PB memory B cells represent pre-malignant, partially transformed remnants that might possess some proliferative advantage over normal memory B cells. They questioned the involvement of CBLs in MM maintenance based on the fact that these cells expressed specific 'early' oncogenes (FGFR3, WHSC1, CCND1) that were deregulated by an IGH translocation but lacked 'late' oncogene (KRAS) mutations.

A large interpatient and interstudy variability led Trepel et al. (2012) to establish patient-individual ligands mimicking the epitope recognized by the myeloma immunoglobulin to specifically target clonotypic surface IGH-positive B cells of MM patients. A new flow cytometric protocol detected clonotypic B cells only in one patient with a sensitivity of 10⁻³, i.e., less than one clonotypic B cell per 1000 PBMCs. These cells accounted for about 0.15% of PBMCs and 5% of B cells. Surprising discrepancies between PCR and flowcytometric approaches could indicate non-specific annealing of the CDR3-primer leading to false positive PCR results. This study suggests that the abundance of CBLs has been enormously overestimated in previous studies. Similarly to Rasmussen et al. (2010), authors consider that CBLs do not represent an essential prerequisite for myeloma maintenance and progression.

Clonotypic pre-switch B cells

An identical rearrangement of the IGH VDJ region with a consistent pattern of hypermutations within the clone is a signature of CBLs. Clonal PCs generally express monoclonal Igs of these isotypes: IgG, IgA, IgD, IgM; in rare cases, they express kappa or lambda light chains or they do not secrete Igs (non-secretory MM) (Basak and Carrier, 2010). However, clonotypic IGHV gene sequences and patterns of hypermutations linked to different classes of Ig heavy-chain constant region genes (including IGHM gene), have been identified in some MM patients and called pre-switch (IgM+) clonotypic B cells (Fig. 2) (Billadeau et al, 1993; Bakkus et al, 1994; Reiman et al, 2001; Corradini et al, 1993). Particular classes of Ig are generated by the mechanism of class switch recombination (CSR), resulting in the formation of a hybrid switch region composed of switch region S_μ and a respective isotype switch region (C_δ, C_{γ3}, C_{γ1}, C_{α1}, C_{γ2}, C_{γ4}, C_ε and C_{α2}) (Bergsagel et al, 1996). The presence of CSR is a hallmark of "post-switch" B cells. However, pre-switch B cells do not seem to undergo CSR because IGH transcript is composed of the clonotypic VDJ sequence, which is still joined to C_μ gene (Corradini et al, 1993).

Pre-switch (IgM+) CBLs have been identified at low frequency in BM and PB of most MM patients (Billadeau et al., 1993; Bakkus et al, 1994). Reiman et al. (2001) described the presence of clinical and nonclinical clonotypic isotypes in PB, BM and G-CSF - mobilized blood autografts of MM patients. Expre-

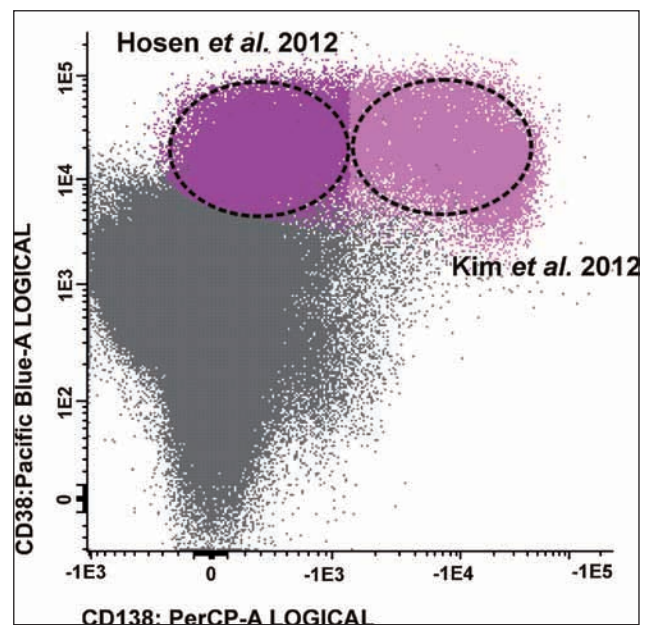
ssion of pre-switch clonotypic transcripts persisted in the blood despite high-dose chemotherapy with stem cell support, suggesting drug resistance of this pre-switch population. The persistence of pre-switch clonotypic isotypes was associated with reduced survival and with a more advanced disease at diagnosis. Moreover, both pre-switched and post-switched cells were able to engraft in non-obese diabetic/severe combined immunodeficiency (NOD/SCID) mice, indicating their potential clinical relevance. However, Taylor et al. (2008) questioned the role of pre-switch (IgM+) clonotypic cells as a progenitor pool for post-switch MM-PCs. Results of specific clonotypic-switch PCR determined the presence of a single, unchanged clonotypic switch junction, and not multiple clonotypic switch junctions. Thus, post-switch MM-PCs most likely originate from a single CSR event, and pre-switch IgM+ cells do not represent MM-PC progenitors.

Clonogenic CD138- cells

Matsui et al. (2004) suggested that the source of MM stem cells might be a minor population of less differentiated cells reminiscent of memory B-lymphocytes with surface markers CD20+CD27+CD34-CD138- (Fig. 3). Results of his study showed that CD138-/CD34- cells derived from MM cell lines RPMI 8226, NCI-H929 and primary clinical samples were clonogenic in vitro. Clonogenic efficiency correlated with disease stage. Clonogenic potential of CD138-/CD34- cells was evaluated by a successful engraftment of NOD/SCID mice during primary and secondary transplan-

Figure 4: Hosen's clonogenic CD138- cells and Kim's clonogenic CD138+ cells

An illustrative figure of bone marrow CD19-CD45-CD38++CD138- cells, violet population (Hosen' et al., 2012); and bone marrow CD19-CD45-CD38++CD138+ cells, pink population (Kim et al., 2012).



tation. CD138⁺/CD34⁻ were unable to form colonies in vitro, and human engraftment was not detected. A chimeric anti-CD20 monoclonal antibody, rituximab, was shown to inhibit clonogenic growth of CD138⁻ cells in vitro (Matsui et al, 2004; Matsui et al, 2008). However, clinical trials failed to confirm an effect of rituximab as a useful maintenance therapy for MM (Moreau, et al 2007, Treon, et al 2002, Zojer, et al 2006).

Paino et al., (2012) re-evaluated the presence and function of CD20⁺ putative MM stem cells in a panel of myeloma cell lines. Although Matsui et al. (2004) described a small population (2-5%) of CD138⁻CD20⁺ cells in NCI-H929 and RPMI-8226 cell lines, Paino et al. (2012) were not able to detect CD20. Only RPMI-8226 cell lines contained a small population of CD20^{dim}⁺ cells (0.3%). These data are consistent with the report of Rossi et al. (2010), which showed U266, NCI-H929 and RPMI-8226 MM cell lines are CD20⁻. On the contrary, CD20^{dim}⁺ cells displayed a myelomatous PC phenotype of CD38⁺CD138⁺CD19⁻CD27⁻CD45⁻ and did not exhibit stem cell properties. Compared to the CD20⁻ population, they showed a lower level of self-renewal potential. Both populations developed plasmacytomas when they were injected into CD17-SCID mice suggesting that CD20^{dim}⁺ cells are not essential for tumor formation. Furthermore, CD20^{dim}⁺ cells did not differentiate into CD20⁻ cells but vice versa, indicating a hierarchical order of differentiation from CD20⁻ to CD20^{dim}⁺ cells. Overall, these results do not support CD20 as a marker associated with MM stem cells phenotype (Paino et al, 2012).

Clonogenic growth of CD138⁺ cells isolated from MM cells was significantly inhibited by dexamethasone, lenalidomide, bortezomib and 4-hydroxycyclophosphamide, but had no significant effect on CD138⁻ cells. This indicates drug resistance, a characteristic feature of cancer stem cell (CSC) (Matsui et al, 2008). Nevertheless, it could not be evaluated in CD138⁺ PCs from MM patients because they lack clonogenic activity in vitro. Detection of a small CD138⁻ population of MM cell lines (< 2%) that displayed stem cell properties mediating drug resistance, such as the capacity to efflux the DNA binding dye Hoechst 33342 and higher relative levels of aldehyde dehydrogenase (ALDH) activity, further supports the existence of a resistant MM stem cells compartment in MM. Moreover, CD138⁻ cells of MM cell lines also exhibited cellular quiescence similar to adult stem cells. Almost all CD138⁻ cells were shown to remain in G0 - G1 phase and less than 1.5 % in S phase, compared to two-thirds of CD138⁺ cells in G0 - G1 and about 20% in S phase (Matsui et al, 2008). On the other hand, results of the first study proved that CD138⁻ cells expressed higher levels of the proliferation marker Ki67 than CD138⁺ cells (Matsui et al, 2004). These discrepancies might come from different passages of cell lines or culture conditions

but cannot conclusively prove a quiescent state of CD138⁻ cells.

Besides the clonogenic population of CD138⁻ cells, Matsui et al. (2004) also isolated circulating clonotypic CD19⁺CD27⁺ B cells in PB of MM patients that were successfully engrafted into NOD/SCID mice. However, it remains unclear whether CD138⁻ clonogenic cells are identical to clonotypic CD19⁺ B cells. Hosen et al. (2012) found that only CD138⁻CD19⁻CD38⁺⁺ cells formed colonies in vitro whereas CD19⁺ B cells did not. Surprisingly, CD138⁺ PCs also gave rise to MM, but more slowly than CD138⁻ cells. Thus, CD138⁻ clonogenic cells might represent a population that have the potential to give rise to MM but does not overlap with the population of CD19⁺ B cells. These results indicate that CD138⁻ clonogenic cells are more PCs than B cells (Fig.4). Although MM stem cells phenotypically resemble memory B cells, they may be modified PCs, while CD138⁺ PCs might represent some 'transit' population that have subsequently lost their mature phenotype. However, Christensen et al. (2012) re-examined CD138⁻ population of the so-called MM stem cells. They analyzed primary CD138⁺ PCs of MM patients, which showed the number of CD138⁻ cells increased in parallel with increasing time from sampling to analysis. Taking into account that myeloma PCs lose expression of surface CD138 in apoptosis, Annexin V was included in all analyses to monitor apoptotic cells. As expected, when CD138⁻ population was detected, these cells were positive for Annexin V. Similar results were also obtained by Chiron et al. (2012). Furthermore, qPCR techniques confirmed similarly high levels of CD138/SDC1 mRNA in both CD138⁻ and CD138⁺ MM cells. CD138⁻ and CD138⁺ subpopulations had no differential expression of CD19 and CD20. These contradictory results would imply that the CD138⁻ population might represent only cells undergoing apoptosis as a consequence of previous sample handling (Christensen et al, 2012). Nevertheless, these new findings cannot completely refute results of previous studies

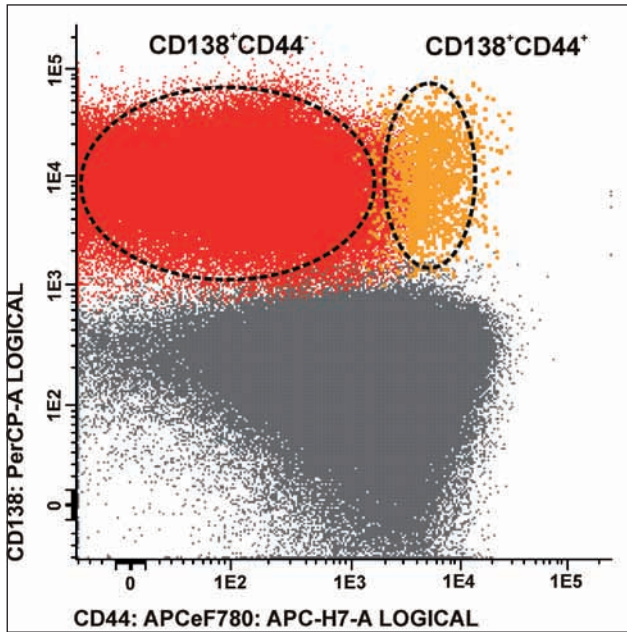
Side population

Side population (SP) cells were defined based on their capacity to exclude dyes such as Hoechst 33342 (Goodell et al, 1996). SP cells have been detected in various cancer cell lines as well as primary tumors (Wu, 2008). Side population possesses CSC characteristics, such as the capacity for re-growth of the tumor, expression of stem cell-like genes and resistance to chemotherapy. This is why SP cells are believed to be the true population responsible for tumor maintenance.

The presence of SP cells were investigated in four MM cell lines, RPMI 8226, U266, OPM2 and KMS-11, as well as primary MM samples (Loh et al, 2008). SP was defined using control cells stained with both Hoechst and verapamil, a calcium channel blocker, to establish the SP gate (Srinivasan et al, 2011). A reduction

Figure 5: Intermediate plasm cell precursors

An illustrative figure of putative multiple myeloma progenitors; red population - bone marrow CD138+CD44-, yellow population - bone marrow CD138+CD44+.



of SP cells was demonstrated in all tested cell lines. The percentage of SP cells ranged from 0 to 4.9%, compared to 0.05% of SP in normal BM. 0.18-0.83% of SP cells express the clonal surface immunoglobulin light chain restriction that matched 89-97% of each patient's PCs. A mean of 96.1% of SP cells were found to be CD138-. However, the CD138+ fraction also contained SP, indicating that SP cells are present in both CD138- and CD138+ compartments. Jakubikova

et al. (2011) also demonstrated that the SP fraction of MM cell lines expressed CD138. Moreover, these results did not prove a correlation between expression of CD19, CD20, or CD27 and the proportion of SP cells. Conversely, SP cells showed more clonogenic potential and proliferation index than the main population.

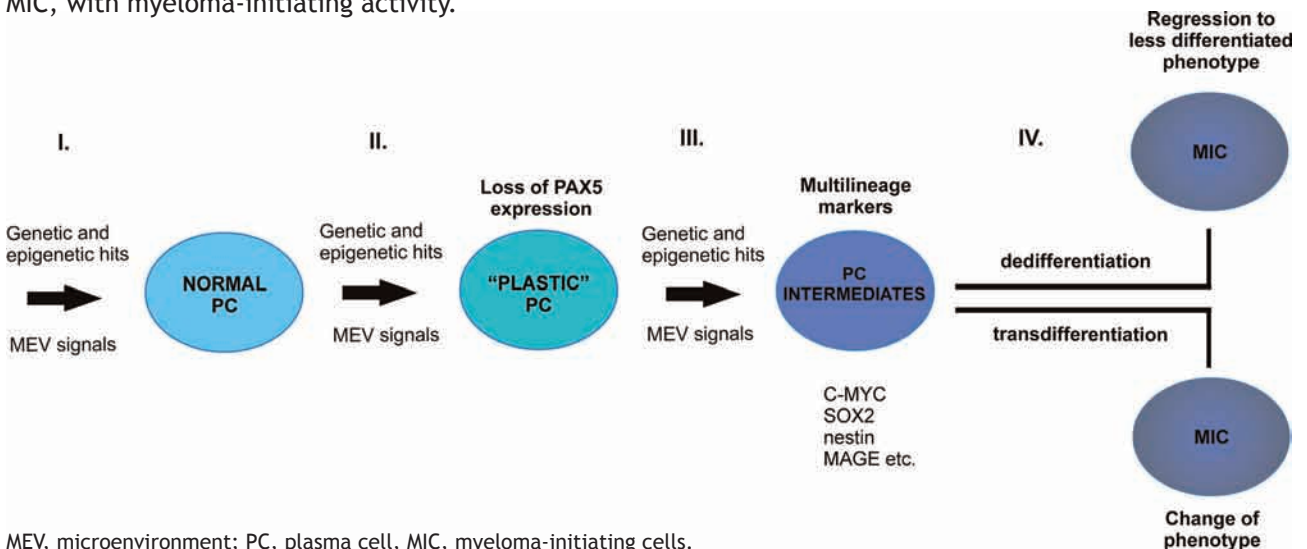
Although SP results seem to be convincing, the method for detection of SP is questioned. Binding of Hoechst to DNA is toxic to live cells, which is why SP cells might represent only a population that survived the lethal effect of Hoechst. SP phenotype might be further affected by staining time, dye concentration or cellular concentration. Different gating strategies might also lead to contamination of the SP fraction by non-SP cells in flow cytometric analyses. Furthermore, the use of verapamil as an inhibitor of efflux does not seem to be specific enough because verapamil-sensitive cells were detected in the negative or SP gate (Montanaro et al, 2004). These findings require more stringent gating strategies to clear doubts about SP.

Clonogenic plasma cells

Abnormal PCs show a low proliferation potential with a plasma cell labeling index (PCLI) ranging from 0.5% in MGUS to 1% in early MM. However, PCLI is one of the most important prognostic factors with a strong impact on overall survival (Bergsagel and Kuehl, 2001). The clonogenic potential of primary MM cells was first demonstrated by Hamburger & Salmon in 1977. They showed that freshly explanted human myeloma cells are able to form colonies of monoclonal PCs. These colonies consisted of immature plasmablasts and mature PCs. Drewinko et al

Figure 6: Model of inducible plasticity in multiple myeloma

Aberrant microenvironmental signals together with genetic and epigenetic factors might cause knock down of PAX5 expression in normal PCs resulting in generation of "plastic" PCs that can be further induced to express of multi-lineage markers, pluripotent factors and/or stem cell genes. Such affected cells, PC intermediates, can change phenotype (transdifferentiate) or regress (dedifferentiate) to less differentiated cells, MIC, with myeloma-initiating activity.



MEV, microenvironment; PC, plasma cell, MIC, myeloma-initiating cells.

(1981) investigated the growth fraction of MM cells. In untreated and nonresponsive patients, the growth fraction represented 4% of MM cells. Patients in relapse had a growth fraction ranging from 14% to 83%. Non-proliferating fraction contained true quiescent cells, some proliferating cells with very long intermitotic times and some proliferating cells that have already entered the maturation phase. Both reports demonstrated clonogenic and proliferative capacity of primary MM tumors, but the cells were not phenotypically defined as whole mononuclear fraction of BM was used for analysis. Therefore, the results of these studies do not answer what kind of cells represent true growth fraction.

First experiments demonstrating the clonogenic growth of phenotypically defined PCs were carried out by Yaccoby and Epstein (1999). They proved that CD38⁺⁺CD45⁻ PCs derived from PB and BM are able to engraft SCID-hu host system with implanted human bone. Circulating clonal PCs grew more rapidly in SCID-hu hosts than those in the BM suggesting this may represent a subpopulation with a higher growth potential. In contrast to previous reports, PC-depleted blood cells did not give rise to MM in SCID-hu hosts (Yaccoby and Epstein, 1999). Yata and Yaccoby (2004) presented an alternative model for the study of MIC that uses rabbit bones implanted subcutaneously in unconditioned SCID mice. The SCID-rabbit model was also successfully engrafted with CD138⁺ PCs of MM patients. Although, these two models did not show a serial engraftment of the disease, they strongly indicate a critical role of specific BM microenvironments for PC survival and proliferation (Yata and Yaccoby, 2004).

The dependence of myeloma PCs on human BM microenvironment was clearly demonstrated in an experiment with NOD/SCID/common cytokine receptor γ chain-deficient (NSG) and recombinase-activating gene 2/common cytokine receptor γ chain-deficient (RAG2^{-/-} γ c⁻) mice (Kim et al, 2012). Results proved that CD138⁺/CD38^{high} cells from MM patients led to a repopulation of CD19⁺CD38^{low} or CD138⁺CD38⁺ B-lineage cells in human bone-bearing mice but no engraftments were detected in human bone-free mice, even after orthotopic intrafemoral injection (Fig. 4). Moreover, serially xenotransplanted CD19⁻CD138⁺ cells preferably engrafted from a human bone graft but were not detected in any mouse hematopoietic tissues. All grafts derived from CD138⁺/CD38^{high} cells were clonally related to myeloma PCs, whereas engraftments of CD19⁺CD38^{low}/⁻ B cells were polyclonal CD19⁺CD38^{low} cells. Further fractionation of CD138⁺/CD38^{high} cells and their subsequent xenotransplantation showed that CD45^{low}/⁻ or CD19⁻ CD38^{high}/CD138⁺ cells had higher engraftment ability than CD45^{high} or CD19⁺ plasmablasts. In accordance with results mentioned above, it was concluded that CD19⁻CD45^{low}/⁻CD38^{high}/CD138⁺ PCs enrich MICs rather than CD19⁺ B

cells or plasmablasts. In addition, analysis of clonogenic potentials of CD138⁺ and CD138⁻ populations derived from plasma cell leukemia (PCL) patients strongly favored these findings (Chiron et al, 2012). This study demonstrated that although CD138⁺ PCs derived from PCL patients formed colony forming units (CFU) in a very low frequency, no CFU were found when CD138⁻ cells were seeded. Harvested cells of CFUs derived from CD138⁺ PCs were strongly positive for CD138 but negative for CD20. These findings further underline an important role of CD20⁻CD138⁺ population as a conceivable reservoir of clonal PCs, at least in PCL.

Intermediate plasma cell precursors

O'Connor et al. (2002) identified post-GC-precursors in a mouse model that might contribute to long-lived humoral immunity. These cells were distinct from splenic B cells, mature or memory B cells as well as mature PCs. Intermediate levels of CD138 indicated that PC precursors might represent a transition state of PC development. PC precursors migrate to the BM where they proliferate and consequently differentiate to mature PCs without antigen stimulation. CD138⁺CD44⁺ give rise to short-lived PCs, CD138⁺CD44⁻ or CD138⁻CD44⁺, which differentiate to long-lived PCs. Two roles of PC precursors were suggested; (i) they might either serve as a reservoir of PCs upon PC attrition or (ii) contribute to post-GC affinity maturation of the humoral immune response. Due to similarities of phenotype, proliferative potential and differential capacity of the PC precursors to putative MM progenitors, authors suggested that these cells are candidates for normal counterpart of transformed MM progenitors (Fig. 5).

HETEROGENEITY OF MULTIPLE MYELOMA

Phenotypic heterogeneity

Normal polyclonal PCs express high CD38 and CD138, along with CD19, a B-lymphocyte antigen, whereas abnormal PCs express a wide range of multi-lineage antigens, such as myeloid, T-cell and natural-killer-associated antigens. In general, abnormal PCs lack CD19 expression. They also show variable expression of CD45, dim expression of CD38 and heterogeneous signals of CD138. Further, they have weaker expression of CD27, increased CD28, CD33, CD56 and variable expression of CD20 and CD117 (Kumar et al, 2010; Paiva et al, 2010). Vast phenotypic variability might be caused by the loss of the lineage master gene, which could lead to dedifferentiation or transdifferentiation into cells of other lineages (Liu et al, 2007).

PCs belong to the B-cell lineage that expresses paired box 5 protein (PAX5) and its target, CD19. PAX5 activation and inactivation is essential for maintenance and commitment of the functional identity of early B cell throughout its development. PAX5 represses B lineage 'inappropriate' genes and simultaneously

activates B lineage-specific genes (Calame 2001). PAX5 and CD19 expression are considered to be downregulated or lost but it has been reported that expression of PAX5 and CD19 is restored in normal PCs of pleural effusion, ascitic fluid and BM aspirate. In contrast to normal PCs, clonal PCs of MM do not express PAX5 or CD19 (> 95% of cases) (Harada, et al 1993, Mahmoud, et al 1996). Therefore, the lack of PAX5 gene expression might affect expression of multi-lineage markers on clonal PCs (Liu et al, 2007). The ability to differentiate into multiple lineages is a characteristic feature of pluripotent embryonic stem cells. However, pluripotency does not necessarily have to be limited to a population of undifferentiated stem cells of the early embryo and irreversibly lost upon terminal differentiation (Allan, 2011). Fully differentiated somatic cells can be reprogrammed into inducible pluripotent stem cells (iPSC) by 'forced' expression of pluripotency/reprogramming factors: OCT4, SOX2, C-MYC and KLF4, or NANOG, LIN28, C-MYC and KLF4 (Takahashi and Yamanaka, 2006; Yu et al, 2007). Reprogramming of mature B cells required additional 'sensitization' by myeloid transcription factor CCAAT/enhancer-binding protein- α (C/EBP α) that causes a specific knockdown of PAX5 or disrupts its functions (Hanna et al, 2008). This indicates the loss of PAX5 expression might be associated with the gain of stem cell features for mature PCs and represent one of the key events in the pathogenesis of MM (Fig. 6).

Intra-clonal heterogeneity

Intra-clonal heterogeneity (evidence of genetically distinct subclones) is present in all stages of MM development. Benign monoclonal gammopathy of undetermined significance (MGUS) shows less complex genotype than MM; however, most mutations found in MM are already present in high-risk smouldering MM (Walker, et al 2013). Subclonal evolution process might be modulated by the administered therapy. It was demonstrated that under selection pressure of therapy, an altering dominance of clones might occur; a resistant clone that was either already present at the time of diagnosis or a new clone selected during therapy expands and competes for dominance with an initially dominant clone (Keats, et al 2012). Recently, Keats et al. (2012) have modified existing Darwinian clonal evolution model of MM development that explains tumor progression as a linear accumulation of genomic aberration over time. Current results indicate that MM develops through mutational branching rather than through linear acquisition of mutation (Bahlis 2012, Keats, et al 2012). Three temporal types of tumors were identified in MM - linearly evolving, genetically stable and heterogeneous represented by a mixture of genetically distinct clones with shifting dominance (Keats, et al 2012). This revolution model of Darwinian mutational branching together with altering dominance

of subclones should be taken into account for future therapeutic regimen of MM.

PLASTICITY OF MULTIPLE MYELOMA

There is growing evidence that MM encompasses a certain degree of plasticity that might be responsible for expression of a wide range of multi-lineage markers or acquiring of stem cell properties. First, shutdown of key lineage commitment factor PAX5 in MM might have crucial consequences for a cell fate. Plasticity of normal pluripotent stem cells requires strict maintenance of balance between expression of pluripotency genes and lineage master genes. Deregulation of these mechanisms may result in dedifferentiation, enabling committed cells to acquire stem cell state (Marjanovic, et al 2013). Interestingly, the hematopoietic system shows considerable lineage plasticity that allows committed cells to transdifferentiate from one lineage to another, e.g. conditional deletion of PAX5 can shift mature B cells back into early uncommitted progenitors (Cobaleda, et al 2007) or pro-B cells lacking PAX5 express genes of different lineage-affiliated programs (Nutt et al., 1999). These examples clearly demonstrate that shutdown of only one key lineage commitment factor can disturb cellular hierarchy.

Secondly, in spite of mature phenotype, MMPCs express pluripotent factors (SOX2, C-MYC or KLF4) and stem/progenitor markers, such as markers of the MAGE family, the hematopoietic progenitor marker CD117 or neural stem cell marker, nestin (Liu et al, 2007; Spisek et al, 2007; Bataille et al, 2008). Some of these factors provide valuable prognostic information. Currently, the role of C-MYC has been growing as the key transforming factor in the progression of asymptomatic MGUS to a symptomatic disease (Chesi et al, 2008). SOX2 and MAGE have been demonstrated to be relevant targets for immunotherapy. CD117 (c-kit) is an essential hematopoietic growth factor receptor with tyrosine-kinase activity. Aberrant expression of CD117 is detected on a subset of MGUS and MM and is associated with a favourable outcome for MM patients (Bataille et al, 2008). Nestin, class VI intermediate filament protein, is a tumor specific marker for CD138+38+PCs of MM (Svachova et al, 2011). However, its presence in terminally differentiated PCs with a low proliferative potential is surprising because nestin is generally found in multipotent proliferative progenitors of developing and regenerating tissues. During terminal differentiation, nestin expression is down-regulated but can be reactivated upon pathological conditions such as injury or cancer. (Michalczyk and Ziman, 2005). Surprisingly, nestin associated with plasticity of terminally differentiated cells in the study of metaplastic conversion of mature pancreatic epithelial cells (Means, et al 2005). Metaplastic changes were accompanied by occurrence of nestin-positive intermediates. This study proved a real trans-differentiation potential of

mature mammalian cells and indicated that plasticity of mature cells may play a role in the generation of neoplastic precursors. Therefore, nestin-positive myeloma PCs might represent particular intermediates/transient population undergoing changes leading to the occurrence of cells with a changed (transdifferentiation) or less differentiated phenotype (dedifferentiation) (Fig. 2). In addition, nestin polymerization/depolymerization influences intracellular signaling, is likely responsible for rapid redistribution of intracellular proteins, cytoskeletal remodeling and/or might function as a scaffold for protein interactions (Michalczyk and Ziman, 2005). Dynamic character of nestin network might represent an important prerequisite for myeloma plasticity.

Thirdly, dedifferentiation might be a key mechanism for the generation of tumor-initiating cells in human cancer (Allan, 2011). The process of dedifferentiation is suggested to be under the control of tumor MEV. Interaction of tumor cells with their MEV might induce altered differentiation; for instance, some solid tumors are known to undergo epithelial-mesenchymal transition (EMT) (Mani, et al 2008, Prindull and Zipori 2004). Similarly to MM, phenotypic plasticity of MMPCs was observed in long-term co-culture with osteoclasts; myeloma PCs lost their mature phenotype and dedifferentiated into an immature, resilient, apoptosis-resistant phenotype (Yaccoby 2005). In addition, CD138⁺ PCs co-cultured with DCs lost expression of CD138 and increased the clonogenic potential (Kukreja et al, 2006). Possibly, signals from the microenvironment can (reversibly) alter the phenotype of PCs and cause obvious heterogeneity of MM. This regulation might keep dynamic equilibrium between CSC and non-CSC compartments (Dhodapkar, 2010). Dynamic state between CSC and non-CSC-like compartments was observed in a subpopulation of differentiated basal-like human mammary epithelial cells that spontaneously converted to stem-like cells *in vitro* and *in vivo*. Moreover, oncogenic transformation enhances this spontaneous conversion. These findings indicate that normal and CSC-like cells can arise *de novo* and indicate the importance of the differentiation state of cells-of-origin as a critical factor determining the phenotype of their transformed derivatives (Chaffer et al, 2011).

Recent work of Chaidos et al. (2013) further supports the theory of plasticity potential of PCs. They demonstrated reversible, bidirectional phenotypic transition between CD19⁻CD138⁻ pre-PC and CD19⁻CD138⁺ PCs. These two subpopulations represented interconvertible phenotypic and functional states and showed myeloma-propagating activity. Interestingly, CD138⁺ PCs predominantly resided in BM, whereas CD138⁻ cells were predominant in the spleen and liver of the engrafted animals. This observation demonstrates a close relationship between MM and MEV and indicates a possible role of tumor MEV in myeloma transition. Moreover, although both subpopulations

shared the same chromosomal abnormalities and immunoglobulin heavy chain complementarity region 3 area sequence, they were epigenetically distinct with a different drug-resistance, which may be a consequence of different microenvironmental conditions. Results confirmed that pre-PC to PC transition is a phenomenon observed irrespective of the primary oncogenic events or clinical stage of disease (Chaidos, et al 2013).

All those findings take into consideration both models of myelomagenesis - hierarchical model of MM stem cells and clonal evolution model of multistep accumulation of mutations. Plasticity model would better explain how slowly proliferating PCs can quickly repopulate the tumor and also resolve inconsistencies among myeloma stem cell theories. Furthermore, mathematical models that involve plasticity provide a more accurate demonstration of stem cell dynamics than does the less flexible concept of differentiation hierarchy. Nevertheless, it is likely that reversible phenotype changes can cooperate with irreversible genetic alternations (Marusyk and Polyak 2010). Certain reconciling demonstrates the ecology model of plasticity and clonal selection (rev. in Holzel et al, 2013). This model suspects an existence of rare resistant 'super-fitness clone' with hardwired mutations that can benefit from plasticity of sensitive bulk of cell populations, termed poor-fitness clone. Therapy-induced inflammation may induce regenerative signals in a local niche and provoke phenotypic changes to support survival of poor-fitness clones. The altered infrastructure of tumor tissue may represent an essential condition to ensure the outgrowth of super-fitness clone. Therapy-induced plasticity of tumor tissue is supposed to be a key mechanism responsible for development of tumor resistance in response to therapy-induced injury. Characteristic hallmarks of therapy-induced injury are inflammation and hypoxia. Both mechanisms were observed to influence spontaneous conversion of tumor cells.

CANCER STEM cell phenotype and tumor microenvironment

Local alterations of tumor MEV naturally occurring during tumor development and progression or under therapeutic stress have a crucial effect on phenotypic changes of tumor cells. MM PCs reside in a close proximity of BM MEV; mutual interactions between PCs and their MEV play a crucial role in MM progression, dissemination and drug resistance. It is becoming evident that cancer stem cell phenotypes is a plastic state induced in cancer cells depending upon microenvironmental signals, such as hypoxia. Hypoxia is a crucial regulator of the stem cell phenotype and together with HIFs is involved in maintaining a stem-like state in normal tissues (Heddleston 2010). Myeloma PCs are long-term exposed to low oxygen levels in the BM microenvironment and both HIF-1 α

and HIF-2 α have been reported to be stabilized in MM patients, resulting in stimulation of angiogenesis (Martin et al, 2010). However, recent studies suggest that hypoxia may have a profound effect on PC behavior. Normal hematopoietic stem cells can represent one example. They reside in regions regulated by oxygen tension. It is hypothesized that undifferentiated phenotypes of these cells relies on HIF activity in hypoxic areas (Parmar, et al 2007). Hypoxic areas in tumors might be an analog to stem cell niches in normal tissues. It is generally known that hypoxia has a great impact on the production of angiogenic factors and generation of new vasculature in tumors but less is known about the role of hypoxia in growth and (de)differentiation of cancer cells. Series of experiments have demonstrated that hypoxia is responsible for altering the cellular phenotype by causing an increase in proliferation, self-renewal and upregulation of stem cell genes in both CSC and non-CSC. Moreover, Yoshida et al. (2009) have shown that hypoxic conditions significantly improve generation of iPSC. It was demonstrated that hypoxia could regulate histone methylation, thus altering the epigenetic status of cancer cells (Heddleston et al, 2009; Xia et al, 2009). Tumor hypoxia also correlates with poor outcome of patients. HIFs were shown to induce pluripotent factors, including OCT4, NANOG, SOX2, KLF4, MYC, and microRNA-302 in cancer cell lines of prostate, brain, kidney, cervix, lungs, colon, liver and breast tumors (Mathieu et al, 2011). Hypoxic microenvironment potentiates biological effect of Notch signaling in adenocarcinoma of lungs or alters gene expression of neuroblastoma cells to induce more immature phenotype (Jögi et al, 2002). CD133, a cancer stem cell marker, has been reported by several groups to be upregulated under hypoxic conditions (Seidel et al, 2010; Soeda et al, 2009). McCord et al. (2009) showed that hypoxia increased the sub-population of CD133+ glioblastoma cells, but also enhanced expression of markers, such as SOX2, OCT4 and nestin. Low oxygen levels also induced HIF-2 α expression, which is able to increase the expression of stem cell-associated genes and confer tumorigenic potential to non-CSC (Heddleston et al, 2009).

Intratumoral hypoxia, followed by stabilization of HIF-1 α , can induce the EMT features and promotes metastasis and the CSC phenotype. EMT is a phenomenon that occurs in solid tumors. However, EMT-like features have been recently identified in MM (Azab, et al 2012). Hypoxic conditions activated EMT-related proteins, such as SNAIL, FOXB, TGF β . Activation of EMT-related machinery led to down-regulation of E-cadherin, an impairment of cell adhesion to BM and egress of PCs to the circulation. Simultaneously, hypoxia increased expression of CXCR4 that plays a major role in the migration and homing of PCs to BM and is up-regulated in EMT. Hypoxia in PCs and surrounding MEV was induced by tumor progression

accompanied by increase expression of hypoxia-induced genes in MM patients compared to healthy donors. Furthermore, HIF-1 α expression correlated with tumor progression. These results demonstrated that PCs acquired metastatic potential under hypoxic conditions resulting in de-adhesion, increase migration and homing. EMT-like mechanism may keep continuous spread of PCs into PB and (re)entrance or homing into new BM niches. It can be assumed that acquiring of EMT-like features to the PCs may be associated with dynamic changes of PC phenotype and CSC plasticity.

CLINICAL TRANSLATION of myeloma stem cell concepts

Despite the achievement of currently used therapy, MM remains difficult to treat with a persistent risk of relapse and disease progression. Myeloma stem cell concepts offer apparently a simple and effective way how to overcome drug resistance and treat MM. Several novel therapeutic strategies have been evaluated to improve long-term clinical outcomes. Based on the presence of clonotypic B-cell precursors that express CD20, phase II trials have been conducted using rituximab (anti-CD20 chimeric monoclonal antibody) as a single-agent therapy (Matsui et al, 2004, Treon et al, 2002; Zojer et al, 2006; Moreau et al, 2007). However, results of those small clinical trials were disappointing. Only in a study of Gozzetti et al. (2008), complete remission was reported in a single patient with CD20+ MM refractory to high dose melphalan (Gozzetti, et al 2008). Other reports focused on self-renewal character of CSCs and targeted signaling pathways, such as Hedgehog (cyclopamine), or telomerase activity (GRN1632) (Agarwal and Matsui 2010, Peacock, et al 2007). However, results of these studies come from only one group and need additional evaluation. It is apparent that inconsistencies among particular concepts complicate clinical translation. Moreover, recent evidence that phenotypic and functional interconvertible states exists between CD138- and CD138+ MIC might explain failure of single-agent therapy targeting only one compartment (Chaidos et al., 2012). It is obvious that currently used therapy does not effectively target all MIC. Furthermore, high intra-clonal heterogeneity of MM incorporates more complexity to this problem. To improve outcomes of future therapy, it is necessary to take into account plasticity of MIC and altering dominance of genetically distinct subclones that can occur based on used treatment. Combination therapy targeting all coexisting subclones and states is required besides detailed screening of genome evolution and new assessment of minimal residual disease including evaluation all MIC.

CONCLUSION

In this review, we discussed inconsistencies among particular myeloma stem cell concepts and the ina-

bility to detect true population responsible for tumor origin and maintenance. Methodological pitfalls of research approaches often caused large interpatient and interstudy variability. This is mainly caused by non-specific annealing of primers in PCR that might overestimate amount of cells, different experimental mouse models, cytometric approaches, culture conditions or sample handling. Discrepancies are expanded further by recent findings that MM possesses plasticity to reversibly change phenotype and functions of MIC. Plasticity of MM is seen to rely on specific signals from aberrant MEV that crucially modulate phenotype and stem cell-like properties. Therefore, an effort to target the specific cell type to yield durable clinical response is not sufficient. Instead, it is necessary to concentrate on pathologic mechanisms responsible for the transition between states and role of surrounding MEV.

ACKNOWLEDGMENTS

This work was supported by research project from: Ministry of Education, Youth and Sports: MSM0021622434, grant from Ministry of Health: IGA NT13190, IGA NT11154, grant from Czech Science Foundation: GAP304/10/1395, Ministry of Health, Czech Republic for Conceptual Development of Research Organization 65269705, Institutional Support of Ministry of Health, Czech Republic no.1 RVO-FNOs/2012 and Institutional Development Plan of University of Ostrava in 2012.

AUTHOR CONTRIBUTIONS

R. Hajek wrote and reviewing the paper. S. A. Okubote co-wrote and corrected the paper. H. Svachova conceived the idea and wrote the paper.

REFERENCES

- Agarwal, J.R. & Matsui, W. (2010) Multiple myeloma: a paradigm for translation of the cancer stem cell hypothesis. *Anticancer Agents Med Chem*, 10, 116-120.
- Allan, A.L., (2011) *Cancer Stem Cells in Solid Tumors*. *Stem Cell Biology and Regenerative Medicine*: Springer, 475.
- Azab, A.K., Hu, J., Quang, P., Azab, F., Pitsillides, C., Awwad, R., Thompson, B., Maiso, P., Sun, J.D., Hart, C.P., Roccaro, A.M., Sacco, A., Ngo, H.T., Lin, C.P., Kung, A.L., Carrasco, R.D., Vanderkerken, K. & Ghobrial, I.M. (2012) Hypoxia promotes dissemination of multiple myeloma through acquisition of epithelial to mesenchymal transition-like features. *Blood*, 119, 5782-5794.
- Bakkus, M.H., Van Riet, I., Van Camp, B., Thielemans, K. (1994) Evidence that the clonogenic cell in multiple myeloma originates from a pre-switched but somatically mutated B cell. *British Journal of Haematology*, 87, 68-74.
- Bahlis, N.J. (2012) Darwinian evolution and tiding clones in multiple myeloma. *Blood*, 120, 927-928.
- Basak, G.W., Carrier, E. (2010) The search for multiple myeloma stem cells: the long and winding road. *Biology of Blood and Marrow Transplant*, 16, 587-594.
- Bataille, R., Pellat-Deceunynck, C., Robillard, N., Avet-Loiseau, H., Harousseau, J.L., Moreau, P. (2008) CD117 (c-kit) is aberrantly expressed in a subset of MGUS and multiple myeloma with unexpectedly good prognosis. *Leukemia Research*, 32, 379-382.
- Bergsagel, D.E., Valeriote, F.A. (1968) Growth characteristics of a mouse plasma cell tumor. *Cancer Research*, 28, 2187-2196.
- Bergsagel, P.L., Chesi, M., Nardini, E., Brents, L.A., Kirby, S.L., Kuehl, W.M. (1996) Promiscuous translocations into immunoglobulin heavy chain switch regions in multiple myeloma. *Proceedings of the National Academy of Sciences USA*, 93, 13931-13936.
- Bergsagel, P.L., Kuehl, W.M. (2001) Chromosome translocations in multiple myeloma. *Oncogene*, 20, 5611-5622.
- Bergsagel, P.L., Masellis Smith, A., Belch, A.R., Pilarski, L.M. (1995a) The blood B-cells and bone marrow plasma cells in patients with multiple myeloma share identical IGH rearrangements. *Current Topics in Microbiology and Immunology*, 194, 17-24.
- Bergsagel, P.L., Smith, A.M., Szczepek, A., Mant, M.J., Belch, A.R., Pilarski, L.M. (1995b) In multiple myeloma, clonotypic B lymphocytes are detectable among CD19+ peripheral blood cells expressing CD38, CD56, and monotypic Ig light chain. *Blood*, 85, 436-447.
- Billadeau, D., Ahmann, G., Greipp, P., Van Ness, B. (1993) The bone marrow of multiple myeloma patients contains B cell populations at different stages of differentiation that are clonally related to the malignant plasma cell. *Journal of Experimental Medicine*, 178, 1023-1031.
- Calame, K.L. (2001) Plasma cells: finding new light at the end of B cell development. *Nat Immunol*, 2, 1103-1108.
- Chaffer, C.L., Brueckmann, I., Scheel, C., Kaestli, A.J., Wiggins, P.A., Rodrigues, L.O., Brooks, M., Reinhardt, F., Su, Y., Polyak, K., Arendt, L.M., Kuperwasser, C., Bierie, B., Weinberg, R.A. (2011) Normal and neoplastic nonstem cells can spontaneously convert to a stem-like state. *Proceedings of the National Academic of Sciences USA*, 108, 7950-7955.
- Chaidos, A., Barnes, C.P., Cowan, G., May, P.C., Melo, V., Hatjiharissi, E., Papaioannou, M., Harrington, H., Doolittle, H., Terpos, E., Dimopoulos, M., Abdalla, S., Yarranton, H., Naresh, K., Foroni, L., Reid, A., Rahemtulla, A., Stumpf, M., Roberts, I. & Karadimitris, A. (2013) Clinical drug resistance linked to interconvertible phenotypic and functional states of tumor-propagating cells in multiple myeloma. *Blood*, 121, 318-328.
- Chesi, M., Robbani, D.F., Sebag, M., Chng, W.J., Affer, M., Tiedemann, R., Valdez, R., Palmer, S.E., Haas, S.S., Stewart, A.K., Fonseca, R., Kremer, R., Cattoretto, G., Bergsagel, P.L. (2008) AID-dependent activation of a MYC transgene induces multiple myeloma in a conditional mouse model of post-germinal centre malignancies. *Cancer Cell*, 13, 167-180.
- Chiron, D., Surget, S., Maïga, S., Bataille, R., Moreau, P., Le Gouill, S., Amiot, M., Pellat-Deceunynck, C. (2012) The peripheral CD138+ population but not the CD138- population contains myeloma clonogenic cells in plasma cell leukaemia patients. *British Journal of Haematology*, 156, 679-683.
- Christensen, J.H., Jensen, P.V., Kristensen, I.B., Abildgaard, N., Lodahl, M., Rasmussen, T. (2012) Characterization of potential CD138 negative myeloma „stem cells“. *Haematologica*, 97, 18-20.
- Cobaleda, C., Jochum, W. & Busslinger, M. (2007) Conversion of mature B cells into T cells by dedifferentiation to uncommitted progenitors. *Nature*, 449, 473-477.
- Colla, S., Storti, P., Donofrio, G., Todoerti, K., Bolzoni, M., Lazzaretti, M., Abeltino, M., Ippolito, L., Neri, A., Ribatti, D., Rizzoli, V., Martella, E., Giuliani, N. (2010) Low bone marrow oxygen tension and hypoxia-inducible factor-1 α overexpression characterize patients with multiple myeloma: role on the transcriptional and proangiogenic profiles of CD138(+) cells. *Leukemia*, 24, 1967-1970.
- Conway, E.J., Wen, J., Feng, Y., Mo, A., Huang, W.T., Keever-Taylor, C.A., Hari, P., Vesole, D.H., Chang, C.C. (2009) Phenotyping studies of clonotypic B lymphocytes from patients with multiple myeloma by flow cytometry. *Archives of Pathology and Laboratory Medicine*, 133, 1594-1599.
- Corradini, P., Voena, C., Omedé, P., Astolfi, M., Boccadoro, M., Dalla-Favera, R., Pileri, A. (1993) Detection of circulating tumor cells in multiple myeloma by a PCR-based method.

- Leukemia, 7, 1879-1882.
24. Dhodapkar, M.V. (2010) Immunity to stemness genes in human cancer. *Current Opinion in Immunology*, 22, 245-250.
 25. Drewinko, B., Alexanian, R., Boyer, H., Barlogie, B., Rubinow, S.I. (1981) The Growth Fraction of Human Myeloma Cells. *Blood*, 57, 333-338.
 26. Goodell, M.A., Brose, K., Paradis, G., Conner, A.S., Mulligan, R.C. (1996) Isolation and functional properties of murine hematopoietic stem cells that are replicating in vivo. *Journal of Experimental Medicine*, 183, 1797-1806.
 27. Gozzetti, A., Fabbri, A., Lazzi, S., Bocchia, M. & Lauria, F. (2008) Reply to „Rituximab activity in CD20-positive multiple myeloma“. *Leukemia*, 22, 1083; author reply 1083-1084.
 28. Hamburger, A., Salmon, S.E. (1977) Primary bioassay of human myeloma stem cells. *Journal of Clinical Investigation*, 60, 846-854.
 29. Hanna, J., Markoulaki, S., Schorderet, P., Carey, B.W., Beard, C., Wernig, M., Creighton, M.P., Steine, E.J., Cassady, J.P., Foreman, R., Lengner, C.J., Dausman, J. A., Jaenisch, R. (2008) Direct reprogramming of terminally differentiated mature B lymphocytes to pluripotency. *Cell*, 133, 250-264.
 30. Harada, H., Kawano, M.M., Huang, N., Harada, Y., Iwato, K., Tanabe, O., Tanaka, H., Sakai, A., Asaoku, H. & Kuramoto, A. (1993) Phenotypic difference of normal plasma cells from mature myeloma cells. *Blood*, 81, 2658-2663.
 31. Heddleston, J.M., Li, Z., Lathia, J.D., Bao, S., Hjelmeland, A.B., Rich, J.N. (2010) Hypoxia inducible factors in cancer stem cells. *British Journal of Cancer*, 102, 789-795.
 32. Heddleston, J.M., Li, Z., McLendon, R.E., Hjelmeland, A.B., Rich, J.N. (2009) The hypoxic microenvironment maintains glioblastoma stem cells and promotes reprogramming towards a cancer stem cell phenotype. *Cell Cycle*, 8, 3274-3284.
 33. Hölzel, M., Bovier, A. & Tüting, T. (2013) Plasticity of tumour and immune cells: a source of heterogeneity and a cause for therapy resistance? *Nat Rev Cancer*, 13, 365-376.
 34. Hosen, N., Matsuoka, Y., Kishida, S., Nakata, J., Mizutani, Y., Hasegawa, K., Mugitani, A., Ichihara, H., Aoyama, Y., Nishida, S., Tsuboi, A., Fujiki, F., Tatsumi, N., Nakajima, H., Hino, M., Kimura, T., Yata, K., Abe, M., Oka, Y., Oji, Y., Kumano-goh, A., Sugiyama, H. (2012) CD138-negative clonogenic cells are plasma cells but not B cells in some multiple myeloma patients. *Leukemia*, 26, 2135-2141.
 35. Huff, C.A., Matsui, W. (2008) Multiple myeloma cancer stem cells. *Journal of Clinical Oncology*, 26, 2895-2900.
 36. Jakubikova, J., Adamia, S., Kost-Alimova, M., Klippel, S., Cervi, D., Daley, J.F., Cholujova, D., Kong, S.Y., Leiba, M., Blotta, S., Ooi, M., Delmore, J., Laubach, J., Richardson, P.G., Sedlak, J., Anderson, K.C., Mitsiades, C.S. (2011) Lenalidomide targets clonogenic side population in multiple myeloma: pathophysiologic and clinical implications. *Blood*, 117, 4409-4419.
 37. Jensen, G.S., Belch, A.R., Mant, M.J., Ruether, B.A., Yacyszyn, B.R., Pilarski, L.M. (1993) Expression of multiple beta 1 integrins on circulating monoclonal B cells in patients with multiple myeloma. *American Journal of Hematology*, 43, 29-36.
 38. Jensen, G.S., Mant, M.J., Pilarski, L.M. (1992) Sequential maturation stages of monoclonal B lineage cells from blood, spleen, lymph node, and bone marrow from a terminal myeloma patient. *American Journal of Hematology*, 41, 199-208.
 39. Jögi, A., Øra, I., Nilsson, H., Lindeheim, A., Makino, Y., Poellinger, L., Axelson, H., Pählman, S. (2002) Hypoxia alters gene expression in human neuroblastoma cells toward an immature and neural crest-like phenotype. *Proceedings of the National Academic of Sciences USA*, 99, 7021-7026.
 40. Keats, J.J., Chesi, M., Egan, J.B., Garbitt, V.M., Palmer, S.E., Braggio, E., Van Wier, S., Blackburn, P.R., Baker, A.S., Dispenzieri, A., Kumar, S., Rajkumar, S.V., Carpten, J.D., Barrett, M., Fonseca, R., Stewart, A.K. & Bergsagel, P.L. (2012) Clonal competition with alternating dominance in multiple myeloma. *Blood*, 120, 1067-1076.
 41. Kim, D., Park, C.Y., Medeiros, B.C., Weissman, I.L. (2012) CD19(-)CD45(low/-)CD38(high)/CD138(+) plasma cells enrich for human tumorigenic myeloma cells. *Leukemia*, 26, 2530-2537.
 42. Kukreja, A., Hutchinson, A., Dhodapkar, K., Mazumder, A., Vesole, D., Angitapalli, R., Jagannath, S., Dhodapkar, M.V. (2006) Enhancement of clonogenicity of human multiple myeloma by dendritic cells. *Journal of Experimental Medicine*, 203, 1859-1865.
 43. Kumar, S., Kimlinger, T., Morice, W. (2010) Immunophenotyping in multiple myeloma and related plasma cell disorders. *Best Practice and Research: Clinical Haematology*, 23, 433-451.
 44. Liu, S., Otsuyama, K., Ma, Z., Abroun, S., Shamsasenjan, K., Amin, J., Asaoku, H., Kawano, M.M. (2007) Induction of multilineage markers in human myeloma cells and their down-regulation by interleukin 6. *International Journal of Hematology*, 85, 49-58.
 45. Loh, Y.S., Mo, S., Brown, R.D., Yamagishi, T., Yang, S., Joshua, D.E., Roufogalis, B.D., Sze, D.M. (2008) Presence of Hoechst low side populations in multiple myeloma. *Leukemia and Lymphoma*, 49, 1813-1816.
 46. Mahmoud, M.S., Huang, N., Nobuyoshi, M., Lisukov, I.A., Tanaka, H., Kawano, M.M. (1996) Altered expression of Pax-5 gene in human myeloma cells. *Blood*, 87, 4311-4315.
 47. Mani, S.A., Guo, W., Liao, M.J., Eaton, E.N., Ayyanan, A., Zhou, A.Y., Brooks, M., Reinhard, F., Zhang, C.C., Shipitsin, M., Campbell, L.L., Polyak, K., Brisken, C., Yang, J., Weinberg, R.A. (2008) The epithelial-mesenchymal transition generates cells with properties of stem cells. *Cell*, 133, 704-715.
 48. Marjanovic, N.D., Weinberg, R.A. & Chaffer, C.L. (2013) Cell plasticity and heterogeneity in cancer. *Clin Chem*, 59, 168-179.
 49. Martin, S.K., Diamond, P., Williams, S.A., To, L.B., Peet, D.J., Fujii, N., Gronthos, S., Harris, A.L., Zannettino, A.C. (2010) Hypoxia-inducible factor-2 is a novel regulator of aberrant CXCL12 expression in multiple myeloma plasma cells. *Haematologica*, 95, 776-784.
 50. Marusyk, A. & Polyak, K. (2010) Tumor heterogeneity: causes and consequences. *Biochim Biophys Acta*, 1805, 105-117.
 51. Mathieu, J., Zhang, Z., Zhou, W., Wang, A.J., Heddleston, J.M., Pinna, C.M., Hubaud, A., Stadler, B., Choi, M., Bar, M., Tewari, M., Liu, A., Vessella, R., Rostomily, R., Born, D., Horwitz, M., Ware, C., Blau, C.A., Cleary, M.A., Rich, J.N., Ruohola-Baker, H. (2011) HIF induces human embryonic stem cell markers in cancer cells. *Cancer Research*, 71, 4640-4652.
 52. Matsui, W., Huff, C.A., Wang, Q., Malehorn, M.T., Barber, J., Tanheco, Y., Smith, B.D., Civin, C.I., Jones, R.J. (2004) Characterization of clonogenic multiple myeloma cells. *Blood*, 103, 2332-2336.
 53. Matsui, W., Wang, Q., Barber, J.P., Brennan, S., Smith, B.D., Borrello, I., McNiece, I., Lin, L., Ambinder, R.F., Peacock, C., Watkins, D.N., Huff, C.A., Jones, R.J. (2008) Clonogenic multiple myeloma progenitors, stem cell properties, and drug resistance. *Cancer Research*, 68, 190-197.
 54. McCord, A.M., Jamal, M., Shankavaram, U.T., Lang, F.F., Camphausen, K., Tofilon, P.J. (2009) Physiologic oxygen concentration enhances the stem-like properties of CD133+ human glioblastoma cells in vitro. *Molecular Cancer Research*, 7, 489-497.
 55. McSweeney, P.A., Wells, D.A., Shults, K.E., Nash, R.A., Bensing, W.I., Buckner, C.D., Loken, M.R. (1996) Tumor-specific aneuploidy not detected in CD19+ B-lymphoid cells from myeloma patients in a multidimensional flow cytometric analysis. *Blood*, 88, 622-632.
 56. Means, A.L., Meszoely, I.M., Suzuki, K., Miyamoto, Y., Rustgi, A.K., Coffey, R.J., Wright, C.V., Stoffers, D.A. & Leach, S.D. (2005) Pancreatic epithelial plasticity mediated by acinar cell transdifferentiation and generation of nestin-positive intermediates. *Development*, 132, 3767-3776.

57. Michalczyk, K., Ziman, M. (2005) Nestin structure and predicted function in cellular cytoskeletal organisation. *Histology and Histopathology*, 20, 665-671.
58. Montanaro, F., Liadaki, K., Schienda, J., Flint, A., Gussoni, E., Kunkel, L.M. (2004) Demystifying SP cell purification: viability, yield, and phenotype are defined by isolation parameters. *Experimental Cell Research*, 298, 144-154.
59. Moreau, P., Voillat, L., Benboukher, L., Mathiot, C., Dumontet, C., Robillard, N., Hérault, O., Garnache, F., Garand, R., Varoqueaux, N., Avet-Loiseau, H., Harousseau, J.L., Bataille, R. & group, I. (2007) Rituximab in CD20 positive multiple myeloma. *Leukemia*, 21, 835-836.
60. Munshi, N.C., Anderson, K.C., Bergsagel, P.L., Shaughnessy, J., Palumbo, A., Durie, B., Fonseca, R., Stewart, A.K., Harousseau, J.L., Dimopoulos, M., Jagannath, S., Hajek, R., Sezer, O., Kyle, R., Sonneveld, P., Cavo, M., Rajkumar, S.V., San Miguel, J., Crowley, J., Avet-Loiseau, H., International Myeloma Workshop Consensus Panel 2. (2011) Consensus recommendations for risk stratification in multiple myeloma: report of the International Myeloma Workshop Consensus Panel 2. *Blood*, 117, 4696-4700.
61. Nutt, S.L., Heavey, B., Rolink, A.G., Busslinger, M. (1999) Commitment to the B-lymphoid lineage depends on the transcription factor Pax5. *Nature*, 401, 556-562.
62. O'Connor BP, Cascalho M, Noelle RJ. Short-lived and long-lived bone marrow plasma cells are derived from a novel precursor population. *J Exp Med*. 2002 Mar;195(6):737-45.
63. Paino, T., Ocio, E.M., Paiva, B., San-Segundo, L., Garayoa, M., Gutiérrez, N.C., Sarasquete, M.E., Pandiella, A., Orfao, A., San Miguel, J.F. (2012) CD20 positive cells are undetectable in the majority of multiple myeloma cell lines and are not associated with a cancer stem cell phenotype. *Haematologica*, 97, 1110-1114.
64. Paiva, B., Almeida, J., Pérez-Andrés, M., Mateo, G., López, A., Rasillo, A., Vidriales, M.B., López-Berges, M.C., Miguel, J.F., Orfao, A. (2010) Utility of flow cytometry immunophenotyping in multiple myeloma and other clonal plasma cell-related disorders. *Cytometry B: Clinical Cytometry*, 78, 239-252.
65. Park, C.H., Bergsagel, D.E., McCulloch, E.A. (1971) Mouse myeloma tumor stem cells: a primary cell culture assay. *Journal of National Cancer Institute*. 46, 411-422.
66. Parmar, K., Mauch, P., Vergilio, J.A., Sackstein, R. & Down, J.D. (2007) Distribution of hematopoietic stem cells in the bone marrow according to regional hypoxia. *Proc Natl Acad Sci U S A*, 104, 5431-5436.
67. Peacock, C.D., Wang, Q., Gesell, G.S., Corcoran-Schwartz, I.M., Jones, E., Kim, J., Devereux, W.L., Rhodes, J.T., Huff, C.A., Beachy, P.A., Watkins, D.N., Matsui, W. (2007) Hedgehog signaling maintains a tumor stem cell compartment in multiple myeloma. *Proceedings of the National Academic of Sciences USA*, 104, 4048-4053.
68. Pilarski, L.M., Hipperson, G., Seeberger, K., Pruski, E., Coupland, R.W., Belch, A.R. (2000) Myeloma progenitors in the blood of patients with aggressive or minimal disease: engraftment and self-renewal of primary human myeloma in the bone marrow of NOD SCID mice. *Blood*, 95, 1056-1065.
69. Pilarski, L.M., Jensen, G.S. (1992) Monoclonal circulating B cells in multiple myeloma. A continuously differentiating, possibly invasive, population as defined by expression of CD45 isoforms and adhesion molecules. *Hematology Oncology Clinics of North America*, 6, 297-322.
70. Pilarski, L.M., Masellis-Smith, A., Szczeppek, A., Mant, M.J., Belch, A.R. (1996) Circulating clonotypic B cells in the biology of multiple myeloma: speculations on the origin of myeloma. *Leukemia and Lymphoma*, 22, 375-383.
71. Prindull, G. & Zipori, D. (2004) Environmental guidance of normal and tumor cell plasticity: epithelial mesenchymal transitions as a paradigm. *Blood*, 103, 2892-2899.
72. Rajkumar, S.V., Leong, T., Roche, P.C., Fonseca, R., Dispenzieri, A., Lacy, M.Q., Lust, J.A., Witzig, T.E., Kyle, R.A., Gertz, M.A., Greipp, P.R. (2000) Prognostic value of bone marrow angiogenesis in multiple myeloma. *Clinical Cancer Research*, 6, 3111-3116.
73. Rajkumar, S.V., Mesa, R.A., Fonseca, R., Schroeder, G., Plevak, M.F., Dispenzieri, A., Lacy, M.Q., Lust, J.A., Witzig, T.E., Gertz, M.A., Kyle, R.A., Russell, S.J., Greipp, P.R. (2002) Bone marrow angiogenesis in 400 patients with monoclonal gammopathy of undetermined significance, multiple myeloma, and primary amyloidosis. *Clinical Cancer Research*, 8, 2210-2216.
74. Rasmussen, T., Haaber, J., Dahl, I.M., Knudsen, L.M., Kerndrup, G.B., Lodahl, M., Johnsen, H.E., Kuehl, M. (2010) Identification of translocation products but not K-RAS mutations in memory B cells from patients with multiple myeloma. *Haematologica*, 95, 1730-1737.
75. Rasmussen, T., Jensen, L., Johnsen, H.E. (2000) Levels of circulating CD19+ cells in patients with multiple myeloma. *Blood*, 95, 4020-4021.
76. Rasmussen, T., Lodahl, M., Hancke, S., Johnsen, H.E. (2004) In multiple myeloma clonotypic CD38- /CD19+ / CD27+ memory B cells recirculate through bone marrow, peripheral blood and lymph nodes. *Leukemia and Lymphoma*, 45, 1413-1417.
77. Reiman, T., Seeberger, K., Taylor, B.J., Szczeppek, A.J., Hanson, J., Mant, M.J., Coupland, R.W., Belch, A.R., Pilarski, L.M. (2001) Persistent preswitch clonotypic myeloma cells correlate with decreased survival: evidence for isotype switching within the myeloma clone. *Blood*, 98, 2791-2799.
78. Rossi, E.A., Rossi, D.L., Stein, R., Goldenberg, D.M., Chang, C.H. (2010) A bispecific antibody-IFN α 2b immunocytokine targeting CD20 and HLA-DR is highly toxic to human lymphoma and multiple myeloma cells. *Cancer Research*, 70, 7600-7609.
79. Seidel, S., Garvalov, B.K., Wirta, V., von Stechow, L., Schänzer, A., Meletis, K., Wolter, M., Sommerlad, D., Henze, A.T., Nister, M., Reifenberger, G., Lundeberg, J., Frisen, J., Acker, T. (2010) A hypoxic niche regulates glioblastoma stem cells through hypoxia inducible factor 2 alpha. *Brain*, 133, 983-995.
80. Shih, A.H., Holland, E.C. (2006) Notch signaling enhances nestin expression in gliomas. *Neoplasia*, 8, 1072-1082.
81. Soeda, A., Park, M., Lee, D., Mintz, A., Androutsellis-Theotokis, A., McKay, R.D., Engh, J., Iwama, T., Kunisada, T., Kassam, A.B., Pollack, I.F., Park, D.M. (2009) Hypoxia promotes expansion of the CD133-positive glioma stem cells through activation of HIF-1 α . *Oncogene*, 28, 3949-3959.
82. Spisek, R., Kukreja, A., Chen, L.C., Matthews, P., Mazumder, A., Vesole, D., Jagannath, S., Zebroski, H.A., Simpson, A.J., Ritter, G., Durie, B., Crowley, J., Shaughnessy, J.D., Jr., Scanlan, M.J., Gure, A.O., Barlogie, B., Dhodapkar, M.V. (2007) Frequent and specific immunity to the embryonic stem cell-associated antigen SOX2 in patients with monoclonal gammopathy. *Journal of Experimental Medicine*, 204, 831-840.
83. Srinivasan, V., Sivaramakrishnan, H., Karthikeyan, B. (2011) Detection, isolation and characterization of principal synthetic route indicative impurities in verapamil hydrochloride. *Scientia Pharmaceutica*, 79, 555-568.
84. Svachova, H., Pour, L., Sana, J., Kovarova, L., Raja, K.R., Hajek, R. (2011) Stem cell marker nestin is expressed in plasma cells of multiple myeloma patients. *Leukemia Research*, 35, 1008-1013.
85. Szczeppek, A.J., Bergsagel, P.L., Axelsson, L., Brown, C.B., Belch, A.R., Pilarski, L.M. (1997) CD34+ cells in the blood of patients with multiple myeloma express CD19 and IgH mRNA and have patient-specific IgH VDJ gene rearrangements. *Blood*, 89, 1824-1833.
86. Szczeppek, A.J., Seeberger, K., Wizniak, J., Mant, M.J., Belch, A.R., Pilarski, L.M. (1998) A high frequency of circulating B cells share clonotypic Ig heavy-chain VDJ rearrangements with autologous bone marrow plasma cells in multiple myeloma, as measured by single-cell and in situ reverse transcriptase-polymerase chain reaction. *Blood*, 92, 2844-2855.

87. Takahashi, K., Yamanaka, S. (2006) Induction of pluripotent stem cells from mouse embryonic and adult fibroblast cultures by defined factors. *Cell*, 126, 663-676.
88. Taylor, B.J., Kriangkum, J., Pittman, J.A., Mant, M.J., Reiman, T., Belch, A.R., Pilarski, L.M. (2008) Analysis of clonotypic switch junctions reveals multiple myeloma originates from a single class switch event with ongoing mutation in the isotype-switched progeny. *Blood*, 112, 1894-1903.
89. Treon, S.P., Pilarski, L.M., Belch, A.R., Kelliher, A., Preffer, F.I., Shima, Y., Mitsiades, C.S., Mitsiades, N.S., Szczepek, A.J., Ellman, L., Harmon, D., Grossbard, M.L. & Anderson, K.C. (2002) CD20-directed serotherapy in patients with multiple myeloma: biologic considerations and therapeutic applications. *J Immunother*, 25, 72-81.
90. Trepel, M., Martens, V., Doll, C., Rahlff, J., Gösch, B., Loges, S., Binder, M. (2012) Phenotypic detection of clonotypic B cells in multiple myeloma by specific immunoglobulin ligands reveals their rarity in multiple myeloma. *PLoS One*, 7, e31998.
91. Walker, B.A., Wardell, C.P., Melchor, L., Brioli, A., Johnson, D.C., Kaiser, M.F., Mirabella, F., Lopez-Corral, L., Humphray, S., Murray, L., Ross, M., Bentley, D., Gutiérrez, N.C., Garcia-Sanz, R., San Miguel, J., Davies, F.E., Gonzalez, D. & Morgan, G.J. (2013) Intraclonal heterogeneity is a critical early event in the development of myeloma and precedes the development of clinical symptoms. *Leukemia*.
92. Wu, C., Alman, B.A. (2008) Side population cells in human cancers. *Cancer Letters*, 268, 1-9.
93. Xia, X., Lemieux, M.E., Li, W., Carroll, J.S., Brown, M., Liu, X.S., Kung, A.L. (2009) Integrative analysis of HIF binding and transactivation reveals its role in maintaining histone methylation homeostasis. *Proceedings of the National Academy of Sciences USA*, 106, 4260-4265.
94. Yaccoby, S. (2005) The phenotypic plasticity of myeloma plasma cells as expressed by dedifferentiation into an immature, resilient, and apoptosis-resistant phenotype. *Clinical Cancer Research*, 11, 7599-7606.
95. Yaccoby, S., Epstein, J. (1999) The proliferative potential of myeloma plasma cells manifest in the SCID-hu host. *Blood*, 94, 3576-3582.
96. Yata, K., Yaccoby, S. (2004) The SCID-rab model: a novel in vivo system for primary human myeloma demonstrating growth of CD138-expressing malignant cells. *Leukemia*, 18, 1891-1897.
97. Yoshida, Y., Takahashi, K., Okita, K., Ichisaka, T., Yamanaka, S. (2009) Hypoxia enhances the generation of induced pluripotent stem cells. *Cell Stem Cell*, 5, 237-241.
98. Yu, J., Vodyanik, M.A., Smuga-Otto, K., Antosiewicz-Bourget, J., Frane, J.L., Tian, S., Nie, J., Jonsdottir, G.A., Ruotti, V., Stewart, R., Slukvin, I.I., Thomson, J.A. (2007) Induced pluripotent stem cell lines derived from human somatic cells. *Science*, 318, 1917-1920.
99. Zojer, N., Kirchbacher, K., Vesely, M., Hübl, W. & Ludwig, H. (2006) Rituximab treatment provides no clinical benefit in patients with pretreated advanced multiple myeloma. *Leuk Lymphoma*, 47, 1103-1109.

SAFETY AND EFFICACY OF ENDOVASCULAR SONOLYSIS USING THE EKOSONIC™ ENDOVASCULAR SYSTEM IN ACUTE STROKE PATIENTS

M. Kuliha, M. Roubec, T. Jonszta, J. Krajča, D. Czerny, A. Krajina, K. Langová, R. Herzig, V. Procházka, and D. Školoudík

From the Comprehensive Stroke Center (M.K., M.R., D.Š., T.J., J.K., D.C., V.P.), Department of Neurology, Faculty of Medicine, Ostrava University and University Hospital Ostrava, Ostrava, Czech Republic; Comprehensive Stroke Center (M.K., R.H., D.Š.), Department of Neurology, Faculty of Medicine and Dentistry, Palacký University and University Hospital Olomouc, Olomouc, Czech Republic; Comprehensive Stroke Center, Department of Radiology (A.K.), Faculty of Medicine, Charles University and University Hospital Hradec Králové, Hradec Králové, Czech Republic; and Department of Biophysics (K.L.), Faculty of Medicine and Dentistry, Institute of Molecular and Translational Medicine, Palacký University, Olomouc, Czech Republic.

Originally published in American journal of neuroradiology 2013; 34(7): 1401-1406

Consent to the publication of 22nd April 2014

ABSTRACT

Background and Purpose:

Sonolysis is a new therapeutic procedure for arterial recanalization. The aim was to confirm the safety and efficacy of endovascular sonolysis using EkoSonic™ endovascular system in subjects with acute ischemic stroke (AIS).

Materials and Methods:

AIS patients with occlusion of the middle cerebral artery (MCA) or basilar artery (BA) occlusion were enrolled consecutively in this prospective study. The control group (44 MCA and 12 BA occlusions) was selected from historical controls. ES started within 8 h after stroke onset. NIHSS upon hospital admission, after 24 h and 7 days, arterial recanalization, early neurological improvement, symptomatic intracerebral hemorrhage (SICH), and favorable 3-month clinical outcome defined as a modified Rankin scale (mRS) score of 0-2 were evaluated by statistical means.

Results:

Fourteen patients (10 males; mean age, 65.1±11.2 years; median NIHSS, 16.5) underwent ES. Arterial recanalization after endovascular treatment was achieved in 6 of 7 (85.7%) patients with MCA occlusion (4 complete recanalizations) and in all 7 (100%) patients with BA occlusion (6 complete recanalizations). No (0%) SICH or periprocedural complications occurred. Seven (50%) patients were independent at 3 months (median mRS=2). Early neurological improvement and favorable clinical outcome were significantly more frequent in ES patients with MCA occlusion than in controls (100% and 71.4% versus 4.6% and 13.6% patients, p=0.0001 and p=0.003, respectively). Three-month mortality was significantly lower in ES patients with BA occlusion than in controls (0% versus 66.7% patients, p=0.013).

Conclusion:

In this small study ES allowed safe and potentially effective revascularization in patients experiencing AIS.

INTRODUCTION

Acute occlusion of cervical or intracranial arteries is the most common cause of ischemic stroke (IS). Detection of arterial occlusion during the first 6 h after the onset of IS is possible in ≤70% of patients [1-4]. Clinical studies have shown that the prognosis of patients with occlusion of the intracranial arteries in the acute phase of an IS is worse when compared with patients without occlusion of a major intracranial artery [5]. One of the most important prognostic factors in patients with occlusion of intracranial arteries is the time to recanalization [6-9].

Data from a meta-analysis of 53 clinical trials (2,066 patients) suggest that early recanalization is present in only 24.1% of patients without specific treatment (spontaneous recanalization), 46.2% of patients treated with intravenous thrombolysis (IVT), 63.2% of patients treated with intraarterial thrombolysis (IAT), 67.5% of patients treated with combined IVT-IAT, and in ≤83.6% of patients treated by mechanical methods [5].

The options for acceleration of recanalization of intracranial-artery occlusion are: IVT, IAT or combined thrombolysis; mechanical recanalization using several mechanical devices for thrombectomy and/or stenting; and remote or local sonolysis [10-24]. Endovascular sonolysis can be used to accelerate and achieve recanalization of intracranial-artery occlusion [22-24].

The aim of the present study was to confirm the safety and efficacy of endovascular sonolysis using the EkoSonic™ Endovascular System in acute IS patients with occlusion of the middle cerebral artery (MCA) or basilar artery (BA) within 8 h after stroke onset.

MATERIALS AND METHODS

Patients

Consecutive patients who fulfilled the following inclusion criteria between August 2009 and September 2011 were recruited into this prospective case-control study: acute IS due to occlusion of the MCA or BA detected using CTA; presenting with a National Institutes of Health Stroke Scale (NIHSS) score of 4-25 upon hospital admission; contraindicated to IVT or with persistent artery occlusion 60 min after IVT commencement; aged 18-80 years; with start of therapy within 8 h of symptom onset. Patients with a modified Rankin score (mRS) >1 before stroke onset, intracranial hemorrhage, or brain tumor detected using CT, were excluded from the study. The control group was selected from consecutive historical controls fulfilling the same inclusion and exclusion criteria hospitalized between July 2006 and January 2008 (i.e. before the era of mechanical recanalization at the Stroke Center in which the study was carried out).

Diagnostics

Upon hospital admission, physical examination, blood samples, electrocardiography (ECG), chest radiography, and standard neurological evaluation by a certified neurologist using the NIHSS were undertaken. These tests were followed by CT of the brain and by CTA of the cervical and brain arteries. Duplex sonography of the cervical portion of the carotid and vertebral arteries, and transcranial color-coded duplex sonography (TCCS) were done before and 60 min after IVT commencement.

Neurological and physical examinations were repeated after 24 h, 7 days and 90 days. Early neurological improvement (ENI) was defined as a NIHSS of 0 or 1 point at 24 h after treatment or a decrease of ≥ 4 points in NIHSS score 24 h after treatment. The mRS was used for the evaluation of clinical outcome 90 days after IS stroke onset with a favorable clinical outcome defined as mRS 0-2. Intracranial bleeding detected in the control brain CT 24 h after therapy onset was recorded. Intracranial bleeding with worsening of neurological symptoms (≥ 4 points in the NIHSS) was classified as "symptomatic intracerebral hemorrhage" (SICH) [25].

Treatment

Patients were treated at a Comprehensive Stroke Center with 24/7 accessibility to IVT and endovascular interventions, and underwent standard treatment [26]. All patients who fulfilled the Safe Implementation of Thrombolysis in Stroke-Monitoring Study (SITS-MOST) criteria for IVT were treated using recombinant tissue plasminogen activator (rt-PA; 0.9 mg/kg) within 4.5 h after IS onset [26,27]. Anticoagulation therapy (oral, subcutaneous or intravenous) and oral administration of acetylsalicylic acid or other antiplatelet agents were used as standard treatment for patients 24 h after IS onset according to guidelines set by the European Stroke Organisation guidelines [26].

Endovascular treatment

For vessel occlusion, verification was confirmed in all patients using four-vessel diagnostic digital subtraction angiography (DSA; General Electric Innova 4100, GE Healthcare, Waukesha, WI, USA). After intraarterial administration of heparin (total dose 50 IU/kg) and placement of the EkoSonic™ Endovascular Catheter (EKOS Corporation, Bothell, WA, USA) within the occluded segment of the artery, the insonation with pulsed high-frequency (2.05-2.35 MHz) and low-power (400 mW/cm²) ultrasound waves and local administration of rt-PA directly into the thrombus were started simultaneously. Patients without contraindication to thrombolysis treatment received rt-PA (15 mg/h). The maximum calculated total dosage was ≤ 20 mg of rt-PA and the endovascular sonolysis was ≤ 60 min.

In the case of partial recanalization or early reocclusion after endovascular sonolysis, patients had additional treatment with angioplasty and stent (Enterprise, Cordis Neurovascular, Miami Lakes, FL, USA or Wingspan, Boston Scientific, San Leandro, CA, USA) implantation. In all patients with stent implantation, 500 mg of ASA was administered intravenously at the end of endovascular procedure. Subsequently, within next 2 hours, 150 mg of oral clopidogrel followed by 6-week dual oral antiplatelet therapy (100 mg ASA daily + 75 mg clopidogrel daily) were used in all cPTAS patients as instituted therapy regimen. Repeated diagnostic angiography of the treated region was undertaken to assess the

Table 1. Thrombolysis in Cerebral Ischemia (TICI) criteria [28].

TICI flow grade	Characteristics
Grade 0	No perfusion
Grade I	Perfusion past the initial occlusion, but no distal branch filling
Grade IIa	Partial perfusion with incomplete distal filling of < 50% of the expected territory
Grade IIb	Partial perfusion with incomplete distal filling of 50-99% of the expected territory
Grade IIc	Near complete perfusion but with delay in contrast runoff
Grade III	Full perfusion with normal filling of distal branches in a normal hemodynamic fashion

recanalization grade according to Thrombolysis in Cerebral Ischemia (TICI) criteria - see Table 1. [28]

Evaluation of recanalization

The efficacy of recanalization was evaluated at the end of the endovascular procedure using TICI criteria. Final recanalization status TICI IIa or IIb were considered to be “partial recanalization” and final status TICI IIc or III to be “complete recanalization”. An experienced, independent radiologists (AK) blinded to the study protocol evaluated all findings before definitive assessment of the diagnosis.

Statistical analyses

Kolmogorov-Smirnov and Shapiro-Wilk methods were used for testing the fit of the parameters calculated to a normal distribution. Data with a normal distribution are reported as the mean \pm standard deviation. All parameters that did not fit a normal distribution are presented as median and interquartile ranges (IQRs); the Mann-Whitney U-test and Fisher exact test were used for comparisons between groups. Statistical analyses were carried out using SPSS 14.0 software (SPSS, Chicago, IL, USA). $P < 0.05$ was considered significant.

Approval of the study protocol by the Ethics Committee

The entire study was conducted in accordance with the Helsinki Declaration of 1975 (as revised in 2004 and 2008). The Ethics Committee of the Stroke Center in which the study was carried out approved the study. All patients signed informed consent forms for treatment. Independent witnesses verified the signatures if there were technical problems.

RESULTS

Fourteen patients (10 males; age, 47-80, (mean 65.1 ± 11.2) years) with acute IS due to MCA occlusion or BA occlusion were enrolled in this prospective study. Five patients fulfilling criteria for IVT commencement received rt-PA within 4.5 h after IS onset. The control group comprised 44 acute IS patients with MCA occlusion and 12 patients with BA occlusion (demographic data are shown in Table 2). Median NIHSS upon hospital admission did not differ significantly between treatment and control groups (MCA: 15 versus 15.5; BA: 27 versus 24; $P > 0.05$). General anesthesia was used in 6 patients treated using the EkoSonicTM endovascular system (EKOS), conscious sedation was applied in 8 patients.

Time of onset to treatment (IVT, endovascular treatment) commencement, length of endovascular procedure and recanalization at the end of endo-

Table 2. Demographic data of the study group

	EKOS	Control	P	EKOS	Control	P
	MCA	MCA		BA	BA	
No. of subjects	7	44	-	7	12	-
Age (mean) (yr)	69.1 \pm 11.4	68.7 \pm 11.2	<.05	61.09.4	68.912.9	<.05
Males (No.) (%)	5 (71.4%)	22 (50.0%)	<.05	5 (71.4%)	9 (75.0%)	<.05
Arterial hypertension (No.) (%)	7 (100%)	33 (75.0%)	<.05	4 (57.1%)	9 (75.0%)	<.05
Diabetes mellitus (No.) (%)	2 (28.6%)	8 (18.2%)	<.05	1 (14.3%)	3 (25.0%)	<.05
Hyperlipidemia (No.) (%)	2 (28.6%)	9 (20.5%)	<.05	2 (28.6%)	5 (41.7%)	<.05
Atrial fibrillation (No.) (%)	2 (28.6%)	19 (43.2%)	<.05	2 (28.6%)	4 (33.3%)	<.05
Smoking (No.) (%)	2 (28.6%)	8 (18.2%)	<.05	1 (14.3%)	2 (25.0%)	<.05
Heavy alcohol consumption (No.) (%)	0 (0%)	1 (2.3%)	<.05	0 (0%)	0 (0%)	<.05
ICA/VA stenosis 50% (No.) (%)	1/0 (14.3/0%)	7/0 (15.9/0%)	<.05	0/3 (0/42.3%)	0/4 (0/33.3%)	<.05
Left hemisphere (No.) (%)	3 (42.9%)	25 (56.8%)	<.05	-	-	-
Use of acetylsalicylic acid (No.) (%)	2 (28.6%)	15 (34.1%)	<.05	2 (28.6%)	4 (33.3%)	<.05
Stroke in medical history (No.) (%)	1 (14.3%)	7 (15.9%)	<.05	1 (14.3%)	3 (25.0%)	<.05
Myocardial infarction in history (No.) (%)	1 (14.3%)	8 (18.2%)	<.05	1 (14.3%)	2 (16.7%)	<.05
IV thrombolysis (No.) (%)	3 (42.9%)	26 (59.1%)	<.05	2 (28.6%)	6 (50.0%)	<.05
IAT (No.) (%)	6 (85.7%)	0 (0%)	-	7 (100%)	0 (0%)	-
cPTAS (No.) (%)	3 (42.9%)	0 (0%)	-	5 (71.4%)	0 (0%)	-

BA-basilar artery; cPTAS-cerebral percutaneous transluminal angioplasty with stenting; EKOS-EkoSonicTM Endovascular System; IQR-interquartile range; IAT-intraarterial thrombolysis; IVT-intravenous thrombolysis; MCA-middle cerebral artery; SD-standard deviation; VA-vertebral artery

Table 3. Recanalization at the end of use of the EkoSonic™ Endovascular System (EKOS) in patients with MCA and BA occlusion and procedural data.

	MCA	BA	All
Complete MCA recanalization (TICI IIc-III)	4 (57.1%)	6 (85.7%)	10 (71.4%)
Partial MCA recanalization (TICI IIa-IIb)	2 (28.6%)	1 (14.3%)	3 (21.4%)
No recanalization (TICI 0-I)	1 (14.3%)	0 (0%)	1 (7.1%)
Time from onset to admission (mean) (min)	139.3±76.6	171.4±76.4	155.4±78.1
Time from onset to EKOS start (mean) (min)	163.6±75.5	210.7±78.6	187.1±80.6
Length of procedure (mean) (min)	67.1±11.4	57.9±9.4	62.5±28.0
Time onset to EKOS start,			
mean±SD (min)	163.6±75.5	210.7±78.6	187.1±80.6
Length of procedure,			
mean±SD (min)	67.1±11.4	57.9±9.4	62.5±28.0

Note:—EKOS indicates EkoSonic Endovascular System.

BA-basilar artery; MCA-middle cerebral artery; TICI-Thrombolysis in Cerebral Ischemia, IVT-intravenous thrombolysis; SD-standard deviation

vascular intervention are given in Table 3. Mean time onset to endovascular treatment start was 187.1 ± 80.6 min and mean length of procedure was 62.5 ± 28.0 min. Complete recanalization of the MCA and BA after endovascular treatment (combined with percutaneous transluminal angioplasty with stenting (cPTAS) if when indicated) was achieved in 4 (57.1%, 95% CI: 18.4-90.1%) and 6 (85.7%, 95% CI: 42.1-99.6%) patients, respectively. Furthermore, partial recanalization was achieved in 2 (28.6%, 95% CI: 3.7-71.0%) patients with MCA occlusion and in 1 (14.3%, 95% CI: 0.4-57.9%) patient with BA occlusion.

NIHSS at day 7 and 90-day mRS were significantly better in acute IS patients after endovascular sonolysis (in combination with cPTAS when indicated) than in controls (Table 4). ENI and favorable clinical outcome at day 90 were achieved in 7 (100%, 95% CI: 65.2-100%) and 5 (71.4%, 95% CI: 29.0-96.3%) patients with MCA occlusion treated using the EKOS in comparison with 2 (4.5%, 95% CI: 0.6-15.5%) and 6 (13.6%, 95% CI: 5.2-27.4%) control group patients (P=0.0001 and P=0.003). SICH did not occur in any patient treated using the EKOS in comparison with 3.6% of control-group patients (Table 4). No periprocedural complication occurred in patients who underwent endovascular treatment.

Seven-day mortality and 3-month mortality were significantly lower in patients with BA occlusion treated using endovascular sonolysis than in the control group (P<0.05) (Table 4). No significant difference in mortality was detected in patients with MCA occlusion.

DISCUSSION

The results of the present study indicated the safety of endovascular sonolysis using the EKOS system without SICH or periprocedural complications. No occurrence of SICH is even more remarkable when

comparing it to the results of the Interventional Management of Stroke (IMS) II trial, in which SICH occurred mainly (all but one) in patients with NIHSS ≥ 20, although in the present study the number of patients with NIHSS ≥ 20 was 6 (42.9%) [23] and, all patients received heparin, 5 (35.7%) IVT, 13 (92.9%) IAT and 8 (57.1%) patients were treated with dual antiplatelet therapy. This result may be biased by a small number of patients.

In the study, three-month mortality was observed in 14.3% of patients. The efficacy of endovascular sonolysis (in combination with cPTAS when indicated) was suggested. Complete or partial MCA recanalization after endovascular treatment was achieved in 92.9% of cases.

In the last decade, the number of methods used for the acceleration of arterial recanalization has increased greatly. In addition to pharmacological methods, especially IVT and IAT, mechanical neuro-interventional methods (e.g. Merci Retrieval System®, Penumbra System®, Solitaire® stent, Trevo Pro®, Catch device®, Phenox Clot Retriever®, BONNET Intracranial Flow Restoration Device® or pRESET Thrombectomy Retriever®, direct stent placement, EKOS) have been introduced into clinical practice [10-19]. One of these, the EKOS is the first tool system approved by the Food and Drug Administration, which allows local, endovascular application of high-frequency (2 MHz) and low-power (400 W/cm²) ultrasound in clinical practice with or without simultaneous catheter-directed thrombolysis by application of thrombolytic drugs [22-24].

Several in-vitro, in-vivo and clinical studies have shown the potential effect of ultrasound (sonolysis) to accelerate clot lysis. The first clinical studies with endovascular sonolysis were used for the recanalization of coronary arteries. In the Analysis of Coronary Ultrasound Thrombolysis Endpoints in Acute Myo-

Table 4. Clinical results in the particular subgroups.

	EKOS	Control	P	EKOS	Control	P
	MCA	MCA		BA	BA	
Baseline NIHSS (median) (IQR)	15 (10-18)	15.5 (12-20)	<.05	27 (14.5-33)	24 (12-32)	<.05
NIHSS 24 hr (median) (IQR)	4 (2-6)	16 (12-20)	.0001	10 (7-25)	24 (14-28)	<.05
NIHSS day 7 (median) (IQR)	2 (1.5-4)	15.5 (7-20)	.0001	6 (4.5-19)	33 (8-33)	.049
Presence of ENI after 24 hours (No.) (%)	7 (100%)	2 (4.6%)	.0001	4 (57.1%)	2 (16.7%)	<.05
90-day mRS (median) (IQR)	1 (1-3.5)	5 (3-5)	.037	3 (2-4.5)	6 (4.5-6)	.034
mRS 0-3 at day 90 (No.) (%)	5 (71.4%)	8 (18.2%)	.008	4 (57.1%)	2 (16.7%)	<.05
mRS 0-2 at day 90 (No.) (%)	5 (71.4%)	6 (13.6%)	.003	2 (28.6%)	2 (16.7%)	<.05
SICH (No.) (%)	0 (0%)	1 (2.3%)	<.05	0 (0%)	1 (8.3%)	<.05
Malignant infarction (No.) (%)	0 (0%)	3 (6.8%)	<.05	0 (0%)	0 (0%)	<.05
7-day mortality (No.) (%)	0 (%)	3 (6.8%)	<.05	0 (%)	6 (50.0%)	.044
3-month mortality (No.) (%)	2 (28.6%)	10 (22.7%)	<.05	0 (0%)	8 (66.7%)	.013

Note:—ENI indicates early neurologic improvement; EKOS, EkoSonic Endovascular System; SICH, symptomatic intracerebral hemorrhage; IQR, interquartile range.

BA-basilar artery; EKOS-EkoSonic™ Endovascular System; ENI-early neurological improvement; MCA-middle cerebral artery; IQR-interquartile range; mRS-modified Rankin scale, SICH-Symptomatic intracerebral hemorrhage

cardial infarction (ACUTE) study, low-frequency (45 kHz) ultrasound was used with high intensity (18 W/cm²) in the treatment of acute occlusion of coronary arteries [29]. Complete recanalization was achieved in 87% patients. No side effects were observed during therapy, and 80% of patients showed clinical improvement. Other studies showed the effect of endovascular sonolysis by EKOS in patients with deep venous thrombosis of the lower extremities and in patients with pulmonary embolism [30-35]. Complete recanalization was achieved in 85.2-96.0% of patients with arterial thrombosis [34,35] and in 83.0% patients with venous thrombosis [31].

Mahon et al. [22] published the first experience with endovascular sonolysis using the EKOS in patients with acute IS. They used a combination of IAT employing rt-PA with endovascular ultrasound in 10 patients with MCA occlusion and in 4 patients with BA occlusion. Partial or complete recanalization was detected in 57% patients, and there were no adverse effects during therapy. Three patients died within the first 24 h, the mean mRS in survivors with MCA occlusion was 2, and in survivors with vertebrobasilar occlusion was 3.

The system was tested subsequently in the Interventional Management of Stroke (IMS) II with promising results [23]. Complete recanalization was achieved within 60 min and 120 min in 12 (41%) and 20 (68.9%) patients, respectively. SICH occurred in 9.9% of subjects in IMS-II, including 3.8% of patients treated with intravenous rt-PA alone. Direct perforation of vessels, primary subarachnoid hemorrhage, or intracranial dissection was not documented in the subjects treated. The results of the present study showed an even higher prevalence of recanalization without SICH occurrence.

The complex effect of ultrasound on the acceleration of thrombus lysis is incompletely understood, but

it is assumed that the ultrasonographic waves accelerate enzymatic fibrinolysis primarily by non-thermal mechanisms. Mechanisms that have been postulated include: increasing the transport of fibrinolytic agents into the thrombus by mechanical disruption of its structure [36]; direct activation of fibrinolytic enzymes (either mechanical dissociation of the complex molecules, in which fibrinolytic enzymes are inactivated by binding to their inhibitors, or irritation of the endothelium with increased production of fibrinolytic enzymes [37,38]); and transient peripheral (capillary) vasodilatation caused probably by increased production of nitric oxide in the endothelium [39,40]. Radiation force and acoustic cavitation are mechanical effects of ultrasound that have also been postulated to be a potential mechanism [41]. Several clinical studies have tested the feasibility and safety of other mechanical devices, especially of the Merci Retrieval System, Penumbra System, Solitaire stents and direct placement of stents. The reported prevalence of recanalization in those studies ranged from 46% for the Merci Retriever System [10], 84% for the Penumbra System [11,12], 90% for the Solitaire stent [13], and up to 100% for direct stent placement [18,19]. Periprocedural complications varied between 3.4% and 9.0%; SICH occurred in 10-11% and the mortality was 32.8-35.0%. Favorable clinical outcome (defined as mRS = 0-2) ranged from 36% up to 74% [10-19]. The present study showed that the prevalence of recanalization and favorable outcome in patients treated by endovascular sonolysis in combination with local or systemic thrombolysis (and cPTAS if indicated) was comparable (or even superior) to other endovascular methods, especially in patients with MCA occlusion. Moreover it seemed to be safer.

Previous studies primarily involved patients with occlusion in the anterior circulation. Nevertheless,

the likelihood of achieving a favorable outcome in patients with a BA occlusion is worse than in those with an MCA occlusion. More than 90% of patients with a BA occlusion and any type of treatment die or have a permanent disability [42,43]. Studies have shown that patients treated by antithrombotic drugs have a chance of favorable outcome of 7% but patients treated by IVT (or by a combination of IVT with intraarterial treatment) had a chance of favorable outcome of 41%. In patients treated intraarterially, partial or complete recanalization (defined as thrombolysis in myocardial infarction (TIMI) of 2-3) of BA at the end of an intraarterial procedure was found in 72% of patients; SICH was reported in 14% of patients [44]. Jung et al. [45] reported similar results in patients with BA occlusion treated by IAT (pro-urokinase) and/or mechanical interventions. Complete or partial recanalization was achieved in 69.8% of patients with favorable 3-month clinical outcome (defined as mRS of 0-3) achieved in 44% patients and with an occurrence of SICH of 0.9%. Those results are in agreement with the results of the present study, in which recanalization was achieved in 100% of patients with a favorable 3-month clinical outcome (defined as a mRS of 0-3, especially for the BA group) achieved in 57.1% of patients and with an occurrence of SICH of 0%.

Several limitations of the present study should be mentioned. It was a case-control study in which the main goal was to assess the safety and prevalence of recanalization of endovascular sonolysis using the EKOS. Although the criteria for SICH evaluation are well defined, the evaluation of recanalization of brain arteries remains subjective (even though in the present study a radiologist blinded to the study protocol evaluated vascular status). Finally, the open-label design of the present study with only blinded evaluation of recanalization in the TICI scale cannot prevent bias in the clinical evaluation of dependency (mRS) after 3 months. Furthermore, a low reliability of TICI scale for stroke trials should be also taken into account [46,47] and, even though independently reviewed, the interobserver correlation of TICI scale was not evaluated in the present study due to a small number of patients.

CONCLUSION

Endovascular treatment using the EKOS in combination with thrombolysis and cerebral percutaneous transluminal angioplasty and stenting seems to be a potentially effective therapeutic method for acute IS patients with MCA or BA occlusion after IVT failure or with a contraindication to IVT. Nevertheless, the efficacy of this endovascular treatment must be confirmed by large, prospective randomized trials.

ACKNOWLEDGEMENTS

The study was supported by grants from the Internal Grant Agency of the Ministry of Health of the Czech

Republic (numbers NT/11386-5/2010 and NT/11046-6/2010) and by grant number CZ.1.05/2.1.00/010030.

REFERENCES

1. Bar M, Školoudík D, Roubec M, et al. Transcranial duplex sonography and CT angiography in acute stroke patients. *J Neuroimaging* 2010;20:240-5.
2. Fieschi C, Argentino C, Lenzi GL, Sacchetti ML, Toni D, Bozzao L. Clinical and instrumental evaluation of patients with ischemic stroke within the first six hours. *J Neurol Sci* 1989;91:311-21.
3. Furlan A, Higashida R, Wechsler L, et al. Intra-arterial pro-urokinase for acute ischemic stroke. The PROACT II study: a randomized controlled trial. *Prolyse in Acute Cerebral Thromboembolism. JAMA* 1999;282:2003-11.
4. Wunderlich MT, Goertler M, Postert T, et al. Competence Network Stroke. Recanalization after thrombolysis: does a recanalization time window exist? *Neurology* 2007;68:1364-8.
5. Rha JH, Saver JL. The Impact of Recanalization on Ischemic Stroke Outcome. A Meta-Analysis. *Stroke* 2007;38:967-73.
6. van der Worp HB, van Gijn J. Clinical practice. Acute ischemic stroke. *N Engl J Med* 2007;357:572-9.
7. National Institute of Neurological Disorders and Stroke rt-PA Study Group. Tissue plasminogen activator for acute ischemic stroke. *New Engl Med* 1995;333:1581-7.
8. Smith WS, Sung G, Starkman S, et al. Safety and efficacy of mechanical embolectomy in acute ischemic stroke: results of the MERCI trial. *Stroke* 2005;36:1432-8.
9. Kerber CW, Barr JD, Berger RM, et al. Snare retrieval of intracranial thrombus in patients with acute stroke. *J Vasc Interv Radiol* 2002;13:1269-74.
10. Smith WS, Sung G, Saver J, et al. Mechanical Thrombectomy for Acute Ischemic Stroke Final Results of the Multi MERCI Trial. *Stroke* 2008;39:1205-12.
11. Penumbra Pivotal Stroke Trial Investigators. The Penumbra Pivotal Stroke Trial: safety and effectiveness of a new generation of mechanical devices for clot removal in intracranial large vessel occlusive disease. *Stroke* 2009;40:2761-8.
12. Grunwald IQ, Wakhloo AK, Walter S, et al. Endovascular Stroke Treatment Today. *Am J Neuroradiol* 2011;32:238-43.
13. Machi P, Costalat V, Lobotesis K, et al. Solitaire FR thrombectomy system: immediate results in 56 consecutive acute ischemic stroke patients. *J Neurointerv Surg* 2012;4:62-6.
14. Costalat V, Machi P, Lobotesis K, et al. Rescue, combined, and stand-alone thrombectomy in the management of large vessel occlusion stroke using the solitaire device: a prospective 50-patient single-center study: timing, safety, and efficacy. *Stroke* 2011;42:1929-35.
15. Nogueira RG, Levy EI, Gounis M, et al. The Trevo device: preclinical data of a novel stroke thrombectomy device in two different animal models of arterial thrombo-occlusive disease. *J NeuroIntervent Surg* 2011. DOI:10.1136/neurint-surg-2011-010053.
16. Mendonça N, Flores A, Pagola J, et al. Trevo System: Single-Center Experience with a Novel Mechanical Thrombectomy Device. *J Neuroimaging* 2011. DOI: 10.1111/j.1552-6569.2011.00666.x.
17. Mourand I, Brunel H, Costalat V, et al. Mechanical Thrombectomy in Acute Ischemic Stroke: Catch Device. *Am J Neuroradiol* 2011;32:1381-5.
18. Levy EI, Siddiqui AH, Crumlish A, et al. First Food and Drug Administration-approved prospective trial of primary intracranial stenting for acute stroke: SARIS (stent-assisted recanalization in acute ischemic stroke). *Stroke* 2009;40:3552-6.
19. Linfante I, Samaniego EA, Geisbüsch P, et al. Self-expandable stents in the treatment of acute ischemic stroke refractory to current thrombectomy devices. *Stroke* 2011;42:2636-8.

20. Skoloudik D, Bar M, Skoda O, et al. Safety and efficacy of the sonographic acceleration of the middle cerebral artery recanalization: results of the pilot thrombotripsy study. *Ultrasound Med Biol* 2008;34:1775-82.
21. Alexandrov AV, Molina CA, Grotta JC, et al. Ultrasound-enhanced systemic thrombolysis for acute ischemic stroke. *N Engl J Med* 2004;351:2170-8.
22. Mahon BR, Nesbit GM, Barnwell SL, et al. North American Clinical Experience with the EKOS MicroLysUS Infusion Catheter for the Treatment of Embolic Stroke. *Am J Neuroradiol* 2003;24:534-8.
23. IMS II Trial Investigators. The Interventional Management of Stroke (IMS) II Study. *Stroke* 2007;38:2127-35.
24. Jonszta T, Czerný D, Skoloudik D, et al. EkoSonicSVTM Endovascular System for Recanalization of the Basilar Artery Occlusion Report of 2 cases. *VASA* 2011;40:408-13.
25. Hacke W, Kaste M, Bluhmki E, et al. Thrombolysis with Alteplase 3 to 4.5 Hours after Acute Ischemic Stroke. *N Engl J Med* 2008;359:1317-29.
26. European Stroke Organisation [ESO] Executive Committee and the ESO Writing Committee 2008. Update Guidelines January 2009 New Elements. Available from: URL: http://www.eso-stroke.org/pdf/ESO_Extended_Thrombolysis_KSU.pdf ESOupdate.
27. Toni D, Lorenzano S, Puca E, et al. The SITS-MOST registry. *Neurol Sci* 2006;27(Suppl 3):260-2.
28. Noser EA, Shaltoni HM, Hall CE, Alexandrov AV, Garami Y, Caccayorin ED, Song JK, Grotta JC, Campbell MSIII. Aggressive mechanical clot disruption. A safe adjunct to thrombolytic therapy in acute stroke? *Stroke* 2005;36:292-296.
29. Rosenschein U, Roth A, Rassini T, et al. Analysis of coronary ultrasound thrombolysis endpoints in acute myocardial infarction [ACUTE trial]. Results of the feasibility phase. *Circulation* 1997;95:1411-6.
30. Ganguli S, Kalva S, Oklu R, et al. Efficacy of Lower-Extremity Venous Thrombolysis in the Setting of Congenital Absence or Atresia of the Inferior Vena Cava. *Cardiovasc Intervent Radiol* 2011. DOI: 10.1007/s00270-011-0247-2.
31. Grommes J, Strijkers R, Greiner A, et al. Safety and feasibility of ultrasound-accelerated catheter-directed thrombolysis in deep vein thrombosis. *Eur J Vasc Endovasc Surg* 2011;41:526-32.
32. Shah KJ, Scileppi RM, Franz RW. Treatment of pulmonary embolism using ultrasound-accelerated thrombolysis directly into pulmonary arteries. *Vasc Endovascular Surg* 2011;45:541-8.
33. Lin PH, Annambhotla S, Bechara CF, et al. Comparison of percutaneous ultrasound-accelerated thrombolysis versus catheter-directed thrombolysis in patients with acute massive pulmonary embolism. *Vascular* 2009;17(Suppl 3):S137-47.
34. Motarjeme A. Ultrasound-enhanced thrombolysis. *J Endovasc Ther.* 2007;14:251-6.
35. Ouriel K, Veith FJ, Sasahara AA. A comparison of recombinant urokinase with vascular surgery as initial treatment for acute arterial occlusion of the legs. Thrombolysis or Peripheral Arterial Surgery (TOPAS) Investigators. *N Engl J Med* 1998;338:1105-11.
36. Francis CW, Blinc A, Lee S, et al. Ultrasound accelerates transport of recombinant tissue plasminogen activator into clots. *Ultrasound Med Biol* 1995;21:419-24.
37. Skoloudik D, Fadrna T, Roubec M, et al. Changes in hemo-coagulation in acute stroke patients after one-hour sono-thrombolysis using a diagnostic probe. *Ultrasound Med Biol* 2010;36:1052-9.
38. Skoloudik D, Fadrná T, Bar M, et al. Changes in haemocoagulation in healthy volunteers after a 1-hour thrombotripsy using a diagnostic 2-4 MHz transcranial probe. *J Thromb Thrombolysis* 2008;26:119-24.
39. Suchkova VN, Baggs RB, Francis CW. Effect of 40-kHz ultrasound on acute thrombotic ischemia in a rabbit femoral artery thrombosis model: enhancement of thrombolysis and improvement in capillary muscle perfusion. *Circulation* 2000;101:2296-301.
40. Bardon P, Skoloudik D, Langova K, et al. Changes in blood flow velocity in the radial artery during 1-hour ultrasound monitoring with a 2-MHz transcranial probe - a pilot study. *J Clin Ultrasound* 2010;38:493-6.
41. Harvey EN. Biological aspects of ultrasonic waves, a general survey. *Biol Bull* 1930;59:306-25.
42. Schonewille WJ, Algra A, Serena J, et al. Outcome in patients with basilar artery occlusion treated conventionally. *J Neurol Neurosurg Psychiatry* 2005;76:1238-41.
43. Baird TA, Muir KW, Bone I. Basilar artery occlusion. *Neurocrit Care* 2004;1:319-29.
44. Schonewille WJ, Wijman CA, Michel P, et al. Treatment and outcomes of acute basilar artery occlusion in the Basilar Artery International Cooperation Study (BASICS): a prospective registry study. *Lancet Neurol* 2009;8:724-30.
45. Jung S, Mono ML, Fischer U, et al. Three-month and long-term outcomes and their predictors in acute basilar artery occlusion treated with intra-arterial thrombolysis. *Stroke* 2011;42:1946-51.
46. Tomsick T. TIMI, TIBI, TICI: I came, I saw, I got confused. *Am J Neuroradiol* 2007;28:382-4.
47. Kallmes DF. If you are not confused, then you are not paying attention. *Am J Neuroradiol* 2012; 33:975-6.

SHOULD MEAN ARTERIAL PRESSURE BE INCLUDED IN THE DEFINITION OF AMBULATORY HYPERTENSION IN CHILDREN?

Terezie Šuláková¹ MD, Ph.D., Janusz Feber² MD, FRCPC

¹ Department of Pediatrics, University Hospital Ostrava, Czech Republic

² Department of Pediatrics, Children's Hospital of Eastern Ontario, Ottawa, Canada

Originally published in *Pediatric nephrology* 2013; 28: 1105-1112

Consent to the publication of 27th March 2014 (3357090030260)

ABSTRACT

Background

The diagnosis of hypertension (HTN)/normotension (NT) on ambulatory blood pressure monitoring (ABPM) is usually based on systolic (SBP) or diastolic blood pressure (DBP). The goal of the study was to analyze whether the inclusion of mean arterial pressure (MAP) improves the detection of HTN on ABPM.

Methods

We retrospectively studied ABPM records in 229 children (116 boys, median age = 15.3 years) who were referred for evaluation of HTN. HTN was made if (A) MAP or SBP or DBP was < 1.65 SDS; (B) SBP or DBP was < 1.65 SDS, during 24h or daytime or nighttime in both definitions.

Results

Using definition A, 46/229 patients had HTN compared to definition B by which only 37/229 patients had HTN ($p=0.001$). The level of agreement between the two definitions was very good ($\kappa = 0.86 \pm 0.04$); however, 9 patients (19.5%) were missed by not using the MAP in the definition of HTN. These nine patients had only mild HTN with a median Z score of 1.69.

Conclusion

The inclusion of MAP in the definition of ambulatory HTN significantly increased the number of hypertensive patients. MAP may be very helpful in detecting mild HTN in patients with normal/borderline SBP and DBP.

Keywords

Mean arterial pressure, ambulatory blood pressure monitoring, hypertension, definition, children

INTRODUCTION

Ambulatory blood pressure monitoring (ABPM) is an important clinical and research tool for evaluation of hypertension (HTN). However, the interpretation of ABPM in children is more complex than in adults (1), as blood pressure (BP) levels (and BP upper limits of normal) vary with growth/body size. The normative pediatric ABPM values include age and height related systolic BP, diastolic BP and mean arterial pressure (MAP) percentiles and Z scores (2); however these

values do not provide an exact definition of ambulatory HTN. Consequently, published reports on HTN in children, suffer from the lack of a standardized approach to diagnose HTN. Most authors used the 95th percentile of the mean systolic and diastolic daytime and night-time BP as the cutoff values for HTN on ABPM (3, 4, 5, 6, 7). Some authors also report MAP (3, 4, 6, 8), night-time dipping (4, 5, 9, 10, 11, 12) and BP loads (8, 13). Moreover, various definitions of awake and sleep periods have been used, which may significantly influence the daytime/night-time BP levels (14, 7, 8). The most recent guidelines for interpretation of ABPM in children, suggest using the BP load in addition to the systolic and diastolic BP for staging of HTN (15) but it is still unclear what type of an elevated BP, (systolic or diastolic or MAP) over what period of time (24 hours, daytime, night-time) should be used to define HTN.

The MAP is not used routinely in clinical practice i.e. for the interpretation of ABPM in children, despite the fact that the MAP normative values have been published (2) and the MAP is directly measured by the oscillometric device (SpaceLab).

The objective of our study was to therefore analyze whether the addition of MAP to the definition of HTN, would increase the diagnostic efficacy of ABPM. We hypothesized that the inclusion of MAP would detect more ABPM-hypertensive children, especially those who have a borderline systolic or diastolic BP and/or those with higher BP loads.

PATIENTS AND METHODS

Patients

We performed a retrospective chart review of children who were referred to the Nephrology clinic in the Department of Pediatrics, University Hospital Ostrava, for assessment of HTN during the period from January 2003 to September 2008. Within this period, 229 patients (116 boys) had the ABPM completed on their initial visit without any anti-hypertensive therapy. The reasons for the investigation were: diabetes mellitus type 1 ($n=84$), primary hypertension ($n=22$), elevated office BP ($n=96$), syncope or collapse ($n=9$) and various kidney diseases

(n=18) including microscopic hematuria (n=5), transient proteinuria (n=3), status post tubulointerstitial nephritis (n=3), post unilateral nephrectomy for multicystic dysplastic kidney disease (n=3), minimal change nephrotic syndrome in long-term remission (n=1), post anaphylactoid purpura (n=1) and autosomal polycystic kidney disease (n=2). All of these patients maintained normal renal function without any significant proteinuria, although 15 diabetic patients had microalbuminuria.

Methods

At the time of ABPM measurements, the body height and weight were recorded. The body mass index (BMI) was then calculated as kg/m² and converted into standard deviation scores (SDS) based on reference values for healthy Czech children (www.oj-rech.cz/lesny/kompendum/foh.htm).

24-hour ambulatory blood pressure monitoring (ABPM)

ABPM was performed using the oscillometric device SpaceLabs 90217 (SpaceLabs Medical Inc., Redmond, Washington, USA). The monitor was programmed to measure the BP every 20 minutes during the day (6 a.m. - 10 p.m.) and every 30 minutes during the night (10 p.m. - 6 a.m.). Parents and children were instructed to keep a diary of daily activities during the ABPM measurement. However, in order to compare our results with the normative values for ABPM, we defined the daytime period as 8 a.m. to 8 p.m. and the night-time period as 12 p.m. to 6 a.m. (2, 16). The cuff size was determined by the measurement of mid-arm circumference and was approximately 40% of the arm circumference; the cuff was placed on the non-dominant arm. The patients were instructed to avoid vigorous physical exercise during ABPM

measurement, but to follow their usual daily activities. A minimum of 40 ABPM recordings was required to consider the ABPM as valid.

For analysis of ABPM results, we used Chronos-Fit software (version 1.05, P. Zuther and B. Lemmer, Chronos-Fit, <http://www.abpm-fit.de>). The following linear ABPM parameters were analyzed: MAP, systolic BP (SBP), diastolic BP (DBP) and BP load, measured over 24h, daytime and night-time periods. Average absolute values for MAP, SBP and DBP for all time periods were subsequently converted into SDS values using the most recent normative values (2). Night-time blood pressure dipping was calculated using the ratio of mean daytime/mean night-time of MAP, SBP and DBP. Non-dipping (absence of nocturnal BP fall of at least 10%) was defined as day/night ratio < 1.1 in MAP and/or SBP and/or DBP. The BP loads were analyzed based on the average BP load (MAP, SBP, DBP) for any given time period separately. BP load was defined as the percentage of valid ambulatory BP measures, above a set threshold value, such as the 95th percentile of BP for gender and height. The highest load from any given time period measured for MAP, SBP and DBP was then considered as the maximum BP load (max BPL).

Definition of normotension/hypertension on ABPM

The diagnosis of NT/HTN was made using two definitions:

(A) MAP included: Patients were considered as normotensive (NT-A) if their average MAP, SBP and DBP during 24h, daytime and night-time periods were simultaneously below 1.645 SDS, (95th percentile) regardless of their BP load and dipping/non-dipping status. Consequently, if one of the BP parameters (MAP, SBP or DBP) during the 24h, daytime or night-time periods was above 1.645 SDS, the patient was

Table 1: Basic characteristics of patients.

Parameter	DEFINITION A (with MAP)		DEFINITION B (without MAP)		P value
	NT	HTN	NT	HTN	
Number of patients	183	46	192	37	0.0001
Number of diabetics	60	24	64	20	< 0.0001
Number of normotensive patients	94/89	22/24	99/93	17/20	N/A
with kidney disease	18	0	18	0	NS
Age (years)	15.3 (12.9;16.8)	15.5 (13.2; 16.8)	15.3 (12.9;16.7)	15.7 (13.2; 17.0)	NS
Gender (male/female)	94/89	22/24	99/93	17/20	N/A
BMI (kg/m ²)	20.9 (18.2;23.9)	20.9 (19.1; 23.6)	21.0 (18.2; 23.9)	20.9 (19.1; 23.1)	NS
	8/33	3/5	8/35	3/3	N/A
BMI (SDS)	0.3 (-0.2; 1.1)	0.2 (-0.1;1.1)	0.3 (-0.2; 1.1)	0.2 (-0.1; 1.0)	NS
Height	168.0 (156.2; 177.0)	162.8 (159.2; 173.3)	168.0 (156.6; 176.0)	162.5 (158.9; 173.5)	NS
Weight	60.6 (47; 72.8)	59 (51.8; 70.4)	60.2 (48; 73)	58.9 (48.9; 70.2)	NS
Overweight/obesity	8/33	3/5	8/35	3/3	N/A

Values are expressed as mean \pm SD or median (interquartile range). DM = diabetes mellitus type 1, NT = normotensive patients, HTN = hypertensive patients, N/A = not available

Table 2: Results of ABPM.

Parameter	Method A		Method B		P value
	NT - A	HTN - A	NT - B	HTN - B	
MAP 24 h (SDS)	-0.01 (-0.5; 0.5)	1.5 (0.9; 1.9)*, **	0.1 (-0.5; 0.5)	1.6 (0.9; 2.1)*, **	<0.0001
MAP day (SDS)	0.01 (-0.7; 0.5)	1.3 (0.8; 1.8)*, **	0.03 (-0.6; 0.6)	1.3 (0.8; 1.9)*, **	<0.0001
MAP night (SDS)	0.3 (-0.4; 0.8)	1.8 (1.3; 2.1)*, **	0.4 (-0.3; 0.9)	1.8 (1.3; 2.1)*, **	<0.0001
SBP 24 h (SDS)	-0.4 (-1.1; 0.2)	1.4 (0.7; 1.8)*, **	-0.4 (-1.1; 0.4)	1.5 (0.8; 1.9)*, **	<0.0001
SBP day (SDS)	-0.4 (-1.0; -0.3)	1.3 (0.6; 1.8)*, **	-0.3 (-1.0; 0.4)	1.4 (0.6; 1.9)*, **	<0.0001
SBP night (SDS)	-0.3 (-0.9; -0.3)	1.3 (0.7; 1.8)*, **	-0.2 (-0.8; 0.3)	1.5 (0.7; 2.0)*, **	<0.0001
DBP 24 h (SDS)	-0.3 (-0.7; 0.3)	1.1 (0.5; 1.9)*, **	-0.2 (-0.7; 0.3)	1.2 (0.4; 1.9)*, **	<0.0001
DBP day (SDS)	-0.2 (-0.9; 0.2)	0.4 (-0.04; 1.5)*, **	-0.2 (0.9; 0.2)	0.3 (-0.02; 1.7)*, **	<0.0001
DBP night (SDS)	0.1 (-0.6; 0.7)	1.5 (0.8; 2.1)*, **	0.1 (-0.5; 0.7)	1.7 (0.8; 2.2)*, **	<0.0001
MAP D/N	1.2 (1.1; 1.2)	1.2 (1.1; 1.2)	1.2 (1.1; 1.2)	1.2 (1.1; 1.2)	NS
SBP D/N	1.2 (1.1; 1.2)	1.1 (1.1; 1.2)	1.2 (1.1; 1.2)	1.1 (1.1; 1.2)	NS
DBP D/N	1.3 (1.2; 1.3)	1.2 (1.1; 1.3)*, **	1.3 (1.2; 1.3)	1.2 (1.1; 1.3)*, **	<0.0001
Dippers all (%)	148 (64.6) +	28 (12.2)++	153 (66.8)	23 (10.0)	<0.0001
Max BPL	25. (15; 4)	67 (52; 78)*, **	25 (15; 4)	70 (50; 79)*, **	<0.0001
Max MAP BPL	19 (9; 31)	57.5 (49; 69)*, **	19 (9; 31)	57 (43; 70)*, **	<0.0001
Max SBP BPL	9 (2; 22)	41 (29; 67)*, **	11 (2; 26)	42 (26; 72)*, **	<0.0001
Max DBP BPL	20 (10; 27)	50 (33; 68)*, **	21 (10; 30)	55 (33; 71)*, **	<0.0001

Values are expressed as mean \pm SD or median (interquartile range)

NT normotensive children, HTN children with hypertension, BP blood pressure, MAP mean arterial pressure, SBP systolic BP, DBP diastolic BP, D/Nday/night ratio, max BPL maximum BP load

*Significantly different from NT-A, **Significantly different from NT-B, + Significantly different from NT-B, ++ Significantly different from HTN-B, NS not significant, N/A not available

Conversion from SDS to percentile: -3 to -2 SDS=0.1 to 2.3rd percentile; -2 to -1.88 SDS=2.3rd to 3rd percentile; -1.88 to -1.645 SDS=3rd to 5th percentile; -1.645 to -1.28 SDS=5th to 10th percentile; -1.28 to -1 SDS=10th to 15.9th percentile; -1 to -0.64 SDS=15.9th to 25th percentile; -0.64 to 0 SDS=25th to 50th percentile; 0 to 0.64 SDS=50th to 75th percentile; 0.64 to 1 SDS=75th to 84.1st percentile; 1 to 1.28 SDS=84.1st to 90th percentile; 1.28 to 1.645 SDS=90th to 95th percentile; 1.645 to 1.88 SDS=95th to 97th percentile; 1.88 to 2 SDS=97th to 97.7th percentile; 2-3 SDS=97.7th to 99.9th percentile.

labeled as hypertensive (HTN-A), regardless of the BP load and dipping status.

(B) MAP excluded: Patients were considered as normotensive (NT-B) if their average SBP and DBP during 24h, daytime and night-time periods were simultaneously below 1.645 SDS, (95th percentile) regardless of their BP load and dipping/non-dipping status. Patients were labeled as hypertensive (HTN-B) if either SBP or DBP Z scores were \geq 1.65 SDS (95th percentile) during the 24h, daytime or night-time periods.

Statistical analysis

Data are shown as mean \pm SD if normally distributed and as median and interquartile range (25th and 75th percentile) in cases of non normal distribution. Continuous variables in patient groups were compared using the analysis of variance (ANOVA) with Bonferroni correction for multiple comparisons, (normally distributed data) and the Kruskal Wallis test with Dunn's correction for multiple comparisons (not normally distributed data). Categorical variables (proportion of patients between groups) were compared using a Chi-square test or Fisher exact

test. The level of agreement between the two definitions was quantified using the kappa coefficient, along with the 95th percentile confidence intervals. Previously published qualitative descriptors, grading the level of agreement according to kappa values, were used (17): <0 no agreement, 0-0.2 slight agreement, 0.21-0.40 fair agreement, 0.41-0.60 moderate agreement, 0.61-0.80 substantial agreement and 0.81-1.0 almost perfect agreement.

Results were considered statistically significant if the p-value was below 0.05. All statistical analyses were performed with the GraphPad Prism software, version 5.0 (GraphPad Software, La Jolla, CA, USA).

RESULTS

Out of the 229 patients, ambulatory hypertension was detected in 46 patients (HTN-A) using the definition A, (including MAP) as compared to only 37 children (HTN-B) by definition B (without MAP), $p=0.001$. Basic characteristics of the study population are given in Table 1. Age, gender distribution, weight and height were not statistically different between

groups. Out of 229 children, only 38 patients were obese (BMI \geq 95th percentile) and 11 were overweight (BMI $>$ 85th but $<$ 95th percentile). The prevalence of being overweight and obese was similar in both groups: 8 and 33 (NT-A), 3 and 5 (HTN-A), 8 and 35 (NT-B) and 3 and 3 (HTN-B), respectively.

ABPM results

ABPM results are shown in Table 2. As expected, patients with HTN (both HTN-A and HTN-B) had significantly higher MAP, systolic and diastolic BP Z scores among all time periods (Table 2). Seven out of 46 hypertensive patients in group HTN-A had an isolated daytime HTN, 18 had isolated nocturnal HTN, and 21 patients had day- and night-time HTN. Similarly, 5 out of 37 patients in group HTN-B had isolated daytime HTN, 13 had isolated nocturnal HTN, and 19 patients had day- and night-time HTN (Chi-square, $p=0.88$). Patients with HTN (both HTN-A and HTN-B) also had significantly lower D/N ratio and higher BP load (Table 2). Out of 229 children, 176 were classified as dippers (77%) without any differences between the groups.

The agreement (kappa statistics) between definitions is shown in Table 3. Even though the level of agreement between the two defined methods of HTN (with or without MAP) was almost perfect (kappa = 0.86 ± 0.04 ; 95% CI 0.78-0.95), the addition of MAP to the definition of HTN allowed for the detection of 9 additional hypertensive patients ($n=46$); they were otherwise missed due to exclusion of MAP within the definition ($n=37$). These nine patients had only mild isolated MAP hypertension with a median MAP Z score of 1.69 (range from 1.66 to 2.16) (Figure 1). Median SBP and DBP Z scores were normal and oscillated around 1.0 (daytime SBP 0.96, night-time SBP 1.04, 24h SBP 0.99, daytime DBP 0.55, night-time DBP 1.1, 24h DBP 0.92), but their BP loads were high (median max BP load = 60, range 49-100) (Figure 2).

DISCUSSION

The main findings of our study are as follows: (a) the inclusion of MAP to the definition of ambulatory HTN significantly increased the number of patients diagnosed as hypertensive, (b) these hypertensive patients

detected by MAP had normal systolic/diastolic blood pressures but a higher BP load.

Ambulatory blood pressure monitoring is an excellent tool for the assessment of hypertension, its daytime and night-time components (blood pressure dipping) and blood pressure load. In adult medicine, the interpretation of ABPM is rather straightforward, as the blood pressure normative values and upper limits of normal BP are based on cardiovascular risk assessment obtained from population studies (1, 18). Consequently, the upper limits of normal blood pressure may be different for certain populations at risk, such as patients with diabetes or chronic kidney disease, but do not change with age, weight or height (1, 19, 20).

In children, the cardiovascular risk of elevated blood pressure is not well studied. Therefore, the normative values and upper limits of normal BP are based on population demographics, (age and height) assuming that an older/taller child may have a higher normal BP than a younger/smaller child. The pediatric normative values for ambulatory blood pressure consist of numerous BP values based on age and height (2, 16). Consequently, the interpretation of ABPM in children is rather challenging. Every BP value obtained by ABPM needs to be compared to a given BP percentile or expressed as a BP Z-score.

The complexity of ABPM further increases with a multitude of BP values generated by the ABPM device: systolic BP, diastolic BP and MAP over 24h, daytime and night-time periods and their respective BP loads. As a result, a total of 9 blood pressure values need to be compared with age/height related normative values.

The correct identification of BP upper limits of normal, are also important for the calculation of BP loads, which seem to play a role in cardiovascular morbidity (21, 22, 23). A normotensive child should theoretically have a normal BP in all 9 BP readings, whereas an increased BP ($>$ 95th percentile) in one or more of these 9 parameters would label the child as hypertensive on ABPM. This approach calls for computer generated age/height related percentiles or Z-scores of all 9 BP readings, in order to allow for a thorough ABPM interpretation. This is probably

Table 3: Comparison of definition of HTN with or without MAP

Definition B	Definition A		Total	Fisher's exact test	kappa 95% CI
	Hypertensive with SBP+DBP+-MAP	Normotensive with SBP+DBP+-MAP			
Hypertensive with SBP+DBP	37	0	37	P value < 0.0001	0.86 \pm 0.04; (0.78-0.95)
Normotensive with SBP+DBP	9	183	192		
Total	46	183	229		

BP blood pressure, MAP mean arterial pressure, SBP systolic BP, DBP diastolic BP, CI confidence interval, HTN hypertension

Table 4

Parameter	Patients									
	1	2	3	4	5	6	7	8	9	All
Gender	M	M	F	M	M	F	F	M	F	
Age (years)	14.9	14.2	15.3	15.3	15.6	12.6	16.2	9.9	17.6	15.3 (13.4;15.9)
Height (cm)	176	152	156.7	166.7	183	159.7	161	163	172	163 (158;174)
Weight (kg)	73	40.3	54	66	59	49	111	56	75	59 (52;74)
BMI-SDS	1.4	-0.8	0.7	1.4	-0.8	0.2	5.5	1.7	1.0	1.0 (-0.2;1.4)
Obesity	No	No	No	No	No	No	Yes	Yes	No	
Diagnosis	DM	DM	DM	DM	PH	PH	PH	PH	PH	
MAP day (SDS)	1.4	0.5	0.7	0.4	1.7	1.5	-0.6	1.7	1.3	1.3 (0.5;1.6)
MAP night (SDS)	2.2	1.7	1.8	1.8	1.2	1.0	2.0	1.1	1.4	1.7 (1.2;1.9)
MAP 24 h (SDS)	1.7	0.9	0.9	0.6	1.5	1.7	0.3	1.2	1.7	1.2 (0.8;1.7)
SBP day (SDS)	1.3	1.0	0.7	0.5	1.4	0.9	0.1	1.1	1.2	0.9 (0.6;1.2)
SBP night (SDS)	1.3	1.3	1.3	1.0	1.5	0.6	1.0	-0.2	0.8	1.0 (0.7;1.3)
SBP 24 h (SDS)	1.4	1.1	0.7	0.6	1.6	0.9	1.0	0.6	1.4	0.9 (0.7;1.4)
DBP day (SDS)	0.8	0.7	0.5	0.2	-0.1	1.3	-1.3	1.6	-0.2	0.6 (-0.1;1.1)
DBP night (SDS)	1.0	1.4	1.6	1.5	0.7	0.7	1.4	1.1	0.9	1.1 (0.8;1.5)
DBP 24 h (SDS)	0.9	0.9	0.8	0.5	1.1	1.4	-0.5	1.1	1.4	0.9 (0.7;1.2)
day MAPL (%)	31	19	16	8	24	50	7	49	38	24 (12;44)
night MAPL (%)	67	55	67	60	55	17	100	40	80	60 (44;74)
24hMAPL (%)	46	38	26	16	40	52	13	49	42	40 (21;48)
day SBPL (%)	31	26	13	8	29	32	14	49	28	28 (14;22)
night SBPL (%)	25	36	50	30	46	8	0	10	42	30 (9;44)
24hSBPL (%)	40	33	22	19	47	38	26	40	37	37(24;40)
day DBPL (%)	28	23	16	6	33	41	11	43	35	28 (14;38)
night DBPL (%)	33	45	50	50	46	8	0	40	63	45 (21;50)
24-h DBPL (%)	32	38	22	18	38	45	13	47	48	38 (20;46)
Average BPL (%)	37	35	31	24	40	32	20	41	46	35 (28;40)
maxBPL (%)	67	55	67	60	55	52	100	49	80	60 (53;74)
SBP D/N	1.14	1.09	1.09	1.09	1.13	1.17	1.08	1.26	1.17	1.13 (1.09;1.17)
DBP D/N	1.25	1.18	1.16	1.13	1.19	1.35	0.99	1.29	1.16	1.18 (1.15;1.27)
MAP D/N	1.15	1.08	1.11	1.08	1.25	1.23	0.99	1.23	1.18	1.15 (1.08;1.23)

Values are expressed as median (IQR=interquartile range)

M male, F female, DM diabetes mellitus type 1, PH primary hypertension, BP blood pressure, MAP mean arterial pressure, SBP systolic BP, DBP diastolic BP, SBPL systolic BP load, DBPL diastolic BP load, MAPL MAP BP load, maxBPL maximum BPL D/Nday-night ratio

Conversion from SDS to percentile: -3 to -2 SDS=0.1 to 2.3rd percentile; -2 to -1.88 SDS=2.3rd to 3rd percentile; -1.88 to -1.645 SDS=3rd to 5th percentile; -1.645 to -1.28 SDS=5th to 10th percentile; -1.28 to -1 SDS=10th to 15.9th percentile; -1 to -0.64 SDS=15.9th to 25th percentile; -0.64 to 0 SDS=25th to 50th percentile; 0 to 0.64 SDS=50th to 75th percentile; 0.64 to 1 SDS=75th to 84.1st percentile; 1 to 1.28 SDS=84.1st to 90th percentile; 1.28 to 1.645 SDS=90th to 95th percentile; 1.645 to 1.88 SDS=95th to 97th percentile; 1.88 to 2 SDS=97th to 97.7th percentile; 2-3 SDS=97.7th to 99.9th percentile.

not feasible in clinical practice where a more simple approach i.e. only systolic and diastolic BP is used. Unfortunately, the definition of ambulatory hypertension in children remains rather vague, even despite publication of recent guidelines (15, 24). The proposed classification and staging of ambulatory BP levels relies solely on systolic BP and its BP load (15, 25). Should we therefore disregard the diastolic BP and the mean arterial pressures? Most authors/centres use both systolic and diastolic BP for the definition of ambulatory hypertension (3, 4, 5, 6, 7), but only few use the MAP (5, 6, 8, 26). There are several advantages to using MAP: 1. it is

directly measured by the oscillometric device i.e. not calculated by the software, which is subject to company's proprietary patents and prone to be outdated; 2. The pediatric ABPM normative values include MAP (2), therefore the MAP percentiles or Z-scores can be obtained similarly to the systolic or diastolic BP levels and may potentially help with the interpretation of ABPM in children; 3. MAP can be regarded as a composite index of BP, assessing both systolic and diastolic blood pressure at the same time; therefore increasing sensitivity for detection of blood pressure abnormalities, especially in the borderline BP range.

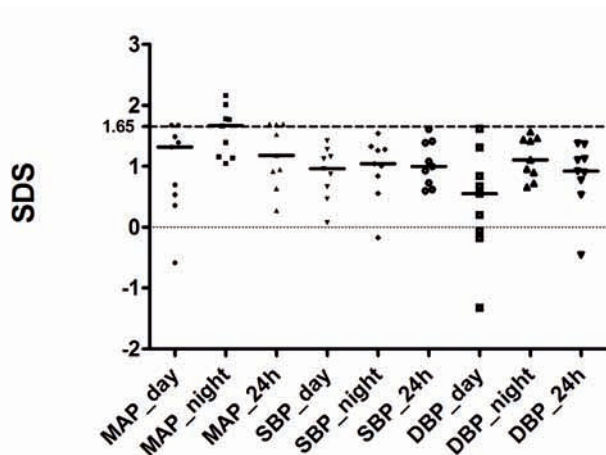


Fig.1. Blood pressure values in 9 patients with MAP hypertension SDS - standard deviation score, MAP - mean arterial pressure, SBP - systolic blood pressure, DBP - diastolic blood pressure (Dot line): 0 SDS (50th percentile), ----- (Broken line): 1.65 SDS (95th percentile)

Our study showed that the addition of MAP in the definition of ABPM normotension/hypertension, significantly increased the number of hypertensive children. These hypertensive children by MAP had normal or borderline systolic/diastolic BP but a significantly elevated BP load. Therefore, they may be considered at risk for cardiovascular damage (21, 22, 23) and may also potentially develop systolic or diastolic HTN later in life. We therefore speculate that the inclusion of MAP into the ABPM definition, may allow for an earlier detection of blood pressure abnormalities in children.

The prognostic relevance of MAP was studied mainly in critical care medicine (27) and gynecology (28), but also in children with chronic kidney disease (ESCAPE) (26). The MAP seems to be a good predictor of survival in spontaneous supratentorial intracerebral hemorrhage, as it maintains adequate levels that are crucial for an increase in cardiac output and improvement of the microvascular flow and reactivity of patients experiencing septic shock (27). The MAP was also found to be a better predictor for pre-eclampsia when compared to systolic or diastolic BP, or an increase of office BP in the first or second trimester of pregnancy (28). The Escape Trial group studied the long-term renoprotective effect of intensified BP control among children with chronic kidney disease (26). They used MAP as the target BP and proved that patients with a MAP < 50th percentile, (intensified BP group) had significantly better renal survival than patients with conventional BP control (MAP between the 50th and the 95th percentile). It seems therefore that the MAP is of prognostic importance and can be successfully used in clinical studies.

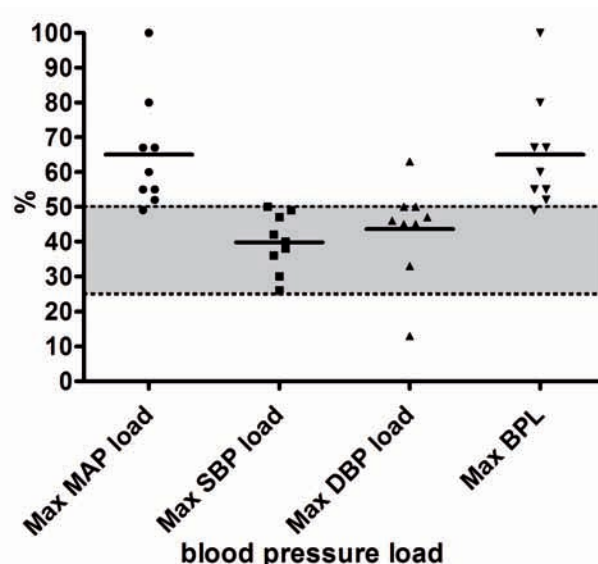


Fig.2. Maximum blood pressure load in 9 patients with MAP hypertension

MAP - mean arterial pressure, SBP - systolic blood pressure, DBP - diastolic blood pressure, Max BPL - maximum blood pressure load --- (Broken line): 25% of blood pressure load (elevated) and 50% of blood pressure loads (predictive for target organ damage) (15)

Our study has several limitations. Firstly, it is a cross-sectional retrospective study in a mixed population of children with normotension, diabetes mellitus type 1 and various mild non-proteinuric kidney diseases. Secondly, the overall sample size is rather small and only one ABPM measurement was performed. Thirdly, no data is available on target organ damage (TOD) in our population; therefore, we could not assess the correlation between an elevated MAP and TOD. However, these patients had only mild hypertension, which may not be necessarily associated with a significant TOD

In conclusion, the mean arterial pressure obtained directly from the ambulatory blood pressure monitoring, can be a useful parameter for assessment of a normotensive/hypertensive status, especially in children with borderline hypertension and/or increased blood pressure load.

Acknowledgement

We thank Brandy Brookings for her help with the revision of this manuscript.

Conflict of interest

The authors have nothing to disclose, nor have any competing financial interest in relation to the work described.

REFERENCES:

1. Mancia G, de Backer G, Dominiczak A, Cifkova R, Fagard R, Germano G et al. (2007) 2007 Guidelines for the Management of Arterial Hypertension. The Task Force for the Management of Arterial Hypertension of the European Society of Hypertension (ESH) and of the European Society of Cardiology (ESC). *Journal of Hypertension* 25: 1105-1187
2. Wühl E, Witte K, Soergel M, Mehls O, Schaefer F (2002) Distribution of 24-h ABP in children-normalized reference values and role of body dimensions. *J of Hypertension* 20: 195-207
3. Torbjörnsdotter TB, Jaremko GA, Berg UB (2001) Ambulatory blood pressure and heart rate in relation to kidney structure and metabolic control in adolescents with Type I diabetes. *Diabetologia* 44: 865-873
4. Torbjörnsdotter TB, Jaremko GA, Berg UB (2004) Nondipping and its Relation to Glomerulopathy and Hyperfiltration in Adolescents With Type 1 Diabetes. *Diabetes Care* 27: 510-516
5. Dost A, Klinkert Ch, Kapellen T, Lemmer A, Naeke A, Grabert M, Kreuder J, Holl RW (2008) Arterial Hypertension determined by Ambulatory Blood Pressure profiles. Contribution to microalbuminuria risk in a multicenter investigation in 2,105 children and adolescents with type 1 diabetes. *Diabetes Care* 31: 720-725
6. Darcan S, Goksen D, Mir S, Serdaroglu E (2006) Alterations of blood pressure in type 1 diabetic children and adolescents. *Pediatr Nephrol* 21: 672 - 6768
7. Šuláková T, Janda J (2008) Ambulatory blood pressure in children with diabetes 1. *Pediatr Nephrol* 12: 2285 - 2286
8. Šuláková T, Janda J, Černá J, Janštová V, Šuláková A, Slaný J, Feber J (2009) Arterial HTN in children with T1DM - frequent and not easy to diagnose. *Pediatric Diabetes* 10: 441- 44
9. Lurbe E, Redon J, Kesani A et al. (2002) Increase in nocturnal blood pressure and progression to microalbuminuria in Type 1 diabetes. *N Engl J Med* 347: 797 - 805
10. Perrin NESS, Torbjörnsdotter TB, Jaremko GA, Berg UB (2004) Follow up of kidney biopsies in normoalbuminuric patients with type 1 diabetes. *Pediatr Nephrol* 19: 1004 - 1013
11. Perrin NESS, Torbjörnsdotter TB, Jaremko GA, Berg UB (2006) The course of diabetic glomerulopathy in patients with type I diabetes: A 6-year follow-up with serial biopsies. *Kidney International* 69: 699 - 705
12. Azar S T. and Birbari A (1998) Nocturnal Blood Pressure Elevation in Patients with Type 1 Diabetes Receiving Intensive Insulin Therapy Compared with that in Patients Receiving Conventional Insulin Therapy. *J Clin Endocrinol Metab* 83: 3190 - 3193
13. Bell C S, Poffenbarger TS and Samuels JA (2011) Ambulatory blood pressure status in children: comparing alternate limit sources. *Pediatr Nephrol* 12: 2211 - 2217
14. Jones HE, Sinha MD (2011) The definition of daytime and nighttime influences the interpretation of ABPM in children. *Pediatr Nephrol* 26: 775 - 781
15. Urbina E, Albert B, Flynn J et al. (2008) Ambulatory Blood Pressure Monitoring in Children and Adolescents: Recommendations for Standard Assessment. A Scientific Statement From the American Heart Association Atherosclerosis, Hypertension, and Obesity in Youth Committee of the Council on Cardiovascular Disease in the Young and the Council for High Blood Pressure Research. *Hypertension* 52: 433 - 451
16. Soergel M, Kirschstein M, Busch C, Danne T, Gellermann J, Holl R, (1997) Oscillometric twenty four-hour ambulatory blood pressure values in healthy children and adolescents: a multicenter trial including 1141 subjects. *J Pediatr* 130: 178 - 184.
17. Landis JR, Koch GG (1977) The measurement of observer agreement for categorical data. *Biometrics* 33: 59 - 174
18. Verdecchia P (2000) Prognostic Value of Ambulatory Blood Pressure. Current Evidence and Clinical Implications. *Hypertension* 35: 844 - 851
19. Chobanian AV, Bakris GL, Black HR, Cushman WC, Green LA, Izzo L Jr, et al (2003) National Heart, Lung, Blood Institute; National High Blood Pressure Education Program Coordinating Committee. Seventh report of the Joint National Committee on Prevention, Detection, Evaluation, and Treatment of High Blood Pressure. *Hypertension* 42: 1206 - 1252
20. O'Brien E, Asmar R, Beilin L, Imai Y, Mallion JM, Mancia G (2003) European Society of Hypertension recommendations for conventional, ambulatory and home blood pressure measurement. *J Hypertens* 21: 821 - 848
21. Sorof JM, Cardwell G, Franco K, Portman RJ (2002) Ambulatory blood pressure and left ventricular mass index in hypertensive children. *Hypertension* 39: 903 - 908
22. Lubrano R, Travasso E, Raggi C, Guido G, Masciangelo R, Elli M (2009) Blood pressure load, proteinuria and renal function in pre-hypertensive children. *Pediatr Nephrol* 24: 823 - 831
23. Chaudhuri A, Sutherland SM, Begin B, Salsbery K, McCabe L, Potter D (2011) Role of twenty-four-hour ambulatory blood pressure monitoring in children on dialysis. *Clin J Am Soc Nephrol* 4: 870 - 876
24. Lurbe E, Cifkova R, Cruickshank JK, Dillon MJ, Ferreira I, Invitti C et al. (2009) Management of high blood pressure in children and adolescents: recommendations of the European Society of Hypertension. *J Hypertens* 27: 1719 - 1742
25. Lurbe E, Sorof JM, Daniels SR (2004) Clinical and research aspects of ambulatory blood pressure monitoring in children. *J Pediatr* 144: 7 - 16
26. The ESCAPE Trial Group (2009) Strict Blood-Pressure Control and Progression of Renal Failure in Children. *N Engl J Med* 361: 1639 - 1650
27. Badin J, Boulain T, Ehrmann S, Skarzynski M, Bretagnol A, Buret J (2011) Relation between mean arterial pressure and renal function in the early phase of shock: a prospective, explorative cohort study. *Critical Care* 15: R135, doi:10.1186/cc10253
28. Cnossen JS, Vollebregt KC, de Vrieze N, ter Riet G, Mol BWJ, Franx A (2008) Accuracy of mean arterial pressure and blood pressure measurements in predicting pre-eclampsia: systematic review and meta-analysis. *BMJ* 336, 7653: 1117 - 1123

ECTOPIC LIVER - DIFFERENT MANIFESTATIONS, ONE SOLUTION

Pavel Zonca, Lubomir Martinek, Peter Ihnat, Jan Fleege

Pavel Zonca, Lubomir Martinek, Peter Ihnat, Department of Surgery, University Hospital Ostrava, 17. listopadu 1790, Ostrava 70852, Czech republic

Pavel Zonca, Lubomir Martinek, Peter Ihnat, Department of Surgical Studies, Faculty of Medicine, University of Ostrava, Syllabova 19, Ostrava 70300, Czech republic

Jan Pleege, MVZ Zentrum für Pathologie und Zytodiagnostik GmbH, Emil-Hoffmann-Straße 7a - 50996 Köln, Germany

Author contributions: Zonca P and Martinek L performed surgical operations; Fleege J performed pathological examinations; Ihnat P and Martinek L were involved in data acquisition and interpretation of data; Zonca P and Ihnat P wrote the manuscript; Zonca P organized the report.

Correspondence to: Pavel Zonca, M.D., Ph.D., FRCS, Ass. Prof., Department of Surgery, University Hospital Ostrava, 17. listopadu 1790, Ostrava 70852, Czech republic. pavel.zonca@hotmail.co.uk

Telephone: +420 597 375 051 Fax: +420 597 375 054

Originally published in *World journal of gastroenterology* 2013; 19(38): 6485-6489

Consent to the publication of 12th April 2014

Conflict of Interest Statement:

The authors have no conflict of interest.

ABSTRACT

Developmental abnormalities are rare in the liver. This study presents two case reports of ectopic liver. The first case was a 31-year old male with clinical indications for laparoscopic appendectomy. Laparoscopy identified a perforated appendix and an unknown tumorous lesion in the ligamentum hepatoumbilicalis. The patient underwent a laparoscopic appendectomy, intraoperative lavage of the peritoneal cavity, and extirpation of the lesion in the ligamentum hepatoumbilicalis. Histopathological examination of the excised tumor revealed that it comprised liver tissue with fibrinous changes. The tumor was completely separate from the liver with no connection. It was classified as an ectopic liver. No further therapy was required. The second case was a 59-year old male with a tumor on the upper pole of the spleen, incidentally diagnosed in an ultrasound examination. The biopsy raised suspicion of hepatocellular carcinoma. A PET-CT examination revealed accumulation of F-18 fluorodeoxyglucose only in the tumor. The patient underwent a splenectomy with a resection and reconstruction of diaphragm. After the hepatocellular carcinoma was confirmed, adjuvant therapy (sorafenib) was initialized. The operations and postoperative recoveries were uncomplicated in both cases. Despite the low incidence of ectopic liver and rare complications, it is necessary to maintain awareness of this possibility. The potential malignancy risk for ectopic liver tissue is the basis for radical surgical removal. Therapy for hepatocellular carcinoma in an ectopic liver follows the same guidelines as those followed for treating the “mother” liver.

Key words:

Ectopic; Liver; Hepatocellular carcinoma; Diagnostic; Treatment

Core tip:

Ectopic liver presents a rare clinical finding resulting from liver tissue migration to various organs during embryogenesis. Although the condition is typically asymptomatic, it can lead to different clinical manifestations such as intraabdominal bleeding or hepatocarcinogenesis. The potential malignancy risk is the basis for radical surgical removal; which represents the only correct solution. Therapy for hepatocellular carcinoma in an ectopic liver follows the same guidelines (National Comprehensive Cancer Network Guidelines) as those followed for treating the “mother” liver. Despite the low incidence of ectopic liver and rare complications, it is necessary to maintain an awareness of this possibility.

INTRODUCTION

The liver is the largest abdominal organ. It occupies a substantial portion of the upper abdominal cavity. Abnormalities in the position or number of liver parts are considered rare developmental anomalies. They are typically asymptomatic, and incidental detection, though extremely rare, may occur during an operation or autopsy. The incidence of ectopic liver is 0.24-0.56%, according to data described in laparoscopic or autopsy studies [1,2,3], but this estimate seems high. Most authors distinguish two types of ectopic liver. The first is an accessory liver lobe connected to the liver, and the second is a truly ectopic liver. Collan classified four types. The first

is the ectopic liver, which is not connected to the mother liver, but is typically attached to the gallbladder or intra-abdominal ligaments. The second is a microscopic ectopic liver, which is occasionally found in the gallbladder wall. The third is a large accessory liver lobe, attached to the mother liver by a stalk (pedunculated liver). The fourth is a small, accessory liver lobe attached to the mother liver [4]. Here, we presented two manifestations of ectopic livers.

CASE REPORT

Case 1

A 31-year-old male patient was admitted with an 8-hour history of pain in the right lower abdominal quadrant with a gradual onset. The patient reported nausea, but no vomiting, normal bowel function, and normal miction. He was subfebrile, but no infection was observed. His medical history included pollinosis. He took no regular medication and had no previous surgeries.

The clinical examination showed right lower quadrant abdominal pain with tenderness. The bowel sounds were diminished. The patient was hemodynamically stable without any signs of sepsis (temperature 37.5 °C, noninvasive blood pressure 120/80 mmHg, heart rate 76 beats/min, respiratory rate 14 breaths/min). The white blood count was 14,800 cells/ml and C-reactive protein was 12.3 mg/l. Other biochemical results were normal and the urinalysis revealed no pathological findings. An abdominal ultrasound showed a small amount of pericaecal fluid. No other abnormal findings were identified by ultrasound in other parts of the abdomen or pelvis.

The signs and symptoms suggested appendicitis; therefore, we performed an acute laparoscopic appendectomy. First, antibiotic therapy was introduced. Initially, the routine diagnostic laparoscopy revealed perforated appendicitis with circumscribed peritonitis. Incidentally, a small oval tumor (3×2×2 cm) was found in the ligamentum hepatoumbilicis next to the liver (Figure 1). No other pathological signs were



Figure 1: Small oval tumor (3×2×2 cm) was found in the ligamentum hepatoumbilicis next to the liver

observed. The appendectomy was performed, followed by an intraoperative lavage of the peritoneal cavity. The tumor was excised. The operation and the postoperative recovery were uncomplicated. The patient was discharged on the third postoperative day. The histology of the appendix revealed an ulcerophlegmonous appendix. The histopathological examination of the tumor from the ligamentum hepatoumbilicis revealed liver tissue with moderate steatosis and a thick fibrotic capsule (Figure 2). The specimen examination showed that the tumor was completely separate, with no connection to the liver. It was classified as the first type of ectopic liver according to the Collan classification. No further therapy was required.

Case 2

During an ultrasound examination, a 59-year-old male was incidentally diagnosed with a tumor (10×8×6 cm) on the upper pole of the spleen. The finding was confirmed with a CT scan (Figure 3 and 4), and a biopsy was performed. A histological examination of the

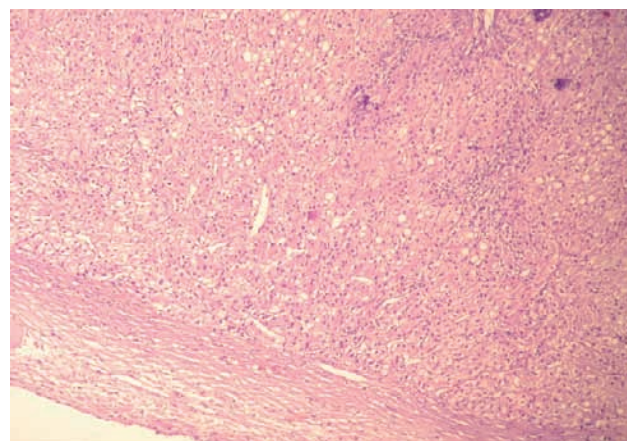


Figure 2: Histopathology of the tumor from the ligamentum hepatoumbilicis (liver tissue with moderate steatosis and a thick fibrotic capsule)

biopsy specimen, including immunohistochemistry, raised the suspicion of a metastatic hepatocellular carcinoma, but bile production was not caught and renal carcinoma could not be reliably ruled out. To detect the primary tumor location, we performed a positron emission tomography-computed tomography (PET-CT) examination. This showed a localized accumulation of F-18 fluorodeoxyglucose only in the suspicious tumor. There was no other pathological finding in the abdominal or thoracic cavities. The medical history included toxonutritive hepatopathy (alcoholic liver disease) and chronic gastritis. The biochemical results were within normal limits, and oncomarkers (CEA, AFP, CA 19-9) were negative. A perioperative examination confirmed that the tumor was located on the upper pole of the spleen and was connected to diaphragm, but did not invade other surrounding tissues. It was classified as the first type of ectopic liver according to the Collan classification.

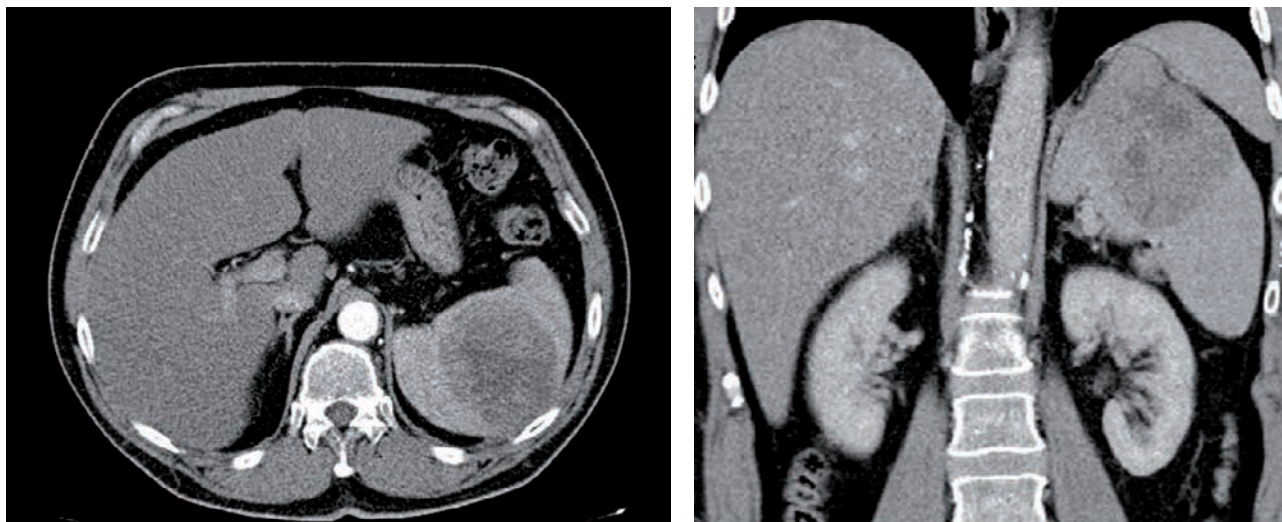


Figure A: Tumor (10×8×6 cm) on the upper pole of the spleen (CT scan, arterial phase with a coronal reconstruction)
 Figure B: Tumor on the upper pole of the spleen (CT scan, arterial phase - axial orientation)

on. No other pathology was found in the abdomen. A splenectomy was performed, with partial diaphragm resection and reconstruction. The postoperative recovery was uneventful. A definitive histological examination, including immunohistochemistry, confirmed a hepatocellular carcinoma (HCC) in the spleen tissue (Figure 5). Two small additional tumor sites (satellite tumors) were found in addition to the main lesion. Several investigations showed that the orthotopic liver tissue was negative for HCC, but a histological verification (a biopsy of the mother liver tissue) was not performed. Due to the high risk of tumor recurrence (additional tumor sites were found), we initialized a targeted adjuvant therapy with sorafenib. The American Association for the Study of Liver Diseases (AASLD) practice guidelines on the management of hepatocellular carcinoma do not recommend the routine use of adjuvant therapy with sorafenib (recurrence rates reduction was not reliably proven) [5], nevertheless, there are data available that indicate that sorafenib was effective for treating patients with advanced HCC [6, 7].

DISCUSSION

In development, the hepatic diverticulum comprises the liver and biliary tree, and it appears late in the third week or early in the fourth week of gestation. The foregut endoderm of the hepatic diverticulum develops into the liver parenchyma (hepatocytes) and the epithelial lining of the biliary tract. The hepatic diverticulum divides to form a small ventral portion, the future gall bladder, and a larger cranial portion, the liver primordium. Developmental errors are relatively rare in the liver. Other errors in foregut development are more frequently observed, like errors in pancreas or duodenum formation [8]. Liver tissue can migrate to various organs during embryogenesis. Sites of ectopic liver include the gallbladder, spleen, retroperitoneum, pancreas, adrenal

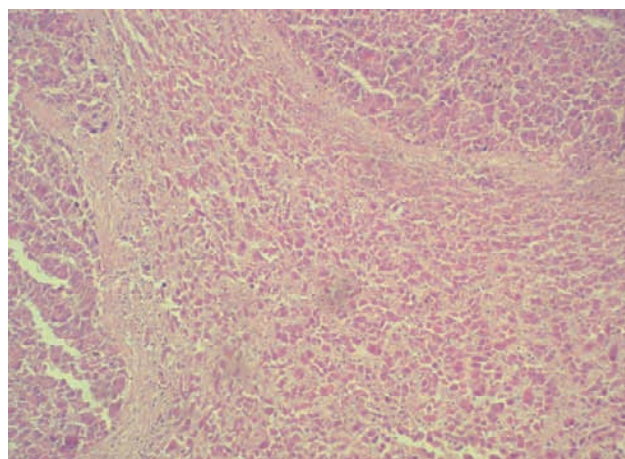


Figure 4: Histopathology of the hepatocellular carcinoma found in an ectopic liver in the spleen

gland, portal vein, diaphragm, thorax, gastric serosa, testes, and umbilical vein [9]. Most authors distinguish ectopic and accessory liver formations, based on whether there is a connection to the mother liver. The Collan Classification mentioned above is not widely used. In many cases, it is difficult to make a clear distinction between ectopic liver and accessory liver. The precise incidence of ectopic liver or accessory liver is unknown. Examination of several studies indicated that the incidence is approximately 0.24-0.56%. Watanabe's series of 1060 patients revealed an incidence of 0.47% for ectopic liver and 0.09% for accessory liver. These numbers could be over-estimated, because histological verification was not performed in all cases. Ectopic and accessory liver are typically asymptomatic, but occasionally they cause unexpected problems, like intra-abdominal bleeding or hepatocarcinogenesis. The first clinical sign of ectopic or accessory liver could be an acute complication that leads to acute surgery and diagnosis of ectopic liver. Various clinical symptoms, like recurrent abdominal pain and impaired

liver function could be caused by ectopic or accessory liver, but in the majority of cases, an ectopic/accessory liver remains undetected.

In some cases, the ectopic or accessory liver may undergo torsion, infarction, rupture, or other disorders. Torsion and subsequent infarction of an accessory liver lobe has been described in children and adults [10, 11, 12, 13, 14]. Ladurner presented a very interesting case of a patient with hepatic ischemia caused by complete vascular occlusion due to a twisted accessory liver lobe. In that case, the accessory liver lobe produced serious, life-threatening problems, and an orthotopic liver transplantation was performed [15]. Ito reported a small omphalocele that involved an accessory liver lobe embedded in the cranial portion of the amniotic sac. In that case, the pedicle of liver tissue was markedly elongated [16].

An ectopic or accessory liver can lead to benign or malignant diseases. Benign cases in the literature report hemangiomas, adenomas, or focal nodular hyperplasia associated with an ectopic or accessory liver [17, 18, 19]. Benign lesions seem to be less frequent; however, the higher frequency of malignancies could be based on the fact that many benign lesions remain undiagnosed because they are asymptomatic. Moreover, due to their abnormal locations, asymptomatic lesions may be misdiagnosed in the absence of histology.

The ectopic liver has been associated with malignancies more often than with benign lesions. Many authors have pointed out that ectopic liver tissue is more predisposed to malignancy than normal liver tissue. Ectopic livers have completely functional architecture, but may be metabolically handicapped; this may facilitate carcinogenesis. Ectopic liver tissue also has increased neoplastic potential compared to orthotopic liver tissue. This may have given rise to the hypothesis that ectopic livers are particularly predisposed to the development of hepatocellular cancer. A high incidence of hepatocellular cancer in ectopic livers was described in Japan [20]. In most cases, a malignant tumor was found in the ectopic liver, but not in the mother liver. Ectopic or accessory livers with cancer may be amenable to surgical resection. Many case reports have described surgical treatments. Some authors suggested that the outcome after resection to remove hepatocellular cancer was superior when it involved an ectopic or accessory liver, compared to when it involved the mother liver. However, long-term follow-up data are poor.

Many anatomical locations have been described for ectopic livers with cancer [20, 21, 22, 23]. The favorable outcome after resection of ectopic livers could depend on the specific anatomical location [24, 25]. Shigemori described a case of ectopic hepatocellular carcinoma in the jejunum [26]. Cardona reported a case of a primary, well-differentiated hepatoce-

llular carcinoma arising from ectopic liver tissue in the pancreas [27]. Leone presented interesting data regarding three cases of hepatocellular carcinomas that arose in ectopic livers. The clinical presentations were very interesting; one patient reported dull epigastric pain; the second reported abrupt onset with signs and symptoms of acute abdomen caused by intra-abdominal bleeding; and the third presented with an unexplained, progressive increase in alpha-fetoprotein serum levels [28]. Seo reported a case of hepatocellular carcinoma that arose from hepatic parenchyma located in the left subphrenic space in the upper portion of the gastrosplenic ligament. The preoperative diagnosis was a nonspecific stomach mass, with suspicion of gastrointestinal stromal tumor. An operation was performed laparoscopically [29]. Takavasu reported another case with high serum alpha-fetoprotein combined with a suspicion of a submucosal stomach tumor [30]. The two latter cases diagnosed the ectopic liver postoperatively, after histological examination.

It is important to consider an ectopic/accessory liver when evaluating perihepatic lesions. It is common to misdiagnose an ectopic liver as a malignant tumor. Stattaus suggested that the diagnosis should be based on a biopsy of ectopic liver or a NMR with liver specific contrast [31]. However, all investigative imaging methods are limited for diagnosing an ectopic/accessory liver, due to its limited volume. Despite the low incidence and rare complications of ectopic liver/accessory, it is necessary to maintain an awareness of this possibility. Because this entity presents with a broad spectrum of clinical symptomatology, it is rarely diagnosed; thus, most discoveries of ectopic and accessory liver are incidental. An elevation in serum alpha-fetoprotein and lack of focus in liver CT image may be the first signs of malignant transformation in an ectopic liver. The suspicion of hepatocellular carcinoma in an ectopic liver is substantial reason for radical surgical removal of an ectopic liver found incidentally. When hepatocellular carcinoma is definitely, histologically confirmed in an ectopic liver, it should be treated with the same approaches used for treating carcinoma in the mother liver (National Comprehensive Cancer Network Guidelines).

REFERENCES

1. Watanabe M, Matsura T, Takatori Y, Ueki K, Kobatake T, Hidakawa M, Hirakawa H, Fukukimoto S, Shimada Y. Five cases of ectopic liver and a case of accessory lobe of the liver. *Endoscopy* 1989; 21: 39-42 [PMID: 2917536, DOI: 10.1055/s-2007-1012892]
2. Asada J, Onji S, Yamashita Y, Okada S, Morino M, Kanaoka M, Ohta Y. Ectopic liver observed by peritoneoscopy: report of a case. *Gastroenterol Endosc* 1982; 24: 309-312 [DOI:http://dx.doi.org/10.11280/gee1973b.24.309]
3. Eiserth P. Beitrage zur Kenntnis der Nebenlebern. *Virchows Arch A Pathol Anat Histopathol* 1940; 307: 307-313 [DOI: http://dx.doi.org/10.1007/BF02593263]

4. Collan Y, Hakkiluoto A, Hastbacka J. Ectopic liver. *Ann Chir Gynaecol* 1978; 67: 27-29 [PMID: 637502]
5. Bruix J, Sherman M. Management of Hepatocellular Carcinoma: An Update. *Hepatology* 2011; 53(3): 1020-1022 [PMID: 21374666 DOI: 10.1002/hep.24199]
6. Llovet JM, Ricci S, Mazzaferro V, Hilgard P, Gane E, Blanc JF. Sorafenib in advanced hepatocellular carcinoma. *N Engl J Med* 2008; 359: 378-390 [PMID: 18650514 DOI: 10.1056/NEJMoa0708857]
7. Cheng AL, Kang YK, Chen Z, Tsao JC, Qin S, Kim JS. Efficacy and safety of sorafenib in patients in Asia-Pacific region with advanced hepatocellular carcinoma: a phase III randomized, double-blind, placebo-controlled trial. *Lancet Oncol* 2009; 10: 25-34 [PMID: 19095497 DOI: 10.1016/S1470-2045(08)70285-7]
8. Sadler TW. *Langman's Essential Medical Embryology*. August 2004 ISBN-10: 0-7817-5571-9
9. Curtis LE, Sheahan DG. Heterotopic tissues in the gallbladder. *Arch Pathol* 1969; 88: 677-683 [PMID: 5357721]
10. Carrabetta S, Piombo A, Podestà R., Auriati L. Torsion and infarction of accessory liver lobe in young man. *Surgery* 2009 Apr; 145(4):448-9. Epub 2008 Mar 24 [PMID: 19303994 DOI: 10.1016/j.surg.2007.12.016]
11. Koumanidou C, Nasi E, Koutrouveli E, Theophanopoulou M, Hilari S, Kakavakis K, Batakis N. Torsion of an accessory hepatic lobe in a child: ultrasound, computed tomographic, and magnetic resonance imaging findings. *Pediatr Surg Int*. 1998 Sep;13(7):526-7 [PMID: 9716687 DOI: 10.1007/s003830050391]
12. Elsayes HB, Elzein MA, Razik AM, Olude IO. Torsion of an ectopic liver in a young child. *J Pediatr Surg* 2005 Mar;40(3):E55-8 [PMID: 15793717 DOI:10.1016/j.jpedsurg.2004.11.009]
13. Umehara M, Sugai M, Kudo D, Hakamada K, Sasaki M, Munkata H. Torsion of an accessory lobe of the liver in a child: report of a case. *Surg Today* 2009;39(1):80-2. Epub 2009 Jan 8 [PMID: 19132476 DOI: 10.1007/s00595-008-3772-0]
14. Khan AM, Hundal R, Manzoor K, Dhuper S, Korsten MA. Accessory liver lobes: a diagnostic and therapeutic challenge of their torsions. *Scand J Gastroenterol* 2006 Feb;41(2):125-30 [PMID: 16484115 DOI:10.1080/00365520500377862]
15. Ladurner R, Brandacher G, Mark W, Iannetti C., Lottersberger C, Steurer W., Königsrainer A, Margreiter R. Complete hepatic ischemia due to torsion of a large accessory liver lobe: first case to require transplantation. *Transpl Int* 2005 Apr;18(4):467-9 [PMID: 15773969 DOI: 10.1111/j.1432-2277.2005.00072.x]
16. Ito F, Ando H, Watanabe Y, Seo T, Murahashi O, Harada T, Kaneko K, Ishiguro Y. An accessory lobe of the liver disturbing closure of the umbilical ring. *Pediatr Surg Int* 1999 Jul;15(5-6):394-6 [PMID: 10415296 DOI: 10.1007/s003830050609]
17. Tsai CC, Yen TC, Tzen KY. Pedunculated giant liver hemangioma mimicking a hypervascular gastric tumor on Tc-99m RBC SPECT. *Clin Nucl Med* 1999; 24: 132-133 [PMID: 9988078 DOI: http://dx.doi.org/10.1097/00003072-199902000-00017]
18. Vilgrain V, Boulou L, Vullierme MP, Denys A, Terris B, Menu Y. Imaging of atypical hemangiomas of the liver with pathologic correlation. *Radiographics* 2000; 20: 379-397 [PMID: 10715338]
19. Leone N, Saettone S, De Paolis P, Carucci P., Brunello F, de Angelis C, Menozzi G, Rizzetto M. Ectopic livers and related pathology: report of three cases of benign lesions. *Dig Dis Sci* 2005; 50: 1818-1822 [PMID: 16187180 DOI : 10.1007/s10620-005-2944-7]
20. Kubota K, Kita J, Rokkaku K, Iwasaki Y, Sawada T, Imura J, Fujimori T. Ectopic hepatocellular carcinoma arising from pancreas: A case report and review of the literature. *World J Gastroenterol* 2007 Aug 21;13(31):4270-3. Review. [PMID: 17696261 DOI: http://www.wjgnet.com/1007-9327/13/4270.asp]
21. Yano T, Ishikura H, Wada T, Kishimoto T, Kondo S, Katoh H, Yoshiki T. Hepatoid adenocarcinoma of the pancreas. *Histopathology* 1999; 35: 90-92 [PMID: 10383723 DOI: 10.1046/j.1365-2559.1999.0728f.x]
22. Paner GP, Thompson KS, Reyes CV. Hepatoid carcinoma of the pancreas. *Cancer* 2000; 88: 1582-1589 [PMID: 10738216 DOI: 10.1002/(SICI)1097-0142(20000401)]
23. Liu CL, Fan ST, Lo CM, Tso WK, Poon RTP, Lam ChM, Wong J. Management of spontaneous rupture of hepatocellular carcinoma: single-center experience. *J Clin Oncol* 2001; 19: 3725-3732 [PMID: 11533094]
24. Caygill CP, Gatenby PA. Ectopic liver and hepatocarcinogenesis. *Eur J Gastroenterol Hepatol* 2004 Aug;16(8):727-9 [PMID: 15256972 DOI:http://dx.doi.org/10.1097/01.meg.0000131037.92864.df]
25. Arakawa M, Kimura Y, Sakata K, Kubo Y, Fukushima T, Okuda K. Propensity of ectopic liver to hepatocarcinogenesis: case reports and a review of the literature. *Hepatology* 1999 Jan;29(1):57-61 [PMID: 9862850 DOI: 10.1002/hep.510290144]
26. Shigemori M, Kondo M, Azechi H, Inue F, Tamura J, Kobayashi H, Saiga T. A case of ectopic hepatocellular carcinoma in the jejunum. *J Gastroenterol* 2006 Sep;41(9):913-8 [PMID: 17048057 DOI: 10.1007/s00535-006-1872-4]
27. Cardona D, Grobmyer S, Crawford JM, Liu Ch. Hepatocellular carcinoma arising from ectopic liver tissue in the pancreas. *Virchows Arch* 2007 Feb;450(2):225-9 [PMID: 17216188 DOI: 10.1007/s00428-006-0353-8]
28. Leone N, De Paolis P, Carrera M, Carucci P, Musso A, David E, Brunello F, Fronda GR, Rizzetto M. Ectopic liver and hepatocarcinogenesis: report of three cases with four years' follow-up. *Eur J Gastroenterol Hepatol* 2004 Aug;16(8):731-5 [PMID: 15256973 DOI:http://dx.doi.org/10.1097/01.meg.0000131044.05434.f7]
29. Seo UH, Lee HJ, Ryu WS, Kwak JM, Shin BK, Kim WB, Lee SI, Park SS, Choi JW, Kim SH, Choi SY, Mok YJ. Laparoscopic resection of a hepatocellular carcinoma arising from an ectopic liver. *Surg Laparosc Endosc Percutan Tech* 2008 Oct;18(5):508-10 [PMID: 18936678 DOI: 10.1097/SLE.0b013e31817e920f]
30. Takayasu K, Itabashi M, Moriyama N. Case report: ectopic hepatocellular carcinoma arising from the left diaphragm. *Clin Radiol* 1994 Aug;49(8):579-81 [PMID: 7955877 DOI: http://dx.doi.org/10.1016/S0009-9260(05)82944-7]
31. Stattaus J, Kühl H, Forsting M. Diagnosis of an accessory liver lobe established by magnetic resonance imaging-guided core biopsy. *Z Gastroenterol* 2008 Apr;46(4):351-4 [PMID: 18393154 DOI: 10.1055/s-2007-963526]

CLINICALLY IMPORTANT INTERACTION BETWEEN METOPROLOL AND PROPRAFENONE

Jana Duricova Mgr, Ilona Perinova Mgr PhD, Nikola Jurckova Mgr, Ivana Kacirova MD, Milan Grundmann MD PhD

Ms Duricova was a postgraduate student in the Department of Clinical Pharmacology, Dr Perinova was a specialist in analytics in the Department of Clinical Pharmacology, Ms Jurckova was a specialist in genetics in the Department of Medical Genetics, Dr Kacirova was a medical doctor and Head of the Department of Clinical Pharmacology, and Dr Grundmann was Associate Professor in the Department of Clinical Pharmacology, all at the University Hospital Ostrava in the Czech Republic.

Originally published in *Canadian family physician* 2013; 59(4): 373-375

Consent to the publication of 2nd April 2014

A combination of antiarrhythmic drugs with β_1 selective blocking agents has often been used. Both these types of drugs are metabolized via the cytochrome P450 (CYP) enzyme system, and therefore potential drug interactions are of considerable clinical significance. The antiarrhythmic agent propafenone undergoes CYP 2D6-dependent metabolism.¹ Propafenone is also an inhibitor of the enzyme; the inhibitory constant has been estimated at 50 nmol/L, similar to that of quinidine (60 nmol/L).² Metoprolol, a β_1 selective blocking agent, undergoes extensive presystemic elimination by CYP 2D6, and it has been shown that metabolites do not substantially contribute to the β_1 -blockade.^{3,4} Metoprolol has a dose-dependent effect; dose is commonly titrated to the highest dose tolerated in order to achieve the maximal effect in the absence of adverse effects.⁵ A 2- to 5-fold increase in steady-state levels of metoprolol has been described after adding propafenone to metoprolol therapy.⁶ The disposition of CYP 2D6 substrates also depends on the CYP 2D6 genotype. In general, 4 subgroups might be differentiated: poor metabolizers (PM), intermediate metabolizers (IM), extensive metabolizers (EM), and ultrarapid metabolizers (UM). Poor metabolizers lack any functional allele. Ultrarapid metabolizers have more than 2 functional alleles. Intermediate metabolizers are heterozygous for a specific variant allele or possess alleles with reduced activity.⁷ We present a case of an interaction between metoprolol and propafenone in which high metoprolol concentrations affect the patient's condition.

CASE

A 66-year-old woman (weight 81 kg) was referred to our outpatient department because of decompensated hypertension (World Health Organization classification grade III). Blood pressure in a sitting position was 154/82 mm Hg, and heart rate was 60 beats/min. The patient had undergone kidney transplantation for polycystic kidney disease several years ago and was taking 175 mg/d of cyclosporine and 50 mg/d of azathioprine. Further comorbidities were ischemic heart disease without angina pectoris syndrome (New York Heart Association class III or IV) and chronic venous insufficiency. At the time of admission, the patient was being treated with the following cardiovascular medication: 200 mg/d of metoprolol, 100 mg/d of losartan, 1 mg/d of rilmenidine, 60 mg/d of furosemide, captopril as needed, 100 mg/d of acetylsalicylic acid, and 20 mg/d of isosorbide mononitrate. To prevent atrial fibrillation, 600 mg of propafenone daily was prescribed. During her follow-up, 5 mg/d of amlodipine was introduced to the therapy. After the medication adjustment, the patient's blood pressure was compensated (**Table 1**); however, she was repeatedly complaining about increased tiredness and dyspnea on exertion. Therefore, determination of metoprolol and α -hydroxymetoprolol serum concentrations was indicated.⁸ Three hours after the patient's metoprolol-dose intake, her metoprolol- α -hydroxymetoprolol metabolic ratio (MR) was used for CYP 2D6 phenotyping.⁹ Genotyping of CYP 2D6 was also performed. A DNA direct sequencing analysis of the whole coding sequence of the CYP 2D6 gene was performed using a genetic analyzer. Copy number variants of the gene were de-

EDITOR'S KEY POINTS

- Propafenone might inhibit metoprolol metabolism, and high metoprolol serum concentrations might have clinical effects. Clinicians should be aware of this potential interaction and start with low metoprolol doses and follow up with patients carefully.
- Therapeutic drug monitoring could serve as a valuable tool in clarifying a patient's condition.

tected using the long-range polymerase chain reaction method and amplified products were visualized on 1% agarose gel electrophoresis. The patient had an IM genotype with detected variant alleles CYP 2D6*4/*9. However, 3 hours after the dose intake, the metoprolol- α -hydroxymetoprolol MR was 104.3, indicative of a PM phenotype. **Table 1** shows metoprolol and α -hydroxymetoprolol serum concentrations. A survey of the patient's concomitant medication revealed her use of propafenone, an inhibitor of CYP 2D6 activity. The patient's metoprolol dose was reduced to 100 mg daily. Her condition improved, and her tiredness and dyspnea disappeared. About half a year later the patient was admitted to the internal medicine department for chest pain on exertion and on rest lasting for about 14 days, with radiation to the right arm, dyspnea, orthopnea, and edema of the lower limbs. Blood pressure on admission was 160/80 mm Hg, and heart rate was 51 beats/min. She was diagnosed as having global cardiac failure with atrial fibrillation with slow ventricular response. Relevant therapy was initiated with an adjustment of her medication. Her metoprolol dosage was reduced to 12.5 mg daily, and propafenone was withdrawn. Two weeks later the patient was hemodynamically stable and was discharged from the hospital. Several days after discharge, the patient herself increased her metoprolol intake to a previous dose of 100 mg daily. During the next outpatient's visit, her CYP 2D6 phenotype after propafenone discontinuation was determined (**Table 1**); a substantial decrease in metoprolol- α -hydroxymetoprolol MR was revealed, switching the patient's phenotype from PM (MR = 104.3) to EM (MR = 1.4).

DISCUSSION

This case demonstrates an inhibitory effect of propafenone on metoprolol biotransformation resulting

in the occurrence of adverse effects due to high metoprolol levels. Propafenone has been shown to be metabolized by the same hepatic enzyme as the sparteine-debrisoquine polymorphism but with higher affinity for CYP 2D6, thereby being able to cause a shift of metabolizer phenotype.¹ Metoprolol undergoes extensive presystemic elimination, with this enzyme accounting for 70% to 80% of its metabolism. In our patient, a marked decrease in metoprolol- α -hydroxymetoprolol MR was observed after propafenone therapy had been stopped, and the patient's phenotype switched from PM to EM. Because the patient's other medications were retained, we attribute this phenotypic shift to vanished inhibitory effect. Labbé et al found that the addition of propafenone to CYP 2D6 substrate mexiletine in people with EM phenotypes caused pharmacokinetic changes of mexiletine to such an extent that differences between those with EM phenotypes and PM phenotypes were almost absent.¹⁰ Thus, results of phenotyping might be falsified by the presence of interfering medications, resulting in discrepancy between the phenotype and genotype. Wagner et al found that the addition of propafenone increased steady-state levels of metoprolol 2 to 5 times in 4 patients. Two patients even developed side effects while receiving the drug combination (severe nightmares and left ventricular failure), which disappeared after the metoprolol dose was reduced or discontinued.⁶ Our patient suffered from tiredness and dyspnea on exertion likely owing to high metoprolol serum concentrations caused by the inhibitory effect of propafenone. Substantial increases in metoprolol concentrations have also been observed after the addition of the antiarrhythmic drug amiodarone and the antihistamine diphenhydramine.^{11,12} The addition of selective serotonin reuptake inhibitors, fluoxetine and paroxetine, has also resulted in severe adverse effects, which subsided

Table 1. Patient's metoprolol and α -hydroxymetoprolol serum concentrations; metoprolol- α -hydroxymetoprolol metabolic ratio; heart rate; and blood pressure before metoprolol intake and 1 or 3 hours after metoprolol intake, with and without propafenone

METOPROLOL DAILY DOSE	METOPROLOL SERUM LEVEL ($\mu\text{g/L}$)	α -HYDROXYMETOPROLOL SERUM LEVEL ($\mu\text{g/L}$)	METOPROLOL- α HYDROXYMETOPROLOL METABOLIC RATIO	HEART RATE (BEATS/MIN)	BLOOD PRESSURE (mm Hg)
200mg with propafenone					
• Before metoprolol intake	152.4	4.4	34.6	66	136/76
• 1 h after	333.2	3.8	87.7	59	134/72
• 3 h after	412.2	4.0	104.3	61	128/76
100mg with propafenone					
• Before metoprolol intake	79.2	7.7	10.3	68	132/68
• 1 h after	168.6	4.0	42.2	67	138/74
100mg without propafenone					
• Before metoprolol intake	10.3	32.0	0.3	55	124/62
• 1 h after	53.8	44.0	1.2	62	126/70
• 3 h after	134.9	97.7	1.4	53	NA

NA - not available.

after discontinuation of the inhibitors.^{13,14}

In our case the patient's genotype was heterozygous for CYP 2D6*4/*9 alleles. Individuals who carry the CYP 2D6*9 allele have an altered ability to metabolize CYP 2D6 substrates and have IM phenotypes, whereas the CYP 2D6*4 allele results in a loss of enzyme activity.¹⁵ The combination of IM phenotype and defective alleles is not associated with a PM phenotype; however, it shows a substantially higher MR than does the EM-PM genotype.¹⁶ The S-enantiomer of propafenone has also been shown to display β -blocking action. The degree of β -blockade reflects genetically determined variations in propafenone metabolism, with subjects with the PM phenotype having considerably more β -blockade.¹⁷ Unfortunately we were not able to determine the propafenone serum concentration and subsequently assess its contribution to the occurrence of adverse effects. However, after the metoprolol dose was reduced to half (100 mg/d), the side effects disappeared. Interestingly, blood pressure and, in particular, heart rate did not change substantially after metoprolol dose reduction and after propafenone discontinuation. Pharmacodynamic modeling of the β_1 -blocking effect of metoprolol shows a steep linear relationship to plasma concentration, with a maximum effect at 400 nmol/L (106.96 μ g/L). However, only 30% of the maximum β_1 -blocking effect is necessary for a clinically significant effect; this limit was observed at a metoprolol plasma concentration of 45 nmol/L (12.03 μ g/L).⁴ We speculate that the permanent metoprolol serum concentrations in our patient above this concentration limit preserved stable heart rate in spite of gradual decline in metoprolol concentrations.

CONCLUSION

Coadministration of propafenone and metoprolol might result in elevation of metoprolol serum concentration and affect a patient's clinical condition. Clinicians should be aware of the potential interaction when prescribing this combination and start with low metoprolol doses, as well as follow up with patients carefully. Therapeutic drug monitoring could serve as a valuable tool in clarifying a patient's condition.

REFERENCES

1. Kroemer HK, Fischer C, Meese CO, Eichelbaum M. Enantiomer/enantiomer interaction of (S)- and (R)-propafenone for cytochrome P450IID6-catalyzed 5-hydroxylation: in vitro evaluation of the mechanism. *Mol Pharmacol* 1991;40(1):135-42.
2. Otton SV, Inaba T, Kalow W. Competitive inhibition of sparteine oxidation in human liver by beta-adrenoceptor antagonists and other cardiovascular drugs. *Life Sci* 1984;34(1):73-80.
3. Frank D, Jaehde U, Fuhr U. Evaluation of probe drugs and pharmacokinetic metrics for CYP2D6 phenotyping. *Eur J Clin Pharmacol* 2007;63(4):321-33. Epub 2007 Feb 2.
4. Abrahamsson B, Lückner P, Olofsson B, Regårdh CG, Sandberg A, Wieselgren I, et al. The relationship between metoprolol plasma concentration and beta 1-blockade in healthy subjects: a study on conventional metoprolol and metoprolol CR/ZOK formulations. *J Clin Pharmacol* 1990;30(2 Suppl):S46-54.
5. Regårdh CG, Johnsson G. Clinical pharmacokinetics of metoprolol. *Clin Pharmacokinet* 1980;5(6):557-69.
6. Wagner F, Kalusche D, Trenk D, Jähchen E, Roskamm H. Drug interaction between propafenone and metoprolol. *Br J Clin Pharmacol* 1987;24(2):213-20.
7. Zanger UM, Raimundo S, Eichelbaum M. Cytochrome P450 2D6: overview and update on pharmacology, genetics, biochemistry. *Naunyn Schmiedeberg's Arch Pharmacol* 2004;369(1):23-37. Epub 2003 Nov 15.
8. Perinova I, Duricova J, Brozmanova H, Kacirova I, Grundmann M. Determination of metoprolol and its metabolite α -hydroxymetabolite in serum by HPLC method with fluorescence detection [article in Czech]. *Ces Farm* 2008;57(6):254-9.
9. Jonkers RE, Koopmans RP, Portier EJ, van Boxtel CJ. Debrisoquine phenotype and the pharmacokinetics and beta-2 receptor pharmacodynamics of metoprolol and its enantiomers. *J Pharmacol Exp Ther* 1991;256(3):959-66.
10. Labbé L, O'Hara G, Lefebvre M, Lessard E, Gilbert M, Adeyoin A, et al. Pharmacokinetic and pharmacodynamic interaction between mexiletine and propafenone in human beings. *Clin Pharmacol Ther* 2000;67(1):44-57.
11. Fukumoto K, Kobayashi T, Tachibana K, Kato R, Kazuhiko T, Komamura K. Effect of amiodarone on the serum concentration/dose ratio of metoprolol in patients with cardiac arrhythmia. *Drug Metab Pharmacokinet* 2006;21(6):501-5.
12. Hamelin BA, Bouayad A, Méthot J, Jobin J, Desgagnés P, Poirier P, et al. Significant interaction between the nonprescription antihistamine diphenhydramine and the CYP2D6 substrate metoprolol in healthy men with high or low CYP2D6 activity. *Clin Pharmacol Ther* 2000;67(5):466-77.
13. Walley T, Pirmohamed M, Proudlove C, Maxwell D. Interaction of metoprolol and fluoxetine. *Lancet* 1993;341(8850):967-8.
14. Onalan O, Cumurcu BE, Bekar L. Complete atrioventricular block associated with concomitant use of metoprolol and paroxetine. *Mayo Clin Proc* 2008;83(5):595-99. DOI:10.4065/83.5.595.
15. The Human Cytochrome P450 (CYP) Allele Nomenclature Database [website]. CYP2D6 allele nomenclature. Stockholm, Sweden: The Human Cytochrome P450 (CYP) Allele Nomenclature Database; 2012. Available from: www.cypalleles.ki.se/cyp2d6.htm. Accessed 2013 Jan 11.
16. Sachse C, Brockmüller J, Bauer S, Roots I. Cytochrome P450 2D6 variants in a Caucasian population: allele frequencies and phenotypic consequences. *Am J Hum Genet* 1997;60:284-95.
17. Lee JT, Kroemer HK, Silberstein DJ, Funck-Bretano C, Lineberry MD, Wood AJ, et al. The role of genetically determined polymorphic drug metabolism in the beta-blockade produced by propafenone. *N Engl J Med* 1990;322(25):1764-8.

OBJECTIVE EVALUATION OF THE EFFECT OF AUTOLOGOUS PLATELET CONCENTRATE ON POST-OPERATIVE SCARRING IN DEEP BURNS

Hana Klosová^{a,*}, Jiří Štětinský^a, Iveta Bryjová^{b,c}, Stanislav Hledík^c, Leo Klein^{d,e}

^a Burn Center, University Hospital Ostrava, 17. listopadu 1790, 708 52 Ostrava-Poruba, Czech Republic

^b VŠB-Technical University of Ostrava, 17. listopadu 15/2172, 708 33 Ostrava-Poruba, Czech Republic

^c Institute of Physics, Silesian University in Opava, Bezručovo nám. 13, 746 01 Opava, Czech Republic

^d Division of Plastic Surgery and Burns Unit, Charles University in Prague, Medical Faculty and Teaching Hospital in Hradec Králové, Sokolská 581, 500 05 Hradec Králové, Czech Republic

^e Faculty of Military Health Sciences, University of Defence, Třebešská 1575, 500 01 Hradec Králové, Czech Republic

Originally Published in *Burns* 2013; 39 (6): 1263-1276

Consent to the publication of 23rd April 2014 (No. 3374580799917)

ABSTRACT

Introduction:

The healing of grafted areas after surgical treatment of deep burns frequently generates mutilating scars, and rises the risk of subsequent scar hypertrophy. Scar assessment based on clinical evaluation is inherently subjective, which stimulates search for objective means of evaluation.

Objective:

The aim of this study was to objectively evaluate the effect of using autologous platelet concentrate (APC) in combination with split thickness skin grafting (STSG) on scarring processes following surgery of deep burns as compared with application of STSG alone.

Method:

Selected viscoelastic properties of 38 scars on 23 patients in total were examined using the Cutometer MPA 580 under controlled conditions for long-term outcomes 1, 3, 6 and 12 months after surgery following deep burns.

Results:

The findings of this study suggest that the STSG + APC combination reduces the time of scar viscoelastic properties recovery as compared with application of STSG alone. This was statistically significant for viscoelastic parameters R2 and Q1.

Conclusion:

APC has been advocated to enhance scarring after surgery of deep dermal and full thickness burns. We objectively demonstrated that the viscoelastic properties of scar treated with STSG + APC combination return more rapidly to the plateau state than are treated with STSG only.

KEYWORDS:

Burns assessment, Scar, Surgical treatment of deep burns, Split thickness skin graft (STSG), Autologous platelet concentrate, (APC), Skin viscoelasticity, Cutometer

1. INTRODUCTION

Increasing emphasis is placed on the functional and cosmetic outcomes following treatment of non-healing deep dermal and particularly full thickness burns which are subject to surgical treatment in the form of sharp tangential excision followed by skin grafting. Such a practice is a golden rule in burns treatment [1]. Meshed Split Thickness Skin Grafting (referred to as STSG hereinafter) represents one of the independent risk factors for postburn pathologic scarring [2]. The healing of grafted areas frequently generates widespread and mutilating scars, thus giving rise the risk of subsequent scar hypertrophy at the same time. The prevalence of pathologic scarring after burn has not yet been well documented [2] and remains in fact unknown [3].

Several scales were proposed and have been routinely used in clinical evaluation of postburn scarring and scars therapy response. The main representatives include the Vancouver Scar Scale (VSS), Patient and Observer Scar Assessment Scale (POSAS), Visual Analog Scale (VAS), and Manchester Scar Scale (MSS), among which the VSS is the most frequently used one [4]. Scar assessment routinely based on the above mentioned scales is inherently subjective and thus highly observer dependent [5]. This lack of objectivity stimulates the search for methods of objective evaluation based on more reliable assessment techniques. Non-invasive suction method has been found to be a reliable for single-observer measurement of scar viscoelastic properties [6].

Autologous Platelet Concentrate (referred to as APC hereinafter) has been used for about 20 years in diverse surgical fields of medicine to improve wound healing and tissue repair. Platelet growth factors have shown its potential to improve healing in many human clinical studies, particularly in oral and periodontal surgery [7-11], orthopaedics and trauma surgery [12-14], and plastic surgery [15,16]. On the other hand, there is a lack of clinical experience

and long-term outcomes of deep burns surgical treatment using APC simultaneously with STSG.

The aim of this retrospective study was to analyze and evaluate the long-term effect of APC in combination with STSG on scarring processes following skin grafting of deep burns, as compared to applying sole STSG by using the objective method. The alternate hypothesis was that using APC in combination with STSG leads to better viscoelastic scar properties and, consequently, to better functional and cosmetic outcomes, against the null hypothesis that no effect is produced by using APC in combination with STSG.

2. METHODS

The study protocol was reviewed and approved by the Institutional Review Board of the University Hospital Ostrava. All patients were fully informed about the study and signed the informed consent with the treatment and subsequent measurements.

The study presented is a retrospective data analysis obtained by the objective testing of long-term outcomes of scarring after deep burns surgery. The assessments were carried out under controlled conditions by objective measuring the viscoelastic properties of skin using the suction method.

2.1. Subjects

From March 2011 till October 2012, a total of 23 patients (10 men and 13 women) underwent measurements of scar and normal skin viscoelastic parameters one, three, six and twelve months after the surgical treatment of full thickness and non-healing deep dermal burns. Total of 38 scars were subjected to those measurements. Both scars healed using STSG + APC (total of 24 scars) and those healed using STSG without APC (total of 14 scars), as well as normal skin sites for comparison (total of 42 sites) were involved. Five patients were treated with the use of STSG only, 5 patients underwent surgery using both STSG with the APC in one area and sole STSG in another area, and 13 patients whose burns were treated with the use of STSG in combination with the APC. The distributions of age, burns extent, surgically treated area (equal to the STSG treated area), STSG in combination with APC treated area, STSG only treated area (all in percent TBSA), and time after injury are given in Table 1 and graphically represented in Figs. 1 and 2. The statistics of scar numbers are graphically represented in Fig. 3. The burns were in most cases caused by flame and by hot liquid (43.5 %), contact (8.7 %), and electricity (4.3 %). Operations were performed on 11th (3.7) day after injury (see Table 1).

2.2. Inclusion and exclusion

Inclusion criteria of the study were: (1) adult patients (18 years of age or above) with full thickness burns and/or non-healing deep dermal burns who underwent skin grafting with or without APC, (2)

signed the informed consent form prior to participation, and (3) intact skin integrity in the areas of viscoelasticity measurements.

Adults unable to give informed consent for the study, patients age under 18 years, patients with impaired skin integrity in the areas of cutometric measurements, skin diseases, current intake of oral anticoagulants, platelet aggregation inhibitors or abnormal bleeding history were excluded.

2.3. Material and instrumentation

The APC and autologous thrombin were prepared by density gradient centrifugation using the Harvest SmartPreP Platelet Concentrate System (manufactured by Harvest Technologies Corporation, Plymouth, MA, USA). The whole process was carried out under strictly sterile conditions right in the operating room simultaneously with the surgery. Hence, the surgery time was not increased at all. The patient's peripheral venous blood was collected in two consecutive steps - from the first batch the autologous thrombin for activation of platelets was prepared, from the second one, about 30 min later, the APC was produced. The blood was centrifuged in accord with the manufacturer's recommendations at 2400 rpm for 14 min at room temperature. 9 ml of blood volume enabled to produce 3 ml of autologous thrombin, 60 ml of blood volume enabled to produce 10 ml of the APC. To get an idea about the quantity needed, the rule of thumb is that 10 ml of APC can cover about 4 % of TBSA.

Table 1 - Basic demographic statistics.

	Min	Mean	Median	Max	SD
Age[years]	21	48.6	40	81	21.7
Surgery PTD	6	10.9	11	22	3.7
% TBSA of Burns	1.25	7.0	6.0	17.0	5.4
Necrectomy	1.0	3.7	3.0	15.5	3.2
STSG total	1.0	3.7	3.0	15.5	3.2
STSG + APC	0.0	2.5	2.5	9.0	2.2
STSG only	0.0	1.2	0.0	8.0	2.1

The APC and autologous thrombin were applied to the skin grafted areas using a special SmartJet Applicator (Harvest Technologies Corporation, Plymouth, MA, USA). APC is a fluid which jellifies within 20-30 s. Gelation is an important factor for graft adherence to the recipient area that prevents grafts displacement and creates favourable input conditions for graft take. After local transplantation of APC and platelet activation by autologous thrombin, the selective sequential release of platelet growth factors improves healing, accelerates scars maturation and reduces

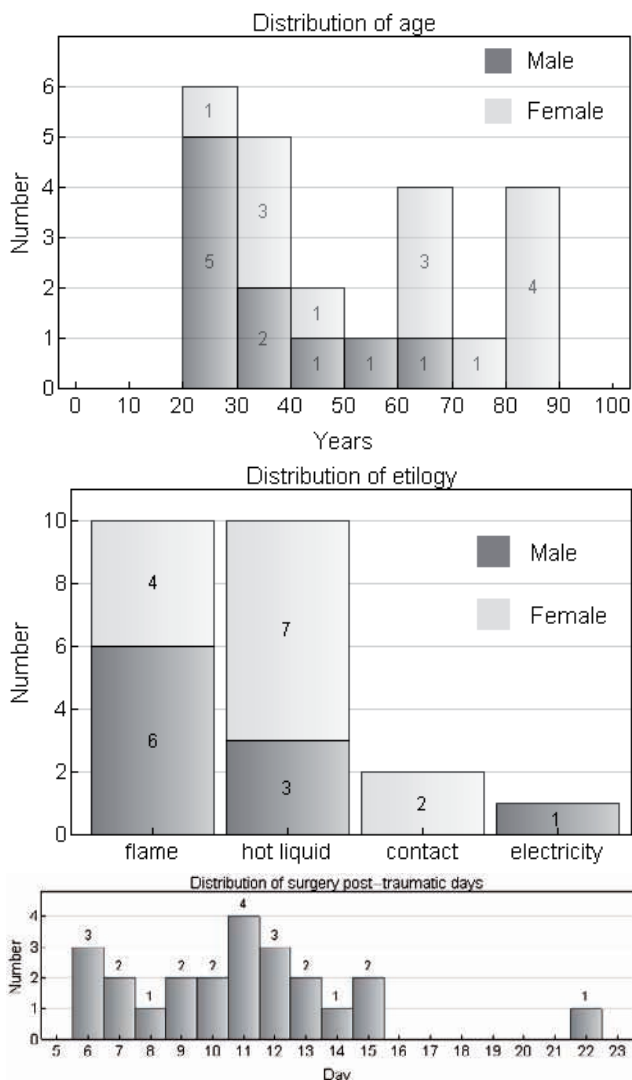


Fig. 1 - (a) Distribution of burned patients by age. The patients aged 20-40 years were 50% of all patients, (b) distribution of burns etiology and (c) distribution of post-traumatic day of the surgery.

subsequent hypertrophic scarring [17]. Since APC is a topically applied autologous material, the risk of blood transfer disease is virtually nonexistent, and no systemic undesirable effects have been identified. The Cutometer MPA 580 by Courage & Khazaka electronic GmbH (referred to as cutometer hereinafter) is a commercially available device for non-invasive contact diagnostics of mechanical properties of skin via measuring its viscoelastic parameters [18-20]. It has been used in the assessment of scar elasticity and in the comparison of dermal skin substitutes and STSG in acute burns and reconstructive surgery [6,21]. The cutometer device consists of a hand held probe with a circular suction opening of 2 mm diameter, a main unit containing a vacuum pump that generates a controlled underpressure inside the probe, and a connecting tube between the probe and the main unit (see Fig. 4). The whole system is connected to and controlled by a computer equipped with dedicated software Cutometer MPA Q supplied together with the hardware [18].

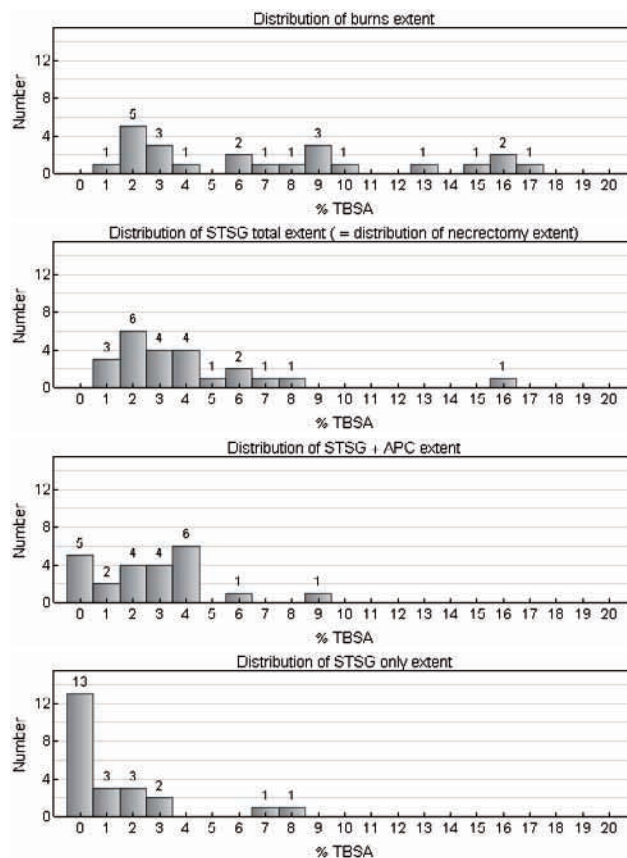


Fig. 2 - (a) Distribution of burns extent, (b) distribution of the STSG total extent which equals to necrectomy extent, (c) distribution of STSG in combination with APC extent and (d) distribution of STSG only extent.

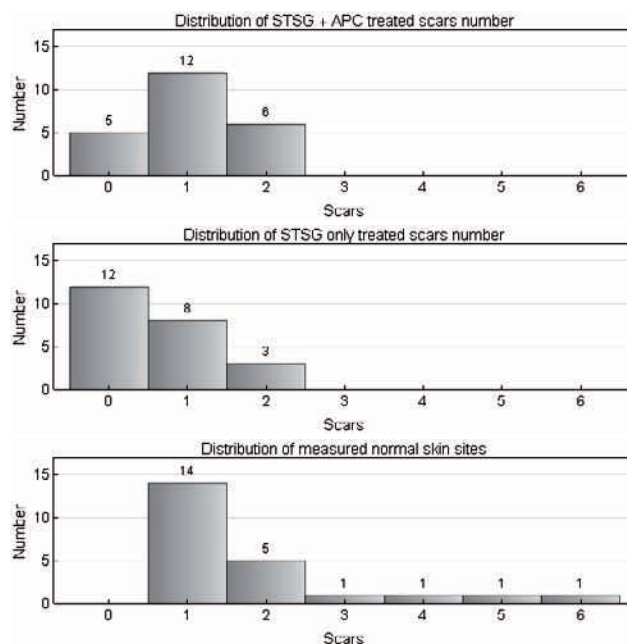


Fig. 3 - (a) Distribution of scar number treated with STSG in combination with APC, (b) distribution of scar number treated with STSG only and (c) distribution of number of measured normal skin sites.

Four measuring modes differing in the time dependence of underpressure are currently implemented for the cutometer. However, only Mode 1, characterized by a constant under-pressure value during a

predefined suction time (also referred to as on-time) immediately followed by an interval of switched off underpressure (referred to as relaxation time or off-time), is almost exclusively used for results published in current literature [18]. During the suction period the skin is drawn into the probe opening, and the depth of the skin penetration (skin deformation) is measured by a precise non-contact optical system with a sampling interval of 0.01 s. The sampled values of skin deformation are then stored for future processing on the attached computer system in the form of digitalized strain-vs-time cutometric curves. The typical shape of a strain-vs-time curve measured in Mode 1 is shown in Fig. 5. Each suction-relaxation cycle has arising part during the suction followed by a decreasing part during relaxation. The ascending part consists of two segments. In the first segment which is dominated by the elastic component of the skin distensibility, the slope of the curve is very steep, and the maximum deformation reached is usually denoted in literature as U_e . Within the second segment the curve gradually flattens more and more which is typical for the viscoelastic component of the skin behaviour [22,23,18]. During this viscoelastic segment the curve increases by U_v , reaching its full extension of $U_f = U_e + U_v$ (see Fig. 5). In highly elastic materials (like a rubber balloon) the value of U_v is negligible in comparison with U_e . The descending part (during the relaxation when the underpressure is released) consists of two segments as well. Similarly to the suction part, the (negative) slope of the strain-vs-time curve in the first segment (which is dominated by the elastic component of the skin retractability) is very steep, and the extension quickly drops by a value referred to as U_r , leaving total residual extension $U_f - U_r$. The values of U_e and U_r are related to the function of elastin fibres [24-26]. Within the second segment of the decreasing part the curve gradually flattens more and more which is again typical for viscoelastic component of the skin relaxation behaviour. During these second segment the curve continues in drop by $U_a - U_r$, reaching its total drop of U_a (relative to the maximum U_f), leaving a residual strain of $R = U_f - U_a$ as shown in Fig. 5. In highly elastic materials the value of U_a is very close to U_f , in other words, the material almost completely restore its original shape when it went out of the probe opening.

The parameters U_f , U_e , U_v , U_r and U_a , and related parameters used in literature ($R_0 \equiv U_f$, $R_1 \equiv R = U_f - U_a$, and $R_8 \equiv U_a$) are all dimensional (usually expressed in millimetres), thus dependent on the skin thickness. In other words, these parameters mix both intrinsic viscoelastic properties of the skin and the probed area spatial dimensions. To get rid of the skin thickness contribution, it is advantageous to introduce intrinsic tissue characteristics U_f , U_e , U_v , U_r and U_a which take into account the corresponding skin

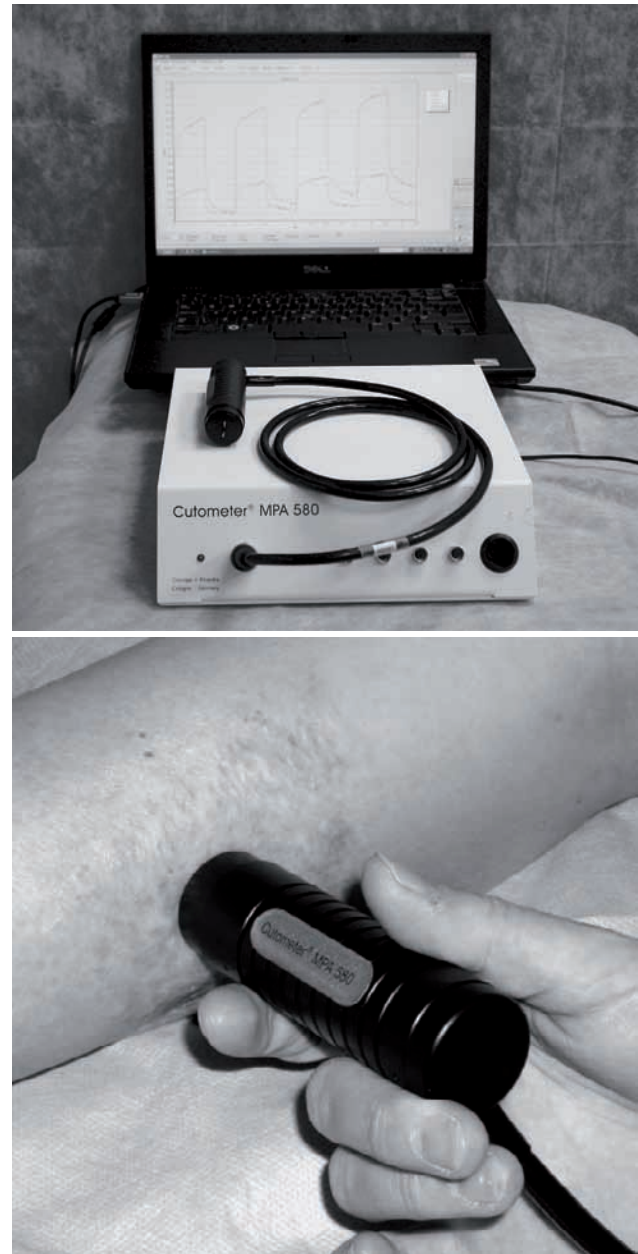


Fig. 4 - The Cutometer MPA 580 device. Top: main unit, probe, connecting tube and computer running the Cutometer MPA Q software. Bottom: Measuring with the probe.

thickness τ in the form of product

$$U_f^* = U_f \tau$$

(and analogously for the remaining parameters), as utilized, e.g., in paper [27]. However, such approach requires time consuming measurement of skin thickness. Another possibility which we finally decided to adopt in this study is to restrict only to dimensionless parameters defined as

$$R_2 = \frac{U_a}{U_f} \quad R_5 = \frac{U_r}{U_e} \quad R_6 = \frac{U_v}{U_e} \quad R_7 = \frac{U_r}{U_f} \quad (1)$$

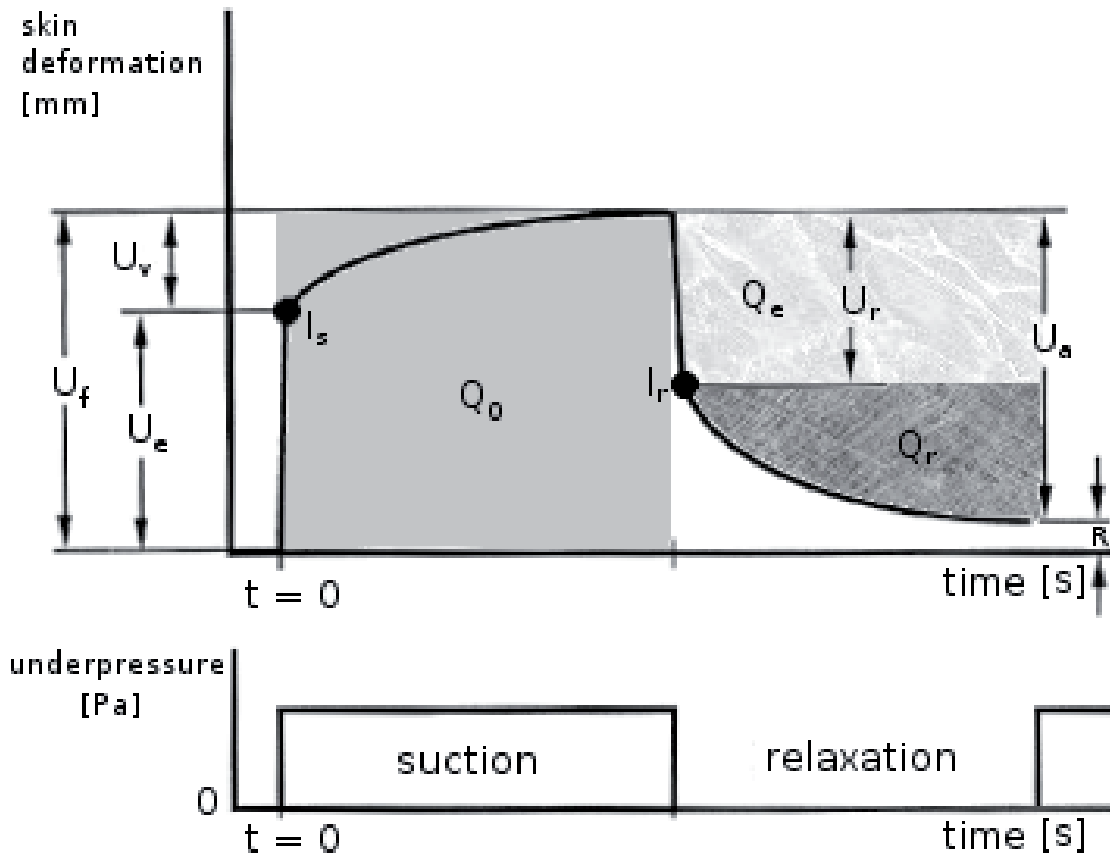


Fig. 5 - Illustration of the cutometric parameters definition for cutometer in Mode 1. Conceptually the area parameter $Q_1 = (Q_e + Q_r) / Q_0$ corresponds to linear parameter $R_2 = U_a / U_f$, the area parameter $Q_2 = Q_e / Q_0$ corresponds to linear parameter $R_7 = U_r / U_f$, and the area parameter $Q_3 = Q_r / Q_0$ corresponds to the difference $R_2 - R_7 = (U_a - U_r) / U_f$. Adapted from [18]

Due to the fractional nature these parameters do not depend on whether the starred form or the plain form of the U-parameters is used, since the skin thickness is eliminated from their definitions. An additional advantage of these parameters lies in the fact that to the first approximation they should be independent on the probe aperture size.

There is another suitable choice in introducing area Q-parameters [18]. They are defined as follows. Let Q_0 be the area of the suction part bounding box (grey filled area in Fig. 5), let Q_e be the elastic recovery area (marbled area in Fig. 5), and let Q_r be the viscous recovery area (paper texture filled area in Fig. 5). Then we define

$$Q_2 = \frac{Q_e}{Q_0} \quad Q_3 = \frac{Q_r}{Q_0} \quad Q_1 = Q_2 + Q_3 = \frac{Q_e + Q_r}{Q_0} \quad (2)$$

The Q-family parameters are dimensionless and more robust than the R-parameters, since they take into account not only values of final strain but they also depend on the path of the strain-vs-time curve within the relaxation period.

Definitions of other cutometric parameters can be found in the literature; worth mentioning are namely R_3 and R_4 related to the last cycle maximum and minimum amplitude, respectively, then parameter $R_9 = R_3 / R_0$, and so called area F-parameters F_0 through F_4 [18]. All these parameters require repetitions of the suction-relaxation cycle (conventionally 10 repetitions) and are not considered in this paper.

At this point it is worth noting that the standard algorithm engaged in determining the inflection points separating the elastic and viscoelastic segments of the strain-vs-time curve relies heavily on the experimental fact that the time T_{infl} elapsed from the instant of under pressure switch-on to attaining the value of U_e approximately equals to 0.1 s; the same value is used for separation the elastic and viscoelastic segment of the relaxation part. These inflection points are denoted in Fig. 5 as I_s and I_r , respectively. The above empirical value of time T_{infl} (which corresponds to 10 sampling intervals) is hardcoded in the configuration file of the cutometer software. Although an experienced user is given an opportunity to change the value by editing the configuration file, the basic principle of a constant elastic segment

duration still survives. This setup leads to a strong dependence of all inflection point based dimensional parameters (i.e., U_e , U_v , and U_r), as well as all derived dimensionless linear parameters (R_5 , R_6 , R_7) on the fixed time T_{infl} . Indeed, a subtle perturbation in the slope of the elastic segment leads either to mutually compensating underestimation or overestimation of these parameters. As a consequence, the parameter R_2 remains the most reliable and robust one. Similar considerations apply also for the Q -parameters. While the values of Q_2 and Q_3 strongly depend on the position of the inflection point I_r (hence, on the value of T_{infl}), the value of Q_1 is independent on the empirical value of T_{infl} . Similarly, the Q_1 parameter is the most reliable one among the Q -parameter family provided the constant elastic segment duration is used.

In the literature, the parameter R_2 is referred to as the gross-elasticity of the skin (it includes the skin viscous deformation), and represents the ability of total reformation of the skin. The parameter R_5 is referred to as net-elasticity of the skin (with the viscous deformation excluded), and it represents the ratio of ability of immediate retraction to the ability of immediate distention. The parameter R_6 represents the portion of viscoelasticity in the elastic part of the curve. Finally, the parameter R_7 is referred to as the biological elasticity of the skin, and it represents the ratio of the ability of immediate retraction to the ability of final distention. For more detailed analysis, see [22] and papers cited therein. To conclude the selection of cutometric parameters to be analyzed, we preferentially take the dimensionless parameters R_2 and Q_1 defined by Eqs. (1) and (2) into account for their independence on the position of the viscoelastic transition point. In order to assess the elastic and viscous part separately, we adopt the area parameters Q_2 and Q_3 defined by Eq. (2) because they are superior to the R_5 , R_6 , R_7 parameters in the sense of their greater robustness.

2.4. Data acquisition

The cutometer was operated in Mode 1 in all patients under the following controlled conditions: the probe aperture of 2 mm, constant suction underpressure of 450 mbar, equal suction and relaxation phases of 2 s each. Until July 2012, the default number of ten cycle repetitions has been used, which resulted in total measurement duration 40 s. As of August 2012, the number of repetitions has been reduced to 4 because none repetition-dependent parameters (such as R_3 , R_4 and R_9 or area F -parameters) have been taken into account. This adjustment shortened a single site measurement down to 16 s without having effect on the results. The measurements were performed on each patient at the same daytime, in the same examination room with controlled room temperature within 22-24 °C and air relative humidity of 50%±10 %. Measured sites were shaved to prevent

penetration of hairs into the probe aperture. All patients were accustomed to the ambient temperature, had been inactive for period of 15 min, and were always examined in the same position with limbs rested. The cutometer was regularly calibrated against the etalon supplied along with the device. The aperture was cleaned if necessary following the manufacturer instructions [18].

The examined areas were (1) scars following surgical treatment using STSG in combination with APC, (2) scars following surgical treatment using STSG only, and (3) normal skin areas in the contralateral or adjacent location (or otherwise best-matched site) to the scars, which acted as the control. All measurements were always carried out by the same physician to avoid introducing various kinds of errors caused by the probe operator. Prior to examination, a digital photo of the measured site was taken.

Since the burn scars are planar, usually having an irregular shape and in homogeneous surface, the measurements were performed in four different representative points of a scar in each patient in order to collect sufficient amount of data characterizing the scar viscoelastic properties in its entirety. For this purpose, as the first step, a "site map" was prepared in the form of a transparent foil placed on the scar area, while the scar borders were marked using indelible marker as shown in Fig. 6. Consequently, four quadrants were identified in the site map, and one measuring point was chosen in the centre of each quadrant. These site maps were filed and served as a guarantee for exact match of sites and reproducibility of measurements.

Total number of 418 curves was measured, of which 24 were excluded because of poor quality of measurement. Although the reasons of such flaws have not been explicitly examined, we are inclined to ascribe them to the most plausible sources - mostly to air leaks around the probe aperture and to soaking up a hair remnants that escaped being shaved into the probe aperture, which resulted in confusion of the measuring optical system. Thus, a net total of 394 curves entered processing and statistical analysis. Examples of both eligible and flawed curves are shown in Fig. 7.

2.5. Data processing and statistical analysis

All measured strain-vs-time curves acquired in the course of study were in the form of DBF and XLS files transferred from the control PC to another computer. Consequently, they were categorized by patient identification, by post-surgery month, and by treatment (STSG only scars, STSG + APC scars, and normal skin areas). The algorithm utilized by the original software to compute cutometric parameters from the curves was reimplemented under system Mathematica® (see, e.g., [28]).

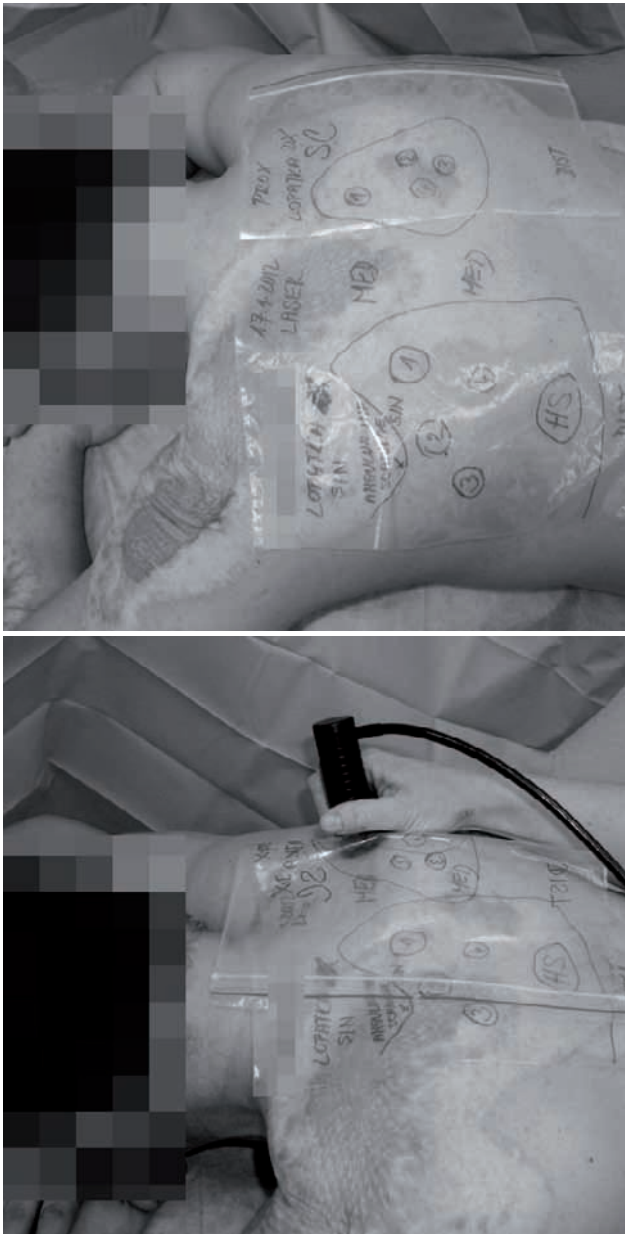


Fig. 6 - Using transparent foil map for exact measurementsite reproducibility.

Measured values of cutometric parameters R2, Q1, Q2 and Q3 were grouped as follows. 2 Values for each parameter were placed into a sample labelled with a specific post-surgery month (PSM 1, 3, 6 and 12) and treatment type/control (STSG + APC, STSG only, and Normal skin) regardless of the patient identification. Thus, total of 12 samples reflecting all possible combinations of post surgery month and type of surgery were formed. These 12 samples were subjected to statistical treatment under the Mathematica® system. However, before any statistical calculations were commenced, an unabridged catalogue of all cutometric strain-vs-time curves had been generated for the purpose of exclusion of all corrupted curves as described in the previous section (see also Fig. 7), having left net total of 394 curves to be subject to statistics.

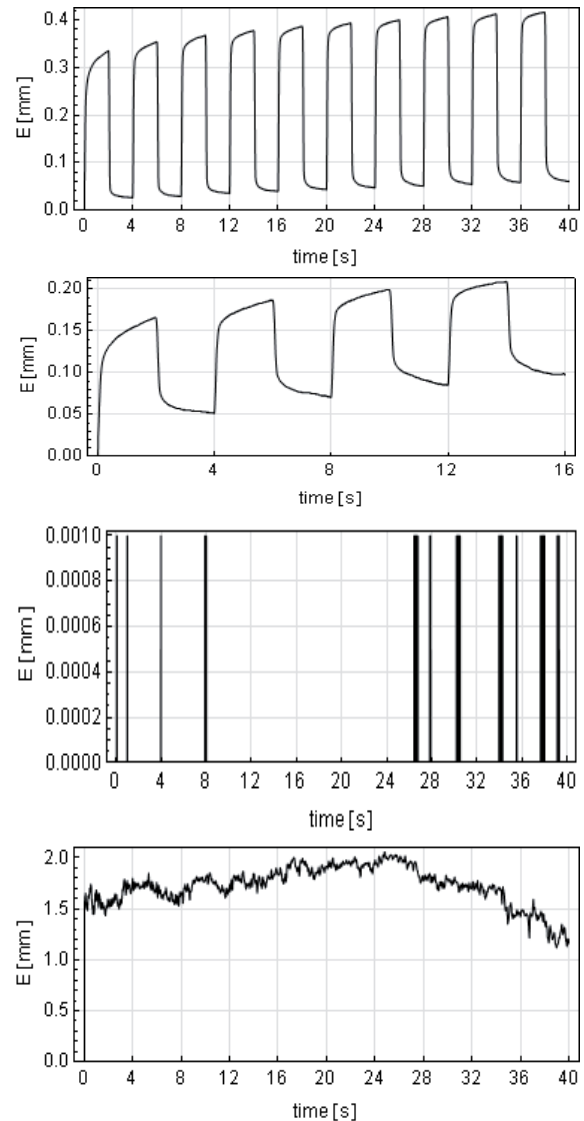


Fig. 7 - (a) Example of eligible cutometric curve with 10 repetitions. (b) Example of eligible cutometric curve with 4 repetitions. (c) Example of cutometric curve corrupted presumably by air leakage around the probe aperture. (d) Example of cutometric curve corrupted presumably by inadvertent penetration of hair remnants into the probe aperture. All 24 cases similar to those in the bottom rows were expunged from the set of eligible curves.

² See the discussion on parameter selection in Section 2.3.

For the purposes of descriptive statistics, box-and-whiskers chart was chosen for its ability to provide comprehensive graphical overview of the basic statistical quantities superior to tabular form (description of basic box-and-whiskers chart anatomy is given in the caption of Fig. 8). The inferential statistical analysis was carried out using multiple comparison tests, both parametric and non-parametric. The former which tested the hypothesis concerning the equality of all 12 means was one-way ANOVA followed by post hoc analysis in the form of Tukey test, the latter which tested the hypothesis concerning the equality of all 12 medians was Kruskal-Wallis test followed by post hoc analysis in the form of Bonferroni test [29]. Significance level of 5 % was adopted.

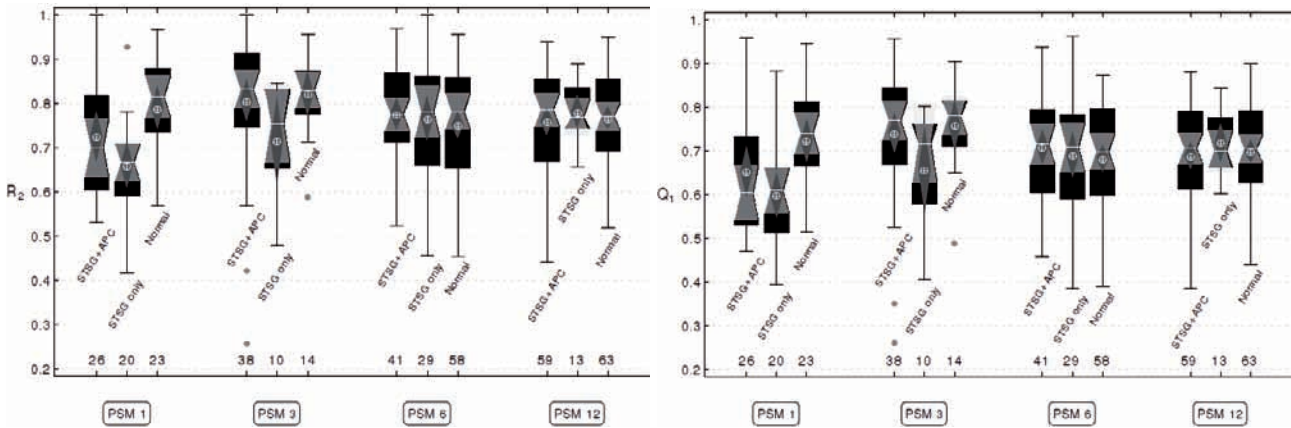


Fig. 8 - Top: Box-and-whisker chart for cutometric parameter R₂. Bottom: Box-and-whisker chart for cutometric parameter Q₁. In each of four post-surgery months 1, 3, 6 and 12, cutometric measurements of viscoelastic properties (including parameters R₂ and Q₁) were carried out on three groups of scars: those treated with combination STSG only, STSG + APC, and control group with normal skin sites. For all resulting 12 samples the box-and-whisker charts were constructed as shown. The upper and lower sides of black boxes mark the upper and lower quartiles, respectively. The upper and lower fences ending the whiskers mark maximum and minimum values, respectively (outliers, if any, are marked by grey dots). White horizontal lines in the narrowest places of the boxes mark median, the light grey notches mark the median confidence intervals. White circled crosshairs mark the location of means, and vertical dimension of the dark grey diamonds centred on crosshairs mark the mean confidence interval. The respective sample sizes are marked by the numbers above the time axis ticks.

Finally, best fits to cutometric data as a function of time were calculated using nonlinear regression (gradient descent algorithm) for parameters R₂, Q₁, Q₂ and Q₃ in both treatment modes STSG + APC and STSG only, as well as normal skin. The model dependence was considered in the form

$$p(t) = p_s - p_d e^{-kt}, \tag{3}$$

where p(t) stands for the value of any cutometric parameter at time t, p_s is its limit steady-state value (to which the parameter value converges for large t), p_d is the difference between the steady-state and initial (t = 0) values, and k can be referred to as a “recovery constant” related to a more suitable characteristics of the decay - the recovery half-time T_{1/2} - by the formula

$$T_{1/2} = \frac{0.693}{k}$$

The meaning of the half-time is that its every elapse reduces the difference between the steady state value and an immediate value in half. Naturally, the model cannot be interpreted literally for time between t = 0 (surgery day) and t = 1 (the first post-surgery month). On the other hand, within the interval of measuring (starting from the first post-surgery month) it is capable to reflect the real progress of healing process reasonably. Typical behaviour of the model function is depicted in Fig. 11.

³ The exponential formula (3) is characteristic of a broad class of natural processes which are gradually steered to a steady, plateau state.

3. RESULTS

The results of descriptive statistics are diagrammatically shown in Figs. 8-12. In Fig. 8, three types of behaviour can be observed for both parameters R₂ and Q₁: (1) In the post-surgery month 1 both kinds of treatment and the normal skin boxes differ from each other. The means and medians of STSG + APC and STSG only treated scars are relatively close, but very distinct from the mean and median of the control box constructed from normal skin data. While the STSG + APC treated scars have the mean greater than the median (the distribution has some excessive higher values that drag the mean up above the median), the opposite applies for the remaining two distributions. (2) In the post-surgery month 3 the STSG + APC treated scars and control normal skin show similar means and medians, but those of the STSG only treated scars seem to be in a somewhat lower position. All means are below medians, suggesting occurrence of some isolated distinctly lower values. (3) In the post-surgery months 6 and 12, a steady state seems to be achieved, neither means nor medians markedly differ from each other.

Cutometric parameters Q₂ and Q₃ charted in Fig. 9 show similar, but more chaotic behaviour. The main distinction lies in completely different behaviour in the first post-surgery month. While the parameter Q₂ has all three medians unequal and rising in the sequence STSG + APC, STSG only, and normal skin, the parameter Q₃ has medians (and means) equal for STSG + APC and normal skin, but with distinctly different STSG only median and mean, similarly to R₂ and Q₁ cases. The Q₂ means of STSG + APC and STSG only are very close but distinctly lower than normal skin mean.

Inferential statistical analysis, both parametric (one-way ANOVA applied to 12 samples combining

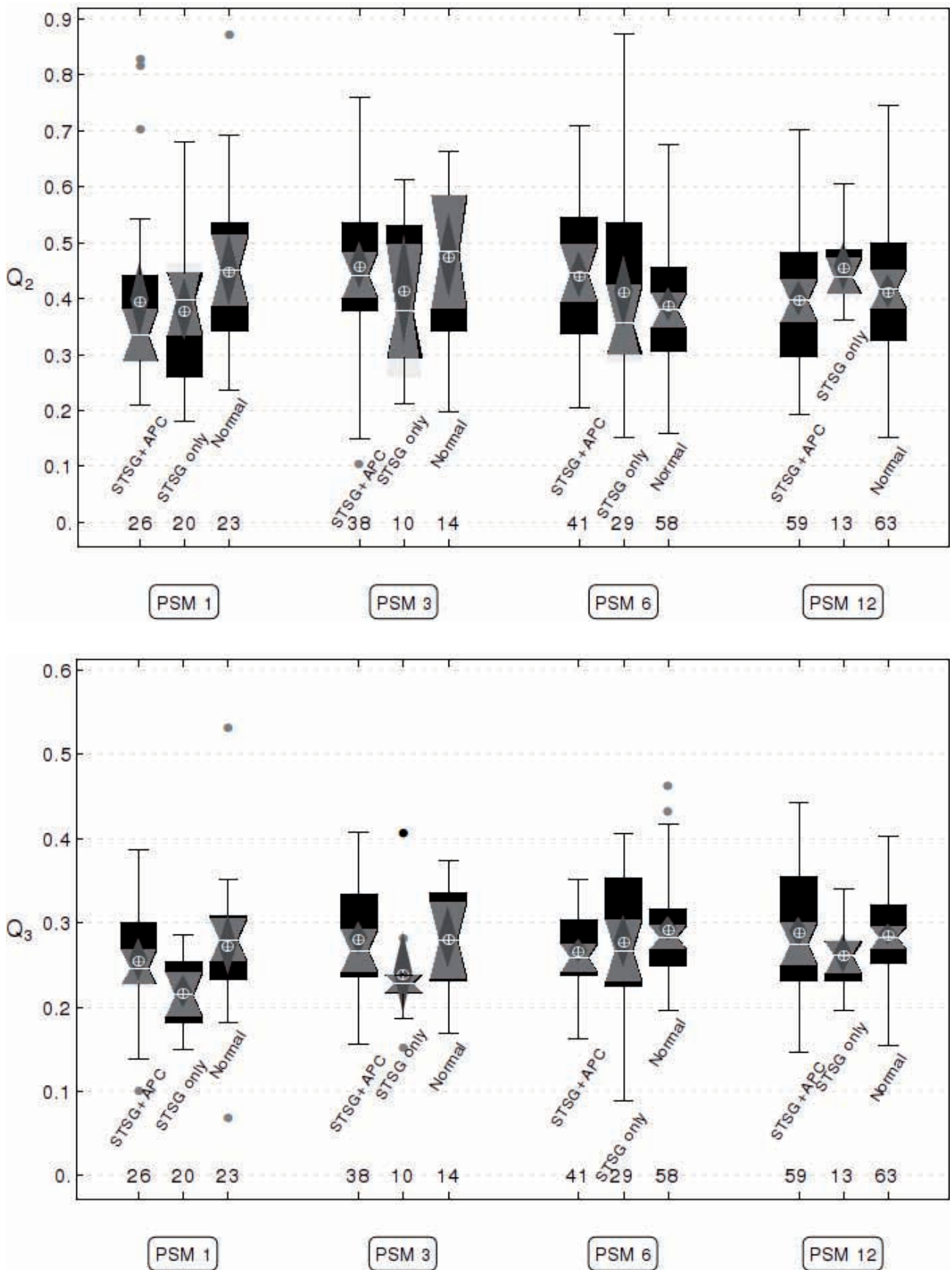


Fig. 9 - Top: Box-and-whisker chart for cutometric parameter Q_2 . Bottom: Box-and-whisker chart for cutometric parameter Q_3 . See also detailed description in Fig. 8 caption.

various combinations of 4 post-surgery months and 3 treatments including control normal skin) and non-parametric (Kruskal-Wallis test applied to the same samples), rejected at the 5% significance level the null hypothesis that the means (medians) are equal. This was obtained for all parameters with the exception of Q2, where only median comparison test (Kruskal-Wallis test) rejected the null hypothesis. The respective p-values are listed in Table 2. Subsequent post hoc analyses detected 5, 2, none, and 5 significantly different pairs using the Tukey post ANOVA test, and 6, 3, none, and 5 significantly different pairs using the Bonferroni post Kruskal-Wallis test for parameters R2, Q1, Q2 and Q3, respectively. And most importantly, the “worst offenders” of rejection were detected: for parameter R2, all 11 pairs (5 coming from ANOVA, 6 from Kruskal-Wallis test) had the sample STSG only in PSM 1 as a member.

Table 2 - p-Values for multiple comparison statistical tests. The sole value above the adopted significance level 0.05 is highlighted.

Parameter	One-wayANOVA	Kruskal-Wallis
R2	0.0055	0.0021
Q1	0.0073	0.0034
Q2	0.14	0.038
Q3	0.00063	0.00019

Similarly for parameter Q1, all 5 pairs (2 coming from ANOVA, 3 from Kruskal-Wallis test) had the same sample STSG only in PSM 1 as a member. In parameter Q2, no significantly differing pairs were detected by post hoc tests despite the fact that the Kruskal-Wallis test rejected the null hypothesis that the medians are equal. Finally, for parameter Q3, all 10 pairs (5 coming from ANOVA, 5 from Kruskal-Wallis test) had the sample STSG only in PSM 1 as a member. All these figures are diagrammatically presented in Fig. 10.

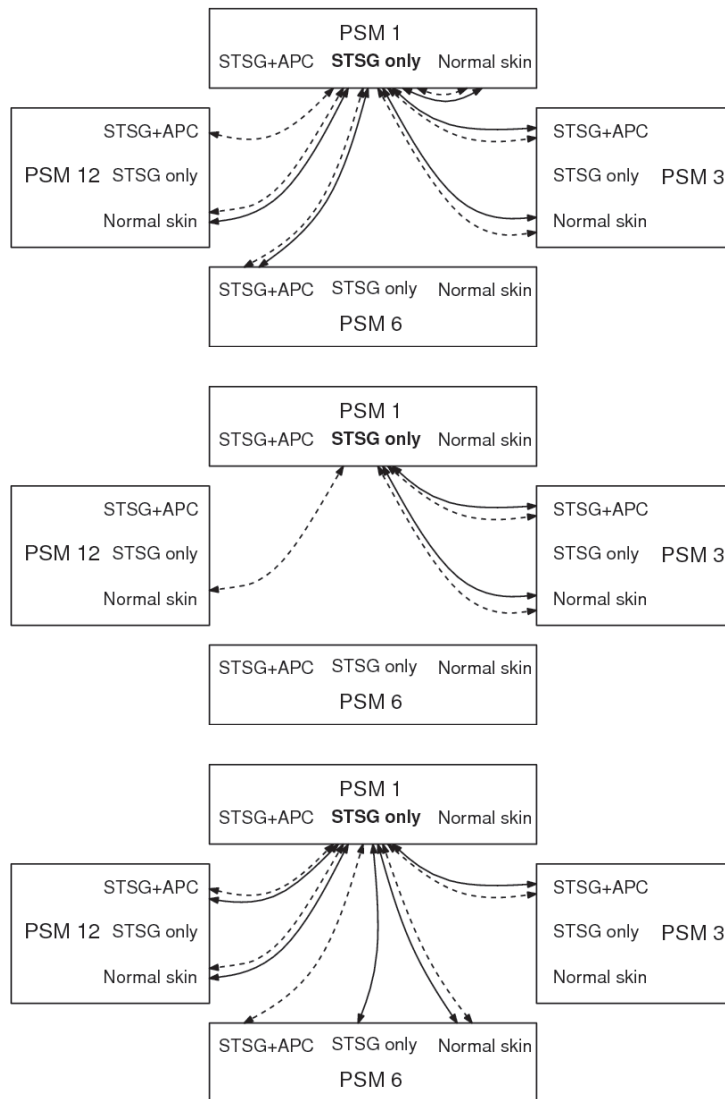


Fig. 10 - Results of post hoc analysis for parametric testing for cutometric parameters (a) R2, (b) Q1, and (c) Q3. Solid lines connect samples that significantly differ in ANOVA post hoc test (Tukey test), dashed lines connect samples that significantly differ in Kruskal-Wallis post hoc test (Bonferroni test).

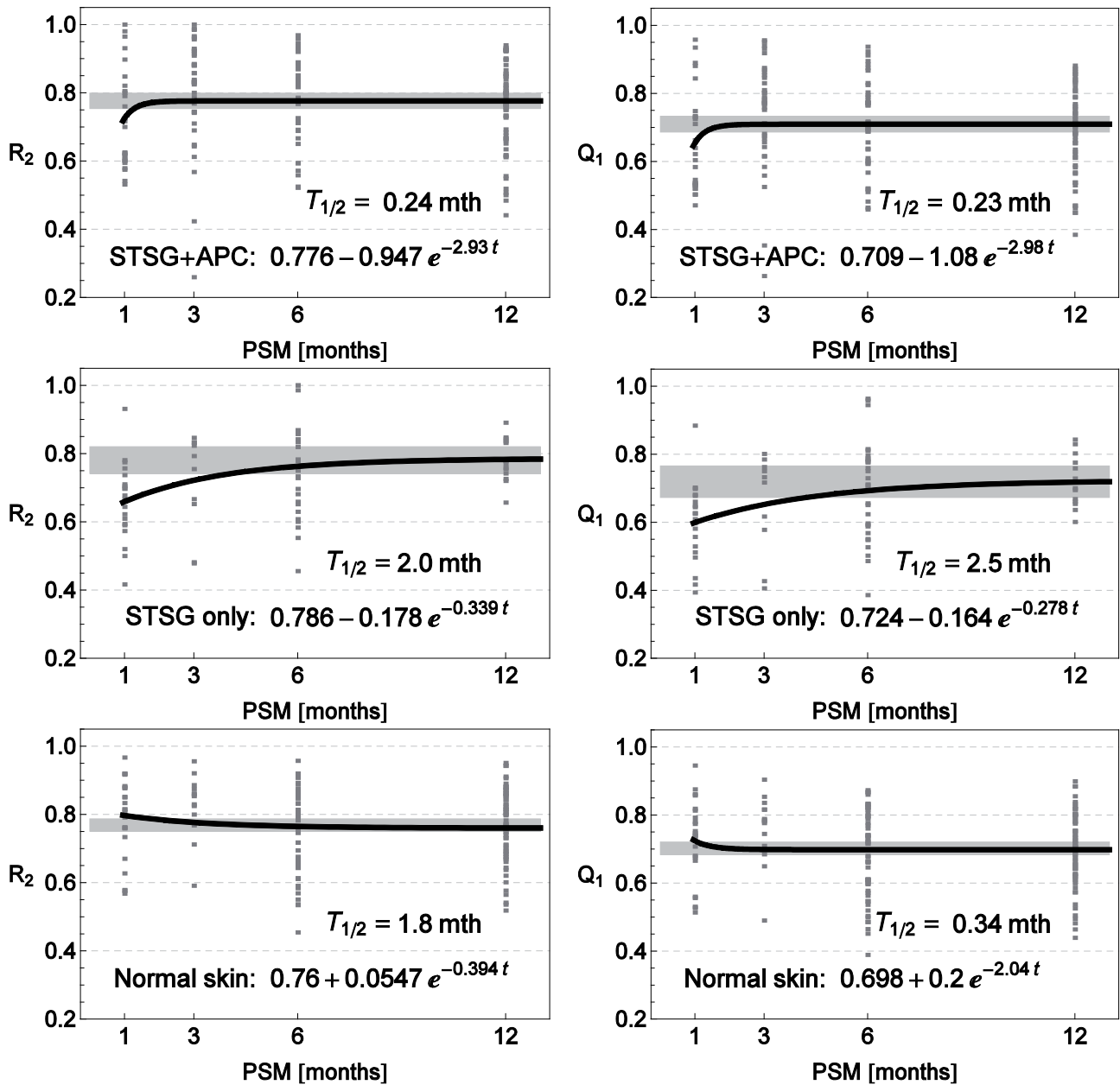


Fig. 11 - Left column from top (a, c, e): Exponential recovery model fits of the cutometric parameter R2 time dependence for STSG + APC, STSG only, and normal skin, respectively. Right column from top (b, d, f): Exponential recovery model fits of the cutometric parameter Q1 time dependence for STSG + APC, STSG only, and normal skin, respectively. The light grey bar defines the confidence interval at confidence level 95 %. The initial part of the model curve between zero and the first post-surgery month is removed due to unacceptability (or at least poor descriptive ability) of the model function within this interval (cf. end of Section 2.5).

The above statistical results suggest that the the parameters R2, Q1 and Q3 can be convicted from being significantly worse for the scars treated with STSG only in the first post-surgery month than the remaining ones.

The results of the exponential recovery model regression are depicted in Fig. 11 for parameters R2, Q1 and in Fig. 12 for parameters Q2, Q3. Each plot contains distributions of cutometric parameters (in dark grey), the model curve (in bold black), confidence interval (in light grey) for the mean calculated from post-surgery months that belong to the steady-state portion of the model curve (confidence level 95 % was adopted), the value of half-time T_{1/2}, and numerically expressed Eq. (3), the leading number

expressing the steady-state cutometric parameter value.

The plots presented in Fig. 11 for parameters R2 and Q1 area like and convincingly demonstrate fast onset of the APC healing effect in the initial phase shortly after the surgery in comparison with STSG only treatment, in addition to the standard statistical approach elaborated above in this section. While the confidence interval strip is reached by the STSG only curve between roughly 4th and 5th PSM, the same is achieved for the STSG + APC combination shortly after the first PSM. It is interesting that the normal skin curve has an opposite, slightly upward bent initial part. A possible explanation of this phenomenon is given at the end of Section 4 below. All

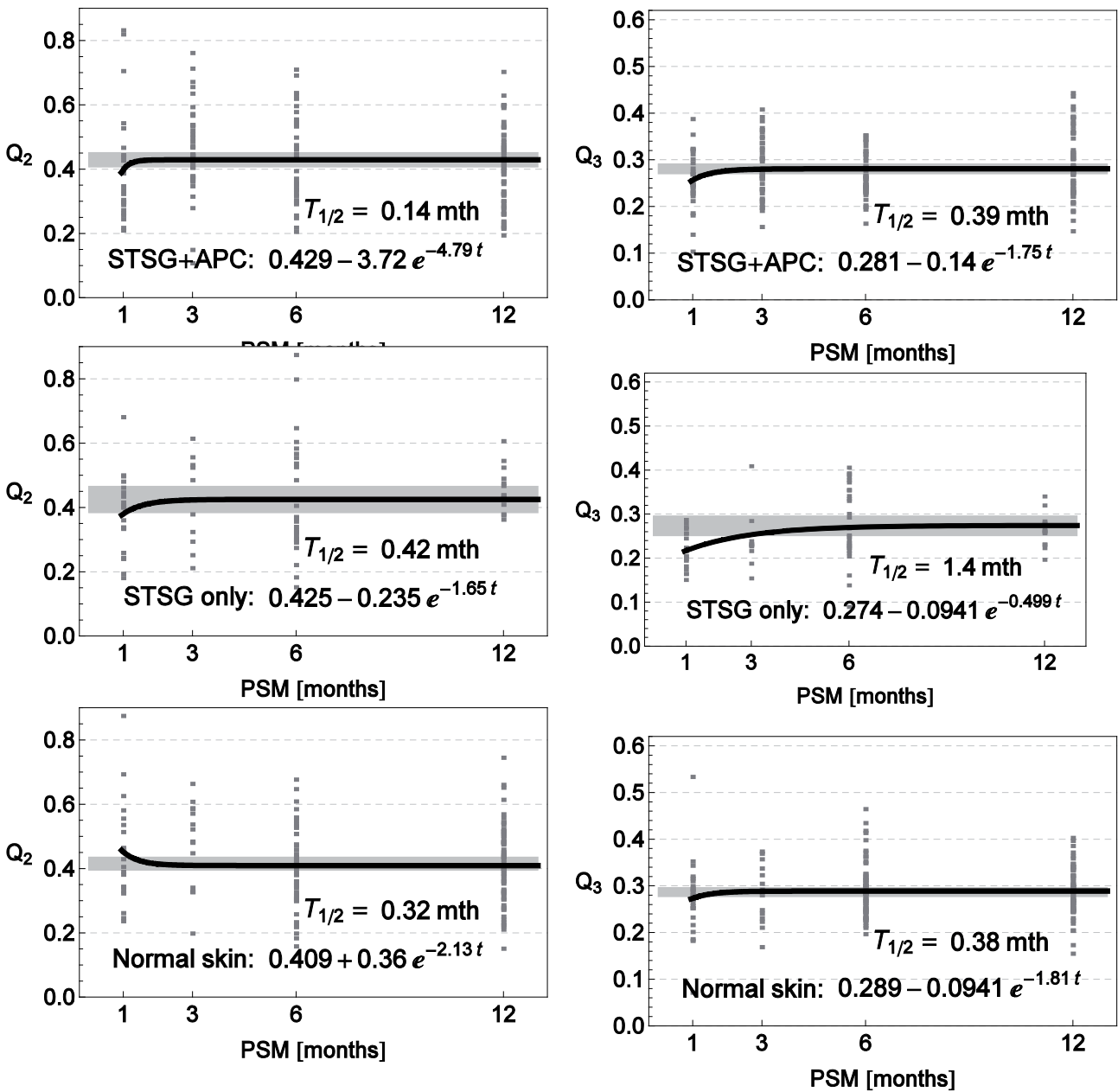


Fig. 12 - Left column from top (a, c, e): Exponential recovery model fits of the cutometric parameter Q₂ time dependence for STSG + APC, STSG only, and normal skin, respectively. Right column from top (b, d, f): Exponential recovery model fits of the cutometric parameter Q₃ time dependence for STSG + APC, STSG only, and normal skin, respectively. The light grey bar defines the confidence interval at confidence level 95 %. The initial part of the model curve between zero and the first postsurgery month is removed due to unacceptability (or at least poor descriptive ability) of the model function within this interval (cf. end of Section 2.5).

three curves eventually converge to approximately common steadystate values $Q_2 \approx 0.77$ and $Q_1 \approx 0.71$. Using the APC reduces the recovery halftime roughly by one order, from about 2 to 3 months to about a quarter of month. It should be pointed out that the cutometric parameters for which such a behaviour is valid are of gross-elasticity type, hence not affected by cutometric curve inflection point (see discussion in Section 2.3). The results presented in Fig. 12 for parameters Q₂, Q₃ do not sound so convincing, but at least for the parameter Q₃, a behaviour similar to that observed for the gross-elasticity type parameters occurs, i.e., STSG + APC healed scars recover to the steady-state value about $Q_3 \approx 0.28$ much more

rapidly than STSG only healed scars (with halftime about 3-4x smaller). The parameter Q₂ does not fit in the remaining parameters behaviour, displaying virtually the same recovery halftimes in both for STSG + APC and STSG only treatment. Nevertheless, the exception of common steady-state value about $Q_2 \approx 0.42$ can also be observed. We can generalize that APC accelerates reaching a steadyplateau for gross elasticity cutometric parameters R₂, Q₁, and for pure viscous portion reflecting parameter Q₃ in the early stages after surgery. On the contrary, the APC-induced improvement of parameter Q₂ (closely related to biological elasticity R₇) remains negligible and insignificant.

4. DISCUSSION

Continual advances in bioengineering methods has increasingly allowed modulation of wound healing and the resultant scars. Autologous platelet concentrate has been used for about two decades in diverse surgical fields to improve wound healing and tissue repair. In this study, autologous platelet concentrate has been advocated to enhance scarring after surgical treatment of non-healing deep dermal and full thickness burns. For objective evaluation of the development of scar viskoelasticity in the course of two year period, the Cutometer MPA 580 device was engaged. This simple but useful bioengineering method enabled fast and reliable routine assessment of the skin viscoelastic properties. Using this method the presented study has objectively demonstrated that the viscoelastic properties of skin areas treated with STSG + APC combination return more rapidly to the viscoelastic properties of normal skin than those treated with STSG only, particularly in the early phases shortly after the APC application.

Despite of the small size of experimental material the statistically significant results were obtained for the parameters R2, Q1 (skin gross elasticity) and Q3 expressing the pure viscous portion of skin retractability. This significance was not seen with the Q2 parameter (pure elastic portion of skin retractability). As already mentioned in Section 2.3, we are inclined to blame such incompatible behaviour on presumptively incorrect definition of the inflection point on the strain-vs-time curves, which can consequently spoil the values of parameters dependent on its correct position. However, it is too early for such a complex issue to be judged.

We are aware of limitations of this study, namely small number of patients, lack of experiences with applications of autologous platelet concentrate in deep burns and still insufficient number of publications dealing with the scarring processes after APC application. Also the way of determining the cutometric parameters from the strain-vs-time curves should be revised in the sense described in the previous paragraph. The factor behind the slight decrease in time of normal skin parameters R2, Q1 and Q2, and slight increase of normal skin parameter Q3 in time remains unknown to the authors. For now we will content ourselves with ascription it to statistical fluctuations. However, a plausible explanation could be based on the changing age of the patients entering respective post-surgery months [30,27]. The factors may be subject to investigation in future studies.

5. CONCLUSION

The findings of this study objectively indicate that the combination of STSG + APC in the surgery of full-thickness and non-healing deep dermal burns reduces the time of scar viscoelastic properties recovery to those of normal skin, as compared with applicati-

on of the sole STSG. This was statistically significant for cutometric parameters R2 and Q1 expressing the gross elasticity of the skin, and parameter Q3 expressing the pure viscous portion of skin retractability. Based on the results of the statistical analysis, parameters R2, Q1 and Q3 showed statistically significantly improved visco-elastic properties of scars in early phases (up to a few months) after the surgery. An alternate wording of the results is that using the autologous platelet concentrate reduces the gross-elasticity and pure viscous recovery halftime roughly by one order.

However, future studies are necessary to complete understanding of the role played by APC in acceleration of recovery in deep burns scars healing.

CONFLICT OF INTEREST STATEMENT

The authors declare that they have no conflict of interest.

ACKNOWLEDGEMENTS

The authors would like to acknowledge the financial support from the following bodies and grants: The Council of the Moravian-Silesian region, Czech Republic (Grant FNO-99-OVZ-09-024-Dot), the ESF Project Integrated Approach (Grant CZ.1.07/2.2.00/28.0271), Student Grant Agency 2012 (Grant SV450 2241 "Biomedical engineering systems VIII"), and TACR (Grant TA01010632 "SCADA system for control and measurement of process in real time").

REFERENCES

- [1] Graham JS, Schomacker KT, Glatter RD, Briscoe CM, Braue Jr EH, Squibb KS. Efficacy of laser debridement with autologous split-thickness skin grafting in promoting improved healing of deep cutaneous sulfur mustard burns. *Burns* 2002;28(8):719-30.
- [2] Gangemi EN, Gregori D, Berchiolla P, Zingarelli E, Cairo M, Bollero D, et al. Epidemiology and risk factors for pathologic scarring after burn wounds. *Arch Facial Plast Surg* 2008;10(2):93-102.
- [3] Bombaro KM, Engrav LH, Carrouger GJ, Wiechman SA, Faucher L, Costa BA, et al. What is the prevalence of hypertrophic scarring following burns? *Burns* 2003; 29(4):299-302.
- [4] Draaijers LJ, Tempelman FR, Botman YA, Tuinebreijer WE, Middelkoop E, Kreis RW, et al. The patient and observer scar assessment scale: a reliable and feasible tool for scar evaluation. *Plast Reconstr Surg* 2004;113(7):1960-5. <http://dx.doi.org/10.1097/01.PRS.0000122207.28773.56> [Discussion p. 1966-7].
- [5] Fearmonti R, Bond J, Erdmann D, Levinson H. A review of scar scales and scar measuring devices. *ePlasty* 2010;10:e43, <http://www.eplasty.com>.
- [6] Draaijers LJ, Botman YA, Tempelman FR, Kreis RW, Middelkoop E, van Zuijlen PP. Skin elasticity meter or subjective evaluation in scars: a reliability assessment. *Burns* 2004;30(2):109-14.
- [7] El-Sharkawy H, Kantarci A, Deady J, Hasturk H, Liu H, Alshahat M, et al. Platelet-rich plasma: growth factors and pro- and anti-inflammatory properties. *J Periodontol* 2007; 78(4):661-9.
- [8] Petrunaro PS. Using platelet-rich plasma to accelerate soft tissue maturation in esthetic periodontal surgery. *Compend Contin Educ Dent* 2001;22(9):729-32. 734, 736 passim; quiz 746.

- [9] Kassolis JD, Rosen PS, Reynolds MA. Alveolar ridge and sinus augmentation utilizing platelet-rich plasma in combination with freeze-dried bone allograft: case series. *J Periodontol* 2000;71(10):1654-61.
- [10] de Obarrio JJ, Araúz-Dutari JI, Chamberlain TM, Croston A. The use of autologous growth factors in periodontal surgical therapy: platelet gel biotechnology - case reports. *Int J Periodont Restorative Dent* 2000;20(5):486-97.
- [11] Moro G, Casini V, Bastieri A. Use of platelet-rich plasma in major maxillary sinus augmentation. *Minerva Stomatol* 2003;52(6):267-71. Article in Italian.
- [12] Dhillon RS, Schwarz EM, Maloney MD. Platelet-rich plasma therapy - future or trend? *Arthritis Res Ther* 2012;14(4):219.
- [13] Edwards SG, Calandruccio JH. Autologous blood injections for refractory lateral epicondylitis. *J Hand Surg [Am]* 2003;28(2):272-8.
- [14] Mishra A, Pavelko T. Treatment of chronic elbow tendinosis with buffered platelet-rich plasma. *Am J Sports Med* 2006;34(11):1774-8. doi: 10.1177/0363546506288850.
- [15] Cervelli V, Gentile P, Scioli MG, Grimaldi M, Casciani CU, Spagnoli LG, et al. Application of platelet-rich plasma in plastic surgery: clinical and in vitro evaluation. *Tissue Eng Part C Methods* 2009;15(4):625-34.
- [16] Cervelli V, Palla L, Pascali M, De Angelis B, Curcio BC, Gentile P. Autologous platelet-rich plasma mixed with purified fat graft in aesthetic plastic surgery. *Aesthetic Plast Surg* 2009;33(5):716-21.
- [17] Ma L, Perini R, McKnight W, Dickey M, Klein A, Hollenberg MD, et al. Proteinase-activated receptors 1 and 4 counter-regulate endostatin and VEGF release from human platelets. *Proc Natl Acad Sci U S A* 2005;102(1):216-20. doi:10.1073/pnas.0406682102.
- [18] Courage+Khazaka electronic GmbH, Cologne, Germany. Information and Operating Instructions for the Cutometer® MPA 580 and the software Cutometer® MPAQ. 2010. 45 pages; URL <http://www.courage-khazaka.de/>.
- [19] Rennekampff HO, Rabbels J, Reinhard V, Becker ST, Schaller HE. Comparing the Vancouver Scar Scale with the cutometer in the assessment of donor site wounds treated with various dressings in a randomized trial. *J Burn Care Res* 2006;27(3):345-51.
- [20] Šin P, Brychta P. Cutometrical measurement confirms the efficacy of the composite skin grafting using allogeneic acellular dermis in burns. *Acta Chir Plast* 2006;48(2):59-64.
- [21] Nguyen DQA, Potokar TS, Price P. An objective long-term evaluation of Integra (a dermal skin substitute) and split thickness skin grafts, in acute burns and reconstructive surgery. *Burns* 2010;36(1):23-8.
- [22] Akhtar N, Zaman SU, Khan BA, Amir MN, Ebrahimzadeh MA. Calendula extract: effects on mechanical parameters of human skin. *Acta Pol Pharm* 2011;68(5):693-701.
- [23] Hendriks FM. Mechanical behaviour of human skin in vivo: a literature review. *Nat. Lab. Unclassified Report 2001/820*. Koninklijke Philips Electronics N.V.; 2001.
- [24] Barel AO, Courage W, Clarys P. Suction chamber method for measurement of skin mechanics: the new digital version of the cutometer. In: Serup J, Jemec GBE, Grove GL, editors. *Handbook of non-invasive methods and the skin*. London: Informa Healthcare; 2006. p. 583-92. chapter 67, ISBN 978-0849314377.
- [25] O'goshi KI. Suction chamber method for measurement of skin mechanics: the cutometer? In: Serup J, Jemec GBE, Grove GL, editors. *Handbook of non-invasive methods and the skin*. London: Informa Healthcare; 2006. p. 579-82. chapter 66, ISBN 978-0849314377.
- [26] Wilkes GL, Brown IA, Wildnauer RH. The biomechanical properties of skin. *CRC Crit Rev Bioeng* 1973;1(4):453-95.
- [27] Escoffier C, de Rigal J, Rochefort A, Vasselet R, Lévêque JL, Agache PG. Age-related mechanical properties of human skin: an in vivo study. *J Invest Dermatol* 1989;93(3):353-7.
- [28] Wellin PR, Gaylord RJ, Kamin SN. *An introduction to programming with mathematica*, 3rd ed., Cambridge: Cambridge University Press; 2005, ISBN 0-521-84678-1, <http://www.cambridge.org/>.
- [29] Upton G, Cook I. *A dictionary of statistics*, 2nd ed., Oxford: Oxford University Press; 2011, ISBN 978-0-19-954145-4.
- [30] Elsner P, Wilhelm D, Maibach HI. Mechanical properties of human forearm and vulvar skin. *Br J Dermatol* 1990;122(5):607-14. <http://dx.doi.org/10.1111/j.1365-2133.1990.tb07282.x>.

EXTRAESOPHAGEAL REFLUX: WHAT IS THE BEST PARAMETER FOR PH-MONITORING DATA ANALYSIS FROM THE PERSPECTIVE OF PATIENT RESPONSE TO PROTON PUMP INHIBITORS?

Karol Zelenik, MD, PhD^{1,2}, Petr Matousek, MD, PhD^{1,2}, Miroslav Tedla, MD, PhD^{3,4}, Jakub Syrovatka, MD¹, Pavel Kominek, MD, PhD¹

1 Department of Otolaryngology, University Hospital Ostrava, 17. listopadu 1790, 708 52 Ostrava, Czech Republic, karol.zelenik@fno.cz, petr.matousek@fno.cz, jakub.syrovatka@fno.cz, pavel.kominek@fno.cz

2 Faculty of Medicine, University of Ostrava, Syllabova 19, 703 00 Ostrava, Czech Republic

3 Medical School of Comenius University, ENT University Department, Bratislava, Antolska 11, 85107 Bratislava, Slovak Republic, miro.tedla@gmail.com

4 University Hospital of Coventry and Warwickshire NHS Trust, Clifford Bridge Road, CV2 2DX, Coventry, United Kingdom

Originally published in *Gastroenterology Research and Practice* 2013; 2013: 736486

Consent to the publication of 1st April 2014

ABSTRACT

Objectives

To analyze the pH-monitoring records of patients with suspected extraesophageal reflux (EER) using three different parameters (number of refluxes (NOR), acid exposure time (AET) and reflux area index (RAI)), with a view to determining which type of analysis is best at selecting the patients who will respond to a proton pump inhibitor (PPI).

Methods

Demographic data were obtained and the level of the complaint was assessed using the Visual Analogue Scale. A dual probe pH-monitoring study was conducted. NOR greater than six, AET more than 0.1% and RAI higher than 6.3mpH were taken to be the thresholds for EER. Subsequently the response to 12 weeks PPI trial was analyzed.

Results

A total of 81 patients were analyzed. The percentages of patients with substantial EER based on NOR, AET and RAI were 36%, 28% and 26% respectively. Statistically significant, often positive PPI trials were confirmed in the group identified as having substantial EER using all three types of analysis. When using AET and RAI, the significance was more pronounced ($p = 0.012$ and $p = 0.013$ respectively) in comparison with NOR ($p = 0.033$).

Conclusions

Patients with EER diagnosed using AET or RAI will respond to PPI significantly often.

Key words

gastroesophageal reflux disease, extraesophageal reflux, pH-monitoring, acid exposure time, reflux area index, proton pump inhibitors

INTRODUCTION

Ambulatory 24-hour dual probe pH-monitoring remains a widely used diagnostic method for detecting extraesophageal reflux (EER). At present, there is a substantial consensus regarding the methodology for this procedure: the upper probe should be placed above the level of the upper esophageal sphincter (UES) [1]. However, there is still a lack of consensus regarding the interpretation of the data recorded, and physicians continue to argue about what constitutes "normal" and what constitutes pathological EER for most patients. Currently, there are three basic parameters being used for data analysis: number of refluxes (NOR), acid exposure time (AET) and reflux area index (RAI) (Figure 1) [2, 3]. NOR is the sum of all reflux episodes per 24 hours, regardless of their duration and the pH level reached. AET, also sometimes called fraction time, is the percentage of time during the study (usually 24 hours) when the pH is below 4.0. This parameter reflects the severity of EER more objectively. Reflux Area (RA) is the sum of the area under the curve for all episodes of pH<4.0 recorded during the study in units of Ph*minutes (mpH). The RAI is the RA corrected for the duration of the study. RAI takes into consideration not only the AET but also the level of pH decline and is currently considered the most accurate parameter for measuring the severity of EER (Figure 1) [2, 3]. Every physician who has evaluated recorded pH-monitoring data is familiar with the fact that results may vary with the parameter used for analysis. The question then becomes which parameter is the most precise and best correlates with the response to proton pump inhibitors (PPI). The aim of the present study was to analyze the pH-monitoring records of patients examined for suspected EER using these three different parameters, compare the re-

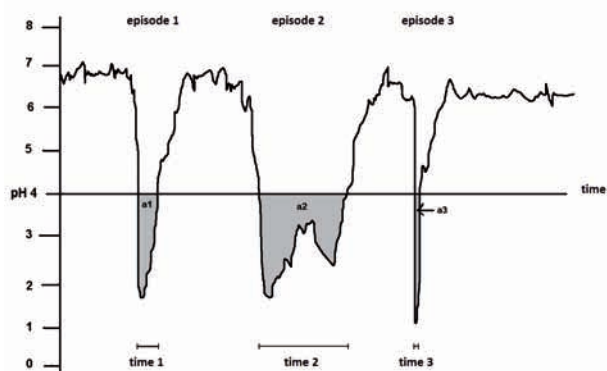


Figure 1: Three different parameters used for pH-monitoring data analysis are compared. There are 3 reflux episodes displayed (episode 1, episode 2 and episode 3). Acid exposure time is the sum of time 1, time 2 and time 3. Reflux area index is the sum of calculated a1, a2 and a3 areas.

sults, and determine which parameter was the best predictor of a positive response to PPI treatment. To our knowledge, this is the first study to compare all three of these parameters and thereby attempt to establish whether using different criteria has any clinical impact.

MATERIALS AND METHODS

The prospective study was performed in accordance with the Declaration of Helsinki, the requirements of good clinical practice and all applicable regulatory requirements, and was approved by the Institutional Review Board. Written informed consent was obtained from all participants before initiating any procedure.

Outpatients aged 18 to 64 years with the complaints commonly attributed to EER (dysphonia, globus, cough and throat cleaning) lasting more than three months were included in the study, conducted between January 2010 and June 2011. Both those patients who had and those who had not been treated for gastroesophageal reflux disease with a PPI were included in the study, since this fact has no bearing on the aim of the study. Patients with acute upper respiratory infection, oropharyngeal and laryngeal cancer and patients with other serious illnesses (e.g. cardiovascular and neurological complaints, diabetes and other illnesses) were excluded from the study, because these conditions can significantly aggravate patient complaints. Epidemiologic data (age, sex, BMI, smoking history, bronchial asthma, professional use of voice) were obtained via questionnaire, and assessment of the severity of the com-

Table 1 Characteristics of the study group

Patients	n = 81
Mean age	50 years (SD± 14)
Sex	31 male, 50 female
BMI	27,29 (SD = 5.33)
Smokers	n = 14 (17.3%)
Voice professionals	n = 21 (25.9%)
Bronchial asthma	n = 15 (18.5%)

plaints commonly associated with EER (dysphonia, globus, cough and throat cleaning) was done using the visual analogue scale (VAS). Reflux Finding Scores (RFS) were assessed using rigid videolaryngoscopy to determine the level of the laryngeal signs of EER. Afterwards, an ambulatory 24-hour dual probe pH-monitoring study was conducted. A digitrapper pH400 device (Alpine Biomed, Denmark, 2007) with double probes with a fixed distance of 15 cm was used. The proximal sensor was placed immediately above the UES using flexible laryngoscopic guidance (Smit technique). The data recorded were analyzed using GastroTrack™ software (Alpine Biomed, Denmark, 2007). Upper probe events with pH < 4.0 were only accepted as EER events when Postma's criteria (the pH decreases to less than 4; the pharyngeal pH drops during or immediately after distal esophageal acid exposure; the pH drop does not occur during an episode of eating; the proximal sensor pH drop is rapid and sharp, not gradual) were met [1]. NOR, AET and RAI were assessed. NOR greater than six, AET greater than 0.1% and RAI higher than 6.3 mpH were considered the thresholds for substantial EER [3, 4, 5, 6]. Subsequently, all patients were put on a PPI (30 mg lansoprasol) twice a day for twelve weeks and were assessed using VAS at the end of this period to ascertain whether their symptoms (dysphonia, globus, cough and throat cleaning) had completely vanished, been relieved or persisted. A drop of at least 3 points in the 10-point VAS, as compared to the VAS value assessed before the PPI trial, was taken to indicate a relief of symptoms, while a decrease of two or less was taken to indicate the persistence of symptoms. A two-sample t-test and Fischer's exact test were used to assess differences in RFS and responses to the PPI trial between the groups analyzed. Stata software (version 10) was used for all statistical calculations.

Table 2 Number (N) and percentage (%) of patients diagnosed with EER (EER+) using three different parameters of pH monitoring analysis (NOR - number of refluxes, AET - acid exposure time, RAI - reflux area index)

Parameter	EER + (N)	EER + (%)	EER - (N)	EER - (%)
NOR	29	35,80	52	64,20
AET	23	28,40	58	71,60
RAI	21	24,93	60	75,07

RESULTS

A total of 90 patients were recruited for the study, nine of whom were excluded from the statistical analysis (five did not tolerate a catheter and four did not come to the last session). A total of 81 patients (31 men, 50 women, mean age 50, $SD_{\pm} 14$) were analyzed (Table 1).

The percentages of patients with substantial EER based on NOR, AET and RAI were 36% (29 patients), 28% (23 patients) and 26% (21 patients) respectively (Table 2).

Statistically significant higher RFS was confirmed in the group with substantial EER in comparison to the group determined not to have EER using all three types (NOR, AET and RAI) of analysis ($p = 0.0166$, $p = 0.0071$ and $p = 0.0007$ respectively) (Table 3).

Statistically significant, often positive PPI trials in the group with substantial EER in comparison to the group without EER as determined using all types of analysis (NOR, AET and RAI) was confirmed as well ($p = 0.033$, $p = 0.012$ and $p = 0.013$ respectively) (Table 4).

Table 3 Average Reflux Finding Score (RFS) and its standard deviation (SD) in group of patients with extraesophageal reflux confirmed by pH-monitoring (EER +) and group of patients without EER (EER -) using three different parameters (NOR - number of refluxes, AET - acid exposure time, RAI - reflux area index). The two sample t-test was for statistical analysis of differences between the EER + and the EER - group.

Parameter	EER +	EER -	p
NOR	8.00 \pm 3.10	6.31 \pm 2.67	0,0166
AET	7.93 \pm 2.65	6.15 \pm 2.83	0,0071
RAI	8.57 \pm 3.00	6.16 \pm 2.59	0,0007

Table 4 Number of patients with a positive therapeutic trial (TT +) and a negative therapeutic trial (TT -) in group of patients with extraesophageal reflux confirmed by pH-monitoring (EER +) and without EER (EER -) using three different parameters (NOR - number of refluxes, AET - acid exposure time, RAI - reflux area index). Fischer's exact test was used for statistical analysis of differences between the EER + and the EER - group.

Parameter	EER +		EER -		p
	TT +	TT -	TT +	TT -	
NOR	25	4	30	22	0.033
AET	20	3	35	23	0.012
RAI	19	2	36	24	0.013

DISCUSSION

Diagnosing EER and establishing its involvement in patient problems continues to be a challenging and controversial business. This has to do with the com-

plicated pathophysiology of EER and the fact that EER symptoms are nonspecific and vary over time, and moreover with the fact that different patients evince different sensitivities to reflux [1]. The lack of diagnostic criteria for EER and inconsistency in the response to therapy is a source of frustration to many physicians. There is as yet no clear answer to that most important of questions: "Which patients will respond to treatment?" Nevertheless, EER causes very real problems and affects hundreds of thousands of patients annually. It is estimated that up to 10-15% of all visits to otolaryngology offices are prompted by manifestations of EER [7].

Ambulatory 24-hour dual probe pH-monitoring for the detection of EER was introduced by Wiener et al. in 1989 [8]. The methodology involved was refined over the years, and over the last two decades the technique has come to be widely used for the diagnosis of EER. At present, there is a substantial consensus regarding the methodology for this procedure: the upper probe should be placed above the level of the UES. This can be achieved using direct laryngoscopy guidance (Smit technique), or else the position of the UES can be ascertained using manometry [1, 2, 3, 9].

The role of pH-monitoring in the examination of patients with suspected EER continues to be a contentious issue. Authors who argue that pH testing should be preceded by a PPI trial make a point of stressing inconsistencies in interpretation criteria and unreliability in predicting the response to therapy [9]. On the opposing side, authors who advocate pH testing before a PPI trial point out the overuse of PPI, its adverse effects (hip fractures, enteritis, anaphylactic reaction, among others), the rebound phenomenon when medication is stopped and the economic impact [10, 11]. Moreover, meta-analysis involving over 790 extraesophageal pH reports in 16 studies over a period of 12 years confirmed that the aggregate number of reflux episodes and the percentage of AET were both significantly greater in persons with EER than in controls [12]. Thus, hypopharyngeal pH-monitoring does appear to be capable of distinguishing persons with EER from normal controls [11, 12].

The dispute over whether pH-monitoring or a PPI trial should be used as a first intervention in patients with suspected EER is fuelled by differences in the definitions of physiological and pathological EER adopted by different authors. Some authors consider any pharyngeal reflux abnormal, while others report small amounts of pharyngeal reflux in healthy individuals and consider a small number of EER refluxes (most often three to six refluxes) a threshold for pathological EER [1, 4, 5, 6]. Moreover, NOR does not seem to be the best parameter for analysis, because the length and severity of individual EER episodes varies significantly. As a result, two other parameters are currently being used for the analysis of pH-monitoring records: AET and RAI. RAI is currently

considered the most accurate parameter as it takes into account the severity of the reflux episode, not just its duration (Figure 1) [3].

In the present study, the data recorded during pH-monitoring were analyzed using all three criteria (NOR, AET and RAI). We did not find any studies in the world literature that compared all three criteria. Our results indicate that AET and RAI are similar parameters, and that pathological EER is diagnosed in 28% and 26% of patients respectively using these methods. They are more specific and less sensitive in comparison to NOR. Using NOR, pathological EER was diagnosed in 36% of patients. The response to the PPI was significantly higher in patients diagnosed with pathological EER using all three types of analysis. However, when AET and RAI were used, the significance was more pronounced ($p = 0.012$ and $p = 0.013$ respectively) than when NOR was used ($p = 0.033$). In practice this means that if we use more specific types of analysis (AET or RAI) we will diagnose fewer patients with pathological EER, but a higher proportion of diagnosed patients will respond to PPI treatment. This result supports the assertion that the response to a PPI can be predicted by the result of pH testing and that the stricter the criteria adopted for pathological EER, the greater the number of patients responding to PPI treatment.

Similar conclusions can be reached by examining the details of the study published by Hartman [13]. He analyzed five randomized placebo controlled trials which tracked the response to a PPI in patients with suspected EER [13]. In two of them, the effect of the PPI was significantly higher as compared to the placebo, and in one the PPI was reported as possibly having an effect [14, 15, 16]. In two other studies, the effect of PPI as compared to the placebo was not confirmed [17, 18]. When we look at these studies closely, a very important fact emerges. In all studies which showed a significant effect of PPI in comparison to the placebo, the diagnosis of EER was arrived at by pH-monitoring, and patients were assigned to the EER group accordingly [14, 15, 16]. And conversely, in studies which did not show a significant effect of PPI as compared to the placebo, patients were assigned to the EER group only according to their symptoms and/or signs [17, 18]. Therefore, it can be assumed that in studies which assigned patients to EER groups without pH testing, more patients believed to have EER suffered from non-EER laryngitis. This also explains why the effect of PPI in the EER group as compared with the non-EER group did not differ in these studies.

The same result was arrived at in our previous study of patients with globus pharyngeus. In the group of patients with globus pharyngeus and pathological EER as confirmed by pH-monitoring, the response to the PPI was significantly higher than in the group of patients with globus pharyngeus but without EER [19].

Even if the use of more specific criteria for the diagnosis of EER improves the practical outcome of pH-monitoring, one has to be aware of the limits of this technique [11]. Hence RFS, designed by Belafsky et al., is recommended as an important part of the examination of patients with suspected EER, to be used as an adjunct to pH testing [11]. RFS has displayed excellent inter- and intra-rater reproducibility [20]. But RFS alone is also limited in specificity because inflammatory changes of the larynx can have many other causes (tobacco, environmental pollutants, infection, excessive voice use, allergy). Thus, laryngoscopy alone cannot be relied upon to make a diagnosis of EER either, and the combination of laryngoscopy and dual-probe pH testing seems to be of much higher diagnostic sensitivity and specificity for EER [11]. Oelschlager et al. reported that 88% of persons with an abnormal RFS and an abnormal pharyngeal pH test improved with anti-reflux therapy, as compared with just 44% of persons with an abnormal pH test but normal RFS [21]. This result strongly indicates that the combination of both diagnostic tools offers the best opportunity to accurately secure the diagnosis of EER and reliably predict the response to anti-reflux therapy.

An additional result of our study was that the sound diagnostic value of RFS was confirmed. RFS was significantly higher in groups of patients with pathological EER diagnosed using all three types of analysis. Moreover, using AET and RAI, which were confirmed to be more specific criteria for the diagnosis of EER, the significance was more pronounced ($p = 0.0071$ and $p = 0.0007$ respectively) in comparison with NOR ($p = 0.0166$).

New devices for the detection of EER - Multichannel Intraluminal Impedance (MII) testing and oropharyngeal pH testing using a Restech™ device - have emerged recently. The main advantage of MII testing is the ability to detect weakly acidic and alkaline EER episodes. Over the past few years, the device has been used primarily for the examination of impedance below the UES. Normative data for pharyngeal probes have only recently been supplied, by Hoppo et al [22]. The authors conclude that EER episodes are very rare in asymptomatic populations [22]. The Restech™ device for the examination of oropharyngeal pH is very sensitive and the examination is well tolerated by patients. Normative data have been available from several recent studies [23, 24, 25, 26]. It is very important to keep in mind that even if these new devices seem to be better in terms of their sensitivity to EER, they will raise exactly the same questions as dual probe pH testing has over the past two decades. Most of these have been discussed and summarized in this article, along with some new perspectives afforded by the results of our study. The most important objective of all methods devised to measure oro- and hypopharyngeal pH is to verify given normative data for different groups of patients

and to determine if the results of these tests can predict the response to anti-reflux therapy.

CONCLUSIONS

When using AET and RAI in the diagnosis of EER, the significance was more pronounced in comparison with NOR. Using these types of analysis (AET or RAI) we will be able to identify the patients who will respond to PPI treatment.

ACKNOWLEDGMENTS

The results reported in this paper were obtained with the financial support of Grant IGA MZ CR NT13500-4/2012 provided by the Ministry of Health of the Czech Republic.

The authors would like to thank Mrs. Hana Tomaskova Ph.D. for her help with statistical analysis.

CONFLICT OF INTEREST STATEMENT

The authors declare that there is no actual or potential conflict of interest in relation to this article. No benefits in any form have been received or will be received from a commercial party related directly or indirectly to the subject of this article.

REFERENCES

- Postma GN. Ambulatory pH monitoring methodology. *Ann Otol Rhinol Laryngol Suppl.* 2000;184:10-4.
- Jecker P, Schuon R, Morales C, Wohlfeil M, Rassouli S, Mann WJ. Normalwertbestimmung des extraösophagealen Reflux (EER) in der 24-h-2-Kanal-pH-Metrie. *HNO* 2008;56:1040-5.
- Reichel O, Issing WJ. Impact of different pH thresholds for 24-hour dual probe pH monitoring in patients with suspected laryngopharyngeal reflux. *J Laryngol Otol.* 2008;122:485-9.
- Vincent DA Jr, Garrett JD, Radionoff SL, Reussner LA, Stasney CR. The proximal probe in esophageal pH monitoring: development of a normative database. *J Voice* 2000;14:247-54.
- Bove M, Ruth M, Cange L, Mansson I. 24-H pharyngeal pH monitoring in healthy volunteers: a normative study. *Scand J Gastroenterol* 2000;35:234-41.
- Richardson BE, Heywood BM, Sims HS, Stoner J, Leopold DA. Laryngopharyngeal reflux: trends in diagnostic interpretation criteria. *Dysphagia* 2004;19:248-55.
- Tauber S, Gross M, Issing WJ. Association of laryngopharyngeal symptoms with gastroesophageal reflux disease. *Laryngoscope* 2002;112:879-86.
- Wiener GJ, Koufman JA, Wu WC, Cooper JB, Richter JE, Castell DO. Chronic hoarseness secondary to gastroesophageal reflux disease: documentation with 24-h ambulatory pH monitoring. *Am J Gastroenterol* 1989;84:1503-7.
- Vaezi MF. CON: Treatment with PPIs should not be preceded by pH monitoring in patients suspected of laryngeal reflux. *Am J Gastroenterol* 2006;101:8-10.
- Altman KW, Radosevich JA. Unexpected consequences of proton pump inhibitor use. *Otolaryngol Head Neck Surg* 2009;141:564-6.
- Belafsky PC. PRO: Empiric treatment with PPIs is not appropriate without testing. *Am J Gastroenterol* 2006;101:6-8.
- Merati AL, Lim HJ, Ulualp SO, Toohill RJ. Meta-analysis of upper probe measurements in normal subjects and patients with laryngopharyngeal reflux. *Ann Otol Rhinol Laryngol* 2005;114:177-82.
- Hartman J. Adult Laryngopharyngeal Reflux. In: Shin et al. *Evidence-Based Otolaryngology*. Springer, 2008, 517-524.
- Noordzij JP, Khidr A, Evans BA, Desper E, Mittal RK, Reibel JF, Levine PA. Evaluation of omeprazole in the treatment of reflux laryngitis: a prospective, placebo-controlled, randomized, double-blind study. *Laryngoscope* 2001;111:2147-51.
- El-Serag HB, Lee P, Buchner A, Inadomi JM, Gavin M, McCarthy DM. Lansoprazole treatment of patients with chronic idiopathic laryngitis: a placebo-controlled trial. *Am J Gastroenterol* 2001;96:979-83.
- Eherer AJ, Habermann W, Hammer HF, Kiesler K, Friedrich G, Krejs GJ. Effect of pantoprazole on the course of reflux-associated laryngitis: a placebo-controlled double-blind crossover study. *Scand J Gastroenterol* 2003;38:462-7.
- Havas T, Huang S, Levy M, Abi-Hanna D, Truskett P, Priestley J, Cox J, Wilson J. Posterior pharyngolaryngitis, double-blind randomised placebo-controlled trial of proton pump inhibitor therapy. *Aust J Otolaryngol* 1999;3:243-6.
- Steward DL, Wilson KM, Kelly DH, Patil MS, Schwartzbauer HR, Long JD, Welge JA. Proton pump inhibitor therapy for chronic laryngo-pharyngitis: a randomized placebo-control trial. *Otolaryngol Head Neck Surg* 2004;131:342-50.
- Zeleník K, Matoušek P, Urban O, Schwarz P, Stárek I, Kominěk P. Globus Pharyngeus and Extraesophageal Reflux: Simultaneous pH <4.0 and pH <5.0 Analysis. *Laryngoscope* 2010;120:2160-4.
- Belafsky PC, Postma GN, Koufman JA. The validity and reliability of the reflux finding score (RFS). *Laryngoscope*, 2001;111:1313-7.
- Oelschlager BK, Eubanks TR, Maronian N, Hillel A, Oleynikov D, Pope CE, Pellegrini CA. Laryngoscopy and pharyngeal pH are complementary in the diagnosis of gastroesophageal-laryngeal reflux. *J Gastrointest Surg* 2002;6:189-94.
- Hoppo T, Sanz AF, Nason KS, Carroll TL, Rosen C, Normolle DP, Shaheen NJ, Luketich JD, Jobe BA. How much pharyngeal exposure is "normal"? Normative data for laryngopharyngeal reflux events using hypopharyngeal multichannel intraluminal impedance (HMII). *J Gastrointest Surg.* 2012;16:16-24.
- Ayazi S, Lipham JC, Hagen JA, Tang AL, Zehetner J, Leers JM, Oezcelik A, Abate E, Banki F, DeMeester SR, DeMeester TR. A new technique for measurement of pharyngeal pH: normal values and discriminating pH threshold. *J Gastrointest Surg* 2009;13:1422-9.
- Wiener GJ, Tsukashima R, Kelly C, Wolf E, Schmeltzer M, Bankert C, Fisk L, Vaezi M. Oropharyngeal pH monitoring for the detection of liquid and aerosolised supraesophageal gastric reflux. *J Voice* 2009;23:498-504.
- Sun G, Muddana S, Slaughter JC, Casey S, Hill E, Farrokhi F, Garrett CG, Vaezi MF. A new pH catheter for laryngopharyngeal reflux: Normal values. *Laryngoscope* 2009;119:1639-43.
- Chheda NN, Seybt MW, Schade RR, Postma GN. Normal values for pharyngeal pH monitoring. *Ann Otol Rhinol Laryngol.* 2009;118:166-71.

CHROMOENDOSCOPY TO DETECT EARLY SYNCHRONOUS SECOND PRIMARY ESOPHAGEAL CARCINOMA IN PATIENTS WITH SQUAMOUS CELL CARCINOMAS OF THE HEAD AND NECK?

Pavel Komínek, MD, PhD, MBA¹, Petr Vitek, MD, PhD^{2,3}, Ondřej Urban, MD, PhD^{2,4}, Karol Zeleník, MD, PhD^{1,2}, Magdaléna Halamka, MD⁵, David Feltl, MD, PhD⁵, Jakub Cvek, MD, PhD⁵, Petr Matoušek, MD, PhD^{1,2}

- 1 Department of Otorinolaryngology, University Hospital Ostrava, Czech Republic pavel.kominek@fno.cz, petr.matousek@fno.cz, karol.zelenik@fno.cz
- 2 Faculty of Medicine, University of Ostrava, Czech Republic ondrej.urban@nemvitkovice.cz, petr.matousek@fno.cz, vitek-petr@seznam.cz
- 3 Department of Internal medicine, City Hospital Frýdek-Místek, Czech Republic, vitek-petr@seznam.cz
- 4 Department of Gastroenterology, Vítkovice Hospital Ostrava, Czech Republic ondrej.urban@nemvitkovice.cz
- 5 Department of Oncology, University Hospital Ostrava, Czech Republic jakub.cvek@fno.cz, magdalenallf@post.cz, david.feltl@fno.cz

Originally published in *Gastroenterology Research and Practice* 2013; 2013: 236-264

Consent to the publication of 1st April 2014

ABSTRACT

Objective: To evaluate the use of flexible esophagoscopy and chromoendoscopy with Lugol's solution in the detection of early esophageal carcinomas (second primary carcinomas) in patients with squamous cell carcinoma of the head and neck (HNSCC).

Methods: All patients with newly diagnosed HNSCC underwent office-based Lugol chromoendoscopy. After flexible esophagoscopy with white light, 3.0% Lugol iodine solution was sprayed over the entire esophageal mucosa. Areas with less-intense staining (LVLs) were evaluated and biopsies taken.

Results: 132 patients with HNSCC were enrolled in this study. The most frequent primary tumors were oropharyngeal (49/132), tumors of the oral cavity (36/132) and larynx (35/132). The majority of subjects (107/132 patients, 81.1%) had advanced HNSCC carcinomas (stages III and IV). Multiple LVLs were discovered in 24 subjects (18.2%), and no LVLs in 108 (81.8%) subjects. Fifty-five LVL biopsy specimens were obtained and assessed. Squamous cell carcinomas were detected in two patients, peptic esophagitis in 11 patients, gastric heterotopic mucosa in two patients, hyperplasia in two patients, and low- and high-grade dysplasia in three patients.

Conclusions: Although only two patients with synchronous primary carcinomas were found among the patients, esophagoscopy should be recommended after detection of HNSCC to exclude secondary esophageal carcinoma or dysplasia.

The study was registered at ClinicalTrials.gov and has this ID: NCT01783158

Key words:

head and neck carcinoma, chromoendoscopy, Lugol's solution, esophageal carcinoma, synchronous tumors, deglutition, deglutition disorders

INTRODUCTION

Patients with squamous cell carcinomas of the head and neck (HNSCC) region show a predisposition to developing second primary squamous cell carcinomas in the aerodigestive tract [1-3]. While the risk of the existence of a second primary tumor in another area of the head or neck varies from 16% to 36%, the incidence of esophageal squamous cell carcinoma (SESCC) in patients with HNSCC varies from 1% to 17% [3,4].

Due to the aggressive nature of esophageal cancer and advanced disease at the time of diagnosis, the prognosis of esophageal cancer is generally poor [3,5,6]. Therefore, the identification of early esophageal lesions localized and limited only to the mucosa and submucosa may enhance the cure rate for patients with HNSCC [1,7,8,9,10,12]. Moreover, these esophageal lesions can potentially be completely removed by endoscopic mucosal resection [7, 8, 10, 11].

Early SESCO is diagnosed almost exclusively by endoscopic methods [11,12]. In contrast to standard white light esophagoscopy, which simply observes the macroscopic appearance of mucosal lesions without any enhancement, chromoendoscopy (Lugol's solution chromoendoscopy or methylene blue contact endoscopy) and "electronic chromoendoscopy" (autofluorescence or narrow band imaging) enable detection of lesions that are not otherwise visible. These methods can be used to accurately assess the extent of the lesions [13-18]. Chromoendoscopy

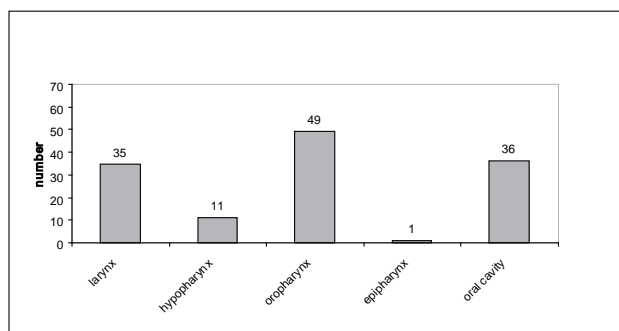


Figure 1
Localization of primary HNSCC in patients screened for the presence of synchronous esophageal pathology by chromoendoscopy.

with Lugol's solution can visualize suspicious areas, called Lugol-voiding lesions (LVLs, also known as Lugol unstained lesions), and thus detect dysplasias/SCCs that are not normally visible [1,3,10,17,19,20]. The aim of this prospective study was to define the benefits of flexible esophagoscopy with chromoendoscopy in the detection of early esophageal carcinomas (second primary carcinomas) in patients with HNSCC. To do so, we used chromoendoscopy with Lugol's solution.

Table 1
Histopathological diagnosis of mucosal biopsies.

Pathology	N
Squamous cell carcinoma	2
High-grade dysplasia	1
Low-grade dysplasia	2
Peptic esophagitis	10
Gastric heterotopic mucosa	2
Hyperplasia	2
Hyperkeratosis	1
Acanthosis	1
Normal mucosa	3
Total	24

MATERIAL AND METHODS

Study design

The study was approved by the Institutional Ethics Committee and performed in accordance with the Declaration of Helsinki, good clinical practice, and applicable regulatory requirements. Informed written consent was obtained from all participants or a legal representative before initiation of any procedure.

A total of 132 patients with newly diagnosed HNSCC underwent chromoendoscopy with Lugol's solution in 2004-2012. Only patients with oral cavity, pharyngeal, and laryngeal carcinomas were included in this prospective study. Patients with iodine allergy were excluded from the study. Patient demographic data were collected, and tumors were staged. The staging included a complete ENT examination, ultra-

sound and CT scans, and a biopsy of mass lesions. Additional staging procedures were performed when necessary. An individual treatment plan was assigned to each patient after completion of the staging.

Chromoendoscopy

Lugol chromoendoscopy of the esophagus was performed as an outpatient procedure. Participants were placed in a recumbent position, and a transoral approach was used for the endoscopy. Video endoscopes were used (models GIFQ140, GIFQ145, GIFH180, GIFN180, and GIFV2; Olympus Optical Company, Hamburg, Germany).

During a conventional examination, the unstained appearance of the esophagus was documented and the esophagus was evaluated. Then, 15-20 ml of a 3.0% Lugol iodine solution was sprayed over the entire esophageal mucosa with a spraying catheter (Olympus PW-205V), moving from the lower to the upper esophageal sphincter over the course of 20 seconds. After a 2-minute waiting period, the areas with less-intense staining were photographed; several biopsies were taken from the unstained areas.

Statistical analysis

For statistical analysis of age, sex, and treatment success, two-sample t-test and Fisher's exact test were used. Results were considered to be statistically significant at $p < 0.05$.

RESULTS

One hundred and thirty-two subjects with HNSCC were prospectively enrolled in this study (117 men and 15 women). The mean age of the cohort was 57.6 years (range 36-78 years).

The most frequent primary tumor site was oropharyngeal (49/132, 37.1%), followed by the oral cavity (36/132, 27.3%), larynx (35/132, 26.5%), hypopharynx (11/132, 8.3%), and epipharynx (1/132, 0.8%) (Fig. 1). Only 9.8% of patients had American Joint Committee on Cancer (AJCC) stage I disease; 9.1% had stage II. The vast majority of the subjects (107/132, 81.1%) had advanced carcinomas: stages III and IV (Figs. 2 and 3). Seventy-eight patients reported severe deglutition problems at the time of the HNSCC diagnosis. It was not possible to distinguish whether these problems originated from the head and neck or esophagus.

Esophagoscopy with chromoendoscopy was performed successfully for all 132 patients. In 25 patients, a percutaneous gastrostomy was performed, due to previously planned surgery for the HNSCC and adjuvant radiotherapy at the same sitting.

Multiple and no LVLs were discovered in 24 (18.2%) and 108 (81.8%) patients, respectively. A total of 55 biopsy specimens from LVL were obtained and assessed histopathologically. For these specimens, the diagnoses were as follows: SESCC in two cases, peptic esophagitis in 11 patients, gastric heterotopic mucosa in two patients, hyperplasia in two patients,

and dysplasia in three patients (Table 1). Three of the 55 biopsies were described as normal. There was only one case of high-grade dysplasia, which was treated with endoscopic mucosal resection (EMR).

Both the SESCCs were visible during the standard esophagoscopy with white light and were more advanced than T1; the primary HNSCCs were stage IV. Both the SESCCs were also evaluated as LVLs; their boundaries were more visible during the chromoendoscopy. Moreover, the extent of the tumors was found to be greater during chromoendoscopy than had been thought prior to the procedure. In both patients with SESCC, the oncological treatment for HNSCC was changed and the intended radical surgical treatment was discontinued.

We experienced complications of chromoendoscopy in one patient. Light bronchospasm that was triggered by aspiration of a small amount of Lugol's solution was treated with standard bronchodilation therapy. The patient was admitted to hospital for observation and discharged the next day. No other complications were observed.

DISCUSSION

In patients with primary HNSCC, the existence of a second primary tumor in another area of the head or neck, such as the esophagus or the lung, varies from 16% to 36% [1-4, 21-23]. The prevalence of synchronous esophageal cancer in patients with head and neck cancer varies from 5.1% to 12.5% [5]. Synchronous multiple primary cancers in the esophagus and the head and neck region adversely affect survival and quality of life, because the mortality rate for patients with a second cancer, especially cancer in the lung and esophagus, is as high as 90% at 2 years after detection [1,5].

The highest incidence of SESCC was found in the Chinese province of Linxian, where the incidence of SESCC is 700 cases per 100,000 people (this is approximately 350 times higher than the incidence of esophageal SCC in the Czech Republic) [6,12,25]. Dubuc et al., in a large European study, discovered esophageal neoplastic lesions in 9.8% of patients with HNSCC [24], whereas the overall incidence of SESCC in the Czech Republic is quite low, approximately two per 100,000 people [25].

The etiology of HNSCC and SESCC is associated predominantly with smoking and drinking [3,6,10,26-

28]. This may be explained by the concept of "field cancerization" proposed by Slaughter et al., in which repeated exposure to carcinogens leads to an accumulation of genetic alterations that results, ultimately, in the development of multiple and independent cancers [1,2]. It is the reason why the upper aerodigestive tract should be examined as part of the staging work-up in patients with HNSCC even in patients without symptoms of deglutition disorders [1,10,14,15,20,22], and why particular attention should be focused on high-risk groups, such as patients with primary HNSCC.

Early detection of SESCC with using neoplasia classification based on cytological and architectural severity and invasion status are essential for effective treatment, and the prognosis strongly depends on tumor stage at the time of diagnosis [1-3,6,9-13,26,27,29-32]. One of the most important reasons for why early SESCCs are not detected is the fact that there is a tendency to carry out cursory examinations of the esophagus using white light only [7]. "Biologic endoscopy" or "detailed endoscopy" can be used for early detection of tumors in the upper aerodigestive tract, because these techniques enable the visualization of lesions that are not otherwise apparent and can provide greater insight into the behavior of target lesions [1,4,13-17,29-31].

Iodine staining of squamous cell epithelium is one of the oldest staining techniques; it was first described by Schiller in 1933 for the detection of early carcinoma of the cervix [32]. Lugol staining patterns correlate well with the degree of glycogen within squamous epithelium, and dysplastic epithelium can be visualized as LVLs [1,5,8,17,33]. Chromoendoscopy is inexpensive and can be performed easily by a gastroenterologist; no special tools or light sources are necessary [1].

Muto et al. reported that 55% of HNSCC patients with many irregularly shaped multiform LVLs had synchronous SESCC. Moreover, Fukuhara et al. reported that 85.7% of HNSCC patients with metachronous SESCC had many irregularly shaped multiform LVLs [1,3]. In contrast with these findings, we observed LVLs in only 24 patients (18.2%), and we found no early SESCCs and only three dysplasias (one of which was treated with endoscopic mucosal resection).

The aim of our study was to define the incidence of esophageal lesions by chromoendoscopy with Lugo-

Figure 2

Tumor staging of head and neck cancer according to TNM classification. Stage I, T1N0M0; stage II, T2N0M0; stage III, T3N0M0; stage IV, T4N0-3M0.

TNM HNSCC stages	N0	N1	N2	N3
T0	0	0	1 (0.7%)	0
T1	13 (9.8%)	3 (2.3%)	8 (6.1%)	1 (0.7%)
T2	12 (9.1%)	6 (4.5%)	14 (10.6%)	2 (1.5%)
T3	14 (10.6%)	6 (4.5%)	24 (18.2%)	1 (0.7%)
T4	6 (4.5%)	2 (1.5%)	15 (11.4%)	4 (3.0%)

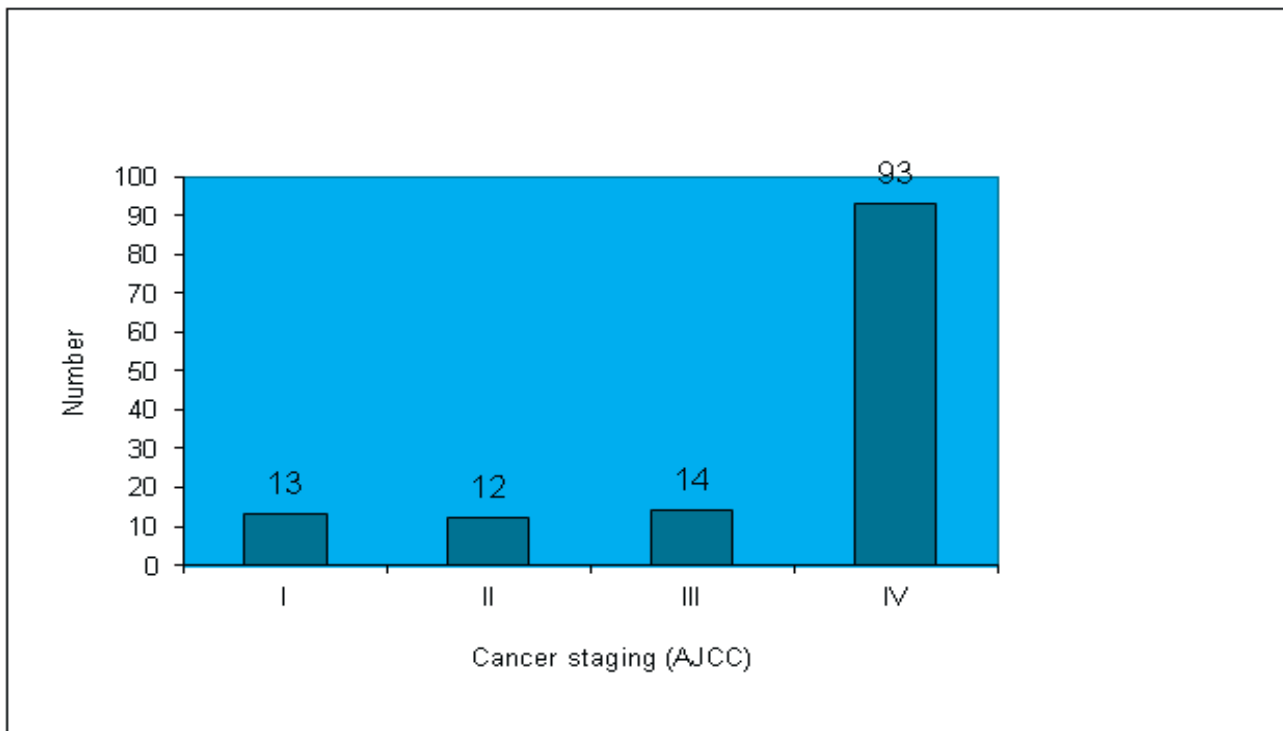


Figure 3

Staging of head and neck carcinomas according to the American Joint Committee on Cancer (AJCC).

l's solution in patients with newly diagnosed HNSCC. Our idea was to detect synchronous early esophageal carcinomas in this high-risk group of patients, in the group in which no or minimal deglutition symptoms are present. From this perspective, our results did not meet our expectations, since we did not find any early SESCCs. However, we believe that detailed endoscopy techniques can improve detection of superficial mucosal areas with dysplasia or early carcinoma and should therefore be considered standard methods during flexible esophagoscopy. This is especially true for high-risk patient groups, such as those

with primary HNSCC. Advanced endoscopic methods should be used not only for staging of the primary HNSCC tumor, but also for follow-up to detect possible second metachronous primary esophageal tumors.

CONCLUSIONS

Patients with HNSCC represent a high-risk group for the development of SESCC. Thus, esophagogastrosfibroscopy should be performed to detect possible synchronous esophageal carcinomas in these patients. Although only two patients with synchronous primary carcinomas were found among the patients with newly diagnosed HNSCC in this study, esophagoscopy

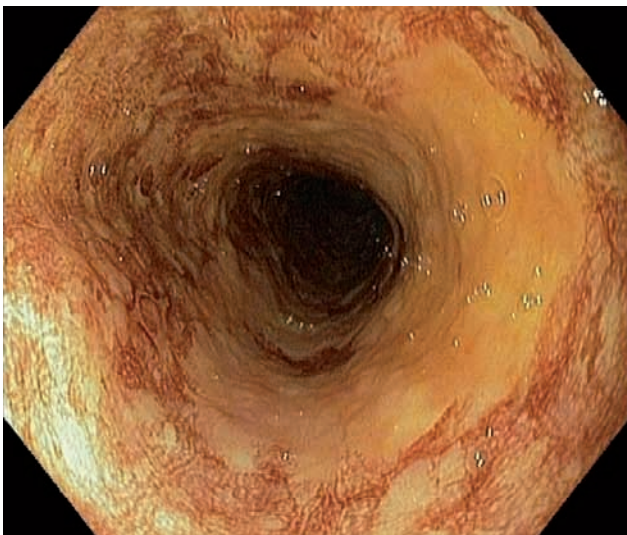


Figure 4

Endoscopic views of Lugol chromoendoscopy in patients with head and neck cancer. (a) Irregularly shaped multifocal LVLs (histologically identified as spinocellular carcinoma). (b) Single LVL on 7 o'clock position (histologically - high grade dysplasia)

and better some of advanced endoscopic methods should be recommended after detection of HNSCC to exclude secondary esophageal carcinoma or dysplasia. Staining of the esophagus with Lugol's solution is an easy and inexpensive option and can be done in most of gastroenterology offices.

Acknowledgments

The authors wish to thank Hana Tomášková from the Institute of Epidemiology and Public Health, Faculty of Medicine of the Ostrava University, Czech Republic, for her help with statistical analysis.

Conflict of interest statement

The authors declare that there is no actual or potential conflict of interest in relation to this article. No benefits in any form have been received or will be received from a commercial party related directly or indirectly to the subject of this article.

The research was supported by the Institutional support of the Ministry of Health No 1 RVO-FNOs/2012

REFERENCES

- Muto M, Hironaka S, Nakane M, et al. Association of multiple Lugol-voiding lesions with synchronous and metachronous esophageal squamous cell carcinoma in patients with head and neck cancers. *Gastrointest Endosc* 56:517-21, 2002.
- Slaughter DP, Southwick HW, Smejkal W Field cancerization in oral stratified squamous epithelium: clinical implications of multicentric origin. *Cancer*. 6:963-8, 1953.
- Fukuhara T, Hiyama T, Tanaka S, et al. Characteristics of Esophageal Squamous Cell Carcinomas and Lugol-voiding Lesions in Patients with Head and Neck Squamous Cell Carcinoma. *J Clin Gastroenterol* 44 (2):e27-33, 2010.
- Shiozaki H, Tahara H, Kobayashi K, et al. Endoscopic screening of early esophageal cancer with the Lugol dye method in patients with head and neck cancers. *Cancer* 66:2068-2071, 1990.
- Möschler O., Spahn TW, Middleberg-Bisping, Ch., et al. Chromoendoscopy is a valuable tool for Screening of High-Risk patients with head and Neck cancer for early Detection of Esophageal Cancer. *Digestion*. 73:160-166, 2006.
- Dawse S, Lewin KJ, Wang GQ, et al. Squamous Esophageal Histology and Subsequent Risk of Squamous Cell Carcinoma of the Esophagus. *Cancer*. 74:1686-92, 1994.
- Fujita J, Sueyoshi S, Yamaha H, et al. Optimum treatment strategy for superficial esophageal cancer: endoscopic mucosal resection versus radical esophagectomy. *World J Surg* 25:424-431, 2001.
- Ponchon T, Makuuchi H, Morita Y, et al. Images of early Cancer: Esophageal Squamous-Cell Carcinoma. *Endoscopy* 36:811-820, 2004.
- Schlemper RJ, Dawsey SM, Itabashi M et al. Difference in Diagnostic Criteria for Esophageal Squamous Cell Carcinoma between Japanese and Western Pathologists. *Cancer*. 88:996-1006, 2000.
- Schlemper RH, Riddel RH, Kato Y, et al. The Vienna classification of gastrointestinal epithelial neoplasia. *Gut*. 47:251-255, 2000.
- Bergman J, Zhang YM, He S, et al. Outcomes from a prospective trial of endoscopic radiofrequency ablation of early squamous cell neoplasia of the esophagus. *Gastrointest Endosc*. 74:1181-90, 2011.
- Wang GQ, Jiao GG, Chang FB, et al. Long-Term Results of Operation for 420 Patients With Early Squamous Cell Esophageal Carcinoma Discovered by Screening. *Ann Thorac Surg*. 77:1740-1744, 2004.
- Piazza C, Bon FC, Peretti G, et al. "Biologic endoscopy": optimization of upper aerodigestive tract cancer evaluation. *Curr Opin Otolaryngol Head Neck Surg*. 19(2):67-76, 2011.
- Nonaka S, Saito Y, Oda I, et al. Narrow-band imaging endoscopy with magnification is useful for detecting metachronous superficial pharyngeal cancer in patients with esophageal squamous cell carcinoma. *J Gastroenterol Hepatol*. 25(2):264-9, 2010.
- Muto M, Minashi K., Yano T., et al. Early Detection of Superficial Squamous Cell Carcinoma in the Head and Neck Region and Esophagus by Narrow Band Imaging: A Multicenter Randomized Controlled Trial. *J Clin Oncol* 28:1566-1572, 2010.
- Piazza C, Dessouky O, Peretti G., et al. Narrow-band imaging: a new tool for evaluation of head and neck squamous cell carcinomas. Review of the literature. *Acta Otorhinolaryngol Ital* 28:49-54, 2008
- Davila RE Chromoendoscopy. *Gastrointest Endoscopy Clin N Am* 19:193-208, 2009.
- Nonaka S, Saito Y Endoscopic diagnosis of pharyngeal carcinoma by NBI, *Endoscopy* 40:347-351, 2008.
- Khosbaten M, Naderpour M, Mohammadi G., et al. Epidemiology of Esophageal Lesions In Patients with Head and Neck Squamous Cell Carcinoma. *Asian Pacific J cancer Prev*, 11:863-865, 2010.
- Papazian A, Descombes P, Capron JP, et al. Incidence of esophageal cancer synchronous with upper aerodigestive tract cancers (100 cases): value of vital staining with Lugol and toluidine blue. *Gastroenterol Clin Biol* 9:16-22, 1985.
- Cohn AM, Peppard SB Multiple primary malignant tumors of the head and neck. *Am J Otolaryngol*. 1:411-7, 1980.
- Muto M, Takahashi M, Ohtsu A, et al. Risk of multiple squamous cell carcinomas both in the esophagus and the head and neck region. *Carcinogenesis* 26(5):1008-1012, 2005.
- Farwel DG, Rees CJ, Mouadeb DA, et al. Esophageal pathology in patients after treatment for head and neck cancer. *Otolaryngol Head Neck Surg*, 143 (3):375-378, 2010.
- Dubuc J, Legoux JL, Winnock, M, et al. Endoscopic screening for esophageal squamous-cell carcinoma in high-risk patients: a prospective study conducted in 62 French endoscopy centers. *Endoscopy* 38:690-695, 2006.
- Vítek P, Komínek P, Kajzrlíková I, et al. Endoscopic diagnosis and treatment of early spinocellular carcinoma of the oesophagus is possible even in a population with low incidence of this disease. *Endoskopie* 18(4): 161-166, 2009.
- Khosbaten M, Naderpour M, Mohammadi G, et al. Epidemiology of Esophagela Lesions in Patients with Head and Neck Squamous Cell Carcinoma. *Asian Pacific J Cancer Prev* 11:863-865, 2010.
- Cancer incidence in Japan, 1985-89: re-estimation based on data from eight population-based cancer registries. The Research Group for Population-based cancer. Registration in Japan. *Jpn J Clin Oncol* 28:54-67, 1998.
- Seitz HK, Poschl, G, Simanowski, UA Alcohol and cancer. *Recent Dev Alcohol* 14:67-95, 1998.
- Ishihara R., Takeuchi Y, Chatani R, et al. Prospective evaluation of narrow-band imaging endoscopy for screening of esophageal squamous mucosal high-grade neoplasia in experienced and less experienced endoscopists. *Diseases of the Esophagus* 23:480-486, 2010.
- Shahid MW, Wallace MB Endoscopic Imaging for the Detection of Esophageal Dysplasia and Carcinoma. *Gastrointest Endoscopy Clin N Am* 20:11-24, 2010.
- Roth MJ, Liu SF, Dawsey SM, et al. Cytologic detection of esophageal squamous cell carcinoma and precursors lesions using balloon and sponge samplers in asymptomatic adults in Linxian, China. *Cancer* 80:2047-2059, 1997.
- Schiller W Early diagnosis of carcinoma of the cervix. *Surg Gynecol Obstet* 56:210-222, 1933.
- Dawsey SM, Fleischer DE, Wang GQ et al. Mucosal iodine staining improves endoscopic visualization of squamous dysplasia and squamous cell carcinoma of the esophagus in Linxian, China, *Cancer* 83:220-231, 1998.

INVESTIGATION OF AN AUTOLOGOUS BLOOD TREATMENT STRATEGY FOR TEMPOROMANDIBULAR JOINT HYPERMOBILITY IN A PIG MODEL

J. Stembírek^{1,2,3}, E. Matalova^{1,4}, M. Buchtova^{1,4}, V. Machon⁵, I. Misek¹

1 Institute of Animal Physiology and Genetics CAS, v.v.i., Brno, Czech Republic;

2 Department of Oral and Maxillofacial Surgery, University Hospital Ostrava, Czech Republic;

3 Faculty of Medicine, Masaryk University, Brno, Czech Republic;

4 Faculty of Veterinary Medicine, University of Veterinary and Pharmaceutical Sciences, Brno, Czech Republic;

5 Department of Oral and Maxillofacial Surgery, Charles University, Prague, Czech Republic

Originally published in *International journal of oral and maxillofacial surgery* 2013; 42: 369-375

Consent to the publication of 28th April 2014 (No. 3377611027768)

ABSTRACT

Many different surgical and non-surgical techniques are used for the treatment of temporomandibular joint (TMJ) hypermobility. One of these methods is autologous blood injection into the TMJ. The fate of the autologous blood used for treatment of recurring condylar dislocation is still not completely understood. The authors used 12 pigs (*Sus scrota f. domestica*) as a model species for autologous blood delivery into the TMJ. Blood injection was followed by histopathological analysis at different times after treatment (1 hour, 1, 2 and 4 weeks). Samples were examined by magnetic resonance imaging, macroscopic and histological methods. The deposition of the remaining blood was observed in the form of clots in the distal parts of the upper joint cavity one hour and one week after treatment. Two weeks after treatment, small blood clots were still apparent in the distal part of the upper joint cavity. Four weeks after surgery, no remnants of blood, changes or adhesions were apparent inside the TMJ. No morphological or histological changes were observed in the TMJ after the injection of autologous blood suggesting another mechanism is involved in the hypermobility treatment.

Keywords:

temporomandibular joint; pig; autologous blood; hypermobility.

INTRODUCTION

The temporomandibular joint (TMJ) provides the junction between the jaw (mandibular condyle) and the neurocranium (temporal bone). Condyle dislocation (or hypermobility) of TMJ is one of the most frequent TMJ disorders in humans¹. In the case of hypermobility, the condyle reaches a position in front of the articular tubercle at wide mouth opening, which can be caused by abnormalities in the shape of the joints, by ligament looseness or by reduced muscle tension². The treatment of TMJ hypermobili-

ty includes surgical or non-surgical approaches.

Surgical procedures can be divided into two categories; those that limit the range of condylar movement, and those that remove the blocking factor that prevents the condyle from returning³⁻⁶.

Non-surgical treatment includes a soft diet, pharmacotherapy, physical therapy, stress reduction, movement limitation and occlusal splint therapy. Joint movement reduction can be caused by the injection of different substances such as autologous blood or sclerosing solutions into the upper joint cavity^{2,7,8}. Although there are many clinical studies about a high success rate of autologous blood injection into TMJ,^{2,3,7,9,10} the effect and the detailed mechanism of this therapy are not well understood.

It has been proposed that autologous blood in the TMJ may result in joint degeneration and/or formation of adhesions inside the joint. There is a lack of studies examining in detail the mechanisms of the effect of autologous blood injection into the TMJ. This type of study can only be carried out using a suitable animal model (human-like size, with similar structure and motion of TMJ) paired with subsequent histological evaluations.

Several studies have been performed to understand the joint pathology and different approaches have been tested for their treatment. A sheep model was used for the evaluation of histopathological changes after intracapsular condylar fracture, the fate of auricular cartilage graft in the surgical treatment of TMJ ankylosis, intraarticular scarring and ankylosis management¹¹⁻¹³. Blood was injected into the rabbit TMJ¹⁴. The rabbit and sheep condyles are adapted to a herbivorous diet so are more rounded than those of humans, which causes greater mobility in the transverse plane and limited mouth opening. In contrast, pigs are omnivorous like humans and therefore the structure of their TMJ resembles that of humans. Their diarthrodial synovial TMJ consists of an articular pit, articular disc and articular condyle surrounded by a ligamentous capsule. The

articular disc, as in humans, divides the joint into two compartments described as two articulations: the meniscotemporal (suprameniscal) joint permitting translational movements, and the condylomeniscal (inframensiscal) joint, which permits rotational movements. The disc has a biconcave shape; the fossa is shallow, and the condyle is elliptic^{15,16}. The masticator muscle arrangement is similar to that in humans, therefore moderate translation movements are allowed in all planes; the major movement is provided by rotation of the joint condyle^{15,17}.

Based on these morphological similarities, the authors selected the pig as a model organism for this study, which aims to confirm or disprove the hypothesis that aseptic inflammation and subsequent formation of lesions and adhesions are responsible for the therapeutic effect of autologous blood used for TMJ hypermobility treatment.

MATERIALS AND METHODS

12 pigs (*Sus scrofa f. domestica*) aged 2 years were obtained from the breeding unit of the Institute of Animal Physiology and Genetics, Academy of Science of the Czech Republic in Libečov. Animals were divided into four groups of three animals, none of which had any previous history of TMJ hypermobility. The first group was killed 1 h after treatment, the second group 1 week, the third group 2 weeks and the fourth group 4 weeks after autologous blood injection. The animals were housed in separate breeding boxes under conventional conditions and provided with water and food ad libitum. The experimental procedure was approved by the Animal Research Committee of IAPG CAS, v.v.i. (Nr. 67985904). All surgical procedu-

res were performed in the aseptic conditions of an operating theatre with disinfectant applied over the operating field. All animals were premedicated with ketamine (22 mg/kg) and atropine (0.04 mg/kg) and anaesthetized with thiopental (15 mg/kg) prior to intubation. Anaesthesia was maintained with inhaled isoflurane (1.5%). The animals were mechanically ventilated with an initial tidal volume of 10 ml/kg and a respiratory rate of 15 breaths per min. The tidal volume was adjusted to maintain an arterial PaCO₂ of 35-40 mmHg during the experiment. Hydration was maintained using lactated Ringer's solution delivered through a cannulated dorsal auricular vein. Body temperature was maintained at 38.0-39.0 °C using a circulating hot water heating pad. Both heart rate and oxygen saturation levels were monitored throughout all surgical procedures.

The lateral approach was carried out from the lateral side of the articular capsule. A small incision was made above the lateral part of the left condyle, approximately 1 cm below the external auditory meatus during a wide mandible opening. The first 20-gauge needle was inserted towards the posterior aspect of the condyle in the posterior part of the superior joint cavity in the anterior-medial direction, before being withdrawn slightly (about 1 mm) to prevent subchondral application and saline solution was injected. During the saline solution application, no protrusive movement of the mandible was observed and the correct position of the needle therefore had to be checked by arthrocentesis with saline solution. The second 20-gauge needle was inserted approximately 0.5-1 cm before the first needle at the same horizontal level but in the posterior-medial direction.

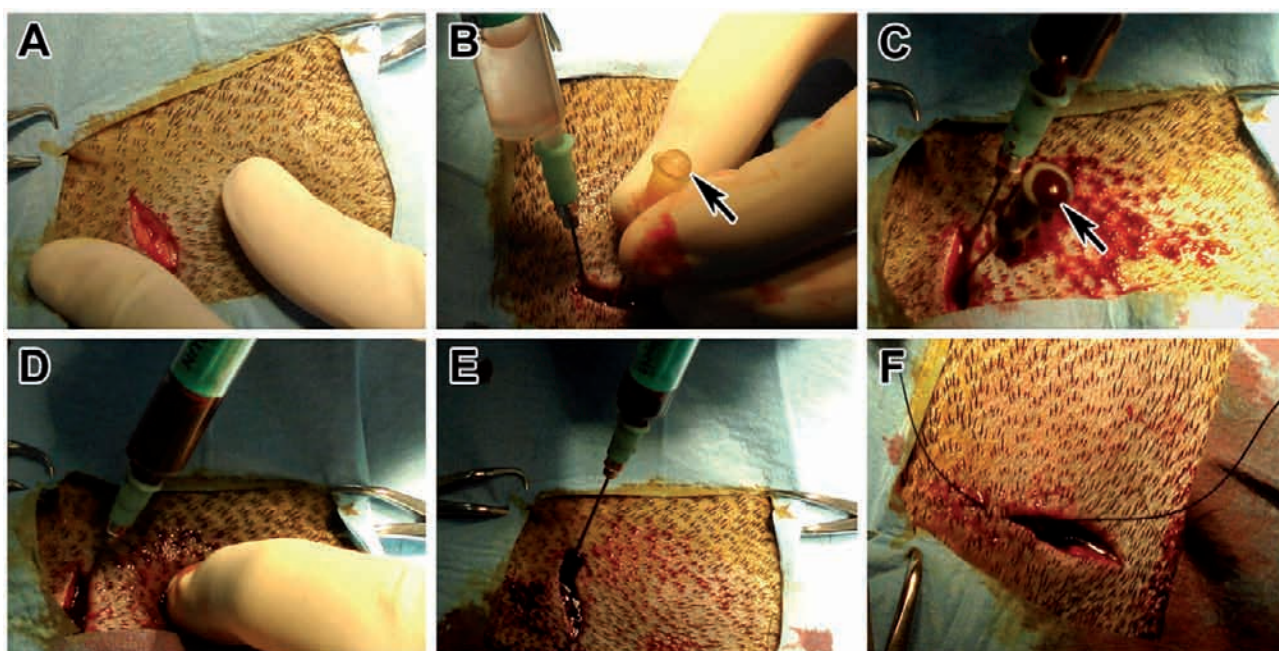


Fig.1. Surgical approach in the pig. (A) Small incision and preparation through the skin and adipose layer. (B) Arthrocentesis with saline solution, black arrow shows positive return of irritant. (C) Recheck of arthrocentesis with autologous blood, black arrow shows positive return of autologous blood. (D) Injection of autologous blood into left upper joint cavity. (E) Injection of autologous blood around left TMJ. (F) Skin suture.

After this procedure, successful arthrocentesis with saline solution was performed in all cases. The next step was collecting blood from the jugular vein and injecting 1.0 ml of this blood into the superior joint cavity and 0.5 ml around the articular capsule, followed by wound suture (Fig. 1). The left TMJ served as the experimental joint for blood application and the right TMJ was left without treatment as the control tissue. As it would be difficult to maintain pigs in a sterile environment after the procedure, antibiotics (amoxicillin Bioventa 15% inj. ad us. vet, 15 ml/kg and day, divided into two doses) were administered to prevent infection.

The experimental pigs were killed by intravenous injection of thiopental at four different time intervals after successful autologous blood delivery (1 h, 1, 2 and 4 weeks after treatment). The whole heads were placed on ice and immediately transported for examination by 3T nuclear magnetic resonance imaging (MRI; Siemens Ltd., Siemens Magnetom Trio 3T) at the Institute of Clinical and Experimental Medicine (Prague, Czech Republic).

After this analysis, both TMJs were dissected, fixed in 10% paraformaldehyde and examined using a stereoscopic microscope (Leica, Germany). After 10 days in paraformaldehyde, decalcification was performed in Livrea's solution (4% HNO₃, 0.15% CrO₃) for approximately 1 month, after which the specimens were embedded in paraffin, cut into 5 mm sagittal histological sections, and split over four parallel slides. Haematoxylin-eosin (HE) was used as the primary staining for the histological analysis, elastic fibres were visualized by Orcein, reticular fibres were stained with Gömöri, and Van Gieson staining was used for the detection of collagen fibres.

RESULTS

In the samples taken 1 h and 1 week after treatment, macroscopic examination revealed deposition of the remaining blood in the form of clots in distal parts of the upper joint cavity. No alterations on the articular surface were observed. 2 weeks after treatment, small blood clots were still apparent in the distal part of the upper joint cavity. 4 weeks after surgery, no remnants of blood, changes or adhesions were apparent inside the TMJ (Fig. 2).

In MRI, the injection injury caused by the needle was visible in the articular disc and surface of the temporal bone 1 h after surgery. There were no apparent morphological changes in the nuclear magnetic resonance (NMR) images when comparing the control and experimental joints (Fig. 3).

Regarding histological analysis, no inflammatory or non-inflammatory morphological lesions were observed at any time after the treatment. The superior and inferior articular spaces showed no sign of joint exudation. The surface of the synovium was covered with small finger-like projections (villi) with no morphological lesions. The fibrous articular discs

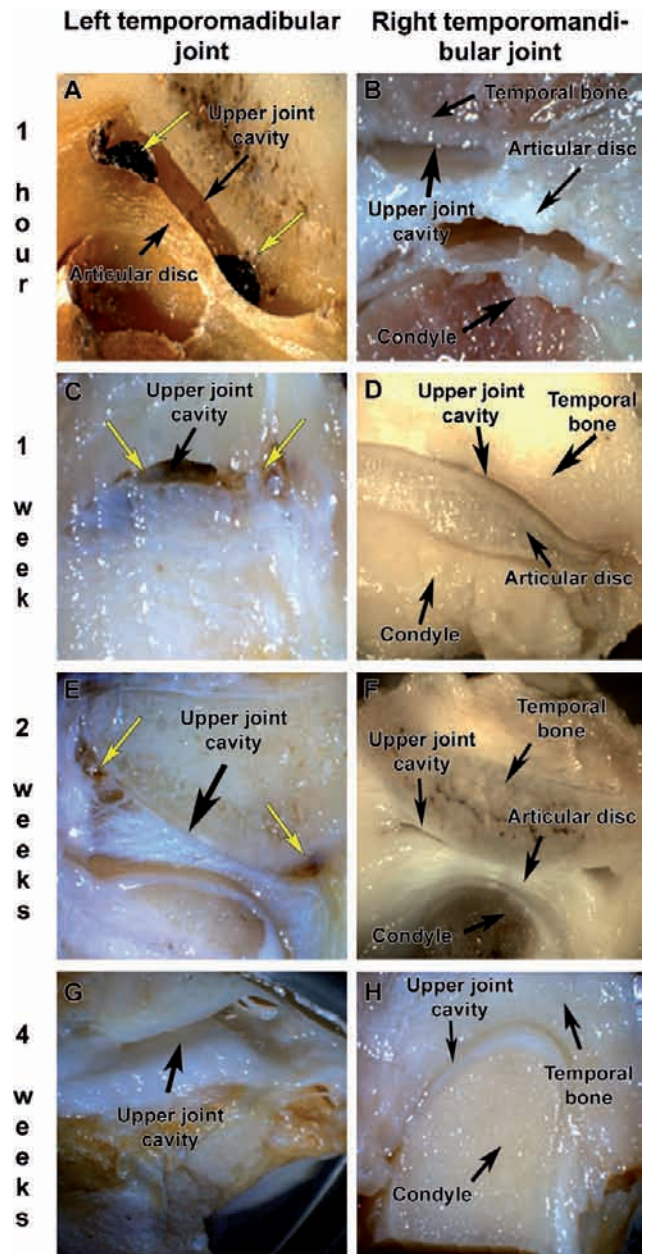


Fig. 2. Macroscopic view of pig TMJ after treatment. (A) Macroscopic view of left TMJ 1 h after treatment, yellow arrows shows visible clots in the upper joint cavity. (B) Macroscopic view of right control TMJ at same stage with physiological anatomical structure. (C) Macroscopic view of left TMJ 1 week after treatment, yellow arrows show remaining blood clots in the distal and central parts of the upper joint cavity. (D) Macroscopic view of right control TMJ 1 week after treatment with physiological anatomical structure. (E) Macroscopic view of left TMJ 2 weeks after treatment, yellow arrows show remaining small blood clots in the distal part of the upper joint cavity. (F) Macroscopic view of right control TMJ 2 weeks after treatment, there are not apparent morphological changes. (G) Macroscopic view of left TMJ 4 weeks after treatment. The upper joint cavity remained with smooth surfaces and without changes or adhesions. (H) Macroscopic view of right control TMJ 4 weeks after treatment. There joint surfaces are still smooth without changes.

(menisci) formed fibrocartilage pads containing bundles of elastic and collagen fibres between opposing surfaces of the joint. Fibroblasts were rare and were dispersed among fibres. Articular cartilage covering the condyle of the mandible and temporal bone was

formed of hyaline cartilage with no apparent erosion or pathological defects (Fig. 4).

The middle and deep layers of cartilage were organized into columns of chondrocytes with normal appearance. Selective histological staining for different types of fibres demonstrated non-fragmented fibres in their typical arrangement. The menisci, peripheral surfaces of the joints and the fibrous tissue of the joint capsule showed no dystrophic or inflammatory lesions (Fig. 4).

DISCUSSION

Autologous blood injection is a simple treatment for TMJ hypermobility in humans. The major advantage of TMJ autologous blood injection is that it is minimally invasive, and being a non-surgical technique it is more acceptable and comfortable for patients. This method does not require surgical incision, tissue dissection, bone preparation or general anaesthesia, and eliminates postoperative complications such as facial nerve injuries, infection and oedema. The disadvantages of the technique are that the needle is advanced without visualization and there is therefore a risk of incorrect application of the autologous blood. Needle insertion can damage the surrounding tissues and cause bleeding in and around the joint. Schulz was the first to report the treatment of human patients using autologous blood for recurrent condyle dislocation¹⁸. He injected autologous blood twice a week for 3 weeks and used intermaxillary fixation for jaw immobilization. 10 of 16 patients were asymptomatic after 1 year. Jacobi-Hermanns et al. injected autologous blood once into the affected side and used intermaxillary fixation for 2 weeks³. This approach was successful in 94% of condyle dislocations. Hasson and Nahlieli reported four patients who received one injection of autologous blood and were then instructed to restrict their mandibular movement for 7 days². Dislocation of condyles did not reoccur, and all patients presented normal mouth opening at follow-up inspections. Kato et al. reported autologous blood injection as a method for treatment of TMJ hypermobility in an 84-year-old woman with subsequent mandible fixation for 1 month. The result was favourable, and no ankylosis occurred⁹. Machon et al. treated 25 patients diagnosed with chronic recurrent TMJ dislocation⁷. The patients were treated by bilateral injections of autologous blood into the upper joint space and around the TMJ capsules. 80% of patients did not require any further treatment during the following year.

Based on clinical data, the presence of autologous blood in the TMJ (injury, surgery) and subsequent immobility may result in adhesion or in development of ankylosis. These studies also reported limited mouth opening in patients with a history of TMJ injury or degenerative diseases¹⁹⁻²². Despite the fact that autologous blood injection is used as a routine therapy in humans, it remains unclear what happens in

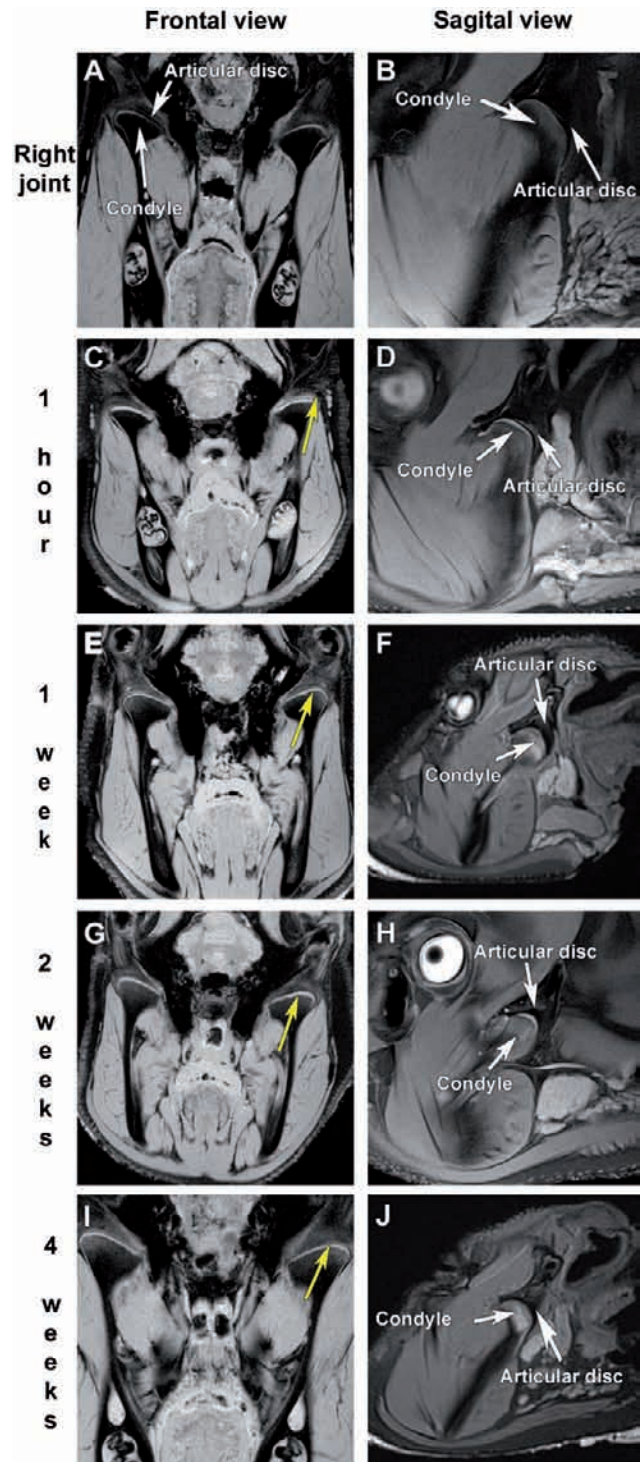


Fig.3. NMR analysis of TMJ after blood treatment. (A) Frontal view of pigs head with both TMJs. (B) Sagittal view of physiological TMJ. (C) Frontal view of both TMJs 1 h after treatment, yellow arrow shows damage of articular disc and temporal bone surface caused by needle. (D) Sagittal view of left TMJ 1 h after treatment with no apparent evidence of blood and damage. (E) Frontal view of both TMJs 1 week after treatment, yellow arrow shows left TMJ but there is no evidence of blood. (F) Sagittal view of left TMJ 1 week after treatment. (G) Frontal view of both TMJs 2 weeks after treatment, yellow arrow shows left TMJ with no apparent changes and blood rests. (H) Sagittal view of left TMJ 2 weeks after treatment with no apparent morphological changes. (I) Frontal view of both TMJs 4 weeks after treatment, yellow arrow shows left TMJ with no apparent changes. (J) Sagittal view of left TMJ 4 weeks after treatment

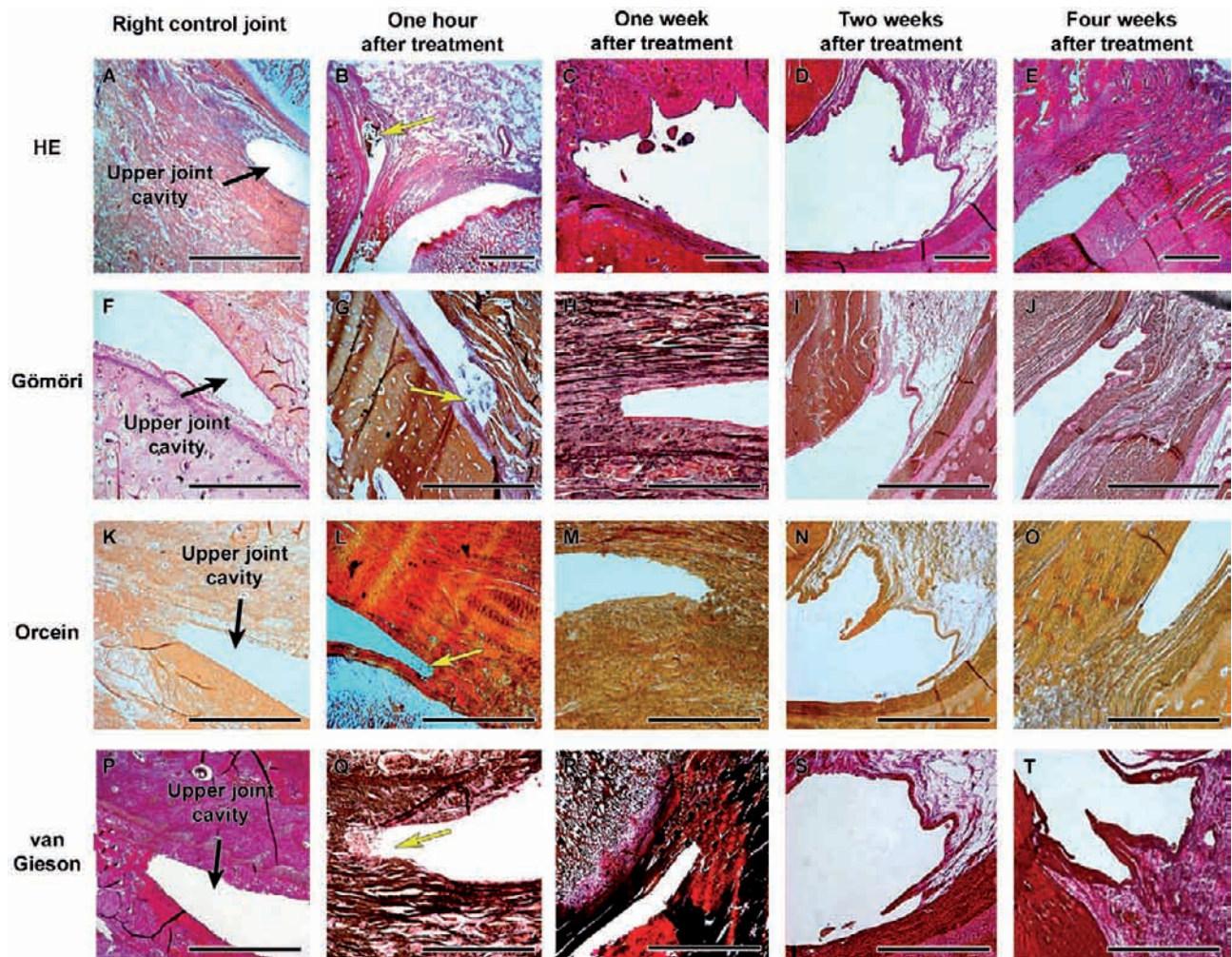


Fig. 4. Microscopic structure of pig TMJ after blood treatment. (A) Right control TMJ stained with HE, (F) with Gömöri for reticular fibres visualization, (K) with Orcein for elastic fibres and (P) with van Gieson for collagen fibres. There are characteristic smooth surfaces in the upper joint cavity. (B,G,L,O) Left treated TMJ collected 1 h after treatment. Yellow arrow shows blood clots in the distal part of cavity, there are not other morphological changes. (C,H,M,R) Left treated TMJ 1 week after treatment; there is no apparent blood or other changes. (D,J,N,S) Left TMJ 2 weeks after treatment. Special staining demonstrated non-fragmented fibres with their characteristic arrangement in the joint without obvious microscopic changes. Scale bar 200µm.

unaffected TMJs after injection. The injection of autologous blood into the knee joint in rabbit and dogs led to joint changes under pathological conditions such as traumatic bleeding, haemophilic bleeding or rheumatoid arthritis²³⁻²⁶. Oxidative stress (injury, arthritis, infection) at the molecular level was shown to contribute to formation of cross-linked proteins that may serve as an initial scaffold for the development of adhesion under pathological conditions²⁷. Some authors suggest that exposure of cartilage to blood alters chondrocyte metabolism, which might lead to unknown alterations and cartilage destruction, plus changes in matrix integrity that may result in lasting joint damage^{23,24,26}. Others suggest that such exposure has only a temporary effect and that a single episode of intra-articular bleeding only leads to reversible cartilage damage^{25,28,29}.

One possible explanation for the effect of autologous blood is an aseptic inflammation resulting in scar and fibrous tissue formation between the surfaces of the articular disc and articular socket, causing a reduction in the extent of condylar movement^{2,9}. No

destructive changes to the bony components of the joint controlled by X-ray have been observed in humans^{2,9,10}.

Until now, experiments involving autologous blood injection into unaffected TMJ in animals have only been performed on rabbits. Candrl et al. used 8 white rabbits for bilateral autologous blood injection into the TMJ. After injection, the mandibles were fixed by orthodontic brackets and elastics for 24 h and the animals killed after 1 month. There was no evidence of degeneration in the joint and no adhesions were found¹⁴.

In the present study on a pig model, the authors have not found any lesions or morphological changes, which could be responsible for the beneficial results of autologous blood injection reported elsewhere. They cannot confirm that injection of autologous blood into the TMJ has any effect based on inflammatory changes. There were some disadvantages of the pig model that should be taken into account when using it for TMJ disease research. The surgery had to be carried out under general anaesthe-

sia. In comparison to experiments on rabbit or dog knee joints, which provide easy access for needle penetration due to the thin layer of subcutaneous tissue, the pig TMJ is situated under a large amount of subcutaneous and adipose tissue and a small skin incision is therefore necessary. The correct needle position could not be confirmed by protrusive movement of the mandible, meaning that in the pig, unlike humans, a double arthrocentesis with saline solution was necessary.

In conclusion, a methodical approach for autologous blood treatment of the TMJ and pathohistological evaluation of specimens in pigs has been demonstrated. Although the human TMJ is unique, the size of the articular structures in the pig, the shape and microscopic characteristics of the meniscus and further similarities favour it as a model species¹⁵⁻¹⁷. Although the injection of autologous blood into the TMJ is a relatively successful treatment in humans, elucidating the effect remains to be determined. The present experiment showed no structural changes in the joints and did not confirm the theory of aseptic inflammation resulting in the formation of adhesions inside the joint. This information can be extended by a detailed cellular and molecular analysis, which may help to explain the therapeutic effect in humans.

Competing interests

The authors report no conflicts of interest.

Ethical approval

The experimental procedure was approved by the Animal Research Committee of IAPG CAS, v.v.i. (Nr. 67985904).

REFERENCES

- Antczak-Bouckoms AA. Epidemiology of research for temporomandibular disorders. *J Orofac Pain* 1995;9:226-34.
- Hasson O, Nahlieli O. Autologous blood injection for treatment of recurrent temporomandibular joint dislocation. *Oral Surg Oral Med Oral Pathol Oral Radiol Endod* 2001;92:390-3.
- Jacobi-Hermanns E, Wagner G, Tetsch P. Investigations on recurrent condyle dislocation in patients with temporomandibular joint dysfunction: a therapeutic concept. *Int J Oral Surg* 1981;10:318-23.
- Poirier F, Blanchereau C, Francfort E, Agostini P, Petavy A, Khorshid M, et al. Surgical treatment of temporomandibular joint: apro-pos of 94 cases. *Rev Stomatol Chir Maxillofac* 2006;107:436-40.
- Shibata T, Yamashita T, Nakajima N, Ueda M, Ishijima T, Shigezumi M, et al. Treatment of habitual temporomandibular joint dislocation with miniplate eminoplasty: a report of nine cases. *J Oral Rehabil* 2002; 29:890-4.
- Tasanen A, Lamberg MA. Closed condylotomy in the treatment of recurrent dislocation of the mandibular condyle. *Int J Oral Surg* 1978; 7:1-6.
- Machon V, Abramowicz S, Paska J, Dolwick MF. Autologous blood injection for the treatment of chronic recurrent temporomandibular joint dislocation. *J Oral Maxillofac Surg* 2009; 67:114-9.
- Matsushita K, Abe T, Fujiwara T. OK-432 (Picibanil) sclerotherapy for recurrent dislocation of the temporomandibular joint in elderly edentulous patients: case reports. *Br J Oral Maxillofac Surg* 2007; 45(September (6)):511-3.
- Kato T, Shimoyama T, Nasu D, Kaneko T, Horie N, Kudo I. Autologous blood injection into the articular cavity for the treatment of recurrent temporomandibular joint dislocation: a case report. *J Oral Sci* 2007;49: 237-9.
- Pinto AS, McVeigh KP, Bainton R. The use of autologous blood and adjunctive 'facelift' bandage in the management of recurrent TMJ dislocation. *Br J Oral Maxillofac Surg* 2009;47(4):323-4.
- Shimizu M, Kurita K, Matsuura H, Ishimaru JI, Goss AN. The role of muscle grafts in temporomandibular joint ankylosis: short-term experimental study in sheep. *Int J Oral Maxillofac Surg* 2006;35(September (9)): 842-9.
- Long X, Goss AN. A sheep model of intra-capsular condylar fracture. *J Oral Maxillofac Surg* 2007;65(June (6)):1102-8.
- Takaishi M, Kurita K, Matsuura H, Goss AN. Effect of auricular cartilage graft in the surgical treatment of temporomandibular joint ankylosis: an animal study using sheep. *J Oral Maxillofac Surg* 2007;65(February (2)):198-204.
- Candrl C, Yu'ce S, Yldrm S, Sert H. Histopathologic evaluation of autologous blood injection to the temporomandibular joint. *Craniofac Surg* 2011;22(November (6)):2202-4.
- Bermejo A, Gonzalez O, Gonzalez JM. The pig as an animal-model for experimentation on the temporomandibular articular complex. *Oral Surg Oral Med Oral Pathol Oral Radiol Endod* 1993;75:18-23.
- Detamore MS, Hegde JN, Wagle RR, Almarza AJ, Montufar-Solis D, Duke PJ, et al. Cell type and distribution in the porcine temporomandibular joint disc. *J Oral Maxillofac Surg* 2006;64:243-8.
- Helland MM. Anatomy and function of the temporomandibular joint. *J Orthop Sports Phys Ther* 1980;1:145-52.
- Schulz S. Evaluation of periarticular autotransfusion for therapy of recurrent dislocations of the temporomandibular joint. *Dtsch Stomatol* 1973;23:94-8.
- Campos PS, Macedo Sobrinho JB, Crusoe - Rebello IM, Pena N, Dantas JA, Mariz AC, et al. Temporomandibular joint disc adhesion without mouth opening limitation. *J Oral Maxillofac Surg* 2008;66:551-4.
- Hase M. Adhesions in the temporomandibular joint: formation and significance. *Aust Dent J* 2002;47:163-9.
- Kim YK, Im JH, Chung H, Yun PY. Clinical application of ultrathin arthroscopy in the temporomandibular joint for treatment of closed lock patients. *J Oral Maxillofac Surg* 2009; 67:1039-45.
- Zhang S, Liu X, Yang C, Cai X, Chen M, Haddad MS, et al. Intra-articular adhesions of the temporomandibular joint: relation between arthroscopic findings and clinical symptoms. *BMC Musculoskeletal Disorders* 2009;10:70.
- Hooiveld M, Roosendaal G, Wenting M, van den Berg M, Bijlsma J, Lafeber F. Short-term exposure of cartilage to blood results in chondrocyte apoptosis. *Am J Pathol* 2003; 162:943-51.
- Hooiveld MJ, Roosendaal G, Jacobs KM, Vianen ME, van den Berg HM, Bijlsma JW, et al. Initiation of degenerative joint damage by experimental bleeding combined with loading of the joint: a possible mechanism of hemophilic arthropathy. *Arthritis Rheum* 2004;50:2024-31.
- Roosendaal G, TeKoppele JM, Vianen ME, van den Berg HM, Lafeber FP, Bijlsma JW. Blood-induced joint damage: a canine in vivo study. *Arthritis Rheum* 1999;42: 1033-9.
- Hooiveld M, Roosendaal G, Vianen M, van den Berg M, Bijlsma J, Lafeber F. Blood-Induced joint damage: long term effects in vitro and in vivo. *J Rheumatol* 2003;30:339-44.
- Dijkgraaf LC, Zardeneta G, Cordewener FW, Liem RS, Schmitz JP, de Bont LG, et al. Crosslinking of fibrinogen and fibronectin by free radicals: a possible initial step in adhesion formation in osteoarthritis of the temporomandibular joint. *J Oral Maxillofac Surg* 2003;61:101-11.
- Safran MR, Johnston-Jones K, Kabo JM, Meals RA. The effect of experimental hemarthrosis on joint stiffness and synovial histology in a rabbit model. *Clin Orthop* 1994;303:280-8.
- Tan AH, Mitra AK, Chang PC, Tay BK, Nag HL, Sim CS. Assessment of blood-induced cartilage damage in rabbit knees using scanning electron microscopy. *J Orthop Surg (Hong Kong)* 2004;12:199-204.

POSSIBLE ROLE OF NANO-SIZED PARTICLES IN CHRONIC TONSILLITIS AND TONSILLAR CARCINOMA: A PILOT STUDY

Karol Zeleník^{1,2}, Jana Kukutschová³, Jana Dvořáčková², Hana Bielníková⁴, Pavlína Peikertová³, Lenka Čabalová¹, Pavel Komínek¹

¹ Department of Otolaryngology, University Hospital Ostrava, Czech Republic

² Faculty of Medicine, University of Ostrava, Czech Republic

³ Nanotechnology Centre, Technical University of Ostrava, Czech Republic

⁴ Department of Pathology, University Hospital Ostrava, Czech Republic

Originally published in *European archives of oto-rhino-laryngology and Head & Neck* 2013; 270: 705-709

Consent to the publication of 8th April 2014 (No. 3364151139022)

ABSTRACT

This study aimed to evaluate the palatine tonsils of patients with chronic tonsillitis and spinocellular carcinoma to determine the presence of nano-sized particles. Tonsil samples from adult patients with chronic tonsillitis and spinocellular carcinoma of the palatine tonsil were dried and analyzed using a scanning electron microscope with the X-ray microprobe of an energy-dispersive spectroscope. Demographic data and smoking histories were obtained. The principal metals found in almost all tissues analyzed were iron, chromium, nickel, aluminum, zinc, and copper. No significant difference in elemental composition was found between the group of patients with chronic tonsillitis and the group with spinocellular carcinoma of the palatine tonsil. Likewise, no significant difference was found between the group of smokers and the group of nonsmokers. The presence of various micro- and nano-sized metallic particles in human tonsils was confirmed. These particles may potentially cause an inflammatory response as well as neoplastic changes in human palatine tonsils similar to those occurring in the lungs. Further and more detailed studies addressing this issue, including studies designed to determine the chemical form of the metals detected, studies devoted to quantitative analysis, biokinetics, and to the degradation and elimination of nanoparticles are needed for a more detailed prediction of the relation between the diagnosis and the presence of specific metal nanoparticles in tonsillar tissue.

Keywords:

tonsillar cancer; chronic tonsillitis; nanoparticles; nanotoxicology; scanning electron microscope; air pollution

INTRODUCTION

Nanosized particles (NPs), having submicron sizes ranging from 10 nm to several hundred nanometers, have been extensively studied during the last few years. This research is encompassed within 2 main fields - nanotechnology and nanotoxicology. Nanotechnology is aimed at the manipulation and utili-

zation of new nanomaterials and products with a vast range of applications such as drug delivery, antibacterial agents, smart materials, etc [1]. Nanotechnology raises many of the same issues raised by the introduction of any new technology, including concerns about the toxicity and potential environmental and health impact of nanomaterials. Hence nanotoxicology, the new branch of toxicology which evaluates the potential health risks associated with exposure to NPs produced, for example, by fossil fuel combustion, smoking, welding and road traffic, has evolved simultaneously [1-3].

There are three common avenues of ingress of NPs into the human body: inhalation, ingestion and skin penetration. The inhalation of NPs, which is considered to be the principal avenue of ingress of NPs into the human body, may lead to deposition in the respiratory tract and lungs [4]. Experimental studies in rats have shown that intratracheal instillation of some NPs can cause pulmonary inflammation, tissue damage, and lung tumors, in contrast to the same materials having an identical chemical composition but in the micrometric size range, which were found to be inert in terms of inflammation and cancerogenesis initiation. These NPs are known to be harmful due to their higher reactivity, given their greater surface area compared to micro-sized particles [5]. Besides, NPs may become "blood-borne" and may be translocated into other organs [1].

Since the palatine tonsils are among the first organs which come in contact with inhaled particles of all sizes below 100 μm in diameter able to enter the respiratory tract (including NPs), it is likely that NPs may enter into the tonsillar tissue and may eventually cause an inflammatory response as well as neoplastic changes. Furthermore, the unique lymphoepithelial structure of the human tonsillar tissue facilitates rapid spread of the NPs into the circulatory and lymphatic systems. Studies dealing with the potential effect of NPs on tonsillar tissue are still lacking. The aim of the present study is to evaluate human palatine tonsils from patients with chronic tonsillitis and spinocellular carcinoma of the

palatine tonsil in order to determine the presence of micro- and nano-sized metallic particles.

MATERIAL AND METHODS

The study was approved by the Institutional Ethics Committee and performed in accordance with the Declaration of Helsinki, observing good clinical practice protocols and all applicable regulatory requirements. Written informed consent was obtained from all participants before initiation of any procedure.

Group selection:

Patients with chronic tonsillitis and patients with spinocellular carcinoma of the palatine tonsil were enrolled in the study. Demographic data, occupational histories and lifetime smoking histories were obtained.

Biopsy and sample preparation:

Fresh tonsil samples were obtained by “cold technique” tonsillectomy. In order to prevent sample contamination from surgical instruments, the central part of each tonsil was chosen for further analysis, and ceramic knives were used for sample preparation. Samples of approximately 1 cm were treated with 4% formalin solution for 24 hours. These samples were then dried in a thermostat at a temperature of 58 °C for 48 hours.

Microscopic analysis:

Dehydrated tissue portions approximately 50x50 mm in size taken from the central part of the samples were placed on target with carbon tape, double coated with gold-palladium (to increase the conductivity of the surface) and analyzed using a scanning

Age	Occupation	Smoking	Metallic particles detected
Group I - Patients with chronic tonsillitis			
49	bus driver	yes	Fe-Cr, Fe-Cr-Ni
41	bus driver	yes	Fe, Fe-Cr, Cu, Ti, Zn, Al
37	locksmith	yes	Fe-Cr
30	policeman	no	Fe, Fe- Cr, Fe-Cr-Ti, Fe-Cr-Ni, Cu, Zn
62	heat power plant worker	yes	Fe, Fe-Ni, Al
45	secretary	no	Cu, Al
42	secretary	no	Fe, Fe-Cr, Fe-Cr-Ni
20	student	yes	Fe, Cu
26	policeman	no	Fe, Zr, Zn
35	locksmith	yes	Zn
35	developer	yes	Fe, Fe-Cr
34	unemployed	yes	Fe
25	metal machinist	no	Fe-Cr-Ni
34	automotive engineer	no	Fe-Cr-Ni, apatite, Zr
45	metal machinist	no	Fe, Al, Cu, Mn
21	student	yes	Fe-Cr-Ni, Cu, Al
Group II - Patients with spinocellular carcinoma of the palatal tonsil			
55	car driver, miner	yes	Fe, Al, Ni, Co, apatite
69	car mechanic	yes	Fe, Al, Zn
47	driver	yes	Fe-Cr-Ni, Fe-Cr, Al, Zr
46	welder	yes	Fe-Cr-Ni, Al
55	locksmith	yes	Fe-Cr-Ni, Al
49	cabinetmaker	no	Fe-Cr-Ni, Al, Cu, apatite
65	senior	yes	Fe-Cr-Ni, Fe-Cr, Al
67	locksmith	no	Fe- Cr- Ni, W
61	mechanic	yes	Fe, Fe-Cr-Ni, Al, Co
69	builder	yes	Fe, Al, Cu
50	coal miner	yes	Fe-Cr-Ni, Cu, apatite
69	driver, car repair	yes	Fe-Cr-Ni, Sn, apatite
63	welder	yes	Fe-Cr-Ni, Al
61	coal miner	no	Fe-Cr-Ni, Al, apatite
62	locksmith	yes	Fe, Ti, Zn

Table 1 Summary of age, occupation, smoking history, and metallic particles detected in the two groups studied

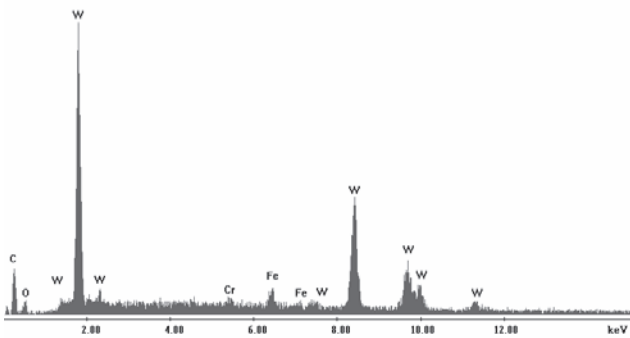


Figure 1: Energy dispersion spectroscopy pattern of a particle analyzed

electron microscope (SEM Philips XL 30 operating at 30 keV) with the X-ray microprobe of an Energy Dispersive Spectroscopy (EDS) in order to identify their elemental composition. Samples were evaluated in the BSE (back-scattered electrons) mode allowing for the detection of changes in elemental composition, e.g. metallic particles scattering electrons appear as lighting spots compared to the tissue absorbing electrons, which manifest as dark spots in the BSE mode.

Statistical analysis:

The presence of metallic particles in the groups studied was compared using the chi-square test. The computer software used for statistical analysis was SPSS (version 17.0, SPSS Inc., Chicago, Illinois, USA). A p-value of $\alpha = 0.05$ was considered statistically significant.

RESULTS

A total of 31 samples of human tonsils were studied between January 2009 and July 2010, 16 from patients with chronic tonsillitis (group I) and 15 from patients with spinocellular carcinoma of the palatine tonsil (group II). The presence of various micro- and nano-structured metallic agglomerates in both groups was confirmed (Table 1). The principal metals found in almost all tissues analyzed were iron, chromium, nickel, aluminum, zinc and copper. However, the peaks of metals detected in the EDS pattern reflect relative amounts and elemental chemical forms only (Fig. 1). No significant differences in elemental composition were found between groups I and II. Likewise, no significant differences were found between the groups of smokers and nonsmokers. In the case of patients exposed to emissions from industrial processes (miners, welders, locksmiths) metals typically associated with the process in question (cobalt and tungsten) were found in the samples analyzed (Fig. 2).

DISCUSSION

Humans are exposed to airborne NPs in everyday life. These particles are produced unintentionally by various anthropogenic activities (e.g. pyrometallurgy, road traffic, smoking and cooking) [6,7]. Development of nanotechnology may increase the risk of exposure to intentionally produced (engineered) NPs used in many products, e.g. pigments, sunscreens, cosmetics, detergents, photocopier toners, electronics, fabrics, clothes, and plastics among others, as well as in manufacturing. Despite their many benefits, NPs are believed to represent potential risks to the environment and to human health [1]. Donaldson et. al suggest that NPs behave quite differently from their larger counterparts and may exhibit unique biological behavior, even when their physical and chemical properties remain identical to those observed in larger particles [2]. Perhaps the most striking example is the ability of NPs to cross barriers that are impervious to larger particles. Research showing the potential for NPs to move up the olfactory nerves to the brain in rodents offers a prime example of this size-unique behavior [8,9]. NPs may be transported via this route directly to the central nervous system after inhalation.

The basic physicochemical and toxicokinetic principles learned from the existing studies are relevant to understanding the potential toxicity of NPs. It is known from studies in animals that NPs due to their small size can be easily translocated within the body, can cross cell membranes and can interact with sub-cellular structures such as mitochondria, where they have been shown to cause oxidative damage and to impair the functioning of cells in cultures [10,11]. NPs have also been shown to localize in or near cell organelles, including mitochondria and nuclei, and have been associated with oxidative stress and cell damage [10,12]. Animal studies have shown that NPs are more biologically active (with greater toxicity) due to their greater surface area per mass compared with larger-sized particles having the same chemist-

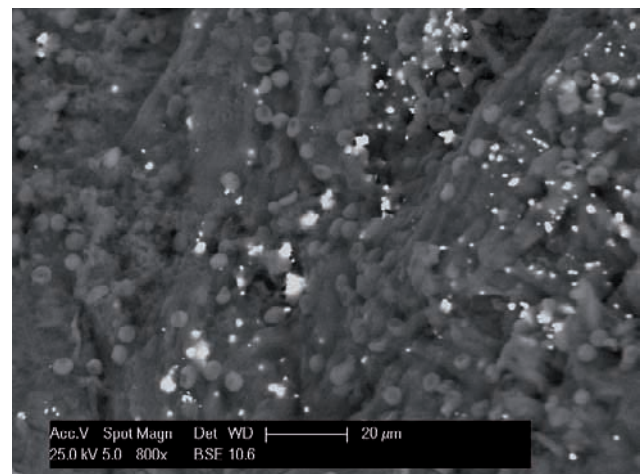


Figure 2: Tungsten particles (*brights spots*) detected in a tonsillar tissue of a welder by scanning electron microscope

ry [5]. More recent studies indicate the possible genotoxicity and cancerogenesis of NPs, as they have been found to cause genotoxic responses such as chromosomal fragmentation, DNA strand breaks, point mutations, oxidative DNA adducts and alterations in gene expression profiles [13,14].

The respiratory tract is by far the most widely studied system in nanotoxicology research. The reason is that the respiratory tract is the major route for unwanted exposure to NPs. Epidemiologic studies have pointed mostly to the adverse effects associated with unintentional anthropogenic materials. Air pollutant NPs have been correlated with several respiratory diseases, such as asthma, chronic obstructive pulmonary disease and cardiovascular disease [15,16]. Welding fumes are the cause of metal fume fever, increased susceptibility to infection, decreased lung function, and pneumonia, and they may be carcinogenic [17]. A specific form of SiO₂, alpha-quartz, is associated with silicosis, emphysema, bronchitis, and an increased risk of lung cancer [18]. Since palatine tonsils are among the first organs to come in contact with inhaled NPs, it is likely that NPs may enter into this tissue and potentially cause an inflammatory response as well as neoplastic changes similar to those that occur in the lungs. Furthermore, the unique lymphoepithelial structure of the human tonsillar tissue facilitates the rapid spread of the NPs through the circulatory system.

We investigated the presence of NPs in human tonsils in two different groups of patients. The presence of various NPs was confirmed in both groups studied (chronic tonsillitis as well as tonsillar carcinoma patients) (Table 1). The particles detected may originate as by-products of many anthropogenic sources, for example cigarette smoke, and may contain metals such as Al, Cd, Ni, Pb, Cu in the form of very fine particles [19]. Other metals (Fe, Cu, Zn, Sn, Ba, Sb and Ti) in the form of NPs are emitted during combustion of fossil fuels, and in the friction produced when automotive brakes and tires make contact with road surfaces [20-22]. It must be mentioned that patients included in the study live in a conurbation with a heavy steel industry and are exposed to the resultant air pollution (including NPs), mostly from pyrometallurgy. Also, welders may be exposed to Fe, Cr, Mn, Ni, Cu, Zn and W, which are present in welding fumes [23]. Figures 1 and 2 show the presence of tungsten particles detected in the tonsillar tissue of a welder. Tungsten welding is carried out at temperatures around 6 000 °C and the boiling point of tungsten is around 5 500 °C [17]. Given these facts, we may assume that NPs originate from tungsten fumes by condensation. Coal dust could contain trace elements such as Ba, Be, Cd, Co, Mo, Nb, Sb, V and W [24].

Based on what we know about NPs, we can hypothesize their possible role in the pathogenesis of both chronic inflammatory as well as carcinomatous

changes of the tonsillar tissue. The fact that we did not find differences between the groups studied does not affect the likelihood that NPs play a role in the pathogenesis of these diseases. The limitation of our study is that the amounts of metals detected by EDS in our samples cannot be quantitatively compared. But this is a pilot study dealing with the presence of micro- and nano-sized metallic particles in human tonsillar tissue and the main aim of the study was to confirm the presence of these particles in human tonsillar tissue.

Interestingly, Fe-Cr-Ni clusters were identified in most samples. Theoretically, these elements may be released from cutting tools during "cold" tonsillectomy. To minimize the risk of contamination from this source, the central part of the tonsils was chosen for further analysis and ceramic knives were used for further preparation of samples. Considering the observed morphology of the Fe-Cr-Ni particles, characterized by sharp edges, we can assume that they are most likely caused by the mechanical wear of stainless steel tools.

CONCLUSIONS

The principal metals found in almost all tissues analyzed were iron, chromium, nickel, aluminum, zinc and copper. No significant differences in elemental composition were found between the groups studied. More experimental data are needed to determine the health risks associated with exposure to metallic nano- and micro-sized particles. The results of existing studies in animals and humans only serve as a basis for preliminary estimates of the possible adverse health effects associated with inhalation exposure to NPs. Hence we may contend that there is still a long way to go before we are able to assess or predict the health impact of NPs with confidence. Further and more detailed studies addressing this issue, including studies designed to determine the chemical form of the metals detected, studies devoted to quantitative analysis, biokinetics, and to the degradation and elimination of NPs are needed for a more detailed prediction of the relation between the presence of a given metal in tonsillar tissue and the diagnosis.

Acknowledgement

Acknowledgments The authors would like to thank MSc. Hana Tomášková, Ph. D. from the Institute of Epidemiology and Public Health, Medical Faculty of the Ostrava University, Czech Republic, for her help with statistical analysis. The research was supported by the Czech Ministry of Education (projects number MSM 6198910016 and CZ.1.05/2.1.00/01.0040).

Conflict of Interest

The authors declare that they have no conflict of interest.

References

1. Monteiro-Riviere NA, Tran CL. (2007) *Nanotoxicology: characterization, dosing and health effects*, Informa Healthcare, Inc; New York
2. Donaldson K, Stone V, Tran CL, et al. (2004) *Nanotoxicology. Occup Environ Med.* 61:727-728
3. Oberdörster G, Oberdörster E, Oberdörster J. (2005) *Nanotoxicology: an emerging discipline evolving from studies of ultrafine particles. Environ Health Perspect.* 13:823-40
4. Singh S, Nalwa HS. (2007) *Nanotechnology and health safety - toxicity and risk assessments of nanostructured materials on human health. Journal of Nanoscience and Nanotechnology* 7:3048-3070
5. HSE (2004). *Health effects of particles produced for nanotechnologies. EH75/6 HSE Books* 2004.
6. Kukutschová J, Roubíček V, Mašláň M et al. (2010) *Wear performance and wear debris of semimetallic automotive brake materials. Wear.* 268:86-93
7. Buonanno G, Morawska L, Stanule L. (2009) *Particle emission factors during cooking activities. Atmospheric Environment.* 43:3235-3242
8. Oberdörster G, Sharp Z, Atudorei V, et al. (2004) *Translocation of inhaled ultrafine particles to the brain. Inhal Toxicol.* 16:437-45
9. Elder A, Gelein R, Silva V, et al. (2006) *Translocation of inhaled ultrafine manganese oxide particles to the central nervous system. Environ Health Perspect.* 114:1172-8.
10. Geiser M, Rothen-Rutishauser B, Kapp N, et al. (2005) *Ultrafine particles cross cellular membranes by non-phagocytic mechanisms in lungs and in cultured cells. Environ Health Perspect.* 113:1555-1560.
11. Geiser H, Kreyling WG. (2010) *Deposition and biokinetics of inhaled nanoparticles. Particle and Fibre Toxicology.* 7:2 doi:10.1186/1743-8977-7-2
12. Li N, Sioutas C, Cho A, et al. (2003) *Ultrafine particulate pollutants induce oxidative stress and mitochondrial damage. Environ Health Perspect.* 111:455-60
13. Singh N, Manshian B, Jenkins GJS, et al. (2009) *NanoGenotoxicology: The DNA damaging potential of engineered nanomaterials. Biomaterials.* 30:3891-3914
14. Donaldson K, Poland CA, Schins RP. (2010) *Possible genotoxic mechanisms of nanoparticles: criteria for improved test strategies. Nanotoxicology* 4:414-420
15. Oberdörster G. (2001) *Pulmonary effects of inhaled ultrafine particles. Int Arch Occup Environ Health* 74:1-8.
16. Delfino RJ, Sioutas C, Malik S. (2005) *Potential role of ultrafine particles in associations between airborne particle mass and cardiovascular health. Environ Health Perspect.* 113:934-46
17. Antonini JM, Lewis AB, Roberts JR, et al. (2003) *Pulmonary effects of welding fumes: review of worker and experimental animal studies. Am J Ind Med.* 43:350-60
18. Shi X, Castranova V, Halliwell B, et al. (1998) *Reactive oxygen species and silica-induced carcinogenesis. J Toxicol Environ Health B Crit Rev.* 1:181-97
19. Kazi TG, Jalbani N, Arain MB, et al. (2009) *Toxic metals distribution in different components of Pakistani and imported cigarettes by electrothermal atomic absorption spectrometer. Journal of Hazardous Materials* 163:302-307
20. Kukutschova J, Roubíček V, Malachova K, et al. (2009) *Wear mechanism in automotive brake materials, wear debris and its potential environmental impact. Wear.* 267:807-817
21. Iijima A, Sato K, Yano K, et al. (2007) *Particle size and composition distribution analysis of automotive brake abrasion dusts for the evaluation of antimony sources of airborne particulate matter. Atmospheric Environment.* 41:4908-4919
22. Cunnell TB, Duckenfield KU, Landa ER, et al. (2004) *Tire-wear particles as a source of zinc to the environment. Environ Sci Technol.* 38:4206-4214
23. Antonini JM, Afshari AA, Stone S, et al. (2006) *Design, construction, and characterization of a novel robotic welding fume generator and inhalation exposure system for laboratory animals. J Occup Environ Hyg.* 3:194-203
24. Gibbs BM, Thompson D, Argent BB. (2008) *Mobilisation of trace elements from as-supplied and additionally cleaned coal: Predictions for Ba, Be, Cd, Co, Mo, Nb, Sb, V and W. Fuel.* 87:1217-1229

TAKAYASU ARTERITIS IN A 10-MONTH-OLD BOY

Tomáš Pískovský¹, Michal Hladík¹, Lenka Kosňovská¹, Jana Čermáková¹, and Katarína Miklošová²

¹ Department of Paediatric Medicine, Medical Faculty of the Ostrava University and University Hospital Ostrava, Czech Republic

² Radiodiagnostic Institute, Medical Faculty of the Ostrava University and University Hospital Ostrava, Czech Republic

Originally published in *VASA* 2013; 42: 134-138

Consent to the publication of 3rd April 2014

KEY MESSAGE

Takayasu arteritis may involve even a very young child. An aggressive immunosuppression is warranted.

INTRODUCTION

Takayasu arteritis (TA) is a chronic inflammatory disease of the aorta and its main branches. TA is characterized by vasculitis of large vessels, and most frequently affects women in the second and third decades of life. It is extremely rare in children [6]. A French study performed in 2007 describes a group of four patients with TA aged 8 - 15 years [1]; however, the condition has also been described in children at several months of age [10]. The youngest child was 6 months old at the time of diagnosis [16]. Initial manifestations of TA are unspecific, and include fever, weight loss, and fatigue. Hence, correct diagnosis of TA may be delayed for several months, or even years [6, 1, 10].

CASE REPORT

In 2010, we examined a 10-month old boy for elevated levels of C-reactive protein (CRP) of unknown aetiology. From the family history: the mother was observed for gestational diabetes in pregnancy; the father and a sister (6 years old) were healthy. There were no autoimmune diseases present in the family. Personal history: the patient was born prematurely during the 35th gestational week, head-first, weight 2650 g, length 49 cm, and was referred for 2 days of phototherapy because of new-born jaundice. There were no other significant oddities. In May 2010, when the boy was 9 months old, he suffered from fever of up to 39°C. The only other clinical manifestation was rhinitis. The laboratory examination showed a haemoglobin level of 85 g/l and a CRP level of 207 mg/l. The general practitioner started treatment with antipyretics, antibiotics (administered orally), and oral Aktiferrin gtt to treat the anaemia. The fever subsided after two days of antibiotics. In July 2010, the general practitioner noticed that the patient was very pale. His haemoglobin level was down to 65 g/l, thrombocytes were 91×10^9 ml/l, and CRP was 180 mg/l. The patient was hospitalized

in a catchment area hospital presenting only with rhinitis and mild conjunctivitis. He had been doing well until that time and had been eating normally, bowel movements and urination were normal. He had significant anaemia, with a haemoglobin (Hb) level of 62 g/l and a thrombocyte count of 1.077×10^{12} cells/ml. The CPR level was 214 mg/l, with a normal procalcitonin level of 0.2 µg/l. Cultures, immunology, paraclinical and imaging tests did not reveal any cause for anaemia or the changes of laboratory values. The patient was admitted to our department at the end of July 2010. He was pale on admission, afebrile, and normotensive. Laboratory tests confirmed the anaemia, with Hb 83 g/l and thrombocytes 6.31×10^{11} cells/ml. Anaemia was hypochromic and microcytic with a Fe level of 1.8 µmol/l, the mean volume of RBCs 62 fl, transferrin 1,85 g/l and ferritin 267 ng/ml. After exclusion of malabsorption, we believed that this was a case of anemia of chronic disease, which is characterized by the reduced level of Fe-S, normal or slightly reduced level of transferrin and normal or slightly elevated levels of ferritin. The CPR level was 210 mg/l, and procalcitonin only slightly elevated (0.34 µg/l). The basic biochemistry examinations (ionogram, alanine transaminase, aspartate aminotransferase, bilirubin, glycemia, cholesterol, triglycerides, albumin, amylase, ammonia) and the leukocyte count were normal. We performed additional cultural examinations (haemoculture, nose, throat, stool, urine), serology (panel of herpetic viruses, campylobacter, helicobacter, Borrelia, chlamydia, coxsackia, respiratory viruses, mycoplasma, Yersinia, parvoviruses, aspergilla, and Candida antigen), and immunological tests (ANA, ENA, IBD, RF, EMA, tTG, ANCA, ASLO, circulating immunocomplexes, C3, C4, total complement), with the discovery of cytomegalovirus positivity in IgM and IgG classes and paroviruses in the IgM class. Except for fever, the child showed no other clinical signs of these infections. Both infections may have contributed to anemia. The test of immunoglobulins revealed an elevated level of gamma globulins of the IgM class at 1.75 g/l, IgG at 15.6 g/l, and IgE at 187 g/l, as well as circulating

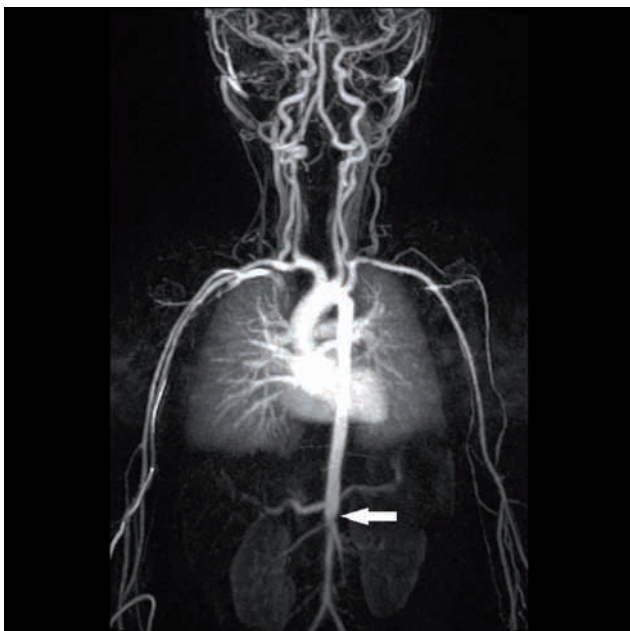


Figure 1: The first MRA examination revealed especially the narrowing of the descending aorta. Maximal stenosis is located above the branching of the renal arteries (arrow).

immunocomplexes of 110 arbitrary units. Tests for basic tumor markers (NSE, hCG, AFP) and hereditary metabolic disorders were negative. Consultative examinations performed included otorhinolaryngological, neurological, and ophthalmological exams, including the slit-lamp test; however, these tests showed no deviations from normal values. Although a bone marrow test revealed sideropenia, there were no pathological findings. The patient was also referred for cerebral ultrasound, abdominal ultrasound, and an X-ray of the chest and heart - all with normal findings. An echocardiographic exam of the heart revealed minor aortic regurgitation. During the one-month hospitalization period, repeated febrile peaks were noted. CRP oscillated between 135 and 210 mg/l, while procalcitonin remained low at all times. It was difficult to measure blood pressure, due to non-cooperation of the child; values measured in arms and legs at rest were within the normal range. Pulses was palpable at both hands and feet. When we considered the possibility of a malignant tumour as part of the differential diagnosis, a positron emission tomography/ computed tomography (PET-CT) exam was performed. The PET-CT yielded a surprising finding that led us to consider arteriitis of the aortic arch and the branching arteries, with an enlargement and blurring of their walls. We subsequently used Magnevist to perform contrast-enhanced magnetic resonance angiography (MRA), which confirmed inflammatory changes in the walls of the ascending aorta, the aortic arch, and the descending aorta, with narrowing of the descending aorta and maximum stenosis above the branching of the renal arteries (Fig. 1). The impairment of the aortic wall was circular (Fig. 2). Doppler ultrasound examination of the carotid arteries revealed a slightly elevated

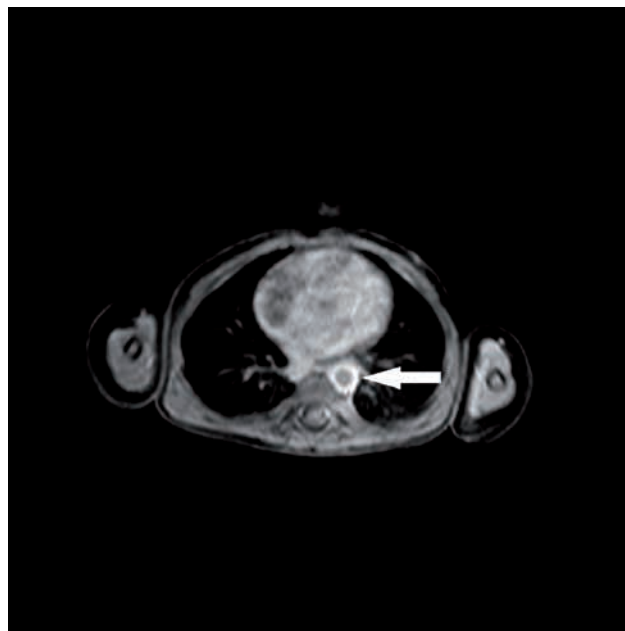


Figure 2: An MRA image (transverse section) depicting the concentric thickening of the aortic wall.

resistance. We established the diagnosis of TA and initiated treatment with pulsed intravenous (i.v.) doses of methylprednisolone 30 mg/kg, administered once weekly for four doses, and subsequently once every two weeks. At the same time, we administered oral methylprednisolone at a dose of 0.8 mg/kg/day. During the treatment course, CRP dropped temporarily; we therefore initiated cyclophosphamide therapy at a dose of 700 mg/m² i. v. administered once monthly. We continued the pulsed i.v. methylprednisolone at a dose of 20 mg/kg once monthly and the daily administration of oral methylprednisolone. A control MRA that was performed after two months of therapy demonstrated partial regression of the findings (Fig. 3). The patient remains normotensive, with palpable symmetric pulsations, without audible murmurs over the chest. CRP has dropped to 15 - 30 mg/l. We continued triple combination therapy for 7 months and then performed a control MRA that demonstrated significant regression of the aortic stenosis; however, a minor stenosis of the right renal artery appeared (Fig. 4). After the examination, the patient was transferred to subcutaneous methotrexate at a dose of 15 mg/m² administered once weekly; he also received continuous oral methylprednisolone therapy. We administered additional pulsed doses of cyclophosphamide at 3 and 6 months after the initial cyclophosphamide series.

The patient is being followed up on a long-term basis by a cardiologist, a rheumatologist, and a nephrologist. During the subsequent course of treatment, we discovered hypertension on 24-hour blood pressure monitoring, together with hypertrophy of the left ventricle on echocardiographic examination. The patient is presently being treated with an angiotensin-converting-enzyme inhibitor and beta-blockers.

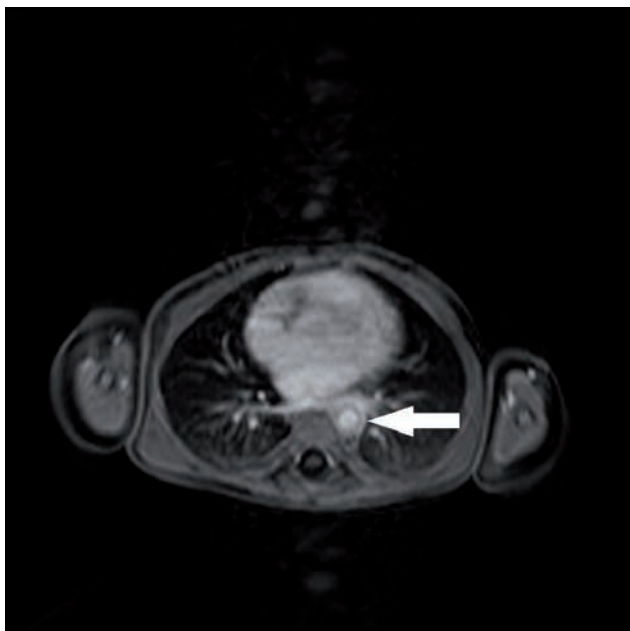


Figure 3: An MRA image (transverse section) depicting partial regression of the aortic wall thickening after 2 months of treatment.

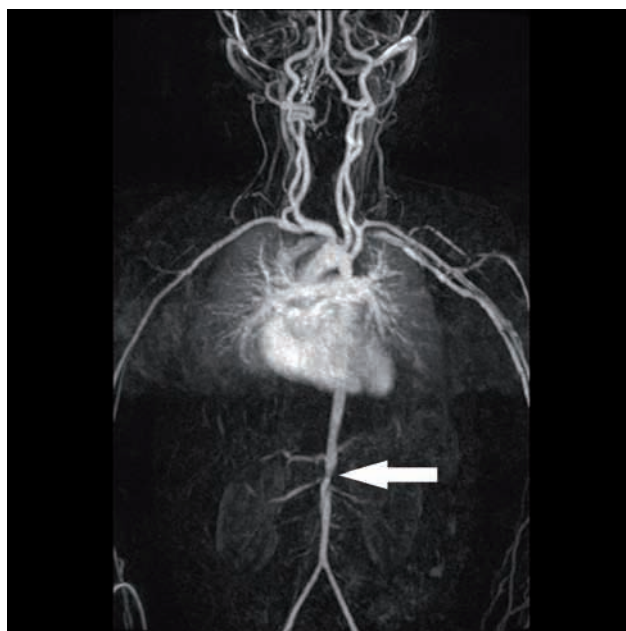


Figure 4: MRA imaging depicts partial stenosis of the descending aorta after 7 months of treatment.

DISCUSSION

The worldwide incidence of TA is estimated at 2 - 3 cases per 1 million people, with a prevalence of women 9:1. Although TA occurs more frequently in the Asian population, it has been reported world wide in other populations [9]. Because initial symptoms are of unspecific nature, it may take a long time to reach the correct diagnosis. This situation is highly problematic, especially in small children [1]. Only 35 % of paediatric patients survive for 5 years after diagnosis [12]. The most common causes of death are rupture of the aorta, cerebrovascular stroke, cardiac failure, peritonitis, and ventricular fibrillation [6]. Due to the rarity of TA and its diagnostic difficulties, it is not surprising that we arrived at a correct diagnosis only as a result of cardiac findings. In autopsies of children with TA who died because of acute rupture of the aorta, multiple aortal dissections are commonly described [16]. The aetiology of TA remains unknown. The presence of hypergammaglobulinemia, circulating immunocomplexes, and circulating antibodies against endothelial cells of the aorta and large arteries, as well as a favourable response to immunosuppressive therapy, suggest significant autoimmunity. Antibodies against aortic endothelial cells play the most important role [11]. Activation of CD4+ T-lymphocytes with antigen deposits in the vascular wall is assumed. The activation of CD4+ cells leads to cytokine release and the chemotaxis of monocytes. These monocytes subsequently change into microphages, which are responsible for endothelial damage. The process results in the formation of granulomas in vascular walls. In some cases, TA occurs together with rheumatoid arthritis, unspecific inflammation of the intestines, systemic lupus, sarcoidosis, or amyloidosis. Although some

studies implicate bacterial and viral infections as the cause, specific infectious agents have not been identified [1, 15]. TA classification arises from the presence of a mandatory primary criterion, and one of five secondary criteria. The mandatory criterion typically manifests as damage to the aorta, its main branches, or pulmonary arteries. Secondary criteria include pulse deficit, claudication, discrepancies of blood pressure of the extremities, presence of murmur, hypertension, and elevation of acute-phase reactants [14].

Concerning differential diagnosis, it is necessary to bear in mind the possibility of malignant disease (acute lymphoblastic leukaemia, Hodgkin's lymphoma), systemic disease (polyarteritis nodosa, Kawasaki disease, rheumatic fever, juvenile idiopathic arthritis), chronic infections (syphilis, tuberculosis, HIV infection, leprosy), congenital defects (coarctation of the aorta, middle aortic syndrome), hereditary disorders (Marfan syndrome, neurofibromatosis, Ehlers-Danlos syndrome), and fibromuscular dysplasia [4]. TA does not have any specific markers. Half of the patients present with normochromic normocytic anaemia, leukocytosis, and thrombocytosis. The acute-phase proteins are usually elevated, and antibodies against endothelial cells may also be present. ANCA are usually negative. We frequently observe elevated levels of all classes of immunoglobulins [9]. Owing to aortic insufficiency, TA may lead to myocarditis and/or hypertension and ultimately to congestive heart failure. The aortal impairment may also give rise to aneurysms, rupture, or thrombosis. An ischemic stroke may also occur, together with myocardial infarction. The complications caused by long-lasting immunosuppressive treatment may also be significant. It is possible to use a number of

imaging methods to diagnose TA. In the light of new developments in radiology techniques, conventional angiography should no longer be considered to be a first choice diagnostic tool in TA. The gold standard is MRA, which may also be used for repeated examinations to monitor the course of the disease. Another suitable method with good results is PET, which led to further diagnostic findings in our patient. The options of high-resolution ultrasound techniques have also improved diagnostic capacity. Duplex sonography might help to establish early disease of TA in a pre-stenotic phase of the extracranial vessels. Alternations in flow velocity can be determined. [3,5]. Therapy aims to suppress the inflammatory process in the arterial walls and to prevent the development of complications. Drug treatment is based on the supposed immunological cause of the disease. A surgical approach may present an alternative in the most serious cases only [16]. The basis of TA pharmacotherapy is immunosuppression. Therapy is usually initiated with the administration of prednisone at a dose of 1 - 2 mg/ kg/day [2]. This dose should be administered for the entire period of disease activity, and should continue for one year after clinical remission is confirmed. Approximately 60 % of patients react to the treatment; however, relapse of the disease is frequently observed in the remaining 40 % patients. Patients that do not respond to prednisone therapy may react well to methylprednisolone at a dose of 30 mg/kg administered by infusion once weekly. Long-term basal treatment arises from the combination of corticoids and other immunosuppressive treatment. This type of treatment includes subcutaneous methotrexate (5 - 15 mg/m² once weekly), or intravenous cyclophosphamide (500 - 1000 mg/m² once monthly). Mycophenolate mofetil can be used in corticoid-resistant patients [6]. We have also gained experience with biologicals. Infliximab and etanercept reportedly induce clinical remission in corticoid-dependent patients [2, 8]. The results of a clinical trial involving six children were published in 2006 (four girls and two boys aged 12 to 17 years at study initiation; the study lasted for 7 years). The children were administered cyclophosphamide induction and corticosteroids followed by methotrexate. The study results suggest that this treatment appears to be effective and safe for paediatric patients [13]. We also observed a favourable outcome of this treatment algorithm in our patient. Long-term solution of stenoses and fibrotic changes may be achieved with surgical therapy, which may include percutaneous balloon angioplasty or insertion of an endovascular stent. These interventions cannot be excluded for our patient in the future owing to the lasting suprarenal aortic stenosis.

CONCLUSIONS

TA is a chronic and relapsing disease. With corticoid treatment, more than one-half of patients may achieve remission. However, relapses are also frequent during this stage, and the prognosis is uncertain.

CONFLICTS OF INTEREST

There are no conflicts of interest existing. Key words Takayasu arteritis, positron emission tomography, magnetic resonance imaging, immunosuppression

REFERENCES

- 1 Al Abrawi S, Fouillet-Desjonqueres M, David L, Barral X, Cochat P, Rolando Cimaz R. Takayasu arteritis in children. *Pediatr Rheumatol Online J* 2008; 6: 17. DOI: 10.1186/1546-0096-6-17
- 2 Buonouomo PS, Bracaglia C, Campana A, Insalaco A, Pardeo M, Cortis E, Ugazio A G. Infliximab therapy in pediatric Takayasu's arteritis: report of two cases. *Rheumatol Int* 2011; 31: 93-5.
- 3 Caspary L. Vasculitides of large vessels. *Vasa* 2011 (40) 2: 89-98.
- 4 Chauhan SK, Tripathy NK, Nityanand S. Antigenic targets and pathogenicity of antiaortic endothelial cell antibodies in Takayasu arteritis. *Arthritis Rheum* 2006, 54: 2326 - 2333.
- 5 Förster S, Tato F, Weiss M, Czihal M, Rominger A, Bartenstein P, Hacker M, Hoffmann U. Patterns of extracranial involvement in newly diagnosed giant cell arteritis assessed by physical examination, colour coded duplex sonography and FDG-PET. *Vasa* 2011 (40) 3: 219 - 227.
- 6 Gedalia A, Cuchacovich R. Systemic vasculitis in childhood. *Curr Rheumatol Rep.* 2009 Dec; 11 (6): 404 - 409.
- 7 Hata A, Noda M, Moriwaki R, Nu-mano F. Angiographic findings of Takayasu arteritis: new classification. *Int J Cardiol* 2004, 54 (Suppl): S155-S163.
- 8 Hoffman GS, Merkel PA, Brasington RD, Lenschow DJ, Liang P. Anti-tumor necrosis factor therapy in patients with difficult to treat Takayasu arteritis. *Arthritis Rheum* 2004, 50: 2296 - 2304.
- 9 Kerr CS, Hallahan CW, Giordano J, Leavitt RY, Fauci AS, Rottem M, Hoffman GS. Takayasu's arteritis. *Ann Intern Med* 1996, 120: 919.
- 10 Ladhani S, Tulloh R, Anderson D. Takayasu disease masquerading as interruption in a 2 years old child. *Cardiol Young* 2001, 11: 244 - 246.
- 11 Lazzarin P, Pasero G, Marson P, Cecchetto A, Zanchin G. Takayasu arteritis. A concise review and some observations on a putative case Reported by Giovanni Battista Morgagni (1761) *Rheumatism* 2005, 57: 305 - 313.
- 12 Miller JH, Gunarta H, Stanley P. Gallium scintigraphic Demonstration of arteritis in Takayasu disease. *Clin Nucl Med*, 1996, 21 (11), 882 - 883.
- 13 Ozen S, Duzova A, Bakkaloglu A, Bilginer Y, Cil B, Demircin M, Davin JC, Bakkaloglu M. Takayasu arteritis in children: Preliminary Experience with Cyclophosphamide Induction and Corticosteroids followed by Methotrexate, *J Pediatr* 2007, 150: 72 - 76.
- 14 Ozen S, Ruperto N, EULARPORES Criteria for childhood Takayasu arteritis, *Ann Rheum* 2010, 69 (5): 798 - 806. 15Rodriguez-Pla A, Stone H. Vasculitis and systemic infections. *Cur Opin Rheumatol* 2006 18: 39 - 47.
- 16 Takayasu arteritis: eMedicine Pediatrics: General medicine, <http://emedicine.medscape.com/article/1007566-overview>

THE ROLE OF ADRENOMEDULLIN AND GALANIN IN RECURRENT VASOVAGAL SYNCOPE: A CASE CONTROL STUDY

Jiri Plasek^a, Vlastimil Doupal^b, Jana Furstova^c, Tomas Furst^d, Kristian Safarcik^e, Alena Krnacova^f, Nadezda Petejova^a, Zuzana Hrabovska^a, Arnost Martinek^a, Milos Taborsky^b

^a *Clinic of Internal Medicine, University Hospital Ostrava and Faculty of Medicine, University of Ostrava, Czech Republic*

^b *Department of Internal Medicine I - Cardiology, University Hospital Olomouc and Faculty of Medicine and Dentistry, Palacky University Olomouc*

^c *First Faculty of Medicine, Charles University Prague*

^d *Department of Mathematical Analysis and Applications of Mathematics, Faculty of Science, Palacky University Olomouc*

^e *Center of Laboratory Diagnostics, University Hospital Ostrava*

^f *Department of Clinical Biochemistry, University Hospital Ostrava*

Originally published in *Biomedical papers* 2013; 157(2):162-167

Consent to the publication of 3rd April 2014

ABSTRACT

Aims. Orthostatic stimuli are known to elicit changes in vasoactive peptide levels. The hypothesis of no difference in adrenomedullin and/or galanin levels in patients with recurrent vasovagal syncope and healthy controls was tested in a passive 35-min head-up tilt test (HUTT).

Methods. Twenty eight persons (14 patients and 14 healthy controls) were tested in a 35-min/60° head-up tilt test with telemetry monitoring. Three blood samples were evaluated for each person during the HUTT. Plasma levels of adrenomedullin and galanin were analysed by the Kruskal-Wallis test for all sampling periods. Vagal influence was indirectly assessed by the break index.

Results. There were no significant differences between groups in median values for either adrenomedullin or galanin plasma levels (all 6 p-values were greater than 0.4). For adrenomedullin, no significant difference between groups was found. For galanin, the rate of change between the 1st and 2nd measurement was significantly greater for patients ($P=0.04$), regardless of HUTT result but between the 2nd and 3rd measurement it was insignificant ($P=0.36$). In the group of positive cases, the break index increased significantly ($P=0.02$).

Conclusion. We confirmed that there is a different galanin secretion pattern during orthostatic provocation in patients with recurrent vasovagal syncope than healthy individuals. For adrenomedullin, no significant difference was found. A significant increment of the break index confirmed increased vagal influence in the subgroup of positive cases.

Key words: adrenomedullin, galanin, vasovagal syncope, head-up tilt test

INTRODUCTION

According to the European Society of Cardiology Guidelines¹ syncope is a symptom defined as a transient, self-limited loss of consciousness and postural tone. The onset of syncope is relatively rapid, and the subsequent recovery is spontaneous, complete, and usually prompt. Vasovagal syncope (VVS) is accompanied by inactivation of sympathetic tone, and paradoxical activation of vagal tone leading to vasodepressor, cardio-inhibitory or mixed reaction. Some vasoactive peptides are reported to be involved in the reaction to orthostatic stress but their particular roles and interactions are complex and poorly understood². In this study, adrenomedullin and galanin were selected and their role in the vasovagal response was assessed. Both peptides are known to affect vasovagal response. However, their specific roles are unclear^{3,4}. Thus the rationale of this study was to ascertain whether either one or both peptides are substantially involved in the course of VVS. Galanin (GAL) is a 30-amino acid peptide with almost ubiquitous presence in organisms within the central and peripheral nervous system, especially cardiac sympathetic neurons⁵. Its amino acid sequence is conserved from vertebrates to mammals which indicates its possible importance⁶. GAL has been proposed to take part in the regulation of cardiovascular homeostasis⁷, more precisely GAL was demonstrated to lower norepinephrine plasma levels and thus attenuate blood pressure response to orthostasis⁸. Further principal actions of GAL are inhibition of acetylcholine, glutamate, and insulin release, stimulation of feeding, stimulation of pituitary hormone release, and inhibition of spinal nociceptive reflexes⁹. The 52-amino acid adrenomedullin (ADM) is a relatively strong vasorelaxant and natriuretic peptide¹⁰. Like GAL, ADM has a very conserved amino acid sequence which places ADM in the

evolutionary line at the pre-dinosaur age¹¹. For this reason, ADM has been studied in many disease states including hypertension, heart and renal failure. ADM is constitutively produced by endothelial cells and regulated on the level of gene expression¹². It has been reported that the ADM plasma levels increase during the head-up tilt test (HUTT) - induced passive orthostasis - followed by a decrease after supination⁴. In the present study, we investigated whether the secretion patterns of GAL and ADM during HUTT differ in patients suffering from recurrent vasovagal syncope (rVVS) and for healthy individuals. We concentrated both on the total level of blood plasma GAL and ADM (absolute values) and on their rates of change (relative values). We also investigated whether the occurrence of a syncope during HUTT affected the secretion patterns. Vagal tone is known to increase during typical vasovagal syncope. Thus we employed the brake index as an indirect measure of vagal influence.

MATERIALS AND METHODS

Subjects

14 patients (7 men, 7 women) with recurrent vasovagal syncope (rVVS), without structural heart or neurological diseases were enrolled as cases. For the purpose of the study we defined rVVS as a history of one or more syncopes and at least one syncope reproducible during HUTT. All cases experienced 2 or more syncopes per month and all had had vasodepressor type of vasovagal syncope during HUTT prior to enrollment. Another 14 healthy individuals (11 women, 3 men, all medical staff volunteers) without a history of syncopes or presyncopal states were used as controls. Absence of structural heart disease, absence of medication, normal ECG and physical status including neurotopic state were the principal inclusion criteria. The BMI of cases was 23.55 ± 3.24 and controls 22.97 ± 2.59 .

Study protocol

Both groups were required to refrain from consuming tea, coffee, chocolate and smoking cigarettes two days before the testing. HUTT was performed between 8:30 and 11:00 AM in a quiet, well ventilated room after overnight fasting and all subjects were well hydrated. Before the HUTT started, antecubital vein cannulation was undertaken for further blood sampling. All patients were asked to rest for 10-15 min in a supine position before the test to allow all the cardiovascular parameters (pulse, blood pressure, respiration rate) to stabilize. The HUTT then proceeded according to the shortened protocol to eliminate late false positive results: the subjects were tilted at 60° head upwards, with their feet secured, for 35 min, without medical provocation. All subjects were further stratified according to HUTT result. Blood samples were taken in the first minute of the test and then, if syncope developed (positive HUTT), in the first 10-15 s and tenth min. after-

wards. After the syncope developed, blood samples were first taken and then the patients were returned to the supine position. If the HUTT was negative (no syncope occurred), blood samples were taken after 1, 25, and 35 min of the test. Blood pressure was measured every two min and then every minute in the presyncopal phase and ECG was recorded continuously for further heart rate variability analysis (brake index). Both blood pressure and ECG were recorded by the Datex Ohmeda S5 monitoring system. ECG recordings were used for brake index calculation ($RR_{max} - RR_{min} / RR_{resting}$), which is a simple heart rate variability measure used to assess the amount of vagal influence. The test procedure was attended by a nurse and a physician. The study protocol was approved by the Local Ethics Committee of the University Hospital in Ostrava. The trial was carried out in accordance with the principles of the Helsinki Declaration. Written informed consent was obtained from all patients prior to enrollment.

Analytical methods

Blood samples were drawn into pre-cooled tubes containing EDTA and aprotinin (Within 30 min, the samples were centrifuged at 1600 g/4 °C for 15 min, and then the plasma was frozen at -80 °C until the analysis which was performed within four months. Plasma ADM levels were measured by commercially available ELISA kit for human ADM containing 52 amino acids (EK-010-01, Phoenix Pharmaceuticals, for research only use). The detection range is 0.13-100 ng/mL. Plasma GAL levels were obtained by means of commercially available RIA kit (RK-026-01, Phoenix Pharmaceuticals, for research only use). The detection range is 10-1280 pg/mL.

Statistical methods

Unless stated otherwise, median values of ADM and GAL plasma levels are provided as non-parametric statistical tests were generally used (the hypothesis of normality of the data was rejected, $P < 0.0001$). All analyses of ADM and GAL levels (including their rates of change) were performed by the Kruskal-Wallis test. Brake index (see the results below) data were analysed using ANOVA or t-tests as the data were normally distributed. P values below 0.05 were considered statistically significant.

RESULTS AND DISCUSSION

A HUTT induced syncope occurred in 4/14 healthy individuals after 3, 26, 27, and 30 min of the test. In the rVVS patients, 8/14 individuals suffered a vasovagal syncope after 4, 11, 21, 22, 24, 24, 26, and 27 min. Although the time to syncope was different in the rVVS group, we believe the pathophysiological mechanisms are uniform. Moreover by holding the blood sampling time frame possible differences are diminished. Basic clinical characteristics and haemodynamic parameters of the groups are shown in

Table 1. Basic characteristics of the study group. All values are provided as the mean ± standard deviation. Normality of the data was not rejected.

		Healthy subjects (controls)			rVVS patients (cases)		
		HUTT negative (n = 10)	HUTT positive (n = 4)	P	HUTT negative (n = 6)	HUTT positive (n = 8)	P
Age (years)		24.5 ± 2.5	26.3 ± 4.3	0.48	41.0 ± 16.0	34.1 ± 12.6	0.36
Sex		9F / 1M	1F / 3M		2F / 4M	4F / 4M	
BMI (kg/m ²)		23.1 ± 2.5	22.6 ± 3.1	0.72	22.7 ± 3.4	23.1 ± 2.7	0.95
Systolic BP (mmHg)	Supine	114.7 ± 8.1	122.5 ± 11.9	0.20	127.8 ± 10.2	124.0 ± 16.3	0.30
	Tilting (3 min)	115.7 ± 9.7	112.3 ± 15.7	0.72	131.7 ± 10.7	119.8 ± 26.2	0.03
Diastolic BP (mmHg)	Supine	69.4 ± 5.7	77.8 ± 5.2	0.02	82.8 ± 6.9	76.5 ± 7.2	0.10
	Tilting (3 min)	74.5 ± 5.3	73.8 ± 14.9	0.94	86.8 ± 11.9	75.4 ± 15.0	0.10
Heart rate (beats/min)	Supine	62.3 ± 5.1	67.0 ± 10.4	0.44	61.2 ± 6.8	59.6 ± 12.7	0.79
	Tilting (3min)	74.5 ± 7.9	77.0 ± 11.2	0.62	74.2 ± 10.6	82.0 ± 19.0	0.44

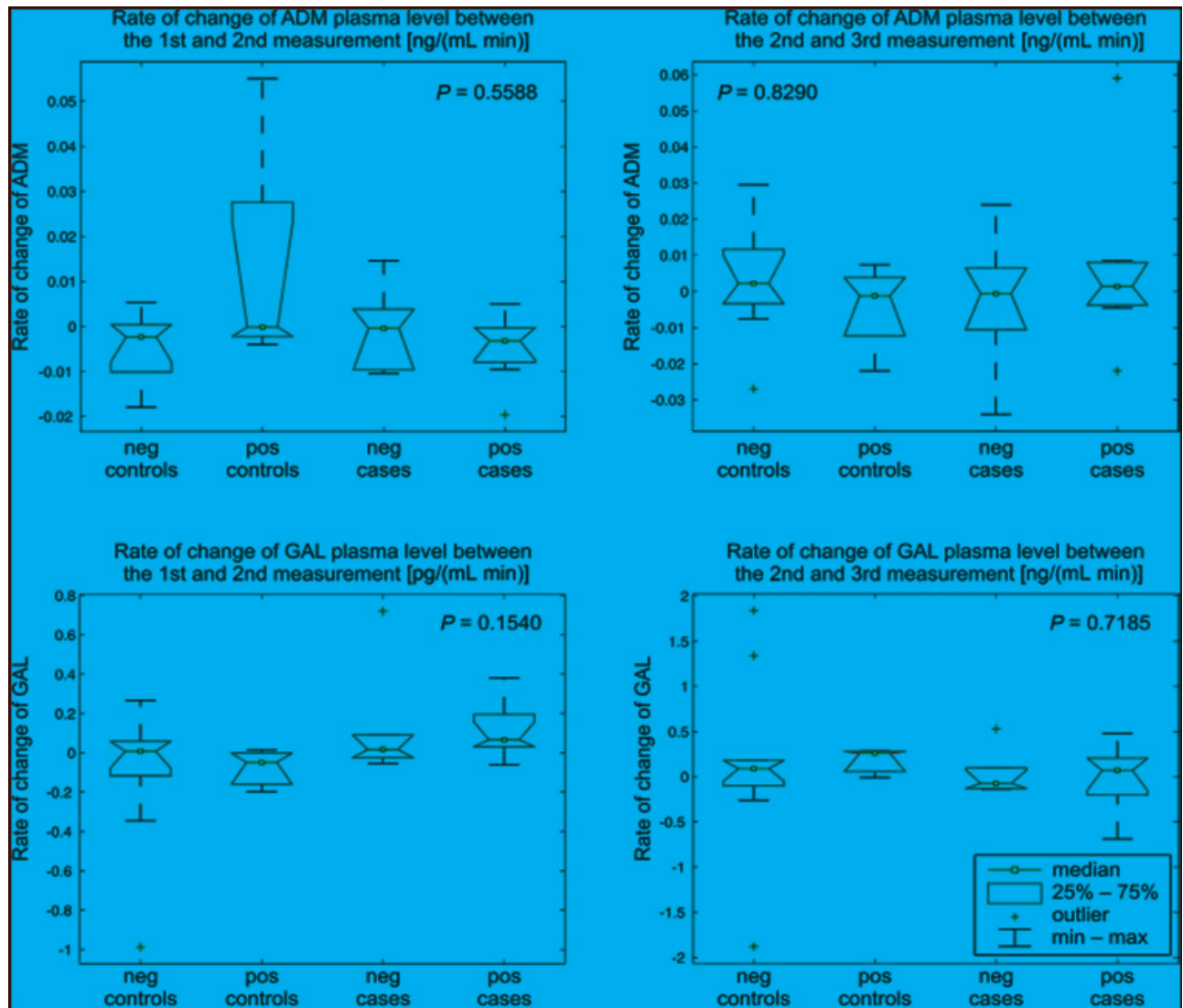


Fig. 1. Rate of change of Adrenomedullin and Galanin plasma level for all four subgroups between the 1st and 2nd, 2nd and 3rd measurement, respectively.

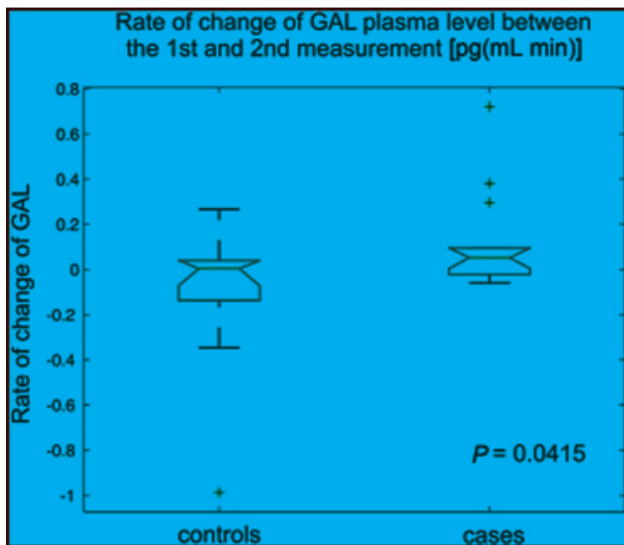


Fig. 2. Rate of change of Galanin between the 1st and 2nd measurement, cases and controls, independent on the result of the HUTT.

(Table 1). First, we compared the plasma levels of ADM and GAL for positive cases and negative controls (where the most profound difference is to be expected) for all three measurements (see the study protocol). No significant difference between the groups was found ($P=0.92$ and $P=0.98$). Next, to capture the dynamics of the regulatory system, we compared the rates of change of the ADM and GAL levels between consecutive measurements (i.e. the change in concentration divided by time). The rate of change of ADM plasma level between the first and second measurement was not significantly different for any of the four subgroups (positive cases, negative cases, positive controls, negative controls, $P=0.56$). Although the box plot (Fig. 1) shows a mild increase in ADM for positive controls, by contrast the remaining three groups show stagnation or slight decrease. The non-significance of this difference may be caused by the small study group. There was also no significant difference in ADM plasma level changes between the second and third measurement: the levels of ADM tend to stagnate for all the four subgroups (Fig. 1). The same analysis was applied to GAL levels. The variation of GAL plasma level change between the first and second measurement is insignificant (Fig. 1), however for the controls, GAL tends to decrease, while for cases there is an opposite tendency. Comparing cases and controls with no further differentiation into positive and negative groups, this difference becomes significant ($P=0.04$, Fig. 2). Patients suffering from rVVS (cases) experience an increase in GAL levels, while healthy individuals experience a decrease, regardless of the HUTT result. The variation in GAL plasma level change between the second and third measurement shows no significant difference between the four groups ($P=0.72$, Fig. 1), not even when only cases and controls are compared

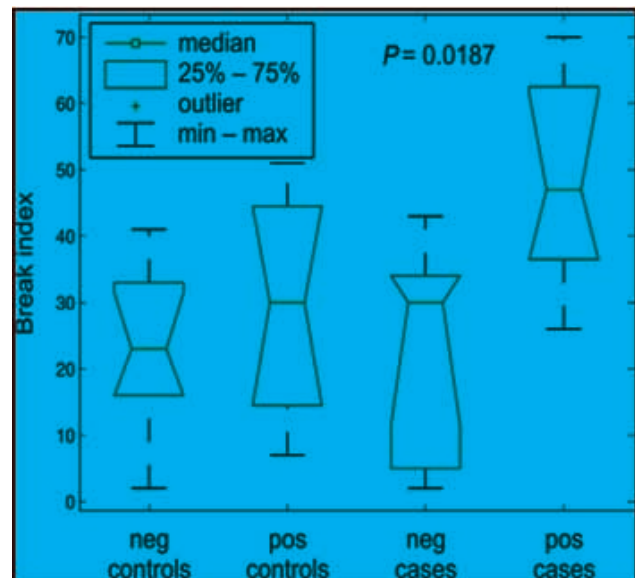


Fig. 3. Brake index, all four groups (positive and negative control, positive and negative cases).

(without differentiating positive and negative). We further tried to capture the secretion patterns for GAL and ADM qualitatively, assigning to each patient one of the three secretion types: an “A-type” for an increase between the first two measurements followed by a decrease, a “V-type” for a decrease followed by an increase, and an “N-type” for any other. This type of analysis showed no significant differences among the groups or subgroups, for either ADM or GAL levels. It is known that the so-called break index¹³, is a good marker of elevated vagal influence. Accordingly, in the positive cases, the values of the break index increased significantly ($P=0.02$, Fig. 3). It is also noteworthy that there is a significant correlation ($r=0.48$, $P=0.01$) between the range of ADM levels (i.e. the maximum level minus the minimum level) and the range of GAL levels in the group of all patients.

As stated a number of neurohumoral factors are involved in triggering and sustaining the vasovagal response. However, neither the roles of individual peptides nor their integrated response is known. In this study, the role of ADM and GAL was addressed to a small group of patients with rVVS. The secretion patterns of both peptides during HUTT were compared to a group of healthy individuals. The authors are not aware of any other HUTT trial without pharmacological provocation performed on rVVS patients while measuring ADM levels though a case/control study exists¹⁴ evaluating GAL levels in patients with rVVS during HUTT. In another trial¹⁵, adrenomedullin response to HUTT in VVS patients was assessed. However, in most patients, the syncope was induced by nitroglycerin administration, and the condition of syncope recurrence was not satisfied. Bondanelli et al.¹⁴ show that GAL levels increase in rVVS pati-

ents who do not develop a syncope (negative HUTT), whereas it remains unchanged in rVVS patients who develop a syncope (positive HUTT). GAL levels are reported to remain unchanged in the control group but there were no positive responses to the HUTT in this group¹⁴. This suggests that GAL could be responsible for preventing a syncope development in susceptible individuals. We observed more stereotypical GAL response to tilting in all subjects. In our trial, GAL increase differentiated cases from controls better than it differentiated positive and negative responses to HUTT, i.e. there was an increase in plasma GAL for rVVS patients during HUTT, regardless whether they developed syncope or not. Our data are thus in a partial conflict with those of Bondanelli et al. Elsewhere it has been demonstrated in healthy individuals that GAL plasma levels increase severalfold with orthostatic stress in the presyncopal phase³, which further questions the reproducibility of the results of Bondanelli. A possible explanation for this conflict may be the absence of a unique GAL secretion pattern. In other words, GAL response to orthostasis might be more complex than its mere increase/decrease, considering the number of other neurohumoral agents involved¹⁶. Our results show that there is no strong adherence of galanin secretion pattern to orthostatic stimuli, although the galaninergic system is involved in the vasovagal response. The galanin secretion pattern better differentiates patients with rVVS from controls than the type of response to HUTT (positive/ negative). This poses the question whether rVVS is just an abnormal autonomic/neurohumoral reaction or a genuine disease¹⁷.

No significant change in ADM plasma levels was observed in our trial, although there was a slight increase in ADM plasma levels in healthy individuals with a positive response to HUTT. It was shown that ADM plasma levels increased significantly with tilting and this correlated with the tilt table inclination level in healthy individuals⁴. Similar results were reported by Gajek et al.¹⁵, who demonstrated increased ADM plasma levels during HUTT immediately after syncope in patients with vasovagal vasodepressor reaction. The opposite was true (i.e. the ADM levels decreased) if nitroglycerin was administered¹⁵. This advocates the role of ADM in a failed prevention of a syncope by excessive paradoxical vasodilatation in healthy individuals and the suppression of this effect by nitroglycerin administration. Our results show an increasing trend in ADM levels in healthy individuals during HUTT which partly supports Rossler et al.⁴. Although a different protocol and tilt angle were used Nishikimi et al.¹⁸ failed to demonstrate ADM increase after 20 min of 70° HUTT in healthy volunteers. The brake index is used as a measure of the activity of the autonomic nervous system as a whole^{13,19}. The significantly elevated brake index for rVVS patients with a positive HUTT result com-

pared with healthy individuals shows that the rVVS patients were well-chosen: increased heart rate variability determinate by the brake index is a sign of increased vagal influence.

CONCLUSION

This study confirms that the galaninergic system is involved in the reaction of rVVS patients to HUTT. It also suggests that GAL accretion throughout HUTT might be used as a marker of vasovagal syncope recurrence. It also poses the question whether rVVS represents an abnormal response to orthostasis/HUTT as a variant of a normal reaction or a genuine disease. To our knowledge, this study represents the first evaluation of ADM in heavily symptomatic rVVS patients during a HUTT which was not accompanied by drug administration. No specific ADM secretion pattern was found for patients with rVVS and our patient's ADM plasma levels were generally lower than the controls. This may be due to fast biodegradation or re-uptake of ADM by the endothelial cells. The significant correlation of GAL and ADM ranges suggests that both peptides are part of the same regulatory pathway, although possibly acting in mutual opposition. The results do not answer all the questions on the involvement of both vasoactive peptides in rVVS and for this reason further research on neurohumoral response to syncope is needed to enhance understanding of this sophisticated system. Small sample size is the major limitation of the study, however, most of the trials cited in this paper have similar numbers of patients enrolled. Cases and controls are gender unbalanced, which might affect especially the GAL plasma levels. It was shown that galanin plasma levels during orthostasis are higher in healthy women (3), however, our data do not confirm this.

ACKNOWLEDGEMENT

This work was financially supported by AstraZeneca Czech Republic s.r.o.

CONFLICT OF INTEREST STATEMENT

Author's conflict of interest disclosure: The authors stated that there are no conflicts of interest regarding the publication of this article.

REFERENCES

1. The European Society of Cardiology Guidelines for the diagnosis and management of syncope reviewed by Angel Moya, MD, FESC, Chair of the Guideline Taskforce with J. Taylor, MPhil. *Eur Heart J* 2009;30:2631-71.
2. Mosqueda-Garcia R, Furlan R, Tank J, Fernandez-Violante R. The elusive patho-physiology of neurally mediated syncope. *Circulation* 2000;102:2898-2906.
3. Hinghofer-Szalkay HG, Rössler A, Evans JM, Stenger MB, Moore FB, Knapp CF. Circulatory galanin levels increase severalfold with intense orthostatic challenge in healthy humans. *J Appl Physiol* 2006;100(3):844-9.
4. Rössler A, László Z, Haditsch B, Hinghofer-Szalkay HG. Orthostatic stimuli rapidly change plasma adrenomedullin in humans. *Hypertension* 1999; 34(5):1147-51.

5. Vrontakis ME. Galanin: A Biologically Active Peptide. *Curr Drug Targets CNS Neurol Disord* 2002;1(6):531-41.
6. Wynn D, Bacon A. Targeted disruption of galanin: new insights from knock-out studies. *Neuropeptides* 2002;36(2-3):132-44.
7. Diaz-Cabiale Z, Narvaez JA, Yanaihara N, Gonzales-Baron SM, Fuxe K. Galanin/alpha2-receptor interactions in central cardiovascular control. *Neuropharmacology* 2000;39(8):1377-85.
8. Degli Uberti EC, Ambrosio MR, Bondanelli M, Trasfori G, Margutti A, Valentini A, Rosi R, Franceschetti P. Human galanin reduces plasma norepinephrine levels in man. *J Clin Endocrinol Metab* 1995;80(6):1894-8.
9. Crawley JN. Biological actions of galanin. *Regul Pept* 1995;59(1):1-16.
10. Brain SD, Grant AD. Vascular actions of calcitonin gene-related peptide and adrenomedullin. *Physiol Rev* 2004;84(3):903-34.
11. Martinez A, Cuttita F. Adrenomedullin. Amsterdam: IOS press;1998.
12. Sugo S, Minamino N, Kangawa K, Miyamoto K, Kitamura K, Sakata J, Eto T, Matsuo H. Endothelial cells actively synthesize and secrete adrenomedullin. *Biochem Biophys Res Commun* 1994; 201:1160-6.
13. Cybulski G, Niewiadomski W. Influence of age on the immediate heart rate response to the active orthostatic test. *J Physiol Pharmacol* 2003;54(1):65-80.
14. Bondanelli M, Alboni P, Margutti A, Franceschetti P, Dinelli M, Gruppilo P, Marchi P, Degli Uberti EC. Plasma galanin response to head-up tilt in normal subjects and patients with recurrent vasovagal syncope. *Metabolism* 2003;52(3):315-21.
15. Gajek J, Zysko D, Halawa B. Adrenomedullin-the link between the sympathetic nervous system activation and peripheral vasodilation in some patients with vasovagal syncope. *Pol Merkur Lekarski* 2004; 17(99):267-70.
16. Sander-Jensen K, Secher NH, Astrup A, Christensen NJ, Giese J, Swarz TW, Warberg J, Bie P. Hypotension induced by passive head-up tilt: endocrine and circulatory mechanism. *Am J Physiol* 1986;251:742-48.
17. Alboni P, Brignole M, Degli Uberti EC. Is vasovagal syncope a disease? *Europace* 2007;9(2):83-7.
18. Nishikimi T, Junichi M, Yasu T, Takeshi S, Kangawa K, Matsuoka H. Two molecular forms of plasma adrenomedullin during tilt test in healthy subjects. *Peptides* 2001;22(11):1867-72.
19. Wieling W, Borst C, Karemaker JM, Dunning AJ. Testing for autonomic neuropathy: initial heart rate response to active and passive changes of posture. *Clin Physiol* 1985;5:23-7.

ENDOSCOPIC VS OPEN SAPHENOUS VEIN HARVEST FOR CORONARY ARTERY BYPASS GRAFTING: A LEG-RELATED MORBIDITY AND HISTOLOGICAL COMPARISON

Radim Brat^a, Jaroslav Horacek^b, Jiri Sieja^a

^a *Cardiosurgical Department, University Hospital Ostrava*

^b *Institute of Pathology, University Ostrava, Faculty of Medicine*

Originally published in *Biomedical papers* 2013; 157(1): 70-74

Consent to the publication of 3rd April 2014

ABSTRACT

Aims

The aim of this study was to compare the leg-related morbidity and to perform histological comparison of the veins for coronary artery bypass grafting (CABG) using endoscopic (EVH) and open harvest (OVH).

Methods

One hundred consecutive patients scheduled for isolated CABG were randomly divided into EVH and OVH group. Perioperative data were recorded. Patients were examined 7 days and 1 month postoperatively focusing on leg-related morbidity. The sample for histological examination was taken from each harvested vein during the surgery.

Results

The postoperative pain was statistically significantly lower in the EVH group 7 days postoperatively. EVH was connected with higher incidence of haematoma, but this difference didn't reach a statistical significance as well as swelling, which was higher in the OVH group. Almost 40% of all histological samples were described as samples with endothelial damage. We found the statistically significant difference between EVH and OVH group in terms of endothelial damage being higher in the EVH group

Conclusions

We have confirmed the advantage of the EVH in terms of leg-related morbidity as well as cosmetic effect but the EVH was associated with higher acute endothelial damage of the graft. These results can support concerns that endoscopic vein harvest could be connected with a detrimental effect on vein endothelium, which may promote a thrombogenic environment leading to a decrease in graft patency, which could be extremely important. Based on this fact we feel further investigation of the long-term patency of vein grafts harvested endoscopically is required.

Keywords:

Saphenous vein harvest; Endoscopic harvest; Histopathology; Endothelial damage; Minimally invasive; Coronary artery bypass grafting.

INTRODUCTION

Coronary Artery Bypass Grafting (CABG) continues to be a widely used therapy for the treatment of ischemic heart disease and it remains the most common procedure in cardiothoracic surgery /1/. Despite the advances in the use of arterial grafts, the long saphenous vein remains the most commonly used conduit for coronary artery bypass surgery /2/.

Traditional methods of vein harvest, in which a wound is opened along the length of the long saphenous vein, often contribute significantly to patient morbidity /3, 4/. Minimally invasive techniques of vein harvest have been developed in order to reduce this significant morbidity. Studies have shown reduced rates of postoperative wound complications following minimally invasive approaches compared to the traditional saphenous vein harvest technique /5, 6/. Despite these studies, there are not enough data about mid-term and long-term results. Also the histological data published in the literature have given a mixed opinion /7, 8/.

The aim of this study was to examine local outcomes with endoscopic vein harvest (EVH) and to give some more data about histological comparison of the veins after endoscopic and open harvest.

MATERIALS AND METHODS

The study was performed as a prospective randomized study including 100 consecutive patients coming to scheduled isolated coronary surgery with the use of great saphenous vein graft. All patients included in this study were acceptable for both saphenous vein harvest methods - open as well as endoscopic. All patients have signed the informed consent form. The ultrasound mapping of both great saphenous veins using the vascular 10MHz probe was done before the surgery. Only patients with patent deep vein system, location of the great saphenous vein at least 4 mm under the skin surface, lumen of the vein from 2,0 to 5,0 mm and the vein wall thickness smaller than 1,5 mm were included in the study.

Patients were randomized into two groups - open vein harvest group (OVH group) and endoscopic har-

Table 1
Clinical characteristics of the patients

	EVH group	OVH group	p-value
No. of patients	50	50	NS
Male (%)	42 (84%)	45 (90%)	NS
Female (%)	8 (16%)	5 (10%)	NS
Age (years)	65±8.94	66.2±8.17	NS
LVEF (%)	53.4±8.85	52.4±9.09	NS
AP (CCS)	1.7±1.0	2.3±1.02	NS
BMI (kg/m ²)	29.1±4.0	28.9±4.08	NS
Diabetics (%)	20 (40%)	22 (44%)	NS
Smokers (%)	18 (36%)	16 (32%)	NS
Smokers and diabetics (%)	6 (12%)	5 (10%)	NS

Where applicable, data are shown as the mean ± the standard deviation.

LVEF...left ventricular ejection fraction

AP...angina

BMI... body mass index

NS... not significant (p>0.05)

Table 2
Perioperative data

	EVH group	OVH group	p-value
No. of patients	50	50	NS
Length of the graft (cm)	36.9±8.35	38.4±11.23	NS
Harvest time (min)	36.2±13.25	37.7±20.46	NS
No. of conversions	0	NA	
No. of 7-0 sutures	1.3±1.57	0.4±0.94	p<0.001
Overall length of skin incisions (cm)	7.6±3.1	40.3±12.81	p<0.001

Where applicable, data are shown as the mean ± the standard deviation.

NS... not significant (p>0.05)

vest group (EVH group). In the OVH group the graft was harvested by advanced surgeon using standard open technique with ligating or clipping the side branches. In the EVH group the endoscopy was performed by surgeon, who was experienced enough in this harvest method. Standardized miniinvasive technique was performed using the Virtuo-Saph (Terumo) endoscopic vessel harvesting system and carbon dioxide insufflation technique. Diathermy was employed to divide side branches in situ with titanium clips applied prior to grafting.

Important perioperative data were recorded. In the follow-up patients were examined 7 days and 1 month after the surgery focusing on leg-related morbidity. The sample for histological examination was taken from each harvested vein during the surgery. The biopsy material was processed using the paraffin technique with basic staining and immunohistochemistry assay. Histological changes were recorded. Assessment of the changes was contributed to by immunohistochemistry assay using Factor VIII, CD34, HAS and Laminin antibodies and by Trichrome and VG

chemical stains.

Comparison between groups was carried out with Student's t-test when appropriate. Values of p=0.001 were considered statistically significant. Informed consent was obtained from all patients and the study was approved by the ethics committee.

RESULTS

From October 2009 to August 2010, 100 consecutive patients scheduled for isolated CABG and meeting the above mentioned criteria were randomly divided into 2 groups. EVH was used in the 1st group and OVH was used in the 2nd group.

The clinical characteristics of the patients are summarized in Table 1. There was no significant difference between groups in the clinical profile. The majority of the patients were male and there was a high proportion of diabetics in both groups. Perioperative data describing the vein harvest are shown in Table 2. There was no difference in the total length of the graft harvested as well as in the harvest time. Statistically significant was the difference in the num-

Table 3
Leg-related morbidity 7 days postoperatively

	EVH group	OVH group	p-value
No. of patients	50	50	NS
Haematoma (%)	31 (62%)	22 (44%)	NS
Leg wound dehiscence (%)	0	0	NS
Swelling (%)	4 (8%)	13 (26%)	NS
Leg wound infection (%)	0	0	NS
Necrosis (%)	0	1 (2%)	NS
Leg wound pain (%)	6 (12%)	22 (44%)	p<0.001
Dysaesthesia (%)	0	5 (10%)	NS

NS... not significant (p>0.05)

Table 4
Leg-related morbidity 1 month postoperatively

	EVH group	OVH group	p-value
No. of patients	50	50	NS
Haematoma (%)	1 (2%)	0	NS
Leg wound dehiscence (%)	1 (2%)	4 (8%)	NS
Swelling (%)	1 (2%)	2 (4%)	NS
Leg wound infection (%)	0	1 (2%)	NS
Necrosis (%)	0	0	NS
Leg wound pain (%)	0	4 (8%)	NS
Dysaesthesia (%)	0	4 (8%)	NS

NS... not significant (p>0.05)

ber of 7-0 sutures (being higher in the EVH group) and first of all in the overall length of skin incisions, which was of course much shorter in the EVH group. Data describing leg-related morbidity 7 days and 1 month postoperatively are shown in Tables 3 and 4 respectively. We can see, that there is a statistically significant difference in the postoperative pain between the groups 7 days postoperatively. The pain was lower in the EVH group. On the other hand EVH was connected with higher incidence of haematoma, but this difference didn't reach a statistical significance as well as swelling, which was higher in the OVH group. The leg-related morbidity has decreased significantly one month postoperatively and haematomas has disappeared almost completely. The only difference between the groups one month postoperatively was in the incidence of swelling and pain being lower in the EVH group, but the difference was not statistically significant.

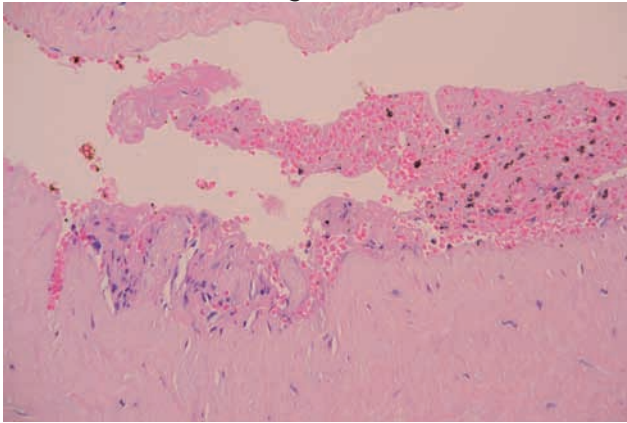
As described in the methodology, the sample for histological examination was taken from each harvested vein during the surgery except of four patients where because of lack of suitable vein for grafting the sample was not taken. The results of remaining 96 samples are summarized in Table 5. We can see, that 38 out of 96 samples were described as samples with endothelial damage, which is almost 40% of all samples. We found the statistically significant difference

between EVH and OVH group in terms of percentage of endothelial damage. This percentage was higher in the EVH group. The typical acute endothelial damage is shown in Picture 1 and 2. They include the desquamation, granulocyte formation with the presence of fibrin, partly with formation of tiny defects with bleeding and leukostasis in capillaries of the vasa vasorum.

DISCUSSION

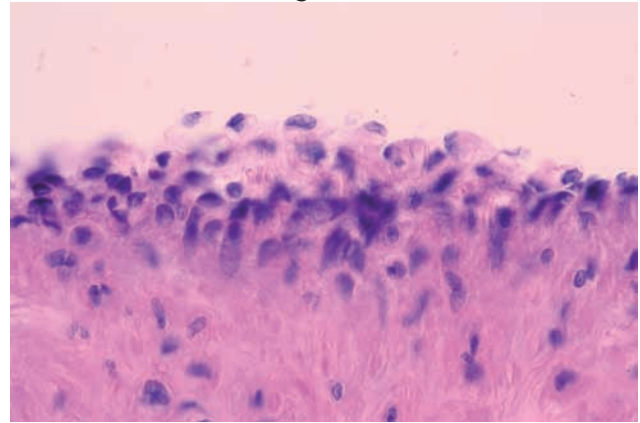
Open saphenectomy has been the technique of choice for vein harvest in coronary artery bypass surgery for several decades; however, minimally invasive techniques have become increasingly popular in a wide range of surgical specialties. Endoscopic vein harvest has become increasingly used as an alternative to the open technique. The advantages of this technique published in the literature (9) includes reduced leg wound complications, postoperative pain, required analgesia and incision length. The disadvantage of the procedure according to the literature is the learning curve (9), risk of carbon dioxide (CO₂) embolism during CO₂ insufflation (10) and lack of data regarding the long-term patency rates of veins harvested by the endoscopic technique(11). Based on our experience the learning curve is not the major problem of the endoscopic vein harvest. In our series the harvest time was almost the same

Picture 1
Acute endothelial damage



Endothelial desquamation with bleeding and fibrin thrombus formation, HE, 400x

Picture 2
Acute endothelial damage



Endothelial desquamation, HE, 1000x

Table 5
Histopatological changes

	EVH group	OVH group	p-value
No. of samples	47	49	NS
Acute endothelial damage (%)	24 (51%)	14 (29%)	p<0.001

NS... not significant ($p>0.05$)

in both groups and all surgeons performing the endoscopic vein harvest were able to adopt this method after a relatively short learning curve.

The most important advantage of the EVH is the reduction of leg-related morbidity(12,13, 14) . In our study we have found the statistically significant difference between groups only in the postoperative pain 7 days after the surgery. The difference in swelling and dysaesthesia didn't reach the statistical significance. The reason for relatively low difference in leg-related morbidity is that generally the incidence of all leg-related mortality in both groups was very low. But in spite of that we have confirmed the superiority of EVH over OVH in terms of reduced leg-related morbidity. The only disadvantage of EVH in this field was relatively high incidence of haematoma in the EVH group. Although the haematoma disappeared in a relatively short time, we recommend using drainage to reduce the incidence of haematoma.

One major limitation of the current literature is that there is very little conclusive data regarding long-term patency rates of endoscopically harvested veins. There are some concerns that endoscopic vein harvest could be connected with a detrimental effect on vein endothelium, which may promote a thrombogenic environment leading to a decrease in graft patency. These results were published for example by Rousou et al. (15) and Zenati et al. (16). In our study we have found the statistically significant difference between EVH and OVH group in

terms of percentage of endothelial damage. This percentage was statistically significantly higher in the EVH group. Based on this experience we can summarize, that there is a difference between the vein harvested endoscopically and the vein harvested by the open technique in terms of histological picture of the vein. This is supported also by the fact, that in our study the pathologist was able to correctly recognize the vein harvested endoscopically in more than 70% of the cases only according to the histological examination.

CONCLUSIONS

Endoscopic vein harvest has become increasingly used as an alternative to the open technique. In our study we have confirmed the advantage of this method in terms of leg-related morbidity as well as cosmetic effect. On the other hand we have found significant histological difference between vein harvested endoscopically and the vein harvested by the open technique showing that the EVH could be associated with higher acute endothelial damage of the graft. These results can support concerns that endoscopic vein harvest could be connected with a detrimental effect on vein endothelium, which may promote a thrombogenic environment leading to a decrease in graft patency, which could be extremely important. But the overall incidence of the endothelial damage in both groups is very high. The reason for that could be, that we have detected minor damages, which will not influence the long-term pa-

tency of the graft. Based on these facts we feel further investigation of the long-term patency of vein grafts harvested endoscopically is required.

ACKNOWLEDGEMENTS:

This study was supported by the grant of the Internal Grant Agency Ministry of Health Czech Republic, No. NS/10611-3.

REFERENCES

1. Caparrelli DJ, Ghazoul M, Diethrich EB. Indications for coronary Artery bypass grafting in 2009: what is left to surgery. *J Cardiovasc Surg (Torino)* 2009;50:19-28.
2. Allen K, Cheng D, Cohn W, Connolly M, Edgerton J, Falk V, Martin J, Ohtsuka T, Vitali R. Endoscopic Vascular Harvest in Coronary Artery Bypass Grafting Surgery: A Konsensus Statement of the International Society of Minimally Invasive Cardiothoracic Surgery (ISMICS) 2005. *Innovations: Technology and Techniques in Cardiothoracic and Vascular Surgery* 2005, 1(2):51-60.
3. Carpino PA, Khabbaz KR, Bojar RM, Rastegar H, Warner KG, Murphy RE, Payne DD. Clinical benefits of endoscopic vein harvesting in patients with risk factors for saphenectomy wound infections undergoing coronary artery bypass grafting. *J Thorac Cardiovasc Surg* 2000, 119(1):69-75.
4. Reed JF. Leg wound infections following greater saphenous vein harvesting: minimally invasive vein harvesting versus conventional vein harvesting. *Int J Low Extrem Wounds* 2008, 7(4):210-219.
5. Allen KB, Heimansohn DA, Robison RJ, Schier JJ, Griffith GL, Fitzgerald EB, Isch JH, Abraham S, Shaar CJ. Risk factors for leg wound complications following endoscopic versus traditional saphenous vein harvesting. *Heart Surg Forum* 2000;3:325-330.
6. Dusterhoft V, Bauer M, Buz S, Schaumann B, Hetzer R. Wound-healing disturbances after vein harvesting for CABG: a randomized trial to compare the minimally invasive direct vision and traditional approaches. *Ann Thorac Surg* 2001;72:2038-2043.
7. Alrawi SJ, Raju R, Alshkaki G, Acinapura AJ, Cunningham JN. Saphenous vein endothelial cell viability: a comparative study of endoscopic and open saphenectomy for coronary Artery bypass grafting. *JLS* 2001, 5(1):37-45.
8. Rousou LJ, Taylor KB, Lu X, Healey N, Crittenden MD, Khuri SF, Thatte HS. Saphenous vein conduits harvested by endoscopic technique exhibit structural and functional damage. *Ann Thorac Surg* 2009, 87(1):62-70.
9. Markar SR, Kutty R, Edmonds L, Sadat U, Nair S. A meta-analysis of minimally invasive versus traditional open vein harvest technique for coronary artery bypass graft surgery. *Interact CardioVasc Thorac Surg* 2010;10:266-270.
10. Lin TY, Chiu KM, Wang MJ, Chu SH. Carbon dioxide embolism during endoscopic saphenous vein harvesting in coronary artery bypass surgery. *J Thorac Cardiovasc Surg* 2003;126:2011-2015.
11. Pranjal D, Soroosh K, Nannan T. Impact of the learning curve for endoscopic vein harvest on conduit quality and early graft patency. *Ann Thorac Surg* 2011, 91(5):1385-1392.
12. Andreasen J, Nekrasas V, Dethlefsen C. Endoscopic vs open saphenous vein harvest for coronary artery bypass grafting: a prospective randomized trial. *Eur J Cardiothorac Surg* 2008;34:384-389.
13. Ouzounian M, Hassan A, Buth KJ, MacPherson C, Ali IM, Hirsch GM, Ali IS. Impact of Endoscopic Versus Open Saphenous Vein Harvest Techniques on Outcomes After Coronary Artery Bypass Grafting. *The Annals of Thoracic Surgery* 2010, 89(2):403-408.
14. Simek M, Bruk V, Nemeč P. Endoskopický odběr vena saphena magna pro revaskularizaci myokardu. *Rozhl.Chir.* 2006;85:211-215.
15. Rousou LJ, Taylor KB, Lu XG, Healey N, Crittenden MD, Khuri SF, Thatte HS. Saphenous vein conduits harvested by endoscopic technique exhibit structural and functional damage. *Ann Thorac Surg* 2009;87:62-70.
16. Zenati M, Shroyer L, Collins J. Impact of endoscopic versus open saphenous vein harvest technique on late coronary artery bypass grafting patient outcomes in the ROOBY (Randomized On/Off Bypass) trial. *J Thorac Cardiovasc Surg* 2011; 141: 338-344.

PRIMARY NEUROENDOCRINE CARCINOMA OF THE KIDNEY

Dvořáčková J¹, Mačák J¹, Brzula P¹, Tomanová R¹, Dokulil J²

¹ Department of Pathology, University Hospital and Faculty of Medicine University of Ostrava, Czech Republic

² Department of Oncology, University Hospital and Faculty of Medicine University of Ostrava, Czech Republic

Originally published in *Biomedical papers* 2013; 157(3):257-260

Consent to the publication of 3rd April 2014

ABSTRACT

Background. The objective of the study was to report a rare case of primary neuroendocrine carcinoma of the right kidney in a 36 year old male.

Methods. The patient was clinically assessed; CT and OctreoScan scintigraphy were performed and levels of 5-HIAA, vanillylmandelic acid and NSE were determined. The tumor and metastases were histologically and immunohistochemically examined.

Results. The imaging methods showed a cystic tumor in the lower pole of the right kidney. Macroscopically, the entire tumor was sized 8x8x7 cm. Histologically, it was made up of ribbon-line or trabecular patterns of tumor cells. Occasional adenomatoid and cystic structures were present. The tumor cell nuclei were round or oval, with no irregularities and fine lumpy chromatin. The mitotic count was < 1 /10HPF and the proliferation marker Ki-67 was < 1 % of tumor cells. Immunohistochemically, the tumor cells were positive with antibodies against chromogranin A, synaptophysin, CD56 (focally), cytokeratins AE1-AE3 (focally), vimentin (most cells), glucagon (focally), and pancreatic polypeptide (PP; focally). Antibodies against serotonin, somatostatin, gastrin, vasoactive intestinal polypeptide (VIP) and calcitonin did not react with the tumor. The results of biochemical markers (5-HIAA, vanillylmandelic acid and NSE) did not correlate with development or treatment of the tumor.

Conclusions. Primary neuroendocrine carcinoma of the kidney was diagnosed both histologically and immunohistochemically. The patient was clinically investigated using CT and OctreoScan scintigraphy. Within two years from nephrectomy, metastases were found in the right humerus and retrocaval lymph nodes. The metastatic lesions were surgically removed. Currently, the patient's condition is good, with no tumor progression detected.

Keywords:

kidney neoplasm, neuroendocrine tumor, carcinoid

INTRODUCTION

Primary neuroendocrine tumors of the kidney are rare. They occur in both the renal parenchyma and

the renal pelvis [1,2,3,4,5,6]. Either individual tumors or series of five or six cases have been reported [7,8]. The largest series of 21 patients with renal carcinoids (well-differentiated neuroendocrine tumors) was investigated by Hansel et al. [6]. The patients were treated in five large US hospitals over a period of 36 years. So far, about 90 cases of the tumor have been described [9]. Most frequently, the tumor develops in the horseshoe kidney [10,11]. Hansel et al. [6] found the horseshoe kidney in 19% of the cases. Sporadically, synchronous well-differentiated neuroendocrine tumor and adenocarcinoma within teratoma of the horseshoe kidney have been reported [11].

CASE REPORT

A 36 year old male was admitted to the university hospital due to epigastric pain and dyspepsia three years previously. The 5-hydroxyindoleacetic acid (5-HIAA) test showed 41.0 µmol/24 hrs (reference range, 10.4- 47.1 µmol/24 hrs). The vanillylmandelic acid level was 31.2 µmol/24 hrs (reference range, 0-33 µmol/24 hrs). During the hospital stay, the vanillylmandelic acid levels fluctuated between 17.9 and 53.2 µmol/24 hrs. Serum neuron-specific enolase (NSE) levels did not exceed 10.3 µg/L (reference cut-off, 12.5 µg/L) throughout the hospitalization. Based on the clinical results, nephrectomy of the right kidney was performed. Two months later, OctreoScan scintigraphy detected two lesions with increased somatostatin receptor density. One lesion was in the proximal third of the right humerus; the other was localized in the epigastrium but not specifically. The former lesion was assessed by CT angiography. Subsequent magnetic resonance imaging (MRI) confirmed a metastasis in the humerus but failed to show alterations in the epigastrium. One year later, a small increase in the right humerus lesion was revealed on X-ray. Subsequent biopsy examination confirmed metastatic neuroendocrine carcinoma. Two and half years after nephrectomy, resection of the humerus was performed. Postoperatively, PET/CT revealed a lesion in the retrocaval lymph nodes of the L1-L2 region. The nodes were surgically removed. Histological examination confirmed a neuroen-

ocrine carcinoma metastasis. At present, the patient is free from tumor symptoms. His levels of the studied markers were of no value and no correlation with tumor development or treatment was found.

MATERIALS AND METHODS

The kidney and lymph nodes were fixed in neutral formalin and the tumor tissue specimens were processed in the Autotechnicon. The paraffin-embedded sections were stained with hematoxylin and eosin. Immunohistological evaluation was carried out using the avidin-biotin complex (ABC) method as usual, according to the manufacturer's instructions. The following antibodies were used (dilutions as shown in the brackets): AE1-AE3, clone AE1-AE3 (1:50), CK20, clone Ks 20.8 (prediluted), CK7, clone OU-TL 12/13 (1:50), NSE, clone 2F111 (1:50), rabbit anti-human gastrin polyclonal antibody (1:2000), vimentin, clone 3B4 (1:100), rabbit anti-human somatostatin polyclonal antibody, code A0566 (1:1000), mouse anti-human serotonin monoclonal antibody, clone 5HT-H209 (1:100), rabbit anti-human glucagon polyclonal antibody, clone A0565 (1:1000) - the antibodies were produced by Dako, Glostrup, Denmark; synaptophysin, clone 27G12 (1:100), chromogranin A, clone 5H7 (1:100), CD56, clone 1B6 (1:50) - antibodies manufactured by Novocastra, Newcastle-upon-Tyne, UK; rabbit anti-pancreatic polypeptide polyclonal antibody, clone 18-0043 (1:100) - Invitrogen, Lofer, Austria; VIP (vasoactive intestinal peptide) (1:500) - Immunostar, USA; rabbit anti-calcitonin polyclonal antibody, clone SP17 (1:20) - Thermo Scientific, Fremont, USA.

RESULTS

Macroscopic findings

In the renal hilum, a 5x5x6 cm cyst was found. The cavity was filled with dark red liquid. The inner surface of the cavity contained brownish soft areas of tissue. The cyst cavity was just adjacent to compact whitish tumor nodules affecting the renal medulla. The overall size of the lesion was 8x8x7 cm (Fig. 1). The cyst was in the close proximity to the renal pelvis.

Histopathology

The tumor itself was made up of ribbon-like or trabecular patterns of cylindrical cells. The nuclei were round or oval, localized mostly in the cell center. Occasional pseudoglandular and cystic structures were present (Fig. 2). At the basal area of the tumor cells, the plasma was of granular appearance. The tumor cells had a mitotic count of <1mitosis/10HPF; the proliferation marker Ki-67 level was much lower than 1%. Metastases in the lymph node and humerus were of a histologically similar appearance to that in the kidney. Also in these places, the mitotic count was 1/10HPF and the Ki-67 index was 1-2%. Immunohistologically, the tumor cells were positive with antibodies against chromogranin A (Fig. 3), synaptophysin (Fig. 4), CD56 (focally), vimentin (most cells), glucagon (focally), pancreatic polypeptide (PP) (focally), and cytokeratins AE1-AE3 (focally). The other markers were negative. The other markers were negative.

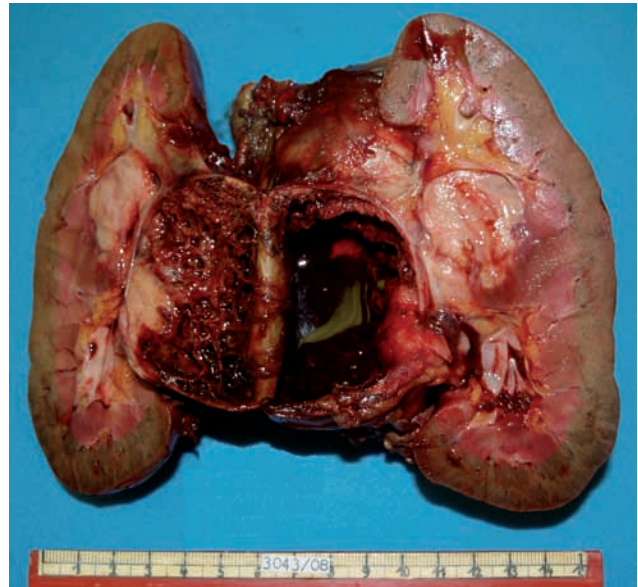


Fig. 1 Section of the kidney with cystic tumor

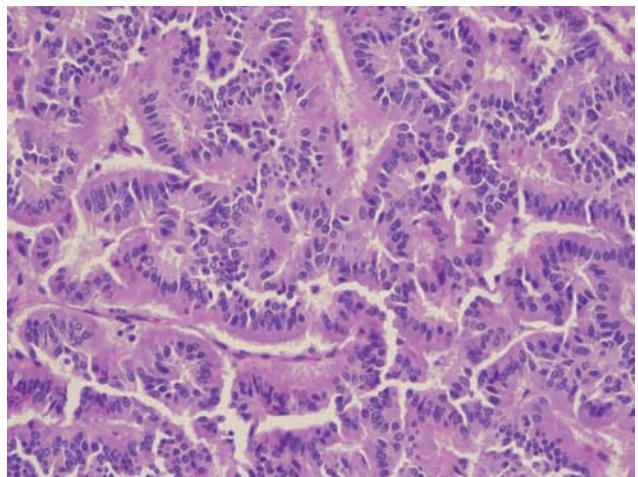


Fig. 2 Cylindrical cells of well-differentiated neuroendocrine carcinoma (HE, 400x)

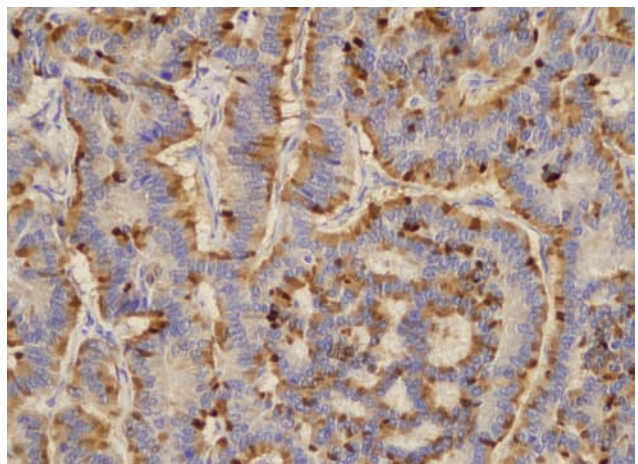


Fig. 3 Tumor cells mostly at the basal area react positively with an antibody against chromogranin (400x)

physin (Fig. 4), CD56 (focally), vimentin (most cells), glucagon (focally), pancreatic polypeptide (PP) (focally), and cytokeratins AE1-AE3 (focally). The other markers were negative. The other markers were negative.

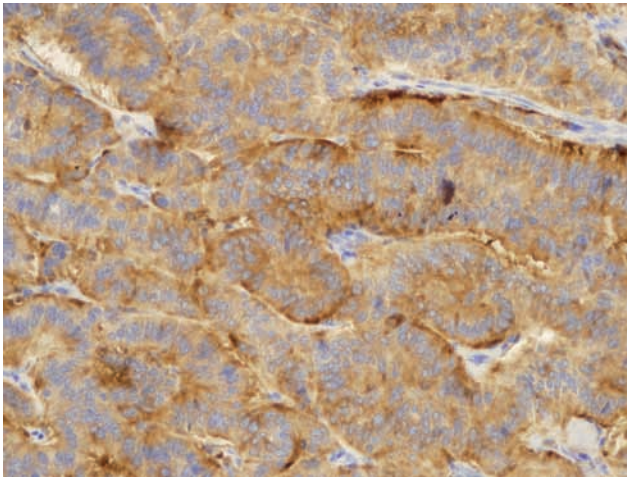


Fig. 4 Positive finding in tumor cells with an antibody against synaptophysin (200x)

DISCUSSION

Well-differentiated neuroendocrine carcinoma is mostly observed in the gastrointestinal tract. Most frequently, it is localized in the small and large intestines and stomach. It is less frequent in the respiratory system. Sporadically, it is seen in parenchymal organs such as the liver and kidneys. In the liver parenchyma, it mostly arises from scattered neuroendocrine cells of bile duct or gall bladder mucosae. In the kidneys, the histogenetic origin of these tumors is unclear. The tumor quite often develops in the horseshoe kidney. In such cases, the clinical course is much more benign than in tumors occurring in normal kidneys¹².

Primary neuroendocrine carcinoma of the kidney is most prevalent in patients around 50 years of age. It is clinically manifested by hematuria and unspecified pain in the lumbar region. Shurtleff et al.¹³ found that in approximately 20% (out of 43 cases), the course is asymptomatic. Gradually, the tumor enlarges and only then clinical symptoms may appear. In our case, it was 8 cm. In more than 48% of cases, the tumor is cystic, such as in our patient. In the aforementioned series of 43 patients with primary neuroendocrine carcinoma of the kidney, metastases in the lymph nodes were found in approximately 18%. Carcinoid syndrome was diagnosed in nearly 14% of cases. In the reported cases, tumor cells most frequently expressed PP, VIP and serotonin¹². In our case, two years and six months after nephrectomy, lesions were found in the proximal humerus and lymph nodes paravertebrally in the subhepatic region. In both sites, metastases of well-differentiated neuroendocrine carcinoma were histologically confirmed. Expression of the proliferation marker Ki-67 was more prominent in these sites than in the primary tumor of the kidney.

The histogenetic origin of primary neuroendocrine carcinoma of the kidney is unclear. Neuroendocrine cells are not mentioned in histological descriptions

of the normal parenchyma of the kidney, renal pelvis or ureter. Progenitor cells incorporated into the renal parenchyma during organogenesis are considered. Some authors^{14,15} found small nests of paraganglionic cells from which neuroendocrine tumors may arise. Nests of these cells were detected in the hilar region of the kidney.

Parada et al.¹⁶ reported chromophobe renal cell carcinoma with neuroendocrine differentiation, an entity described in the only case. According to the authors, both types of lesions have a common origin in renal tubular cells. Neuroendocrine differentiation was suggested by not only immunohistochemical assay but also neurosecretory granules found in tumor cell cytoplasm by elektron microscopy. Rarely, neuroendocrine differentiation is observed in microcystic urothelial cell carcinoma of the renal pelvis¹⁷. Primary neuroendocrine carcinoma of the kidney may be mimicked by neuroendocrine cancer metastasis as reported in Merkel cell carcinoma metastatic to the kidney¹⁸.

Some authors think that the tumors arise from neuroendocrine cells occurring in the mucosa of the renal pelvis in intestinal metaplasia^{19,20}.

The histological picture of the neuroendocrine carcinoma of the kidney was medium-sized tumor cells arranged into trabecules or ribbons. That is, structures similar to those observed in these tumors in the gastrointestinal tract. In our case, glandular structures were also seen that tended to form cyst cavities. One such cavity occupied a considerable part of the tumor. Less frequently, large cell neuroendocrine carcinoma is seen^{21,22}. Some authors^{23,24} claim that neuroendocrine carcinoma of the renal pelvis is more frequently associated with transitional cell carcinoma, adenocarcinoma or squamous cell carcinoma than with the same tumors arising in the renal parenchyma.

At the molecular genetic level, abnormalities of chromosome 3 were detected¹.

ACKNOWLEDGEMENT

Authors thank Dr. O. Koperek, Department of Pathology, AKH Vienna, for his help with immunohistochemical examinations.

REFERENCES

1. Kuroda N, Alvarado-Cabrero I, Sima R, Hes O, Michal M, Kinoshita H, Matduda T, Ohe CH, Sakaida N, Vemura Y, Lee GH. Renal carcinoid tumor: an immunohistochemical and molecular genetic study of four cases. *Oncology letters* 2010;1:87-90.
2. Kuroda N, Katto K, Tamura M, Hes O, Michal M, Hayashi Y, Lee GH. Carcinoid tumor of renal pelvis: consideration on the histogenesis. *Pathol Int* 2008;58:51-54.
3. Yoo J, Park S, Lee HJ, Kang SJ, Kim BK. Primary carcinoid tumor arising in a mature teratoma of the kidney a case report and review of the literature. *Arch Pathol Lab Med* 2002;126: 979-981.
4. Romero FR, Rais-Bahrami S, Permpongkosol S, Fine SW, Kohanian S, Jarrett TW. Primary carcinoid tumor of the kidney. *J Urol* 2006;176:2359-2366.

5. Murali R, Kneale K, Lalak N, Delprad W. Carcinoid tumors of the urinary tract and prostate. *Arch Pathol Lab Med* 2006;130:1693-1706.
6. Hansel DE, Epstein JI, Berbesco E, Fine S, Young R, Cheville J. Renal carcinoid tumor: a clinicopathologic study of 21 cases. *Am J Surg Pathol* 2007;31:1539-1544.
7. Raslan WF, Ro JY, Ordonez NG, Amin MB, Troncso P, Sella A, Ayala AG. Primary carcinoid of the kidney. Immunohistochemical and ultrastructural studies of five patients. *Cancer* 1993;72: 2660-2666.
8. Lane BR, Chery F, Jour G, Sercia L, Nagi-Galluzzi C, Novick AC, Zhou M. Renal neuroendocrine tumours: a clinicopathological study. *BJU Int* 2007;100:1030-1035.
9. Jain D, Sharma CH, Singh K, Gupta NP. Primary carcinoid tumor of the kidney: case report and brief review of literature. *Ind J Pathol Microbiol* 2010;53:772-774.
10. Isobe H, Takashima H, Higashi N, Murakami Y, Fujita K, Hanazawa K, Fujime M, Matsumoto T. Primary carcinoid in a horseshoe kidney. *Inter J Urol* 2000;7:184-188.
11. Armah HB, Parwani AV, Perepletchikov AM. Synchronous primary carcinoid tumor and primary adenocarcinoma arising within mature cystic teratoma of horseshoe kidney: a unique case report and review of the literature. *Diagn Pathol* 2009;4:1-10.
12. Krishnan B, Truong LD, Saleh G, Sirbasku DM, Slawin KM. Horseshoe kidney is associated with an increased relative risk of primary renal carcinoid tumor. *J Urol* 1997;157:2059-2066.
13. Shurtleff BT, Shvarts O, Rajfer. Carcinoid tumor of the kidney: case report and review of the literature. *Rev Urol* 2005;7:229-233.
14. Guy L, Bégin LR, Oligny LL, Brock GB, Chevlier S, Aprikian AG. Searching for an intrinsic neuroendocrine cell in the kidney. *Pathol Res Pract* 1999;195:25-30.
15. Kawabata K. Searching for an intrinsic neuroendocrine cell in the kidney. Letter to the editor. *Pathol Res Pract* 1999;195:865-866.
16. Parada DD, Pena KB. Chromophobe renal cell carcinoma with neuroendocrine differentiation. *APMIS* 2008;116:859-865.
17. Pacchioni D, Bosco M, Allia E, Mussa B, Mikuz G, Bussolati G. Microcystic urothelial cell carcinoma with neuroendocrine differentiation arising in renal pelvis. Report of a case. *Virchows Arch* 2009;454:223-227.
18. Pollheimer VS, Bodo K, Pollheimer MJ, Zigeuner R, Langer C. Merkel cell carcinoma metastasizing to the kidney mimicking primary neuroendocrine renal cancer. *APMIS* 2007;115:774-777.
19. Gordon A. Intestinal metaplasia of the urinary tract epithelium. *J Pathol Bacteriol* 1963;85:441-445.
20. Shurtleff BT, Shvarts O, Rajfer J. Carcinoid tumor of the kidney: case report and review of the literature. *Rev Urol* 2005;7:229-233.
21. Dunder P, Pešl M, Povýšil C, Bauerová L, Soukup V. Primary large cell neuroendocrine carcinoma of the kidney. *Pathol Oncol Res* 2010;16:139-142.
22. Jiang SX, Mikami T, Umezawa A, Saegusa M, Kameya T, Okayasu I. Gastric large cell neuroendocrine carcinomas: a distinct clinicopathologic entity. *Am J Surg Pathol* 2006;30:945-953.
23. Mazzucchelli A, Morichetti D, Lopez-Beltran A, Cheng L, Scarpelli M, Kirkali Z, Montironi R. Neuroendocrine tumours of the urinary system and male genital organs: clinical significance. *BJU Int* 2009;103:1464-1470.
24. Guillou L, Duvoisin B, Chobez C, Chapuis G, Costa J. Combined small-cell and transitional cell carcinoma of the renal pelvis. A light microscopic, immunohistochemical and ultrastructural study of a case with literature review. *Arch Pathol Lab Med* 1993;117:239-243.

Sborník vybraných impaktovaných prací za rok 2013

Vydavatel: Fakultní nemocnice Ostrava
Periodicita: roční
Počet výtisků: 100 ks

ISBN 978-80-905684-2-6



Sborník vybraných impaktovaných prací za rok 2013

Vydavatel: Fakultní nemocnice Ostrava
Periodicita: roční
Počet výtisků: 100 ks

ISBN 978-80-905684-2-6 (print)
ISBN 978-80-905684-3-3 (on-line)

ISSN 2336-4041 (Print)
ISSN 2336-405X (On-line)